Heat Pump Integrated Thermal Storage for Building Demand Response and Decarbonization

A Dissertation Presented for the

Doctor of Philosophy

Degree

The University of Tennessee, Knoxville

Sara Sultan

August 2023

Copyright © 2023 by Sara Sultan.

All rights reserved.

DEDICATION

To my beloved husband for always having my back.

To my parents for tremendous support.

To the wizarding world of Harry Potter for comforting me.

To my love of art for keeping me sane.

And to myself, for not giving up…



ACKNOWLEDGEMENTS

I wholeheartedly thank my advisor, Dr. Kyle R. Gluesenkamp for his tremendous support and guidance throughout my Ph.D. I also wish to thank my doctoral committee members Dr. Orlando Rios, Dr. William A. Miller, Dr. Hongyu Nick Zhou and Dr. David J. Keffer for their patience and assistance.

I couldn't have completed this milestone without my wonderful husband, Syed Muhammad Aqib, who helped me calm down in my most depressed moments, who attended every big exam and presentation of mine to support me, and who also taught me programming to troubleshoot my model. A special thanks to my father Sultan Mehmood, my mother Zahida Firdous and my siblings Aisha Sultan, Fatima-Tuz-Zahra, Abeer Sultan, and Muhammad bin Sultan, for always rooting for my success and being there for me whenever I needed them.

Additional thanks to Dr. Xiaobing Liu, Dr. Tim LaClair, and Dr. Monojoy Gosowami for the use of lab equipment, inspiration, guidance, and providing helpful resources. I feel blessed to have worked with talented people at Oak Ridge National Lab who inspired me and helped me throughout my journey including Dr. Tugba Turnaoglu, Dr. Saad Ayub Jajja, Dr. Navin Kumar, Dr. Borui Cui, Dr. Zhenning Li, Dr. Joseph Randell, Dr. Lingshi Wang, Dr. Jason Hirschey and Dr. Damilola Akamo. Thanks to Isis Fukai and Dr. Terry Hazen for providing me a convenient alternate office space on UTK campus.

Thanks to the team of directors and coordinators at the University of Tennessee Bredesen Center for their support and encouragement: Dr. Lee Riedinger, Dr. Suresh S. Babu, Dr. Phillip Rack, Dr. Yanfei Gao, Wanda Davis, Allie Burns, Rebecca Christ and Rachel Roberts. I am grateful to the Bredesen Center ORII Program and the U.S. DOE Building Technologies Office for financial support of this research and my education.

And last but not the least, thanks to my friends for understanding my struggles and being truly amazing as they are; Kashif Janjua, Dr. Saad Saleem, Yusra Farhatullah, Lesli Burton Portoff, and Lee Leadbetter.

ABSTRACT

This work presents a novel thermal energy storage (TES) integrated with existing residential heat pump (HP). The research focuses on controls and configuration for energy, demand, cost and carbon emissions savings for residential buildings' energy consumption. This work will be significant in developing a framework especially for reduced energy demand and carbon emissions associated with space heating and cooling in residential buildings. Since buildings account for about 40% primary energy consumption in U.S. and half of that is associated with HP.

An existing air source HP in integrated with a phase change material (PCM) based TES via active configuration where HP mediates the heat transfer. In this novel configuration, TES is indirectly coupled to the building and behaves as heat sink or source, only providing heating or cooling via HP equipment. We used a single TES for both heating and cooling applications and performed a parametric analysis to determine the best phase change temperature and storage capacity for maximum performance. The performance parameters are energy savings, demand savings, and cost savings, achieved by shifting the peak load and using rule-based control strategies.

There are very few studies available in literature on heat pump integrated with thermal energy storage (HP-TES) and no standards are available to compare them. There's no complete experimental system found in literature that addresses controls, configurations, and performance of HP-TES altogether. Furthermore, no simulation works have analyzed and compared different climate zones for HP-TES performance.

We address this gap by contributing a simulation-based system and validating it experimentally for a single-family residential building. The simulation compares different climate zones in U.S. to determine the impact of configuration and controls on performance.

Commercializing such HP-TES will have a broader impact on research community and this work aligns with DOE's goals of decarbonizing and reducing demand by 2030. Flexible installation of HP-TES allows use of existing HP equipment for controls with minimal space footprint, reducing installation and consumer cost that will appeal to residential homeowners.

Keywords

Thermal Energy Storage, Residential Buildings, Heat Pumps, Phase Change Material, Demand Response, Carbon Mitigation

TABLE OF CONTENTS

INTRODUCTION 1

Overview 1

Relevance of Research 2

Research Gap 3

Problem Statement 5

Research Significance and Contribution 5

Research Questions 7

Research Objective 7

Dissertation Outline 7

CHAPTER I HEAT PUMP INTEGRATED WITH THERMAL ENERGY STORAGE 10

Abstract 11

Research Question 12

Introduction 13

Knowledge Gaps 16

Existing Reviews 16

Objectives 17

Scope and Organization 18

Background 19

DR and Building Flexibility 19

Utility Rate Structures 20

TES in Buildings 22
HP-TES Configurations and Definitions 24
Literature Review 26
Controls for HPs without TES 26
HP-TES Configurations 32
Passive HP-TES 32
Active HP-TES 39
Building Envelope 41
Air Distribution 41
Vapor Compression System 42
Comparative Research Trends 54
HP-TES Research 54
PCMs for HP-TES 54
Climate Zones and TES Application 56
Impact Analysis 56
Comparison of Active HP-TES Configurations 58
Utility Cost Savings 58
Energy Savings 60
Demand Impact 62
Comparison of Active and Passive HP-TES 64
Load Shifting 65
Payback Period 65

Performance Analysis with and without TES 67
Discussion and Future Work 70
Conclusions 73
CHAPTER II PHASE CHANGE MATERIAL FOR HEAT PUMP INTEGRATED WITH TES 74
Abstract 75
Research Question 76
Background 76
PCM for HP-TES 80
PCM Selection 80
Integration in Heat Pump Components 81
Heat Pump Integration 84
Application and Configuration 84
Results and Discussion 87
Melting Temperature 87
Configuration 87
Conclusions 90
CHAPTER III CASE STUDY – ECONOMIC IMPLICATIONS OF RESIDENTIAL BUILDINGS 91
Abstract 92
Research Question 93
Background 93
Methodology 97

System Overview 97
System Operating Modes and Controls 98
Component Models 103
Weather Data 103
Building Model 103
Building Thermostat Model 105
VCS Model 105
TES Model 106
Utility Rate Analysis 106
Results and Discussion 108
Conclusions 113
CHAPTER IV OPTIMISING PHASE CHANGE TEMPERATURE FOR HEAT PUMP INTEGRATED WITH TES 114
Abstract 115
Research Question 116
Background 116
State of the art 117
Research Gap and Objectives 119
Methodology 121
System Overview 122
Operating Modes 124
Component Models 125

Weather Data 125
Utility Data 128
TES Model 128
Thermostat Controls 131
Heat Pump Model 132
Building Model 135
Results 137
Birmingham, Alabama 138
New York City, New York 144
Houston, Texas 147
Discussion 153
Conclusions 158
CHAPTER V ANALYSIS ON HP-TES IN VARIOUS CLIMATE ZONES IN U.S. AND EXPERIMENTAL VALIDATION 160
Abstract 161
Research Questions 161
Background and Literature Review 162
Marginal Grid Emissions 164
Case Study 167
Methodology 168
Component Models 174
Results and Discussion 179

Figure 58: Utility Cost reduced using TES.ConclusIONS 183
Annual Simulations 185
Overview 185
MATLAB flow chart 185
Thermostat model 188
Building Model 188
HP Model 192
Operating modes 192
Configurations 194
TES Model 194
Controls logic 203
Experimental Validation 203
Building RC Model 206
Experimental setup with HP in FRP-2 211
PCM Heat exchanger and HP-TES integration 211
Analysis 215
Climate Zone and Input Data 215
Analysis on Baltimore, MD 221
Analysis on Golden, CO 221
Analysis on Sacramento, CA 221
Conclusions 225
Discussions 225

DISSERTATION CONCLUSIONS 227
Summary 228
Broader Impact 229
Future Work 234
REFERENCES 235
APPENDIX 265
Appendix A: HP-TES configurations review 265
Comparative Analysis 265
Payback Period 266
Load Shifting 267
Demand Impact 268
Energy Savings 269
Utility Cost Savings 270
Appendix B: Alabama case study analysis 271
Payback Period 271
Appendix C: HP Analysis on California Case Study 272
Appendix D: HP-TES Technoeconomic Analysis 273
VITA 282

LIST OF TABLES

Table 1: Table showing gap in literature and scope of this work. 4

Table 2: Definitions of active, passive, direct, and indirect TES configurations 27

Table 3: Demand management without TES 31

Table 4: Passive TES configurations with cooling only 35

Table 5: Passive TES configurations with heating only 36

Table 6: Passive TES configurations with both heating and cooling 38

Table 7: Active PCM configurations with cooling only 46

Table 8: Active PCM configurations with heating only 50

Table 9: Active PCM configurations with both heating and cooling 51

Table 10: PCMs for HP-TES 82

Table 11: Active HP-TES Configurations with Salt hydrate PCMS 85

Table 12: Active HP-TES Configurations with other PCMS 86

Table 13: PCM-based active TES for load shifting. 96

Table 14: Literature review on PCM temperature optimization 120

Table 15: Electric utility rates 130

Table 16: Operating mode examples 134

Table 17: Annual results summary 155

Table 18: Load shifting, and carbon mitigation reported in literature using PCM-TES 163

Table 19: Table showing gap in literature and scope of this work. 166

Table 20: Thermostat logic to trigger actions at T_{indoor}, setpoint, and deadband. 189

Table 21: Building Thermal Energy Simulation Model Parameters 191

Table 22: Buildings selected for analysis. 191

Table 23: Definitions of SOC 198

Table 24: Cases for comparative analysis..... 200

Table 25: HP capacity and COP 212

Table 26: TOU Utility Schedule 216

LIST OF FIGURES

Figure 1: Gaps in literature filled by this work and final contribution. 6

Figure 2: Dissertation chapters and publications. 8

Figure 3:PCM-TES in active and passive storage 25

Figure 4: Possible configurations for PCMs integrated in a building..... 33

Figure 5: Passive storage locations in the building..... 40

Figure 6: Indirect PCM-integrated HVAC configuration..... 45

Figure 7: Active storage locations in the building and HP components..... 53

Figure 8: Historical trend of HP-TES research..... 55

Figure 9: Historical trend of PCMs used for HP-TES. 55

Figure 10: Phase change temperatures in various climate zones. 57

Figure 11: Active HP-TES and utility cost savings in literature. 59

Figure 12: Active HP-TES and energy savings in literature..... 61

Figure 13: Active HP-TES and demand impact in literature. 63

Figure 14: Load shifting of active and passive HP-TES in literature. 66

Figure 15: Payback period of active and passive HP-TES in literature..... 66

Figure 16: Overall comparison: (A) phase change temperature, (B) demand impact, (C) energy savings, and (D) utility cost savings. 69

Figure 17: Comparison of load shifting benefits for Active and Passive TES 79

Figure 18: Demand Impact and PCM Temperature..... 88

Figure 19: Demand Impact and heat pump configurations..... 89

Figure 20: Comparison of temperature gradients for a) normal VCS operation and b) TES-assisted cooling 99
Figure 21: Energy flows in the four operating modes for summer (cooling only) 100
Figure 22: Controls decision tree 102
Figure 23: Total system information flow and relation between sub-models 102
Figure 24: Ambient dry bulb temperature for the simulated week 104
Figure 25: VCS operating power for normal, charging, and discharging modes. 107
Figure 26: Ambient Temperature and Utility Data 109
Figure 27: Electric Consumption comparison with and without TES 110
Figure 28: Total electrical utility cost with and without TES 110
Figure 29: PCM SOC 112
Figure 30: Indoor Temperature Profile 112
Figure 31: Comparison of temperature gradients for baseline and TES cases. 123
Figure 32: Cooling Operating modes with TES. 126
Figure 33: Heating Operating modes with TES. 126
Figure 34: Operation flow chart showing the submodels and direction of information flow. 127
Figure 35: Average dry-bulb temperature. 129
Figure 36: Controls decision tree. 133
Figure 37: T-s diagram for cooling cycle 136
Figure 38: Birmingham results for peak energy consumption. 140
Figure 39: Birmingham results for energy consumption. 141
Figure 40: Birmingham results for utility cost. 143

Figure 41: New York City results for peak energy consumption. 145
Figure 42: New York City results for energy consumption. 146
Figure 43: New York City results for utility cost. 148
Figure 44: Houston results for peak energy consumption. 149
Figure 45: Houston results for energy consumption. 151
Figure 46: Houston results for utility cost. 152
Figure 47: Electric Consumption. 154
Figure 48: Summary of annual results for all three locations. 156
Figure 49: One representative reference reporting emission reduction by using PCM in various locations and configurations. 165
Figure 50: HP-TES configuration in cooling mode (A. TES Discharging B. TES Charging) 169
Figure 51: Operating modes in cooling. 171
Figure 52: Controls decision tree used in this work. 173
Figure 53: Information Flow Diagram 175
Figure 54: Ambient Temperature and Utility data for cooling day 176
Figure 55: Fresno annual grid emissions during 2022 180
Figure 56: Emissions reduced using TES 181
Figure 57: Electric Consumption with and without TES. 181
Figure 58: Utility Cost reduced using TES.ConclusIONS 183
Figure 59: Simplified information flow 186
Figure 60: MATLAB Model flow 187
Figure 61: Indoor temperature setpoints. 190

Figure 62: Models integration for HP-TES in MATLAB. 190
Figure 63: HP-TES cooling operating modes. 193
Figure 64: HP-TES heating operating modes. 193
Figure 65: Vapor Compression Cycle for Normal Cooling. 195
Figure 66: Vapor Compression Cycle for Normal Heating. 195
Figure 67: Vapor Compression Cycle for Charging Cooling 196
Figure 68: Vapor Compression Cycle for Discharging Cooling 196
Figure 69: HP-TES integration and energy flow 199
Figure 70: Operating mode controls for base case 204
Figure 71: Operating mode controls for case 1 and 2 204
Figure 72: SOU controls for case 1 204
Figure 73: SOU controls for case 2 204
Figure 74: Conceptual figure of HP-TES with building 205
Figure 75: Schematic of the simplified building thermal network model 207
Figure 76: HP Charging and Discharging rate. 212
Figure 77: Measured PCT using sensors. 213
Figure 78: Experimental setup at ORNL. 213
Figure 79: PCM-HX integrated with DSHP. 214
Figure 80: Hydronic piping and data points. 214
Figure 81: Representative MGE Data for Summer in all locations. 217
Figure 82: Representative MGE Data for Winter in all locations. 217
Figure 83: Ambient Weather and Utility Rate on the coldest day in Baltimore 218

Figure 84: Ambient Weather and Utility Rate on the hottest day in Baltimore 218
Figure 85: Ambient Weather and Utility Rate on the coldest day in Sacramento 219
Figure 86: Ambient Weather and Utility Rate on the hottest day in Sacramento..... 219
Figure 87: Ambient Weather and Utility Rate on the coldest day in Golden 220
Figure 88: Ambient Weather and Utility Rate on the hottest day in Golden..... 220
Figure 89: Control Strategy Comparison for Winter Typical week in Baltimore 222
Figure 90: Control Strategy Comparison for Winter Extreme week in Baltimore 222
Figure 91: Control Strategy Comparison for Winter Typical week in Golden..... 223
Figure 92: Control Strategy Comparison for Winter Extreme week in Golden 223
Figure 93: Control Strategy Comparison for Summer Extreme week in Sacramento.... 224
Figure 94: Control Strategy Comparison for Winter Extreme week in Sacramento 224
Figure 95: Broader Impacts of research. 230
Figure 96: Business model development. 232
Figure 97: Market adaptation framework. 233
Figure 98: Historical trend of PCMs for HP-TES 265
Figure 99: Historical trend of HP-TES research with TES type..... 265
Figure 100: Payback period comparison against configurations 266
Figure 101: Payback period comparison against application 266
Figure 102: Load shifting comparison against application..... 267
Figure 103: Load shifting comparison against configuration 267
Figure 104: Demand Impact comparison against application..... 268
Figure 105: Demand Impact comparison against climate zone 268

Figure 106: Energy savings comparison against application 269
Figure 107: Energy savings comparison against PCM type 269
Figure 108: Utility cost comparison against climate zone 270
Figure 109: Utility cost comparison against TES type 270
Figure 110: Alabama Ambient TMY 271
Figure 111: HP-TES Normal mode COP 272
Figure 112: HP-TES Charging mode COP 272
Figure 113: Electric Consumption of Winter Typical week in Baltimore, MD 273
Figure 114: Utility Cost of Winter Typical week in Baltimore, MD 273
Figure 115: Grid Emissions of Winter Typical week in Baltimore, MD 274
Figure 116: Electric Consumption of Winter Extreme week in Baltimore, MD 274
Figure 117: Utility Cost of Winter Extreme week in Baltimore, MD 275
Figure 118: Grid Emissions of Winter Extreme week in Baltimore, MD 275
Figure 119: Electric Consumption of Winter Typical week in Golden, CO 276
Figure 120: Utility Cost of Winter Typical week in Golden, CO 276
Figure 121: Grid Emissions of Winter Typical week in Golden, CO 277
Figure 122: Electric Consumption of Winter Extreme week in Golden, CO 277
Figure 123: Utility Cost of Winter Extreme week in Golden, CO 278
Figure 124: Grid Emissions of Winter Extreme week in Golden, CO 278
Figure 125: Electric Consumption of Summer Extreme week in Sacramento, CA 279
Figure 126: Utility Cost of Summer Extreme week in Sacramento, CA 279
Figure 127: Grid Emissions of Summer Extreme week in Sacramento, CA 280

Figure 128: Electric Consumption of Winter Extreme week in Sacramento, CA 280

Figure 129: Utility Cost of Winter Extreme week in Sacramento, CA 281

Figure 130: Grid Emissions of Winter Extreme week in Sacramento, CA 281

INTRODUCTION

The introduction is organized to lay a framework for this work and to highlight its importance. It talks about residential buildings' energy consumption and peak demand associated with heat pumps and proposes thermal energy storage integrated with heat pump as a solution to shift the peak loads. The research gap is established, and contributions of this work are listed at the end of this section.

Overview

Heating, cooling, and ventilation loads in residential buildings account for about 10% of energy consumption and CO_2 emissions worldwide and comprises 50% of the building electricity consumption [1]–[3]. More than 74% of electric use in United States is attributed to buildings where heat pumps (HP) exacerbate the demand issues, as, during the summer peak times, 50% of the electric load comes from residential buildings, which is largely HVAC (Heating, Ventilation, and Air Conditioning) load [4]. The potential of onsite thermal energy storage (TES) has mostly been underestimated even though its significance for decarbonization and demand reduction has been established by researchers [2].

TES systems locally decouple heating or cooling demand from its production. The thermal storage properties can be leveraged from phase change materials (PCM) to not only design a demand response strategy for peak load shifting, but also for decarbonization. PCM which can be incorporated as passive or active storage, have the capability to store the off-peak energy that can be released during on-peak time.

Researchers have used TES as a building material, but those systems do not have control over when and how to use TES [5], [6]. Such systems are often utilized as a passive storage. They can meet high cooling and heating demands while maintaining occupant comfort [7], but that effort also poses challenges such as complex installation, material encapsulation, space constraints, and additional controls and components [8]–[12].

TES can be coupled with existing air source, ground source, or dual source HPs in buildings [13]–[16]. Integrating TES not only increases the HP efficiency and coefficient of performance (COP) [17]–[19] but also offers controls, configuration, and design flexibility [20]–[22]. HP-integrated TES (HP-TES) has a smaller space footprint and does not require additional equipment [23], [24]. HPs can control TES charging and discharging using existing equipment [25] while providing load shifting and cost saving benefits when coupled with a utility tariff [26]–[29]. PCM integrated with an HP via active storage could save energy, shift the HP loads and energy use from peak to off-peak times, and provide grid flexibility by reducing grid stress during high-demand periods [30]–[32].

Relevance of Research

TES has gained popularity in the past few years for demand management. Researchers have analyzed different PCM and ice-based TES for demand response (DR) using utility controls but decarbonization potential hasn't been assessed.

Passive TES has been more popular and there are very few experimental studies on active TES. Furthermore, there can be number of active TES configurations that haven't been explored yet. Very few studies integrated HP with TES, hence, both the configuration and controls haven't been investigated. HP-TES provides degree of freedom in hardware design and controls choices. Number of possibilities exist for integration using existing equipment with minimum modifications. However, literature on HP-TES performance and simulation is non-existent, and there are no standards or models to compare against. In addition to providing a complete model and validated experimental prototype with a focus on configurations and controls, we also use a single PCM for both heating and cooling in active TES which hasn't been done before.

TES is integrated with HP via novel coupling method and performance is analyzed using single PCM for both heating and cooling in different climates to compare the utility cost, electric consumption, carbon emissions and peak demand savings.

Research Gap

This work will fill a gap in literature by providing a literature review on heat pump integrated TES with a focus on configurations. The papers that are reviewed have reported energy savings, cost savings, or load shifting benefits of HP-TES configuration. The review includes type of PCM used, utility-based controls for demand response, charging and discharging operation, and location of PCM within building envelop and heat pump components for passive and active TES, respectively.

The research gaps are identified from the literature review. To the best of our knowledge, an HP-TES model doesn't exist for configurations where heat pump is mediating the heat transfer. This work will develop the model and validate the simulations via full scale experimental setup. A salt hydrate PCM will be used with a single-phase change temperature for active heating and cooling via heat pump, aided by TES. Technoeconomic analysis will be performed using pre-defined utility rates and grid emissions-based controls to report energy savings, cost savings, peak load shifting, and carbon mitigation.

The key to using TES to provide economic and grid benefits is the development of materials and packaging in optimized configuration and temperature range. This work is focused on active heat pump integrated TES and technoeconomic analysis is conducted based on,

1. **Configuration** for integrating TES with heat pumps.
2. PCM with **single phase change temperature** for both heating and cooling.
3. **Controls** for peak load shifting and carbon mitigation.

Table 1 shows the scope of this work and compares with the literature to identify gap. The comparison includes active heat pump integrated TES systems studied in literature where either carbon emissions analysis or technoeconomic analysis is performed reporting load shifting benefits and energy or cost savings. Some papers have reported demand reduction or peak load shifted based on utility controls, others have reduced high cooling or heating demands and shifted diurnal loads by pre-cooling the building at night.

Table 1: Table showing gap in literature and scope of this work.

Reference	Single PCM for both heating and cooling	Active HP-TES mediated by heat pump	Carbon Emission controls for Hp-TES	Emissions reported	Electric heat pump baseline for emissions	Utility based controls for Hp-TES
[33]	×	×	×	■	×	×
[34]	×	×	×	■	×	■
[35]	×	×	×	■	×	■
[36]	×	×	×	■	×	■
[37]	×	×	×	×	×	■
[38]	×	×	×	×	■	■
[39]	×	×	×	×	■	■
[40]	×	×	×	×	■	■
[41]	×	×	×	×	×	■
[3]	×	■	×	×	■	■
[42]	×	×	×	×	■	■
[43]	×	×	×	×	■	■
[44]	×	×	×	×	■	×
[45]	■	×	×	×	×	×
[46]	×	×	×	×	■	■
[47]	×	×	×	×	■	×
[48]	×	×	×	×	×	■
This work	■	■	■	■	■	■

This work will use TOU utility rates and marginal grid emissions data to optimize the heat pump operation and use TES when utility price and emissions are low. The demand reduction and cost and energy savings are compared against the heat pump integrated TES as proposed case and electric heat pump without TES as a base case.

Problem Statement

This work will first fill a gap in literature by providing a review on heat pump integrated TES with a focus on configurations and PCM materials used. The main contributions of this work will be,

1. A complete HP-TES model with single PCM for heating and cooling in an active heat pump-mediated configuration, using controls based on utility cost and grid emissions, to demonstrate energy savings, grid benefits, and carbon mitigation potential for various climate zones in U.S.
2. Experimental validation of the simulations based on a full-scale experimental prototype of a PCM heat exchanger integrated with heat pump.

Figure 1 illustrates the contributions of this work and gaps in literature that are filled by this study.

Research Significance and Contribution

This work will be a significant contribution to the literature by reviewing configuration and PCM for heat pump integrated thermal storage for building demand response and decarbonization.

Deliverables are an **HP-TES full-scale prototype** and a **validated model with an active HP-TES configuration using single PCM for both heating and cooling**.

The model and prototype will demonstrate grid benefits, energy savings, cost savings, and emission reduction. It might impact the policy for building decarbonization and demand response as well as will present a strong business model for commercialization.

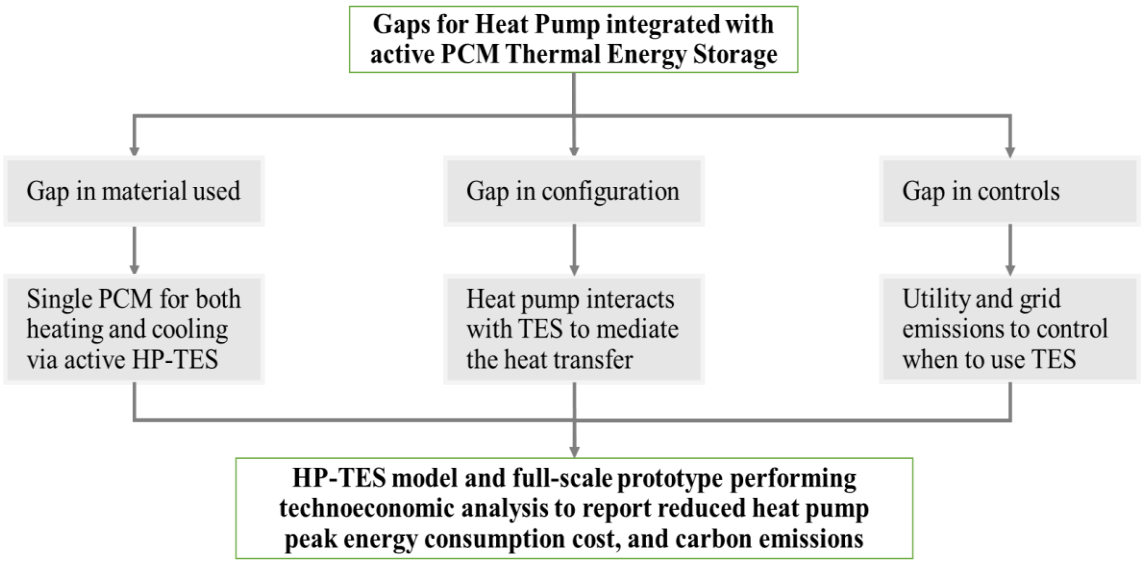


Figure 1: Gaps in literature filled by this work and final contribution.

Research Questions

1. How much reduction in cost of electricity and carbon emissions is possible by shifting the load from peak to off-peak hours for residential buildings in various climates?
2. How can PCM based Thermal Energy Storage be integrated into a heat pump for carbon mitigation, demand response, and reduced electric consumption of heat pumps in residential buildings?
3. What is the optimum PCM temperature and heat pump configuration for maximum economic and grid benefits of heat pump integrated TES?

Research Objective

Design heat pump integrated thermal storage using a salt hydrate PCM for heating and cooling in residential buildings to demonstrate 50% peak demand and carbon emission reduction using control strategies while maintaining occupant comfort.

Dissertation Outline

Dissertation is organized into 5 main chapters preceded by Introduction and followed by Conclusions (Figure 2).

Chapter 1 will provide a review on HP-TES. TES can be integrated with HP via many different configurations. Researchers have either coupled TES with HP via building envelop in passive configurations, or with HP components via vapor compression cycle or air distribution system in active configurations. The chapter provides a review on HP-TES configurations, charging operation, and demand impact.

Chapter 2 will review suitable PCMs for HP-TES system. Both organic and inorganic PCMs have been used in literature for HP-TES. The chapter focuses on performance analysis of PCMs used in various configurations, in different phase change temperature range and TES applications.

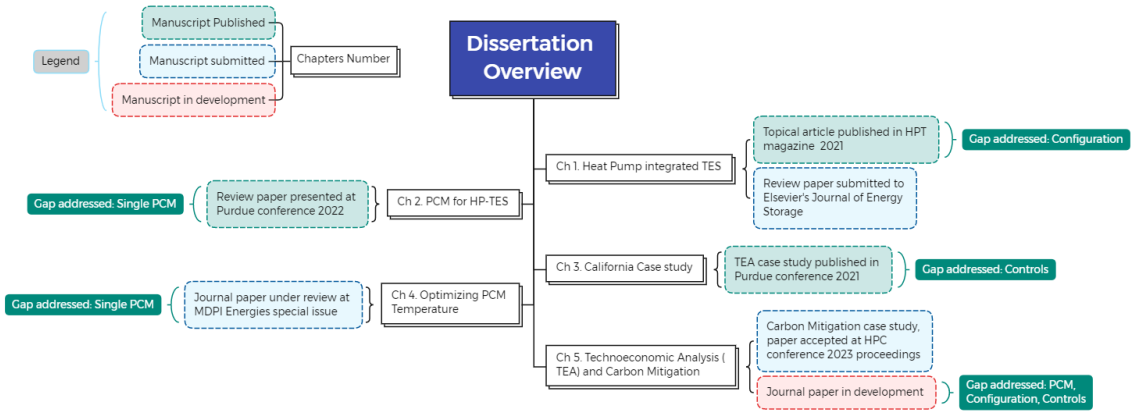


Figure 2: Dissertation chapters and publications.

Chapter 3 will present a case study on techno-economic analysis for residential utility rates in California to discuss economic implications and potential of HP-TES. A control strategy is developed using pre-defined Time-of-Use utility tariff for load shifting. Technoeconomic analysis is performed to evaluate energy savings, cost savings, carbon emission reduction, and demand impact of an active HP-TES in a novel configuration. TES is integrated with heat pump in such a way that it does not directly interact with the building, heat transfer is mediated by the heat pump.

Chapter 4 will determine optimized phase change temperature and energy storage by performing a parametric analysis for various climate locations in the U.S. It is established that for active HP-TES, different phase change temperatures are used for both heating and cooling. No study has used a single PCM with constant phase change temperature for both heating and cooling in an active configuration. This chapter will perform a parametric study to select a single PCM and phase change temperature for both heating and cooling in an active HP-TES configuration.

Chapter 5 will present a detailed annual simulation of HP-TES and validated experimental prototype. Controls are compared for demand reduction and decarbonization for various climate zones in the U.S.

CHAPTER I

HEAT PUMP INTEGRATED WITH THERMAL ENERGY STORAGE

A version of this chapter was originally published by Sara Sultan and Kyle R. Gluesenkamp:

Sultan, S., & Gluesenkamp, K. R. (2021). “The State of Art of Heat-Pump integrated Thermal Energy Storage for Demand Response.” *IEA Heat Pump Technologies Magazine*, *40*(2), 27–30

A version of this chapter is submitted for publication to the Elsevier “Journal of Energy Storage” by Sara Sultan and Kyle R. Gluesenkamp:

Sultan, S., Turnaoglu T., Hirschey J., Kumar N., Rendall J., LaClair T., Liu X., Rios O., Miller W. A., & Gluesenkamp, K. R. (2023). “Heat Pumps Integrated with Thermal Energy Storage in Buildings: System Configurations and Performance Review.” *Journal of Energy Storage*

Conceptualization, data collection, and original manuscript draft was prepared by Sara Sultan. Jason Hirschey, Tugba Turnaoglu, Navin Kumar, Joseph Rendall, Tim LaClair, and Xiaobing Liu provided help with editing and analysis. Review and supervision by Orlando Rios, William A. Miller, and Kyle R. Gluesenkamp.

Abstract

Buildings account for approximately 40% of the US energy consumption and 78% of the US peak electricity usage, almost half of which is for HVAC systems. Literature suggests that thermal energy storage (TES) can shift building peak load to off-peak periods, allowing buildings to help alleviate the challenges associated with electric peak demand. Numerous researchers have investigated coupling TES with heat pumps (HPs) in various configurations and control strategies. HP-integrated TES (HP-TES) has been demonstrated to be effective for load shifting and to provide economic benefits if combined with price-based tariffs and controls. This study provides a critical review of HP-TES using phase change materials (PCMs) and various control strategies. It is a comparative study on HP controls without TES for demand response, passive HP-TES (in the building envelope), and active HP-TES (in HP components with mechanically controlled heat transfer). The

study provides an analysis of possible HP-TES configurations with a focus on PCM location and system performance to compare cost savings, energy savings, demand impact, and payback period.

Research Question

How can PCM based Thermal Energy Storage be integrated into a heat pump for carbon mitigation, demand response, and reduced electric consumption of heat pumps in residential buildings?

INTRODUCTION

Buildings account for approximately 40% of the US primary energy consumption. The residential sector represents about 21% of total US energy consumption [1], [49], [50]. The major electric load from the residential buildings comprises 80% of the total electricity use in the U.S., and 78% of the peak period use during 2-8 PM [51]–[53]. Buildings are already responsible for more than two-thirds of electricity consumption in the U.S., and energy consumption and peak demand is often attributed to air conditioning applications. The heat pumps (HPs) used in buildings exacerbate demand issues [4].

Buildings can play a significant role in reducing energy demand [54]–[57] and increase the building flexibility while maintaining the temperature in a comfortable range, by designing a load shifting strategy [54]–[57].

About 80% of American homes are detached single-family houses of an average area of about 2600 ft2, with an average occupancy of 2.5 [1]. Typically, in US residential buildings, there is no mechanical outdoor air exchange, or cross ventilation using natural resources, therefore, HPs are important to regulate the humidity inside the house as well as the indoor temperature.

HP technology offers cooling and heating from residential and commercial buildings to chemical, petroleum, and food industries, to name a few. Although various HP types exist, such as absorption, adsorption, or chemical reaction cycles, most commercial HP operate based on a vapor compression cycle. HP can provide heating during cold weather and cooling during hot weather throughout the year in mild climates as they can be operated in both heating and cooling mode by simply reversing the operating cycle. HP might also be considered an environmentally friendly HVAC system due to the possible utilization of waste heat. However, even though HP technology evolved over the years and continues to find new applications, the most efficient use of energy in the HP systems while maintaining or improving the overall performance is crucial to reduce the net energy consumption and consequently the greenhouse release into the environment.

It is often cost-prohibitive to rebuild houses or update the conventional methods, but the HP systems can be made smart to respond to the peak demand changes. Today's high-efficiency HVAC and appliance products can provide energy savings, but do not generally help with demand management and grid stress [23].

Efficient heating and cooling appliances, combined with HP controls for demand response (DR), can provide grid and building flexibility [58]–[60], but they have numerous challenges such as heavy dependence on user data, compromise on comfort levels without additional storage, demand rebound issues, and need for complex controls [61]–[64]. Overall operational cost can also increase in some cases [65].

Thermal energy storage (TES), which has capability to decouple the energy generation from its demand and usage, can be a crucial tool to shift the thermal loads. TES systems can be easily incorporated in small to large single-family or multi-family residential buildings. When properly controlled, thermal storage can be useful in an economic or behavioral curtailment scenario for demand response. Major factors influencing an appropriate TES system's choice include the energy storage period and duration, cost and economic feasibility, and operational conditions.

The thermal storage properties can be leveraged by using phase change materials (PCM). which can store energy to release later. Researchers have used various configurations to employ the economic and grid benefits of PCM-TES for heating and cooling applications in buildings. The most common configurations are to install the material in building envelope via passive storage where the charging and discharging process is the function of ambient temperature. High cooling and heating demands can be met by passively using TES while maintaining occupant comfort [7], but that effort also poses challenges such as complex installation, material encapsulation, space constraints, and additional controls and components [8]–[12]. Researchers have used TES as a building material, but those systems do not have control over when and how to use TES [5], [6], hence the grid benefits can't be maximized.

Active storage configurations allow real-time control of TES and are proven to be more effective than passive configurations. Active TES systems mechanically transfer the heat and hence can control when to charge or discharge the TES. This allows the TES systems to achieve grid flexibility, making them more suitable for load shifting and demand management. Another benefit of active configuration is the flexibility to be installed in an existing building infrastructure without needing a significant construction.

The active TES may be separate and removed from the space. PCM-TES can behave as a standalone isothermal heat exchanger when integrated with HP. TES systems when integrated with HP, can offer advantages by shifting the peak demand while maintaining an adequate internal temperature in comfort range, without excessively using HP equipment.

TES can be coupled with existing air source, ground source, or dual source HPs in buildings [13]–[16]. Integrating TES not only increases the HP efficiency and coefficient of performance (COP) [17]–[19] but also offers controls, configuration, and design flexibility [20]–[22]. HP-integrated TES (HP-TES) has a smaller space footprint and does not require additional equipment [23], [24]. HPs can control TES charging and discharging using existing equipment [25] while providing load shifting and cost saving benefits when coupled with a utility tariff [26]–[29]. Phase change material (PCM) TES (PCM-TES) integrated with an HP could save energy, shift the HP loads and energy use from peak to off-peak times, and provide grid flexibility by reducing grid stress during high-demand periods [30]–[32].

This study provides a comparative review of TES in buildings integrated with HPs. An analysis of cost and demand reduction is provided by comparing HP controls without TES and comparing different configurations of HP-TES. System performance of HP-TES is provided to compare energy savings, demand impact, and payback period against different configurations, TES types, and heating and cooling applications for various climate zones.

Knowledge Gaps

Previous reviews have discussed TES in various applications, including residential buildings [66], [67] and PCMs [68]–[71], but none of them reviewed TES integrated with existing HPs with a focus on controls, configuration, and installation of TES in buildings.

Existing Reviews

Navarro et al. [72] discussed active storage systems integrated in buildings. Additionally, various reviews discussed the state of the art of PCMs in the building envelope and passive storage [73]–[76]. Waqas et al. [77] presented a comprehensive review of free cooling and discussed design challenges. Some articles studied both active and passive PCM-TES for heating and cooling [78], [79]. Wahid et al. [80] discussed the thermal performance of PCMs in buildings to reduce electric demand. Pasupathy and Velraj [81] also reviewed PCMs integrated in buildings and coupled with heating and cooling systems for thermal management.

Another comprehensive article with an overview of thermal storage systems discussed diurnal TES systems and briefly analyzed the hot and cold storage of building HVAC systems [82]. Yang et al. [83] presented a review of active storage using PCM and discussed the shortcomings of PCMs for active building energy savings. They also briefly reviewed PCMs in HP and ventilation systems.

HVAC systems and control strategies for HVAC energy savings have also been reviewed [84], [85]. Neil Hewitt [86] presented an overview of HPs and energy storage for thermal load management. Rashidi et al. reviewed the potential of combining PCMs with heat pipes and HPs [87]. They discussed various types of HPs, modeling of materials, and energy saving benefits of combining PCMs with different HPs and types.

In a recent review of a compression HP coupled with TES for space conditioning, Osterman and Stritih [88] analyzed HP-TES performance for economic and continuous operation and to enable a larger share of renewables. They compared different storage mediums and studied the impact of TES implementation on the system operation, energy

efficiency, and cost-effectiveness. They studied various types of HPs for heat recovery and to exploit their efficiency while using low-grade energy. The performance indicators were TES size, COP, storage capacity, and greenhouse gas emissions.

Takudzwa Muzhanje et al. [89] presented a review of PCM-TES applications for A/C with a focus on PCM heat transfer and potential benefits such as energy savings and COP improvement. Ermel et al. [90] performed a bibliometric analysis of thermal storage with an air source heat pump (ASHP). Gu et al. [91] examined combining PCMs with HPs in applications such as heat storage, defrosting, and renewable energy integration.

Objectives

In this chapter, we reviewed HPs integrated with latent TES to reduce the space conditioning cost, save energy, and shift electric demand in buildings and present a detailed analysis of reported results. The study provides a comparison of active and passive HPs integrated with TES systems and how different configurations influence performance. Although many reviews cover PCMs in buildings, a review has not been published on HP-TES in buildings to present a technoeconomic analysis. This work provides a review of HP-TES with a focus on system configuration, heat exchanger types, charging methods, and available operating modes. The configuration includes TES location with regard to HP components and within the building. This study presents an analysis of the impact on DR, energy consumption, and cost for these systems. The analysis was conducted for three systems:

- An HP without TES, discussing control strategies for demand impact.
- Passive HP-TES connected to an A/C or ventilation system.
- Active HP-TES embedded in or coupled with HP components.

Scope and Organization

This study presents a comparative review of TES in buildings integrated with HPs with a focus on configurations and controls. The impact of various configurations on performance is evaluated for energy, cost, and demand reduction.

The chapter is divided into seven sections.

Section 1 introduces the study, defines the scope and objectives, and highlights the gaps in existing literature. Section 2 provides the background on DR and TES in buildings and provides definitions used in this work.

Section 3 provides a literature review of HP controls for DR and cost savings without TES and an impact analysis of HP-TES configurations. It presents an analysis on passive and active HP-TES configurations by comparing performance metrics (energy savings, cost savings, and demand impact) against the PCM type, temperature, and location in HP-TES. We focused on evaluating plumbing configurations, refrigerant integration, and a hydronic heat exchanger (HX) for TES installation in an HP-TES system.

Section 4 explains the results from the literature review and focuses on comparative research trends on HP-TES in literature. A bibliographic analysis is presented on different PCMs used for heating or cooling HP-TES applications in various climate zones. A historical trend is provided for experimental and simulation studies on HP-TES in various configurations.

Section 5 provides a technoeconomic analysis on active HP-TES configurations, comparing energy, cost, and demand reduction. It further provides a comparative cost and demand analysis (payback period and load shifting) of active and passive HP-TES. Finally, an overall performance analysis of cost savings and load shifting is presented to compare cases with and without TES.

Section 6 provides a discussion and summarizes possible future work. Section 7 summarizes the conclusions of this study.

Background

The power grids around the world are undergoing major changes to address the ever-increasing energy demand and maintain physical and economic stability [92]. The technological advances and flexibility in the design and operation of HPs can allow them to overcome these new load patterns. Modern high-efficiency HPs and appliances can provide some energy savings but do not generally help with demand management and grid stress. Many researchers have used different HP control strategies for DR. Section 2.1 explains these controls to achieve building flexibility.

DR and Building Flexibility

Building energy flexibility, as defined by IEA EBC Annex 67 is "the building ability to manage its demand and generation according to local climate conditions, user needs, and energy network requirements" (IEA EBC Annex 67). The building structure and HVAC system can achieve this flexibility while maintaining the occupants' comfort [56], [57].

The Demand Response ‘D.R.’ can be defined as “changes in electric use by demand-side resources from their normal consumption patterns in response to changes in the price of electricity, or to incentive payments designed to induce lower electricity use at times of high wholesale market prices or when system reliability is jeopardized” [50]

A DR strategy can be designed for load shifting [93], [94]. Many utility providers have a rate schedule that defines peak and off-peak hours of operations. During the high-demand (peak) period, the utility rate is usually higher than the normal (off-peak) hours. Consumers can take advantage of this scenario by load shifting, in which loads are shifted from peak to off-peak hours. Load shifting can also reduce grid stress, providing more flexibility as the energy usage during the high-demand periods decreases [95].

Utility Rate Structures

Several types of utility rate structures may be available depending on the building type and purpose, the availability within the electrical provider and municipality, and the metering capabilities.

The most common and historical utility plan is a flat-rate pricing structure. At all hours and all energy usage levels, the consumer will pay the same price for each unit of energy from the grid. A tiered plan will adjust the price according to the quantity of energy the customer uses, often restarting monthly. Two or more tiers are corresponding to specific electrical usage quantities for which the price of electricity changes in each tier, often increasing the price as the customer uses more energy. All other utility rate tariffs may have tiers.

EPRI [96] in their technical report has divided demand-side management strategies into event-based and non-event-based treatments. An event-based treatment activates in response to certain immediate signals from the environment that are unplanned or unpredictable. A non-event-based treatment may follow a predetermined schedule or be a systematic change to the building and is enacted regardless of the immediate environmental factors.

Examples of event-based treatments related to building energy include a thermostat that monitors ambient weather conditions and adjusts indoor temperature setpoints and humidity, a thermostat equipped with motion sensors that monitor building occupancy and conditions spaces accordingly, building reactions to real-time pricing, and networked electrical plugs that activate in response to specific data such as excess grid supply, low carbon energy sources, or proximity of the user to the building. There are many more event-based treatments. The distinguishing feature is communication between the building and external systems, with the building having some autonomy in its energy usage.

Non-event-based treatments include time-of-use utility pricing in which the electrical energy is priced hourly based on a predetermined schedule, improving building insulation

and thermal capacitance, replacement of appliances with more efficient versions, and occupant-operated changes to the building operation such as seasonal thermostat adjustment. There are many more non-event-based treatments not listed here. These treatments are often conscience decisions of the occupants onto the building which seek to fortify the building's energy efficiency.

Real-time pricing (RTP) is, as the name suggests, electrical pricing at or near the bulk wholesale price. RTP plans can change prices hourly for residential customers or at even greater frequencies for commercial and industrial customers. A variation of the RTP rates is day-ahead pricing where the next day's hourly electrical pricing is determined based on model forecasts of supply, demand, and weather.

Time-of-use (TOU) pricing follows fixed schedules for the duration of the contract. The price is determined for all time periods, often hour blocks, in the year. The electrical price varies with the month, day of the week, hour, and whether it is a holiday. On-peak refers to the hours with the highest daily utility cost, off-peak to the lowest. Some TOU plans may have several levels of pricing suggesting there can be several mid-peaks.

Variable peak-pricing (VPP) follows a schedule throughout the year similar to TOU, however, the utility may adjust the mid-peak or on-peak pricing under certain circumstances. For many residential customers, there may be restrictions on the maximum price, duration, advance notice given, and several instances in which these events occur depending on the governing body overseeing the utility provider. Commercial and industrial customers may have fewer protections and could be subject to more events, unforeseen price changes, or even short-notice power cuts. In some instances, the timing, frequency, and price change may be codified explicitly into the utility agreement.

A non-event treatment such as TOU utility rate is effective even after it is onset, rather than only during critical events, so it can be hypothesized that these treatments can reduce the overall energy use in addition to the usage shift towards targeted times of the day. Real-

time pricing (RTP), and variable peak pricing (VPP) have the characteristics of both kinds of treatments as prices vary according to the supply conditions. [96].

These treatments can reduce the overall energy use in addition to the usage shift toward targeted times of the day [96].

DR strategies and HP controls can provide some cost and demand reductions, which are reviewed in Section 3.1. Meanwhile, TES can decouple the energy generation from its demand and usage and can be a crucial tool to shift the thermal loads. By using TES to store the energy for later use during peak hours, demand management systems can be designed to take advantage of lower utility rates during off-peak hours.

TES in Buildings

Thermal energy storage (TES) is becoming increasingly popular as a tool to level out electrical grid demand and add stability to the grid as more intermittent renewable energy sources are installed. TES systems locally decouple heating or cooling demand from its production.

Thermal energy storage stores high- or low-temperature energy temporarily to be used later [97]. TES systems can be easily incorporated into small to large single-family or multi-family residential buildings and all types of commercial buildings. They are designed to trim the building's electrical demand profile by reducing the energy usage and high demand costs arising from summer cooling and winter heating needs [98].

Major factors influencing an appropriate TES system's choice include the energy storage period and duration, cost and economic feasibility, and operational conditions. The building's thermal load is highly dependent on the weather conditions and the thermal quality of the building envelope. Therefore, improving the heating or cooling systems' efficiency and building thermal quality is essential in conserving the energy and environment [99]. These systems can optimize thermal equipment; they can be an effective and economical replacement of the energy resources on a large scale, thus reducing the

disparity between thermal energy demand and supply. If a system is designed carefully and smartly, it could also cut down the preliminary cost and maintenance expenditures [97].

TES is classified into three types based on the principle of energy storage: sensible, latent, and thermochemical. Sensible storage systems accumulate energy by increasing or decreasing the temperature of the storage media (e.g., salt, water, soil, etc.). The energy by phase transition (e.g., frozen water storage in ice and storing heat by melting paraffin waxes) is stored as latent heat. In thermochemical storage, a chemical reaction is used to store or release energy [99]–[101].

The thermal storage properties can be leveraged by using PCMs to allow conventional HPs to function more during off-peak hours.

For an effective system, the phase change materials (PCM) must perform their phase change at temperatures in the operational range of the designated thermal application. Often, the phase change occurs over a small temperature range, thus these systems are near isothermal in operation. When a PCM melts from a solid to a liquid state, energy is absorbed from the surroundings. Solidification is the opposite of the melting process, where the energy is lost to the surroundings [102].

PCM-TES can behave as a standalone isothermal HX when integrated with an HP and can offer grid flexibility while maintaining an adequate internal temperature for occupant comfort without excessively using HP equipment. The overall load on HVAC can be reduced by storing energy in a PCM, depending on the melting temperature in the phase change process.

For buildings, HVAC systems are needed to maintain a comfortable temperature inside during warmer weather months. However, the temperature for the PCM-based building materials will only tend to increase until it gets to the point of phase change. The incident energy at this point is continually absorbed through the latent heat of fusion while maintaining the same temperature. The load on HVAC could be significantly lowered if this temperature can match the comfortable temperature range of the building. This is

predominantly suitable in the regions with a wide-ranged climate, where heat could be used through the sun during the day, while there will also be cool nights, where heat will be released from the PCM [102].

Generally, two classifications of PCMs are suitable for building systems: organic PCMs and inorganic PCMs. Organic PCMs such as paraffins, have low heat conductivities and are flammable, whereas inorganic PCMs, such as salt hydrates, are relatively inexpensive, are easily synthesized, are nonflammable, and possess high storage capacity and higher thermal conductivity compared with organic PCMs [103].

The application of PCMs in buildings to harness energy could be produced either naturally, such as with seasonal heat and cold, or by artificial means, such as electric heating elements or HPs. Any energy storage system should at least possess the following components:

- Material with the desired phase change temperature range
- HX or storage tank suitable for PCMs

HP-TES Configurations and Definitions

Building integration with TES can be divided into three types: active, passive, and hybrid systems. Active TES systems rely on some mechanical work to transfer heat between the space and the PCM, and the decision of when to charge and discharge is determined by controller hardware. However, for passive TES systems, the heat transfer requires no mechanical work; TES charging and discharging occur according to an uncontrolled independent variable such as ambient temperature and PCM phase change temperature. Hybrid TES can be a combination of either active and passive TES, or an additional system like solar heater is coupled. Figure 3 shows various active and passive TES methods of integrating PCMs into buildings.

PCMs in passive TES are incorporated into the building envelope and are thermally coupled directly with the space to be conditioned.

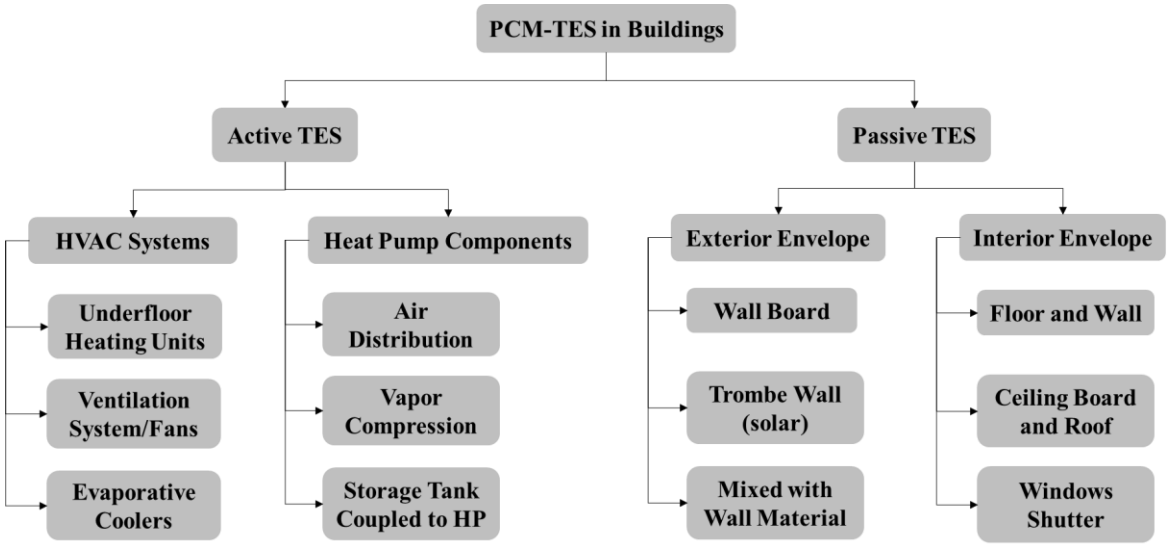


Figure 3:PCM-TES in active and passive storage

PCMs can be in exterior building walls, separating conditioned from unconditioned spaces, or in interior walls, separating two conditioned spaces. PCMs could also be mixed with building wall materials, such as concrete or gypsum, either directly or with encapsulation [66], [70], [75], [79], [104], [105]. PCMs in active TES are integrated into HP components or coupled with the building's heating, cooling, or ventilation system. The TES may also be separated and removed from the space via standalone HX. Active HP-TES allows real-time control over when the TES is charged and discharged. One advantage of active configurations is the ability to add TES to existing building infrastructure without significant construction. Active HP integrated configurations can be further categorized as direct and indirect configurations depending on the heat transfer control mechanism. Detailed definitions of these terms are provided in Table 2.

Literature Review

Researchers have investigated DR management systems with price- or demand-based control strategies for cost and peak demand reduction without using TES. To provide a comparison of cases with and without TES, Section 3.1 presents a literature review on cost savings and peak load shifting without TES, and Section 3.2 discusses HP-TES configurations.

Controls for HPs without TES

The impact of time-based utility pricing on residential electricity use with different load and demand control strategies has been investigated [106]. The results suggested that the A/C cost and peak demands in buildings can be reduced, depending on utility rate structure, weather, building occupancy and thermal capacitance, and characteristics of the cooling system [107].

A few models with no thermal storage have been developed for diurnal load shift by preconditioning the building at night. Rabl and Norford [108] developed a model to reduce summer peak load in buildings by preconditioning the preceding night.

Table 2: Definitions of active, passive, direct, and indirect TES configurations

HP-TES configuration	Definition
Passive HP-TES	TES charging and discharging occur according to an uncontrolled independent variable such as ambient temperature and PCM phase change temperature. HP is indirectly used by overheating or cooling buildings
Active HP-TES	TES is directly or indirectly coupled with HP and the decision of when to charge and discharge is determined by controller hardware
Direct HP-TES	Heat is exchanged directly between the TES and the conditioned space. TES is directly used to heat or cool the building
Indirect HP-TES	An HP mediates all heat exchanges between the TES and the conditioned space. The TES and conditioned space thus do not directly exchange heat. TES is used as heat sink or heat source of HP

A building model based on internal load, temperature, and solar data was developed and integrated with dynamic thermostat control strategies. The researchers, however, lacked data to predict the amount of peak load that could be shifted [108]. A dynamic building control strategy to reduce the A/C cost and peak demands in buildings was also investigated [107]. The state of the building's thermal storage was controlled by varying building zone temperatures over time within the comfort region. The cooling load was shifted from daytime to nighttime to utilize low utility rates and reduce the peak demand. The reduced cost was found to be a function of utility rate structure, weather, building occupancy and thermal capacitance, and cooling system characteristics [107].

Researchers have achieved building flexibility and reported energy and cost savings by developing a dynamic control model for HPs and buildings without using TES. Gottwalt et al. [109] presented a model to generate the load profile of a house under flat tariffs and simulated the varying profiles using TOU tariffs with smart appliances to investigate the impact on utility bills. Besides heat pumps for space heating, they used a variety of appliances including kitchen appliances, water heaters, and washing and drying appliances. The simulations were carried out in reference to the households in Germany and they concluded that except for the heating devices like water heaters and heat pumps, the economic benefit of investing in other smart appliances is low. They recommended that for the U.S. households, with a majority using electric water and space heating, the economic benefit will be promising. The air conditioning was not included in the study because of less relevancy to German households either and is recommended for the U.S. case study. Since, TOU tariffs could create new demand peaks, building flexibility can be achieved no matter the appliance or region, and the utilities can balance the demand and supply since they need a large hourly load to be shifted. TOU tariffs could achieve grid and building flexibility by creating new demand peaks regardless of the appliance or region.

Vrettos et al. [110] investigated the residential buildings' response to three price signals; day-night tariff, day-ahead dynamic tariff, real-time dynamic tariff. DR was evaluated for five appliances, including HPs. They demonstrated that most of the energy

shifting potential could be achieved by a price step with a duration of up to two hours. The building was more responsive to the known price signals such as day-ahead tariffs.

Yoon et al. [111], and [112] modeled a demand response controller (DRC) for homes in Austin, Texas, based on historical real-time data for the Electricity Reliability Council of Texas (ERCOT). They demonstrated that, depending on the house's size and utility price structure, up to 24.7% of HVAC peak demand loads can be reduced, reducing annual electricity consumption by 4.3% and providing up to 10.8% cost savings while maintaining occupant thermal comfort.

Schibuola et al. [113] simulated HP control based on real-time pricing, using three control strategies for DR, and showed up to 30% savings in electricity consumption cost. The HP was integrated into the smart grid and coupled to water heater. The system was simulated in EnergyPlus, and an 18% efficient PV panel was used for on-site energy generation. They demonstrated better performance for the control strategy that forces the HP to turn on when the PV system generates electricity.

Farrokhifar et al. [114] investigated the energy usage of 15 appliances in the building and recommended that HPs could be investigated to provide better energy management. The appliances were classified into two categories, non-programmable appliances such as T.V., computer, lights, etc., and smart appliances like the dishwasher to respond to the fluctuating time prices by programming their time of operation. They presented an energy management system with reduced electric consumption costs, based on real-time pricing, and preventing the high peak demands. All appliances were investigated for total building energy usage and studied with five cases based on different energy-cost ratios and compared by varying the number of peak hours, peak demand charge, and the run-time and energy usage of appliances. The maximum cost saved was 22.4% in case 5, where double-peaked tariff has been considered and the energy-cost ratio was 0.48.

Romero Rodríguez et al. [115] evaluated the energy consumption and cost for an HP using dynamic pricing and benefitting from the building’s thermal mass. They reduced the

peak time usage of heat pumps and reported 25% cost savings using optimal strategies. The building became overheated because dynamic pricing control caused infrequent activation of the HP.

Arabzadeh et al. [116] developed a predictive cost-optimal DR control for HPs in residential buildings with on-site, roof-integrated PV energy generation under cold climate conditions. The model predicts a building's heat demand one day ahead, which is implemented to optimize the grid electrical energy consumption. The excess energy generated by PV was sold back to the grid.

Table 3 summarizes the cost savings and demand impact for systems without TES, using various demand and price control strategies.

The role of HPs and TES was also investigated for load shifting and demand-side management [94]. TES was coupled with an HP with radiators or underfloor heating to study the impact on thermal comfort. With the HP turned off during peak hours, the electricity bill was reduced without compromising comfort, but no significant demand reduction was reported.

Ali et al. [118] evaluated the DR potential of residential HVAC loads. They maintained that value can be added by supporting the HVAC system with even a small TES system. In a study to investigate the DR impact on thermal comfort and cost in a residential building with an electric HP, 10% energy cost savings were reported using a predictive control strategy [119], and 12% of energy was saved in addition to the cost savings when a hot water storage tank was coupled with an HP with the predictive DR control [120].

The DR control strategies without TES can reduce the overall cost but cannot provide energy savings, so the demand impact is not comparable to the grid flexibility provided by HP-TES. When properly controlled, thermal storage can be useful in an economic or behavioral curtailment scenario for DR. The DR control and TES together offer more stability and grid benefits, as discussed in the upcoming sections.

Table 3: Demand management without TES

Reference	Control strategy	Tariff	Appliance	Cost savings	Demand impact
[109]	Dynamic building control	Day-ahead hourly TOU	HP (heating) and water heater	Not reported	Hourly load shift
[110]	Dynamic building control	Day-night tariff, day-ahead dynamic tariff, real-time tariff	Five appliances, including an HP	Not reported	2 h of load shifted
[113]	Dynamic price control	RTP	HP (heating and cooling) with a smart grid, coupled with a water heater	30%	Not reported
[114]	Dynamic price control	RTP, TOU	15 appliances	22.4%	Peak load shift
[115]	DR control	Dynamic electricity pricing	HP coupled with the building's thermal mass	25%	HP did not operate during peak hours
[116]	Predictive DR control	Dynamic electricity pricing	HP (heating) and on-site PV energy generation	12% with predictive control, 43% with on-site PV	24% less energy consumed due to PV
[117]	Precooling for various climates	Predefined peak times from TOU rates	Low thermal mass building with HVAC	Not reported	50%–75% peak load shifted
[111]	Dynamic price control	RTP	HVAC (cooling)	12%	24.7% HVAC cooling load reduced

HP-TES Configurations

PCM-TES can be integrated with HPs via various configurations, as shown in Figure 4. Passive configurations (shown as ovals in Figure 4) are integrated in the building envelope. Active configurations (shown as horizontal cylinders in Figure 4) are integrated in HP components or an HX coupled with an HP. Some locations in the building envelope provide both possibilities, so PCMs can be directly embedded in ceiling, wall, or floor via passive storage and installed via active storage in an HX placed at these locations.

The research on passive HP-TES and active HP-TES configurations is reviewed in this section. This section discusses different configurations investigated in the literature. Based on PCM type and configuration and on price- and demand-based controls, these performance metrics are summarized:

- Energy savings (energy, COP, power, and load reduction)
- Cost savings (daily/annual cost and payback period)
- Demand impact (load shift, instantaneous power during peak, and demand reduction)

Passive HP-TES

Various passive storage configurations have been investigated in literature. PCMs can be coupled with a ventilation system or standalone cooling or heating systems via passive storage [121]–[123]. This section discusses HP-coupled passive configurations in which PCMs are integrated in the attic [124], [125], floor [126], [127], internal building envelope [128], [129], wallboard [130], [131], frame wall [132], or window [133] for load shifting and energy and cost savings. The performance of passive TES is highly dependent on the occupant's choice of indoor set point temperature, and passive TES does not have controllable parameter that can be manipulated in real time by a controller.

Numerous studies have demonstrated energy savings using free cooling or heating to charge PCMs, usually overnight, and passively blocking thermal loads.

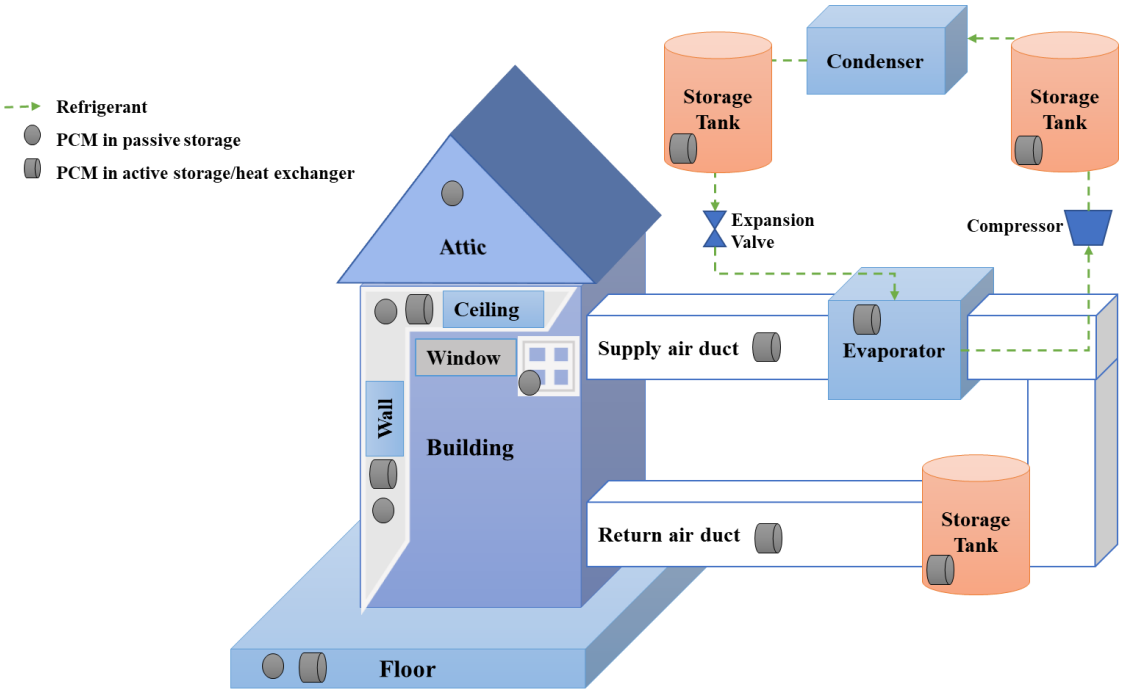


Figure 4: Possible configurations for PCMs integrated in a building

Halford et al. [124] shifted the peak A/C cooling load using a salt PCM perlite mixture with a melting temperature range of 28°C–40°C. The PCM melting temperature varied relative to the ambient temperature. The material and temperature were selected to change the phase during peak times of the day by absorbing heat from the ambient and releasing it later when the temperature lowers or A/C causes the solidification. The material was stored in the attic in two layers of insulation. The developed model was based on a simple geometry with many simplified assumptions to explore the approximate value of the resistive, capacitive, resistive configuration. The simulation results were compared against varying heat flow without the PCM application as an insulation-only baseline in which the heat transfer takes place through the resistive wall.

Barzin et al. [126] and Devaux et al. [134] used underfloor heating systems in combination with natural solar irradiation to charge PCMs for heating. Though significant savings per day and per week were achieved, the indoor comfort was compromised often because of overheating. Plytaria et al. [127] combined a solar collector and PV system with a water-to-water HP, and an underfloor heating system contained PCMs. A storage tank was also used for hot water, which provided convective heating.

Kosny et al. [125] modeled a passive attic insulation and compared two configurations using a 30% condensed and a 90% dispersed paraffin PCM layer. The melting temperature range was 22°C–27°C, and the freezing range was 20°C–26°C. The model was complex and was analyzed in detail, and the building model considered internal gains and construction material properties. The configuration with the condensed PCMs performed better than the other. Within that configuration, PCM locations were also analyzed, and the PCMs installed on the bottom of the attic floor insulation yielded the best results with the 13 mm PCM layer.

Tables 4, 5, and 6 summarize the configuration and impact analysis of passive TES systems coupled with the conventional HP or A/C system. Tables 4 and 5 describe the cooling-only and heating-only cases, respectively. Table 6 provides information on both heating and cooling cases.

Table 4: Passive TES configurations with cooling only

	Study parameters					Study outcomes		
Source	**PCM type & phase change temperature**	**PCM location**	**Climate & study approach**	**Notes**	**Charging method**	**Energy savings**	**Demand impact**	**Cost savings**
[124]	Salt PCM perlite mixture	In attic	Simulation Las Vegas, Nevada, United States	Peak load shift	PCM stores heat from ambient during peak times to solidify later	Not reported	19%–57% peak load reduced	Not reported
[129]	Bio PCM (23°C)	In walls to enhance envelope of air-conditioned building	Simulation, Termoli, Italy	Retrofit to reduce cooling demand, no tariff reported	Night convective cooling. PCM prevents overheating	Summer energy consumption reduced by 11.7%	HVAC load reduced by 6.1%	30 year payback period

Table 5: Passive TES configurations with heating only

	Study parameters					Study outcomes		
Source	**PCM type & phase change temperature**	**PCM location**	**Climate & study approach**	**Notes**	**Charging method**	**Energy savings**	**Demand impact**	**Cost savings**
[126]	Paraffin (28°C)	In wallboard with underfloor heating	Experiment, Auckland, New Zealand	Price-based control	PCM charged during the night using underfloor heating and an A/C unit	44.4% energy savings per day	3–4 h of peak load shifted	35% cost savings per day
[127]	Bio PCM Q29 (29°C)	In an underfloor heating system	Simulation, Athens, Greece	Hybrid system	Solar-assisted HP and underfloor system used for charging	42%–67% electricity savings (winter)	Heating demand reduced by 40%	9.61–22.06 year payback
[130]	Fatty acids (21°C–22°C)	In wall (direct solar gain)	Experiment, Helsinki, Finland, and Madison, Wisconsin, United States	Diurnal load shifting	Passive solar gain	5%–20% energy savings	Not reported	Not reported
[131]	Ammonium chloride (21.7°C)	In DuPont wallboard	Experiment Auckland, New Zealand	Price-based control	PCM charged using solar heat gains	60% energy savings per day	5 h of peak load shifted	62.64 % cost savings per day

Table 5 Continued

[132]	7 PCMs (3°C–20°C)	In frame wall of an air-conditioned building	Simulation, Jeddah, Saudi Arabia	Effect on air handling unit energy usage	PCM wall stores heat from solar radiations, energy losses minimized	10%–11.2% energy savings	Air handling unit power usage decreased by 11.73%	18.6 year payback
[134]	PCM gypsum board (27°C–29°C)	In wall, ceiling, and an underfloor heating system	Experiment and simulation, Auckland, New Zealand	10 day period analyzed	Combined solar and underfloor heating to charge PCMs	32% energy savings	2.5%–9% peak load shifted	42% cost savings per week

Table 6: Passive TES configurations with both heating and cooling

	Study parameters					Study outcomes		
Source	**PCM type & phase change temperature**	**PCM location**	**Climate & study approach**	**Notes**	**Charging method**	**Energy savings**	**Demand impact**	**Cost savings**
[125]	Paraffin (cooling: 22°C–27°C; heating: 20°C–26°C)	In attic insulation	Simulation, Phoenix, Arizona, United States	Dynamic load shift	Passive cooling and heating depending on ambient	3.6%–6.2% heating and 3.1%–5.6% cooling load savings annually	Reduced peak load by 25%–35%	Not reported
[128]	Bio PCM (29°C)	In building envelope (ceiling, floor, wall)	Simulation, Tempe, Arizona, United States	Peak load shift	PCM melts or solidifies based on ambient	9%–30% energy savings	1 h of peak load shifted	10%–30% cost savings
[133]	Paraffin wax (16°C–23°C)	In ventilated window	Simulation, New York, United States	Demand control strategies	Preheating and precooling through ventilation	Energy savings of 10.1%–12% in summer and 26.6%–32.8% in winter	Demand-based savings of 14.7% in summer, 30.4% in winter	Not reported
[135]	n-paraffin (20°C–30°C)	In frame wall of air-conditioned building	Experiment, Lawrence, Kansas, United States	Peak load shift	PCM charged using ambient temperature and diurnal swing	8.6%–10.8% cooling load reduced	Peak load shifted, spread over 13 h	Not reported

Figure 5 shows the locations of different passive HP-TES systems in building, as reported in literature. All of these are embedded in the interior or exterior envelope of the building.

The energy and cost saving benefits are more prominent for heating-only systems than for cooling-only systems. Most of the heating systems use solar heat gains passively to charge the PCM, and the diurnal temperature difference works in the building's favor to discharge PCM at night, simultaneously shifting the demand to off-peak hours. In the cooling-only case, for the free or passive cooling, the building's thermal capacity is enhanced. PCMs store the solar heat during the day that otherwise would be accumulated by the building and solidify when the ambient temperature drops. Such systems do not necessarily provide A/C and depend on ambient temperature, solar radiation, and diurnal temperature swing range. An additional system is required to control and charge the PCMs to achieve significant savings.

For both systems, indoor comfort is often compromised, and combined annual benefits are not as promising as for heating-only systems. Thus, the payback period for most systems is more than 10 years.

Active HP-TES

Ideally, passive TES configurations can offset the peak demand by shifting loads. However, they cannot control the charging or discharging operation to optimize grid benefits. Active HP-TES configurations offer a high level of control of indoor conditions and improve heat energy storage [23] by allowing real-time charging and discharging for grid-interactive operation.

We categorized active TES configurations into three types based on PCM location and integration, and each type is addressed in the following sections. The three types are as follows:

1. Building envelope integration
2. Air distribution system

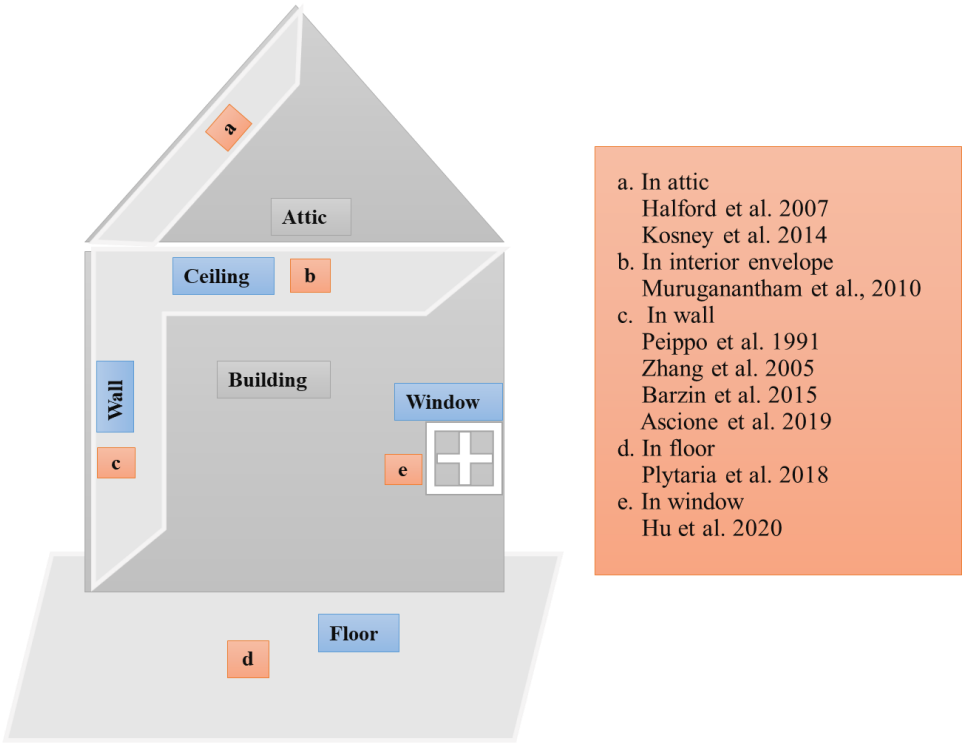


Figure 5: Passive storage locations in the building.

3. Vapor compression system (VCS): load side and source side

Building Envelope

Few studies have examined active configurations in the building envelope. In these studies, PCMs are installed in an HX coupled with an HP or HVAC unit.

Mazo [46] developed a model to simulate a PCM radiant floor system coupled with an HP that operates during the night to supply hot water to the system. The stored energy is discharged during the day to shift the electric energy consumption from peak hours.

Kondo [136] enhanced a PCM ceiling board to reduce the air handling unit (AHU) load for A/C using peak shaving controls. The cold air from the AHU passes through the ceiling chamber, charging the PCM overnight using a less expensive nighttime tariff. The stored cooling energy is then used to precool the return air during peak hours, thus reducing the thermal load.

Zhu et al. [137] studied the influence of different demand-limiting control strategies on energy consumption and electricity cost of air-conditioned buildings using PCMs in the wall to enhance the envelope of the air-conditioned PCM building. They developed and used two control strategies for load shifting and demand management. The load-shifting strategy reduced energy consumption by using off-peak electricity to store the cooling energy, and the demand management strategy reduced the peak demand by resetting the temperature set point. The PCMs were precooled during the off-peak period and discharged during peak hours.

Air Distribution

PCMs can be installed in the supply or return air distribution loop, which is the most used configuration in HP-TES literature. Notable studies are described in this section; others are covered in Tables 6, 7, and 8.

Yamaha and Misaki [138] evaluated peak shaving using PCM-based storage equipped with an air distribution system for cooling. The A/C was turned off during peak hours, and

the stored energy was discharged through night-cooled PCMs. The paraffin-based PCMs with a 19°C melting temperature maintained the comfort level during the discharge period.

Tyagi et al. [139] assessed the thermal performance and economic evaluation of PCM encapsulated in thermal management systems equipped with A/C to reduce the cooling peak demand by offsetting the peak period cooling energy. The proposed system was tested in India's hot climate by discharging at three different heat loads. The study suggests that the system can be economical and efficient in hot and humid areas around the world.

Chaiyat [140] and Chaiyat and Kiatsiriroat [141] improved the cooling efficiency of a conventional HVAC system using PCM-TES for the climatic conditions of Thailand. The PCM was solidified during the night by the cold air from the HP. During the day, return air from the room was passed through the PCM, liquifying it and reducing the cooling load at the evaporator.

Vapor Compression System

PCMs can be installed in or coupled with HP components of the VCS (i.e., compressor, evaporator, and condenser). Some studies are described in this section, and others are summarized in Tables 7, 8, and 9.

PCMs in a chiller were investigated by Bruno et al. [142]; energy savings were achieved by using PCMs for off-peak cooling. The cooling energy was provided through the chiller to the PCMs for solidification or to the building during off-peak hours. Although about 85% of the cooling energy could be offset using an ice-based system, the overall energy demand increased by 7.6% because of the exergy loss by using TES. A PCM with a 10°C melting temperature could save 13% energy. The authors suggested optimizing the charging time and duration depending on the outside temperature to minimize energy consumption.

Many researchers have used PCMs in one or two storage tanks for heat and cold dissipation [143], [44], [144]–[146]. Real et al. [143] used PCMs to enhance HP performance using two thermal tanks for cold and hot storage. A cold tank was used to cool

the PCMs at night, and the other tank acted as an alternative hot reservoir to increase system flexibility. This system was efficient because the COP did not depend on the outside temperature. In total, 18.97% energy savings were achieved; however, the system must be verified in real conditions because this was a Solar Decathlon project. Moreno et al. [147] also integrated two storage tanks into the evaporator of an HP. The HP was turned off during the day and was operated at night to charge the PCMs.

Mosaffa et al. [44] used a combination of PCM TES coupled with a refrigeration system for A/C and performed experiments for cooling analysis and peak load shifting. Air was cooled by a PCM during the day, and the heat was extracted from the thermal storage through A/C at night. Three different PCMs were used: RT27, S27, and SP25. The system with S27 had the lowest cost, and the one with SP25 reported the highest COP of 3.434.

Jaber et al. [144] coupled PCMs in an HX with the indirect evaporative cooling system. The PCMs only provided for 80% of the cooling demand, but the cost was reduced.

Long et al. [145] and Zou et al. [146] used an HX coupled with the compressor. Long et al. [145] developed an ASHP water heater with PCMs and used fin-type HXs to improve the heat transfer because the paraffin PCMs had a slow heat transfer rate. During off-peak hours, the refrigerant absorbed heat through an evaporator at the air side and released the heat to the PCMs through a condenser. The PCMs solidified during peak hours, and the heat from the PCMs was used for water heating. The space requirements for a water tank were eliminated with this system. Zou et al. [146] improved the heat capacity and COP of an ASHP water heater with a PCM integrated water storage tank. The heat transfer was improved using fin-type HXs for PCM installation, and the condenser was coated with PCMs to increase the heat transfer area.

Dong et al. [3] improved the efficiency of a PCM TES integrated with an electric HP and enabled grid-responsive HP control. They used a novel PCM integration employing indirect use of PCMs mediated by an HP, and TES indirectly provided conditioning

through an HP during discharge by improving its COP (Figure 6) instead of commonly used configurations in which PCMs directly exchange heat with the building.

Tables 7, 8, and 9 summarize the configuration and impact analyses of active TES systems coupled with conventional HPs or A/C systems. Tables 7 and 8 summarize systems that address cooling only and heating only, respectively. Table 9 provides information on both heating and cooling cases.

Figure 7 shows the locations of active HP-TES systems in building as reported in literature. Active HP-TES are coupled to building or HP components via HX or storage tank.

A notable experimental study by Gohar and Farid [148] compared the thermal performance of passive and active TES systems and confirmed that PCM in active HP-TES can be easily installed or removed from a standalone storage tank without modifying the construction. Two experimental huts were designed with controls to evaluate energy savings and load shifting potential. An A/C unit, a solar heater, and an electric heater provided necessary heating and cooling for the base case in both huts. The PCMs in wallboards were installed in walls, floor, ceiling, and attic for passive heating through solar or free night cooling. For the active system, the PCM storage unit was installed, and PCMs were charged by circulating indoor return air through the storage unit during off-peak hours. The active system was more feasible for heating application during winters, consuming 22% less energy than the passive system and reducing 32% electricity cost due to load shifting. The authors argued that the passive storage can have environmental problems because detaching the PCMs from the building construction material at the end of the building's life is difficult.

In summary, the literature confirms that significant heating and cooling costs can be saved, and grid flexibility can be achieved by using an active HP-TES system. The flexibility to install PCMs in active storage and control the operation provides greater energy and demand savings and cost benefits as compared with passive HP-TES.

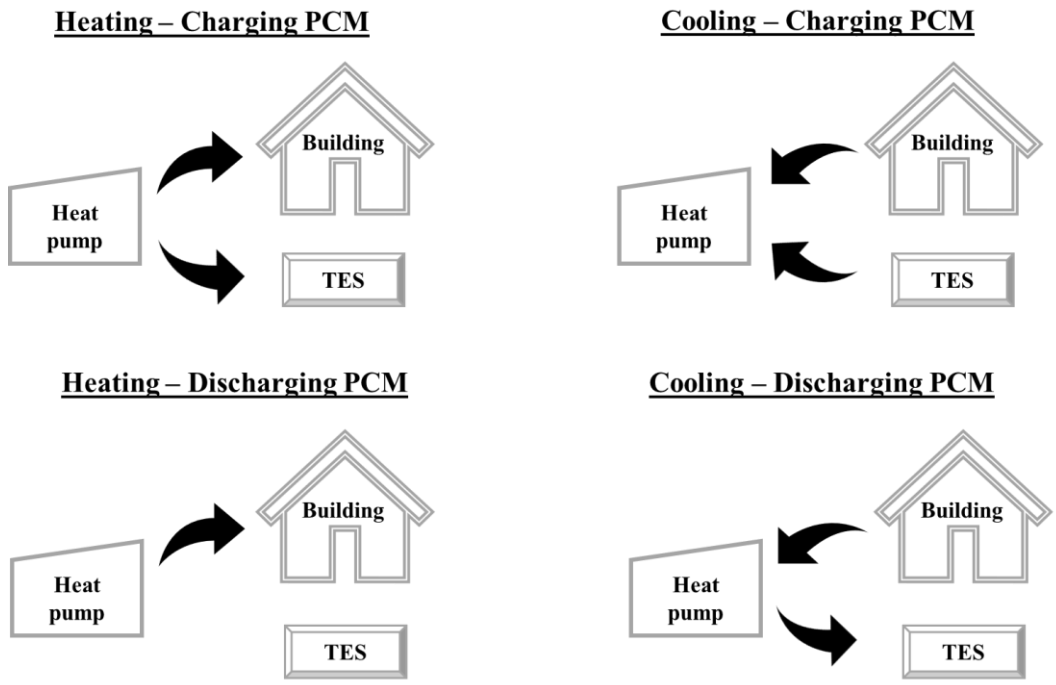


Figure 6: Indirect PCM-integrated HVAC configuration

Table 7: Active PCM configurations with cooling only

	Study parameters					Study outcomes		
Source	**PCM type & phase change temperature**	**PCM location**	**Climate & study approach**	**Notes**	**Charging method**	**Energy savings**	**Demand impact**	**Cost savings**
[136]	Microcapsulate (25°C)	In ceiling board coupled with the AHU	Simulation, Tokyo, Japan	Peak shaving	PCM charged overnight using AHU	9.4% load reduction	Not reported	Not reported
[137]	Paraffin and polyethene (23°C)	In walls to enhance envelope of air-conditioned PCM building	Simulation, Hong Kong, and Beijing, China	Demand-based pricing	PCM precooled during off-peak hours using A/C system	Daily electricity consumption reduced by 10%	17%–20% peak demand reduction	11% cost savings
[140]	RT20 paraffin (20°C)	In return air duct coupled with the evaporator	Experiment, Thailand	TOU tariff	Supply air from evaporator used to solidify PCMs during off-peak period	Cooling load decreased by 3.09 kWh/day, 9% energy savings	3 h load shifted to off-peak hours	9.1% cost savings, 4.15 year payback
[44]	RT27 (27°C), S27 (27°C), S25 (25°C)	In storage tank coupled with the vapor type compressor of a HP	Simulation, Tehran, Iran	Peak cooling load shifting	PCMs solidified using air conditioner during off-peak hours	7%–9% energy savings	Not reported	Not reported

Table 7 Continued

[144]	Commercial salt hydrates (14°C–26°C)	In HX coupled with indirect evaporative cooling	Simulation, Jordan	Utility tariff of Jordan	Energy stored when there is no cooling demand	Not reported	Not reported	7.8 year payback
[3]	Ice/water	In HX coupled to VCS of HP	Simulation, Knoxville, Tennessee, United States	TOU utility tariff for cooling load shifting	Subcooler used to melt ice	13% less power consumed	12.7% peak load shifted*	19% electricity cost savings
[149]	35% paraffin GR25 composite	Under floorboard in the supply A/C system	Simulation, various climate zones in Japan	Analysis for eight cities in Japan to reduce ventilation load	PCMs solidified during night using the cool air from the AHU supplied through the PCM bed rather than vents	Not reported	Ventilation load reduced by 62.8%	Not reported
[150]	Paraffin (20°C)	In supply air duct of the underfloor ventilation system	Experiment, Sapporo, Japan	Night load shift	Cool air circulated through the duct to charge PCMs at night	Not reported	89% cooling load shifted	10 year payback
[151]	Ice/water	In ice storage coupled with the chiller	Simulation, offices in various US climate zones	DR assessment tool and peak load shifted	Chiller makes the ice during off-peak hours	Energy consumption slightly increased for off-peak hours	39% maximum peak energy savings	35% annual cost savings

Table 7 Continued

[152]	Ice/water	In storage tank used as an evaporator	Simulation, Ahwaz, Iran	Demand analysis not conducted	Energy from the evaporator used to make ice during off-peak hours	Energy consumption reduced by 9%	Not reported	3.4 year payback
[42]	Ice and salt hydrate (0°C), S4 (4°C), S10 (10°C)	In HX coupled with a chiller	Simulation, Adelaide, Australia	Off-peak cooling	Chiller provides cooling to PCM during off-peak hours	13% cooling energy savings	Peak electricity consumption reduced by 36.6%	Not reported
[153]	RT20 (20°C), RT25 (25°C), RT27 (27°C)	In fresh air-cooling system with a chiller and coil	Simulation, various climates	Night precooling	Chiller used to store cold energy during nonworking hours	7%–41% energy savings	Not reported	Not reported
[40]	Salt hydrate PCM 18T (18°C)	In storage tank coupled with an ASHP	Simulation and experiment, Australia	Demand tariff and usage	Return air from room passes through PCMs before entering the evaporator; COP increased	Energy consumption reduced by 7%–14%	Half-hourly peak demand reduced by 10%–32%	7%–14% with usage tariff, 13%–14% with demand tariff; 10 –year payback
[41]	RT11HC organic PCM (10°C–12°C)	In storage tanks coupled with HPs and water pumps	Simulation, Fuzhou, China	Demand tariff	HP cools water and directs it to storage tank to solidify PCM	Electricity consumption reduced by 1.17%–2.47%	9.07%–11.28% peak demand charges reduced	Not reported

Table 7 Continued

[39]	Slurry ice	Embedded in the condenser of a personal A/C device	Simulation, various US climate zones	Various building types, old (pre-1980) and new (post-2004)	Refrigerant from compressor used to solidify PCMs in air-to-refrigerant HX	Cooling energy savings of 7%–11% for new office buildings, 6%–15% for new apartments	10%–70% energy savings during peak hours with adjusted thermostat settings	Up to $3,000 cash savings depending on location
[154]	Ice	In storage tank as a condenser or evaporator	Simulation, California, United States	TOU tariff (1 week analysis)	PCMs used as evaporator for charging; COP improved	14.5% electricity consumption reduced	Peak energy consumption reduced by 87.5%	20% cost savings per week
[38]	PureTemp (15°C)	In supply air duct of an A/C system	Experiment, El Paso, Tempe, and Houston, United States	TOU tariff	Cold supply air solidifies PCM during off-peak hours	Slightly more energy consumed for charging	Peak energy consumption reduced by 20%–25%	9.6%–14.5% cost savings, 4.3-year payback

*Calculated from the data available in paper

Table 8: Active PCM configurations with heating only

	Study parameters					Study outcomes		
Source	**PCM type & phase change temperature**	**PCM location**	**Climate & study approach**	**Notes**	**Charging method**	**Energy savings**	**Demand impact**	**Cost savings**
[46]	Composite PCM (27°C)	In radiant floor system coupled with an HP	Simulation, Córdoba, Spain	Spanish legislation for peak utility pricing	PCM floor system stores heat from HP during night	No significant energy savings using PCMs (0.76%)	1 h load shifted per day	17.9% cost savings
[155]	$CaCl_2.6H_2O$ (28°C)	Coupled with solar-assisted HP	Experiment, Trabzon, Turkey	Building heat load and HP COP calculated	Hot water from solar collectors used to melt PCMs	12,056 kW energy saved each season	Not reported	Not reported
[47]	Composite PCM	Integrated with an HP via a condenser storage tank	Simulation, United Kingdom	Peak clipping, condenser energy transfer to PCM	Ground source heat pump used to charge PCMs during off-peak hours	Not reported	6 h load shift	Not reported
[48]	Sodium acetate trihydrate (58°C)	In storage tank coupled with a condenser and electric heater	Simulation, Stockholm, Sweden	Off-peak charging and various configurations	HP condenser used to charge PCMs during off-peak hours	Heating load increased with off-peak charging	3–6 h of peak load shifted	15 –year payback period
[156]	ATS 30 (28°C–33°C)	In supply air system of an HP	Simulation and experiment, Denmark	Three cases with varying heating set points	PCMs charged by warm air of HP at lower rates of electricity	6.7% energy consumption reduced compared with no-PCM case	Not reported	7% utility cost savings, 7 –year payback

Table 9: Active PCM configurations with both heating and cooling

	Study parameters					Study outcomes		
Source	**PCM type & phase change temperature**	**PCM location**	**Climate & study approach**	**Notes**	**Study approach**	**Energy savings**	**Demand impact**	**Cost savings**
[143]	S10 (10°C), S27 (27°C)	In two storage tanks (hot and cold) coupled with HVAC	Simulation, Madrid, Spain	Solar Decathlon project, additional storage tank	Cooling energy stored in cold tank at night using HVAC system; waste heat stored in hot tank at high ambient temperature	18.97% energy savings	Not reported	Not reported
[45]	PureTemp 18 (18°C) hybrid system	In HX coupled with the return water loop of an air-water HP	Simulation, Copenhagen, Denmark	Demand analysis not conducted	PCMs charged during the night using forced air convection with ambient cold air	67% energy savings	Not reported	Not reported
[157]	RT25HC (22°C–26°C)	Air-PCM storage coupled with A/C and solar heater	Experiment, Auckland, New Zealand	Solar and electric heaters	Cooled or heated indoor air passed through PCM storage for charging	Energy savings of 10.3%–40% for heating, 10%–30% for cooling	Not reported	Not reported

Table 9 Continued

[37]	RT25HC (22°C–26°C)	Air-PCM storage coupled with an HP and solar heater	Experiment, Auckland, New Zealand	Price-based control	PCMs stored energy during peak hours from an HP and/or solar (heating) or ambient (night cooling)	47% daily savings in winter, 23% daily savings in summer	Heating and cooling peak loads shifted	65% in winter, 42% in summer

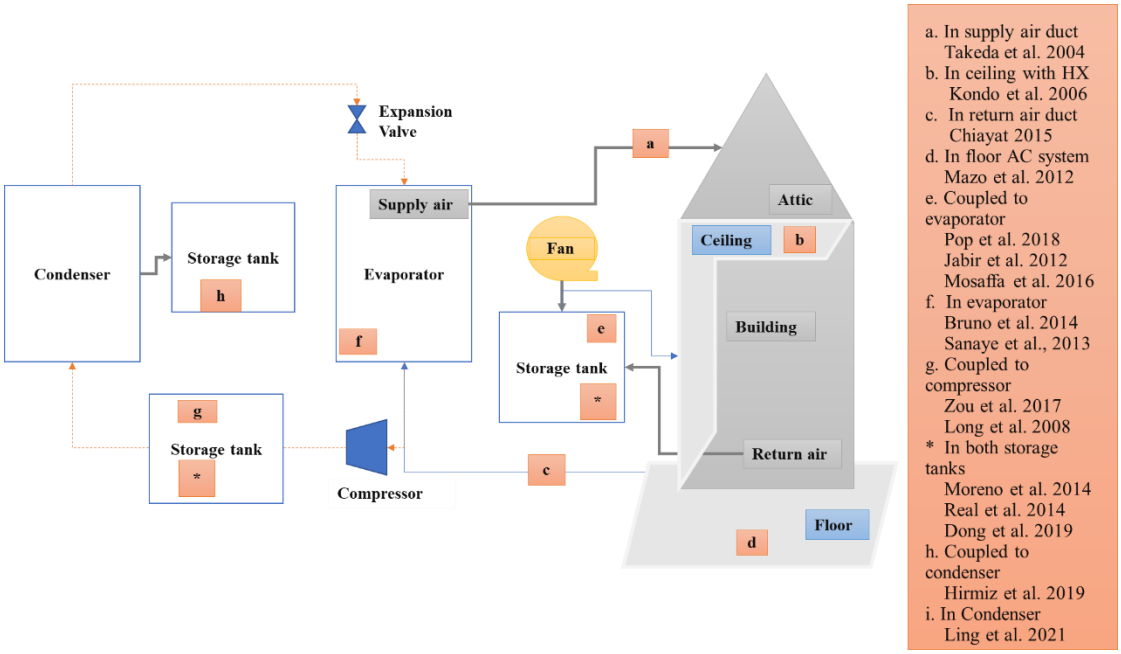


Figure 7: Active storage locations in the building and HP components

Active HP-TES is more financially viable in regions that have higher electricity prices during peak hours and where cooling systems dominate the demand.

Comparative Research Trends

This section presents an overview of results from literature to compare PCM type and temperature, TES applications, HP-TES configuration, and climate zone for different studies. A historical trend and bibliographic analysis are presented for PCMs and configurations of HP-TES in various climate zones.

HP-TES Research

Figure 8 shows a historical trend of research conducted on ice or PCM based HP-TES in the past 30 years. The technology has garnered more attention since the past decade.

HP-TES can be installed in the building envelope, air distribution loops, or VCS itself. For active HP-TES installed in the building envelope, an HX is used and coupled with an AHU [136]. In the VCS, the TES is directly installed in the condenser, evaporator, or both, or the TES is coupled via a standalone storage tank [42], [158]. Besides the building envelope for passive TES systems, air distribution has been the most used configuration in active TES in which PCMs are installed in the supply or return air ducts or the water loop [141], [38].

PCMs for HP-TES

Figure 9 compares the different PCMs used in simulation and experimental studies. Paraffins are the most commonly investigated PCMs by far. Salt hydrates are gaining more attention recently because they are inexpensive, are easily available, and offer wide range of temperatures. A detailed analysis of PCMs for HP-TES is provided in another review [20].

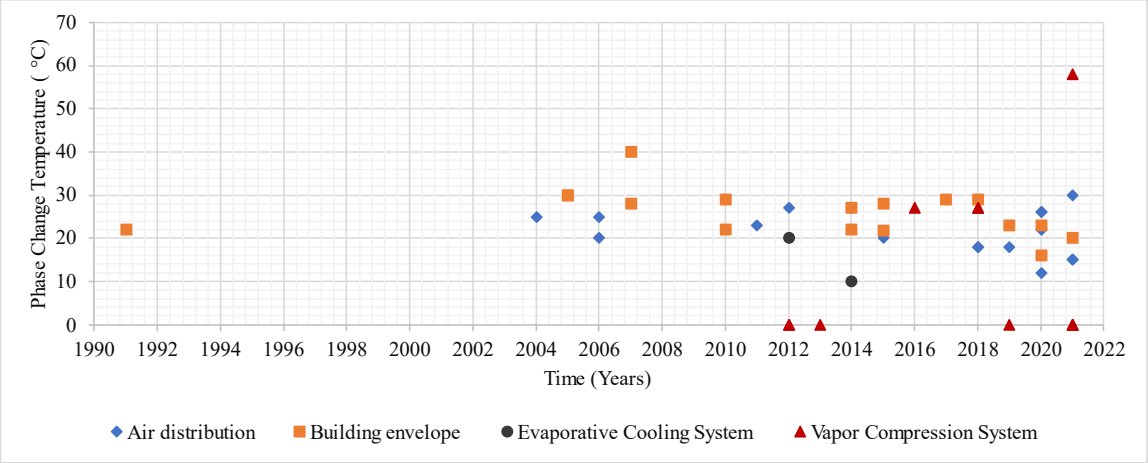


Figure 8: Historical trend of HP-TES research

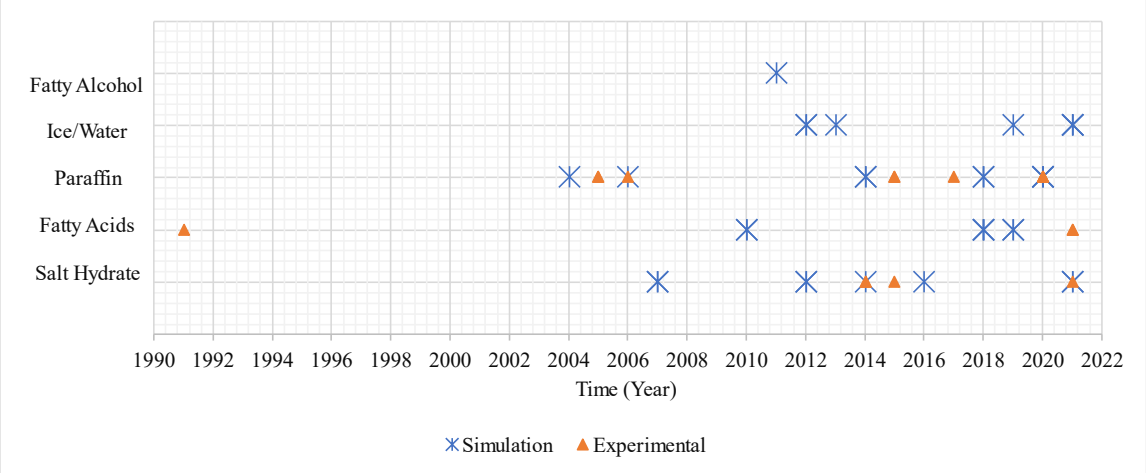


Figure 9: Historical trend of PCMs used for HP-TES.

The research conducted on HP-TES is mostly based on simulations, and very few works present an experimental analysis of both heating and cooling systems. Figure 7 shows an increase in experimental systems during the past decade.

Most active TES experimental systems are integrated via an air distribution system with the PCMs in the supply or return air duct [37], [38], [141], [156], [157].

Climate Zones and TES Application

Figure 10 shows PCM phase change temperatures for space heating and cooling via active and passive TES in various climate zones. Humid continental and oceanic climates are suitable for all kinds of systems, especially active heating, but only active cooling has been investigated for humid subtropical climates. A hot arid climate is suitable for both active and passive cooling, but hot subtropical climates have only been investigated for passive cooling.

HP-TES performance measured by reported cost savings, electricity consumption, and peak load reduction greatly depends on the climate and the TES type. Passive heating TES systems in oceanic and dry climates demonstrated more than 40% energy and cost savings with phase change temperatures close to room temperatures (between 20°C and 29°C) and an organic PCM embedded in the building's interior envelope [126], [127], [131], [134]. Active TES is mostly investigated for cooling in humid climates in which PCMs are mostly installed in an air distribution system [41], [45], [137], [149], [150], [156].

Impact Analysis

This section presents an impact analysis of HP-TES performance with various configurations and controls. It first provides a technoeconomic analysis of active HP-TES configurations, comparing energy savings, utility cost savings, and demand reduction. Then a comparative analysis of active and passive HP-TES is provided by focusing on the load-shifting potential and payback period.

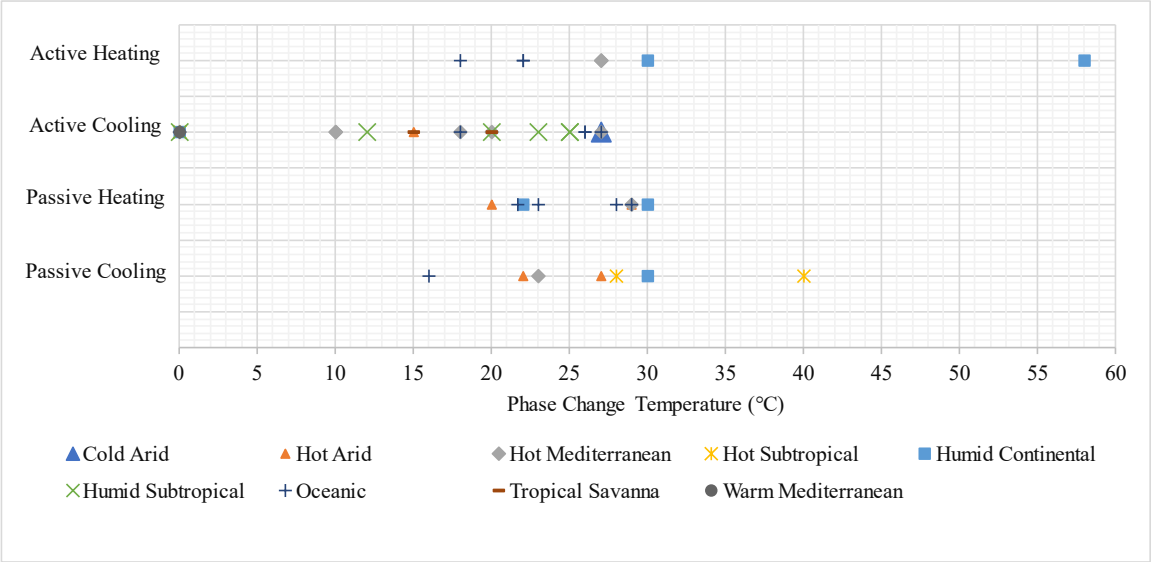


Figure 10: Phase change temperatures in various climate zones.

Finally, the comparison is performed for cases with and without TES to provide an overall performance analysis on cost savings and load shifting.

Comparison of Active HP-TES Configurations

This section focuses on active HP-TES configurations and their impact on utility cost savings, energy savings, and peak electric demand. These performance metrics are discussed further, in which plumbing configurations, refrigerant integration, and hydronic HX are evaluated. Energy savings are calculated from power consumption and HP heating and cooling loads. Utility cost is calculated from daily or annual energy consumption for space heating or cooling. Demand is the instantaneous power during peak hours. These metrics were compared against the TES type, utility tariff, study approach, TES integration, and charging method.

Utility Cost Savings

Figure 11 shows no clear trend or correlation when phase change temperature is plotted against cost savings for active HP-TES configurations. The results demonstrate that savings depend on the climate location, type and size of TES, TES location within the HP, and the utility tariff.

Ice storage is implemented where strong economic incentives exist and the difference between the utility tariff for peak and off-peak hours is large. Dong et al. [125] and Sultan et al. [154] reported similar cost savings of about 20% using ice storage for residential buildings. Both used an indirect configuration in which TES was used as a heat sink or heat source, and space cooling was provided through an HP directly without TES exchanging heat directly with the building. Sehar et al. [151] reported cost savings of 35% using ice storage coupled with a chiller for commercial office buildings in the United States. The simulation-based study used EnergyPlus, and a demand tariff was used to shift the peak load.

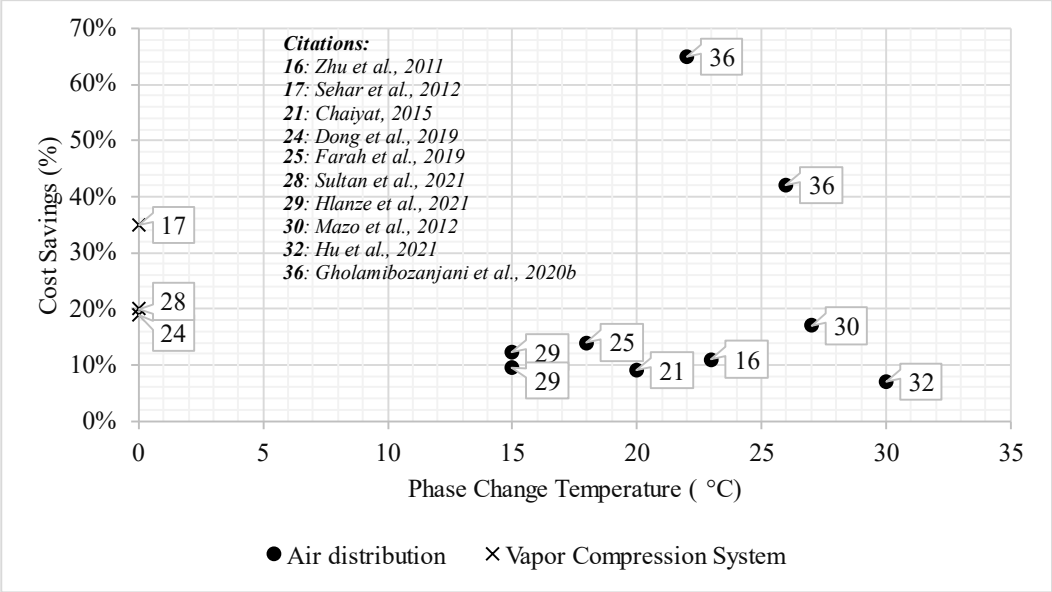


Figure 11: Active HP-TES and utility cost savings in literature.

All other HP-TES systems that have been studied are residential systems coupled with an HP via a return or supply air duct. Cost savings are 10%–15% for a phase change temperature range within 5°C–10°C of room temperature.

Most of the investigated active TES systems that reported cost savings were for cooling only. Hlanze et al. [38] investigated different US climates and reported 12.3% cost savings for El Paso, Texas, and 9.6% for Miami, Florida. Mazo et al. [46] and Hu et al. [156] used heating-only systems and were the only two studies that used a salt hydrate PCM.

Maximum savings were reported by Gholamibozanjani et al. [37] for a hybrid system designed for office buildings in Auckland, New Zealand. Both heating and cooling systems were experimentally investigated, and price-based controls were used for peak load shifting. A solar heater was coupled with an active PCM storage unit for charging, TES was used to provide heating, and a split A/C unit was used to cool the PCMs installed in the supply air loop. In total, 65% cost savings were achieved during winter and 42% during summer.

Energy Savings

Figure 12 shows the percent energy savings and phase change temperatures for HP-TES configurations. No correlation was found between savings and phase change temperature, but besides depending on TES type, configuration, and size, energy savings highly depend on climate and on space heating or cooling application. Most systems reported low energy savings compared with cost and demand savings because energy consumption is not a function of the utility tariff or demand charges. PCMs can sometimes use more energy during off-peak hours.

Maximum savings were reported by Maccarini et al. [45] for a multizone hybrid system in a large office building in Copenhagen, Denmark. District heating and cooling through a thermal plant was considered the baseline compared against three systems: an air-to-water HP, an HP with a dry cooler, and an HP with a PCM HX.

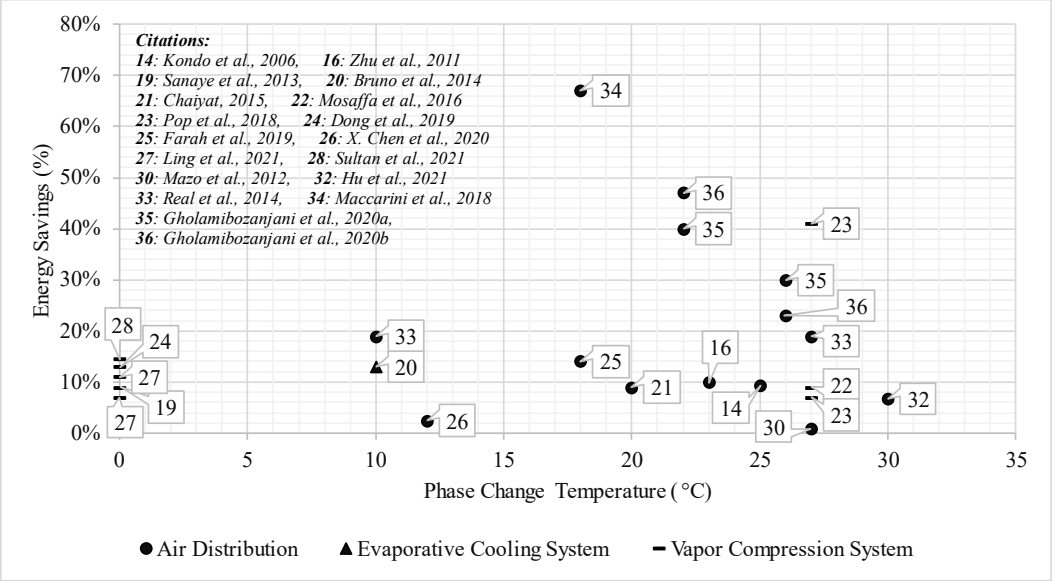


Figure 12: Active HP-TES and energy savings in literature.

PCMs were installed in a return water loop and charged during the night using forced air convection with ambient cold air. In total, 67% energy savings were reported using PCMs.

Gholamibozanjani et al. [157] and Gholamibozanjani et al. [37] performed experiments for a commercial building in Auckland, New Zealand, using a paraffin PCM with a phase change temperature between 22°C and 26°C for both heating and cooling. It was a hybrid system with PCMs in a return air loop coupled with a solar heater in the heating mode and a split A/C unit in the cooling mode. The authors reported 23%–30% energy savings during summer and 40%–47% during winter.

Mazo et al. [46] reported minimal savings for a radiant floor heating system in Spain. PCMs stored heat at night from the HP. Although they reduced cost using a utility tariff and shifted 1 h of peak load, only 0.76% energy savings were reported.

Other PCMs (shown in Figure 10) with a phase change temperature of 18°C–26°C had energy savings of 10%–30% and were integrated via an air distribution configuration.

Ice storage systems had energy savings of 7%–15% and were coupled with a vapor compression cycle [39], [154]. Ling et al. [39] investigated office and mid-rise apartment buildings and reported 7% energy savings for Chicago and 11% for San Francisco. Sultan et al. [154] reported 14.5% savings for residential ice storage in California. The savings were driven by diurnal temperature change.

Demand Impact

Figure 13 shows the demand impact of various active HP-TES configurations. Demand impact is the percentage of heating or cooling demand reduced or percentage of peak load shifted.

Most studies of the active HP-TES systems that reported demand impact investigated a cooling system, which shows that cooling demand dominates in centrally air-conditioned residential homes. Other factors that influence the demand impact are system size and configuration, demand charges and utility tariff, and climate conditions.

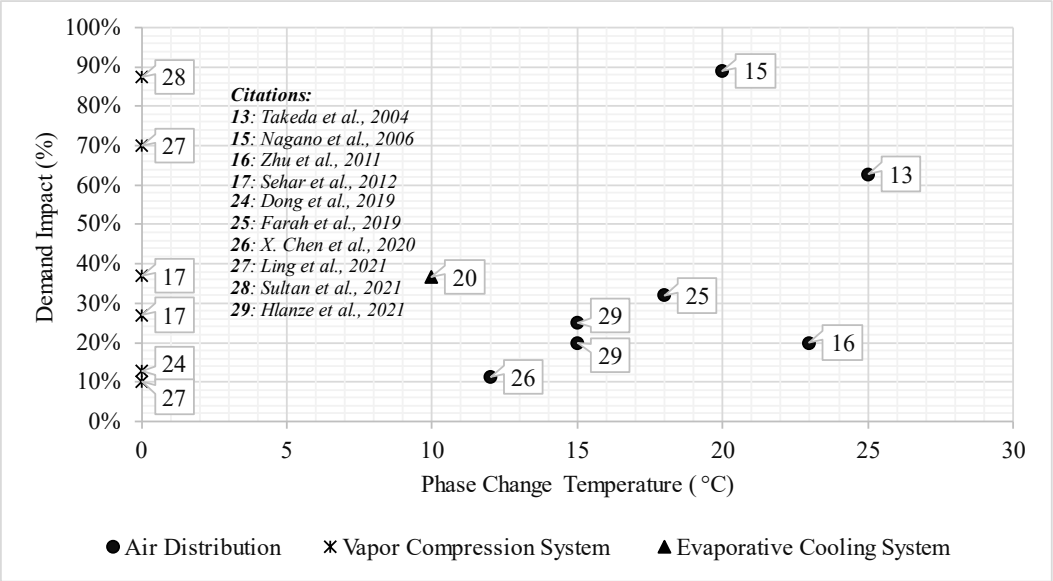


Figure 13: Active HP-TES and demand impact in literature.

Ice storage was beneficial for commercial systems and savings depending on climate, tariff, and configuration. Sehar et al. [151] investigated a commercial ice storage system coupled with a chiller. The chiller made ice during off-peak hours for cooling. In total, 39% peak energy was saved for Seattle, Washington, and 27% for Las Vegas, Nevada. Ling et al. [39] experimentally investigated slurry ice in the condenser of a personal conditioning device for office buildings and mid-rise apartments. They reported 10%–70% peak savings depending on climate zone and building type.

All ice systems were integrated with a vapor compression cycle. In total, 87% of peak cooling load shifting was reported for a residential ice storage system using a TOU tariff in Fresno, California [154]. TES was used as an evaporator and condenser in charging and discharging modes, respectively.

For systems with PCM phase change temperatures between 12°C and 25°C, air distribution was a common configuration with PCMs in the supply or return air duct. Hlanze et al. [38] investigated organic PCMs in a supply air duct for different climate zones in the United States. In total, a 20% peak energy savings were reported for El Paso, Texas, and 25% for Miami, Florida.

Only a few studies were experimental. Bruno et al. [42] experimentally investigated an evaporative cooling system coupled with a chiller with salt hydrate PCMs. PCMs were cooled using a chiller during off-peak hours, and peak electricity consumption was reduced by 36.6%. Nagano et al. [150] reported 89% of cooling load shift for an experimental setup in Japan. Paraffin was installed in a supply air duct of an underfloor ventilation system for night cooling.

Comparison of Active and Passive HP-TES

This section provides a comparative analysis of the payback period and peak load shifting of active and passive HP-TES in literature.

Load Shifting

Figure 14 shows hours of peak load shifted for active and passive HP-TES. No clear trend or correlation was found between TES and load shifting, but active HP-TES systems demonstrated the highest load shifting.

Barzin et al. [126], [131] reported 3–5 h of peak load shift. PCMs were installed in a wallboard and were passively charged using solar heat gains in Auckland, New Zealand. However, indoor comfort was often compromised by overheating.

Muruganantham et al. [128] and Mazo et al. [46] reported the lowest peak load shift of 1 h. Muruganantham et al. investigated passive PCM-TES in an interior envelope of the building; the PCMs melted or solidified based on ambient temperature. Mazo et al. studied active storage with PCMs installed in the floor heating system. They applied Spanish peak utility pricing and used an HP for off-peak night charging. Furthermore, 1 h of peak load was shifted per day.

Sultan et al. [154] and Xu et al. [48] reported the highest load shift of 6 h. Both actively coupled PCMs with a VCS. Sultan et al. investigated cooling only using ice storage, and an evaporator was used to charge the PCMs. The authors used thermostat controls for load shifting and implemented a TOU utility tariff. Xu et al. investigated a heating-only system coupled with an electric heater, and a condenser was used to charge a sodium acetate trihydrate PCM with a 58°C phase change temperature.

Payback Period

Figure 15 shows that passive HP-TES has a payback period of more than 15 years, whereas active HP-TES has a payback period of less than 10 years, except for as reported by Xu et al. [48].

The trends of energy savings of passive TES were not significantly different from active TES, but because of installation complexities, the investment and installation cost was much higher than that of the active TES.

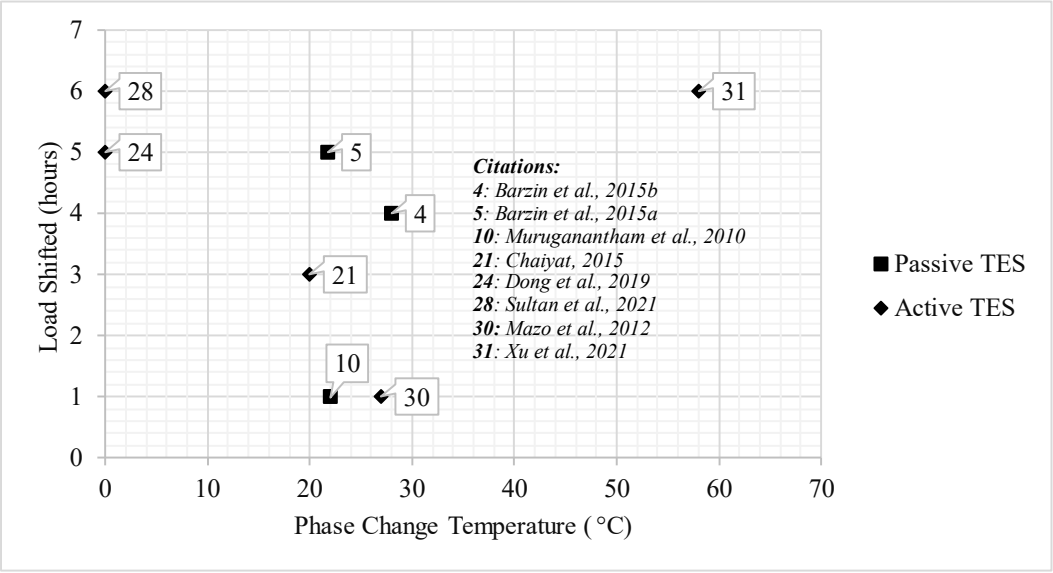


Figure 14: Load shifting of active and passive HP-TES in literature.

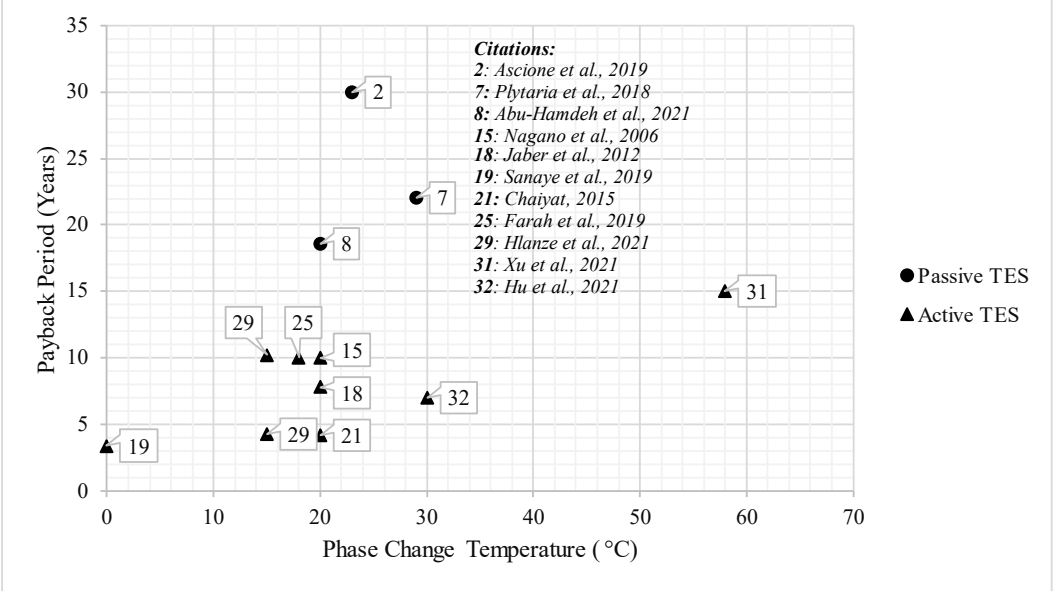


Figure 15: Payback period of active and passive HP-TES in literature.

Furthermore, cost and demand reduction were not as prominent as in active HP-TES because of no control of passive HP-TES over TES equipment and operation.

Ascione et al. [129] reported the longest payback period of 30 years for passive HP-TES. PCMs were installed in interior walls of a public educational building that was refurbished to reduce cooling demand in a hot Mediterranean climate. The investment costs, maintenance and operating costs, and disposal costs were considered to calculate the payback period. The authors suggested additional measures such as using inexpensive PCMs and applying discount rates that could shorten the payback period to 12 years.

Abu-Hamdeh et al. [132] reported the shortest payback period of 18.6 years for passive HP-TES. They also installed PCMs in the interior wall for space heating to reduce AHU energy usage. In an arid climate such as Jeddah, Saudi Arabia, passive TES can take advantage of ambient temperatures for heating, which reduces heat demand; hence, the payback period is shorter.

Xu et al. [48] reported the longest payback period of 15 years for active HP-TES. PCMs were installed in a storage tank coupled with a condenser for charging. The heating load was increased with off-peak charging.

Sanaye et al. [152] had the shortest payback period of 3.4 years for active HP-TES. Ice-based TES in a storage tank was used as an evaporator and made ice during off-peak hours.

All other active HP-TES works shown in Figure 13 had PCMs installed in the supply or return air ducts and reported a payback period between 4 and 10 years [38], [40], [127], [140], [144], [150], [156]. Most of these are cooling-only systems, except for a heating and cooling system reported by Hu et al. [156], which had a payback period of 7 years.

Performance Analysis with and without TES

A statistical (box-and-whisker) analysis was performed on the groups of data sets for active TES, passive TES, and no TES systems where at least two of the outcomes are

reported out of energy savings, demand impact, and cost savings (Figure 16). The skewness of the mean results does not indicate that the studies were erroneous but were identified to allow an improved discussion of the mean. Furthermore, the results with the highest performance should be examined in great detail for replication. Studies that fall significantly below the mean should be noted to determine methods of improvement. Identifying the success factors or discussing the improvements is outside the scope of this study.

As shown in Figure 16(A), few studies were conducted at high temperatures, and the active TES mean is about 10°C below the passive TES mean—both means are high because of the heating studies. Most studies examined PCMs with phase change temperatures closer to the room or ambient temperature; however, active TES have more acceptable temperature range. The demand impact (Figure 16(B)) shows a good distribution around the mean for active TES. Because the median was used in determining the quartiles and the outliers included in the mean, the mean can lie outside the middle quartiles, which is the case for active TES in Figure 16(C). This suggests one study was very successful compared with the others in active TES [45]. The cost savings results (Figure 16(D)) have the most outliers. The passive TES cost savings are notably skewed high and low, whereas the active TES mean is skewed high only.

Passive TES tends to be closer to ambient conditions, whereas active TES can use temperatures above and below ambient conditions.

Demand impact can be reduced by control schemes without using TES, but TES provides additional energy and cost saving benefits. Passive systems tend to have a lower demand impact (about 20%), whereas active systems have a higher average impact of 40%.

Passive and active TES generally save energy at similar percentages, although passive systems have a slightly higher average of 22% than active systems, which have an average of 15%.

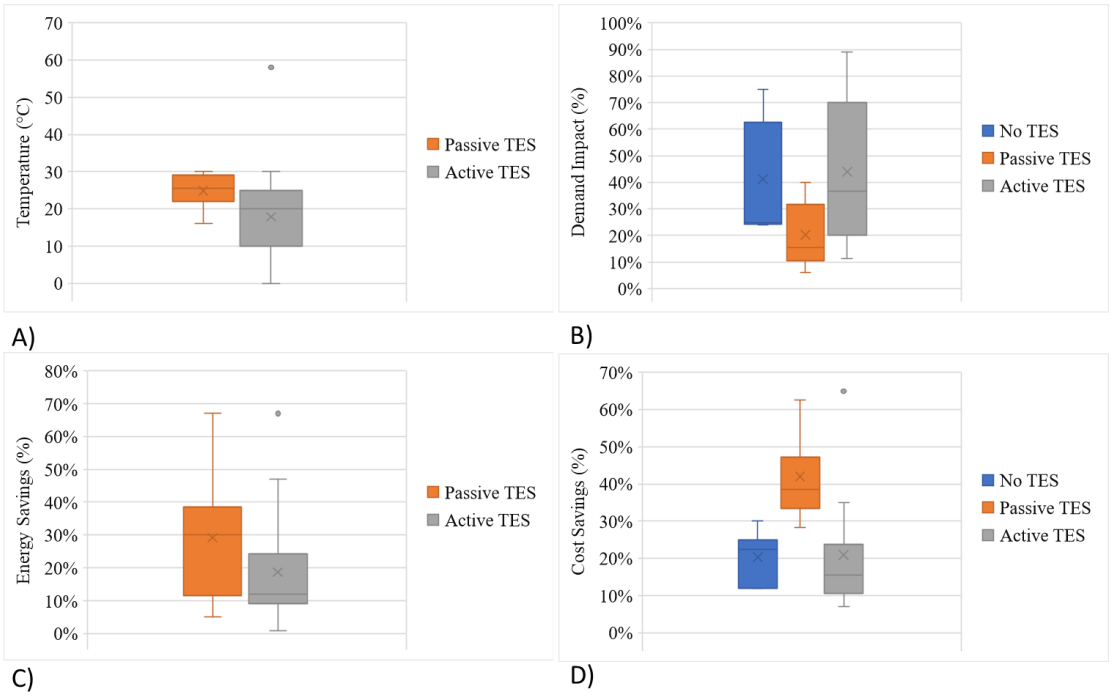


Figure 16: Overall comparison: (A) phase change temperature, (B) demand impact, (C) energy savings, and (D) utility cost savings.

The utility cost savings in all three building types can be significant (e.g., >10%). Passive systems have the highest average (>35%), and active systems have an average of about 15%.

Discussion and Future Work

This study compares various configurations of active and passive HP-TES for space heating and cooling applications. We included PCM and ice storage as TES integrated with HP. There are some works that investigate commercial buildings, but HP-TES systems were mostly studied for residential buildings. The reviewed studies reported energy savings, cost savings, peak load shifted, demand reduction, and payback period. The reported outcomes were compared against the PCMs used; the temperature, configuration, and TES location within the building envelope; and the HP components, type of TES, and application. DR potential was assessed and compared with and without TES, and peak demand shifting using dynamic price-based controls was examined.

DR strategies and HP controls can provide some cost and demand reduction, but with TES having the capability to decouple the energy generation from its demand and usage, energy can be stored during off-peak hours for later use during peak hours.

HP-TES allows for the use of established technology and resources with minimal equipment, which can reduce the installation complexity and cost. HPs can provide heating and cooling at different times of day or year, and their weather-dependent performance can be exploited by TES and controls. Passive HP-TES systems can offset the peak demand by shifting loads, but they cannot control the charging or discharging operation to optimize grid benefits. Active HP-TES can be packaged into various configurations that require small modifications and offer maximum benefits to the consumer and the grid while minimizing the TES footprint.

System performance of HP-TES was reviewed to compare energy savings, demand impact, and payback period against different configurations, TES types, and heating and cooling applications for various climate zones. For passive TES, heating energy and utility

cost savings can benefit from passive solar gains and diurnal temperature swing in some climates. However, additional controls and equipment are required to achieve cooling energy savings, and these controls and equipment can be costly. Indoor comfort can also be compromised by the lack of control in passive TES. Active HP-TES equipment is programable with a thermostat for DR and offers installation flexibility and better TES control, providing greater demand savings and cost benefits. Active HP-TES is more financially viable in hot climates with higher demand or utility tariffs.

Besides being influenced by the utility tariff and climate, system performance is influenced by TES type, size, and configuration. Active HP-TES can be installed in the building envelope, air distribution loops, or VCS itself. Most active TES systems are integrated via an air distribution system with PCMs in the supply or return air duct. Paraffins and salt hydrates were commonly used materials with phase change temperatures ranging between 15°C and 30°C.

Passive TES systems tend to use temperatures closer to ambient temperatures, whereas active TES systems can use temperatures above and below ambient. Demand impact can be reduced by control schemes without using TES, but TES provides additional energy and cost saving benefits. Passive systems tend to have a lower demand impact (about 30%) compared with active systems, which have a higher average demand impact of 40%. Both passive and active systems generally save money and energy at similar percentages, although passive systems have a slightly higher average than active systems. However, the payback period for active systems is much shorter than that of passive systems, which indicates that passive systems require significant initial investments. On average, active systems have payback periods of less than 10 years, whereas passive systems have payback periods of more than 25 years.

TES can sometimes use more energy during off-peak hours. Most systems reported low energy savings compared with their cost and demand savings because energy consumption is not a function of the utility tariff or demand charges. Many advances in

materials have occurred, but more research is needed on the system side to improve the energy storage performance and enhance the charge–discharge cycle efficiency of TES.

Very few studies have examined HP-TES overall, and there are even fewer experimental studies. TES can be coupled with an HP in many configurations that have not yet been explored. There is much to uncover in integrating TES experimentally with HP.

Although the historical trend indicates an increased interest in the technology during the past decade, all the HP-TES systems in literature highly differ from each other. No standards exist, and it is hard to compare these systems. More comprehensive and comparative simulation work is needed to compare different PCMs for HP-TES and compare optimum storage and configurations for different climates.

CONCLUSIONS

Buildings can alleviate peak demand challenges by shifting peak load to off-peak periods via TES. This chapter provided a review of HP-TES with various configurations and control strategies. The study compared HP controls without TES for DR, passive HP-TES (in the building envelope), and active HP-TES (in HP components). DR can lower some costs but cannot provide energy savings without TES. Passive TES provides up to 60% energy savings but cannot optimize grid benefits because of their lack of control over TES operation. Active HP-TES improved energy storage and provided up to 80% demand reduction through real-time charging and discharging. The utility cost savings for active HP-TES depend on the type and size of TES, TES location within an HP, and utility tariff, and energy savings highly depend on the climate and TES application. The financial viability of active HP-TES is higher in cooling-dominated climates with higher peak electricity prices. These conclusions are largely based on simulation studies, and only studies that provided some technoeconomic analysis were reviewed. Few experimental HP-TES systems are presented in literature, but the historical trend demonstrates an increasing interest in this technology over the past decade.

CHAPTER II

PHASE CHANGE MATERIAL FOR HEAT PUMP INTEGRATED WITH TES

A version of this chapter was originally published by S. Sultan *et al*:

Sultan, Sara; Turnaoglu, Tugba; Akamo, Damilola; Hirschey, Jason; Laclair, Tim; Liu, Xiaobing; and Gluesenkamp, Kyle R., "PCM Material Selection for Heat Pump Integrated with Thermal Energy Storage for Demand Response in Residential Buildings" (2022). *International High Performance Buildings Conference*. Paper 427.

Conceptualization, data collection, and original manuscript draft was prepared by Sara Sultan. Jason Hirschey, Tugba Turnaoglu, Damilola Akamo, Tim LaClair, and Xiaobing Liu, provided help with editing and analysis. Review and supervision by Kyle R. Gluesenkamp.

Abstract

PCMs can be used for space heating and cooling applications in residential buildings by integrating into the HP equipment or building envelope via several possible configurations. The HP integrated active PCM storage can provide significant energy savings and reduce peak demand, but the benefits vary substantially depending on the system configuration, storage capacity, and the temperature range of the PCM used. Low temperature salt hydrate PCMs with melting point closer to the room temperature have garnered interest for near ambient TES systems because of their high storage density. However, the PCMs in this range often have low thermal conductivity that impacts the storage capacity. As such, modifications are needed to enhance the stability and thermal properties of PCM. It is critical to provide a review of the materials and their suitability in HP integrated PCM systems. This chapter will present an analysis of the PCM material selection for heat pump integrated TES in various configurations. The comprehensive review will compare PCMs with different melting temperatures, and configurations, corresponding to the energy savings and demand impact reported in the literature. This work is significant to guide the design of high-performance heat pump integrated PCM systems.

Research Question

What is the optimum PCM temperature and heat pump configuration for maximum economic and grid benefits of heat pump integrated TES?

Background

Building's energy consumption and peak demand is often attributed to air conditioning applications. More than half of the energy consumed in the residential buildings is used for air conditioning and space heating. According to the DOE report, 54% of the site energy consumption is accounted for space heating and cooling combined, driving major portion of the residential energy demand [49], [52]. The residential buildings can play a major role to reduce energy demand and increase the building flexibility while maintaining the temperature in a comfortable range, by designing a load shifting strategy [54]–[57]. The major electric load from the residential buildings comprises 80% of the total electricity use in the U.S., and 78% of the peak period use during 2-8 PM [53].

About 80% of American homes are detached single-family houses of an average area of about 2600 ft^2, with an average occupancy of 2.5 [1]. Furthermore, 90% of homes in the U.S. use air conditioning as of 2019, and 75% of those air-conditioned homes use central units. In 2019, the average annual electricity consumption for a U.S. residential utility customer was about 877 kWh per month. The consumers end up paying additional peak demand charges due to stress on the utility grid.

Though, the energy consumption and demand in the U.S. declined by 14% in response to the COVID-19 pandemic, however, the residential buildings energy consumption rose by 8% due to the increased residential demand shift as a result of working from home [159]. Power generation grids around the world are undergoing major changes to cope with the increasing energy demand and maintain physical and economic stability in response to the growing need for renewable energy generation [92]. The technological advances and flexibility in the design and operation of HVAC systems can allow them to help the grid overcome these new load patterns challenges if properly managed.

Typically, in US residential buildings, there is no mechanical outdoor air exchange, or cross ventilation using natural resources, therefore, heat pumps are important to regulate the humidity inside the house as well as the indoor temperature. It is often cost-prohibitive to rebuild houses or update the conventional methods, but the heat pump systems can be made smart to respond to the peak demand changes. Today's high-efficiency HVAC and appliance products can provide energy savings, but do not generally help with demand management and grid stress [23].

Thermal energy storage (TES), which has capability to decouple the energy generation from its demand and usage, can be a crucial tool to shift the thermal loads. TES systems can be easily incorporated in small to large single-family or multi-family residential buildings. They are designed to trim the building's electrical demand profile by reducing the energy usage and high demand costs arising from summer cooling and winter heating needs [98]. When properly controlled, thermal storage can be useful in an economic or behavioral curtailment scenario for demand response. Major factors influencing an appropriate TES system's choice include the energy storage period and duration, cost and economic feasibility, and operational conditions. The building's thermal load is also dependent on the weather conditions and the thermal quality of the building envelope.

Phase Change Materials (PCMs) are widely used commercial thermal storage materials that could be used for space heating and cooling applications in various configurations. PCM-TES can store and release energy through charging and discharging process, respectively. By utilizing TES to store the energy for later use during peak hours, demand management systems can be designed to take advantage of lower utility rates during off-peak hours.

Researchers have used various configurations to employ the economic and grid benefits of PCM-TES for heating and cooling applications in buildings. The most common configurations are to install the material in building envelope via passive storage where the charging and discharging process is the function of ambient temperature, hence the grid benefits can't be maximized. Active storage configurations allow real-time control of TES

and are proven to be more effective than passive configurations. Active TES systems mechanically transfer the heat and hence can control when to charge or discharge the TES. This allows the TES systems to achieve grid flexibility, making them more suitable for load shifting and demand management. Another benefit of active configuration is the flexibility to be installed in an existing building infrastructure without needing a significant construction. The TES may be separate and removed from the space.

PCM-TES can behave as a standalone isothermal heat exchanger when integrated with heat pump (HP), and can offer advantages by shifting the peak demand while maintaining an adequate internal temperature in comfort range, without excessively using heat pump equipment. HP-TES in an active configuration, can enhance these benefits with a better performance if heat transfer is controlled by the heat pump [3].

The key to using TES to provide economic and grid benefits is the development of materials and packaging in optimized configuration and temperature range. Low temperature salt hydrate PCMs with melting point closer to the room temperature have garnered interest for near ambient TES systems because of their high storage density. However, the PCMs in this range often have low thermal conductivity that impacts the storage capacity. As such, modifications are needed to enhance the stability and thermal properties of PCM. Researchers have used single material in passive configurations for both high and low temperature applications but for active configuration, the materials with different melting temperature are selected for each application. Melting temperature for cooling applications is below 10°C, while for heating is above 40°C.

The benefits also vary largely due to other factors such as PCM material and temperature, configuration, and climate zone. Figure 17 below shows the demand impact and load shifting benefits reported in literature for Heat pump coupled passive and active TES. Active TES dominate mostly because the high level of control, allows designing and incorporating effective load shifting strategy.

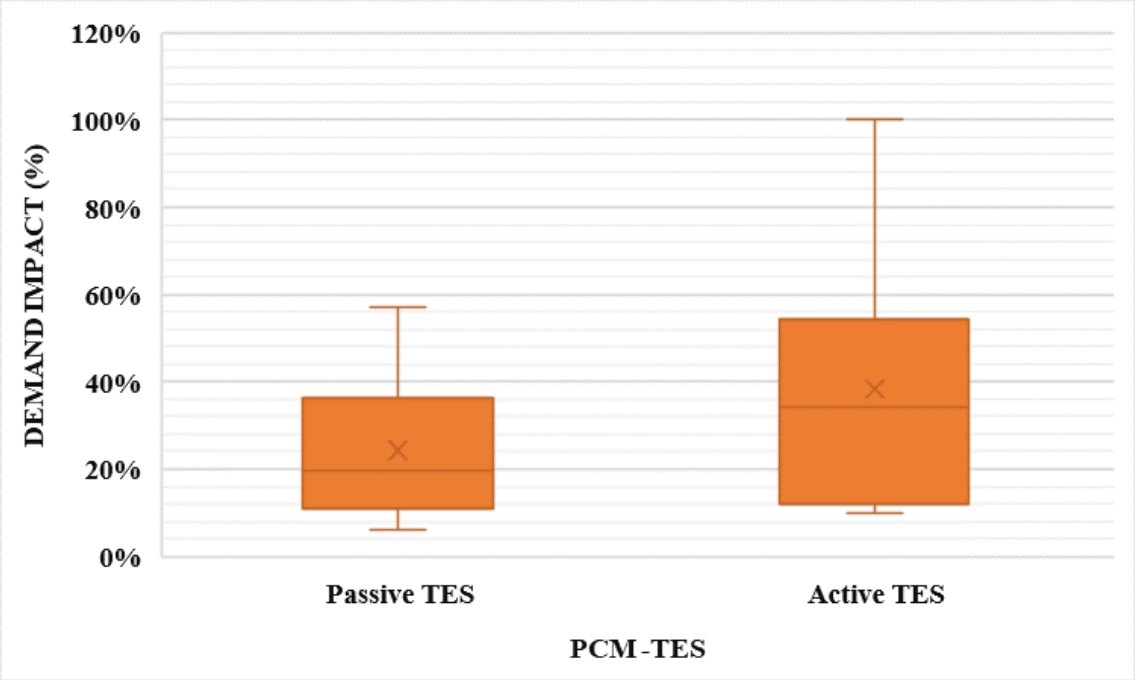


Figure 17: Comparison of load shifting benefits for Active and Passive TES

The focus of this chapter is to review PCM used in active HP-TES. Literature review is conducted to evaluate the properties of PCM used in active HP-TES, as well as to compare the different configurations.

Next section will discuss the salt hydrate PCMs, focusing on melting temperature and storage capacity. It is further explained how PCMs are integrated in heat pump via different configurations. The demand impact is also reported and compared against the PCM types, heat pump configurations, and TES application.

PCM for HP-TES

PCMs perform solid-liquid phase changes at temperatures in the operational range of the designated thermal application. When a phase transformation from a solid to a liquid occurs, the energy is absorbed by the phase transitioning material from the surroundings, though maintaining almost the same temperature [102]. There are generally three classifications of PCMs; organic PCMs, inorganic PCMs, and eutectics. Organic PCMs are attributed to low heat conductivities and are flammable, while inorganic PCMs are relatively inexpensive, easily synthesized, nonflammable and possess high thermal conductivity and high storage capacity [103].

Any energy storage system should at least possess the following components:

- A PCM with the desired temperature range
- A compatible heat exchanger

This section reviews important factors and parameters for PCM selection to be integrated in heat pump components or coupled to the vapor compression system. The salt hydrate PCMs integrated with HP for space heating or cooling applications are reviewed.

PCM Selection

PCM temperature and storage capacity are considerably important to design the TES that can meet the buildings' load and provide necessary comfort. Various approaches can

be found in literature to choose the melting point of PCMs to maximize their performance for space conditioning in buildings. Free cooling for continental climates was studied by Medved and Arkar [121], and they found the PCM with a melting point equal to the average temperature of hottest month, most appropriate choice. The melting temperature range 20 and 22 °C was found suitable for passive cooling. Waqas and Kumar [160] demonstrated an optimum PCM storage unit performance by selecting a PCM with the melting point equal to the comfort temperature of hottest month for free cooling.

The PCM temperature optimization studies [161]–[170] have commonly utilized passive cooling with organic PCMs. Paraffins are the frequently investigated materials with 20-30 °C melting temperature range. Furthermore, for a given TES, different PCM melting temperatures have been studied for both heating and cooling applications.

Table 10 below reviews salt hydrate PCMs integrated with different types of HPs via HX for space heating and cooling.

Most of the active TES studies reported in literature, as shown in the table above, have selected a melting temperature closer to the typical room temperature. A few of these works have investigated more than one type of PCM and have reported that the salt hydrate PCMs performed better than the organic PCMs in terms of storage capacity, and economic benefits.

Integration in Heat Pump Components

Active PCM-TES can be coupled to heat pump in various configurations. Table 10 in previous section described different types of heat exchangers and heat pumps. This section will particularly focus on PCM location within the heat pump and charging operation for the configuration. Researchers have reported energy and cost savings, and demand impact benefits for off-peak heating and cooling. Besides the PCM type and melting temperature, the savings and benefits largely depend on how and when PCM has been charged and discharged.

Table 10: PCMs for HP-TES

Author	PCM material	Application	Heat Exchanger	Thermophysical Properties	Performance
[171]	S8, S17, S27 (8 °C, 17 °C, 27 °C)	Geothermal heat pump for heating and peak load shifting	Single U-Tube ground heat exchanger	S27 showed highest savings and had thermal conductivity of 0.540 W/m.K	COP increased from 3.8 to 5.5
(Xin Jin et al., 2021)	Composite modified SAT (47.8°C)	Coupled to air source heat pump for heating	Shell and tube heat exchanger	Latent heat 219.8 kJ/kg (presented longer cycling lifetime)	Heat pump COP increased by 5.1%, 10 year payback period
[173]	$CaCl_2.6H_2O$ (29.9 °C)	Solar assisted ground source heat pump	U-Tube soil exchanger	PCM thermal conductivity 1.09 W/m.K	COP increased from 3 to 5.95
[174]	$Na_2SO_4.10H_2O$ (32 °C)	Coupled to floor heating system for heating	Tube heat exchanger	PCM thermal conductivity 1.09 W/m.K	COP reported 3.0
[155]	$CaCl_2.6H_2O$ (28°C)	Coupled to solar and heat pump for heating	Fin tube heat exchanger	PCM thermal conductivity 1.09 W/m.K	COP increased to 4.0
[175]	$CaCl_2.6H_2O$ (28°C)	Coupled to ground source heat pump for green house heating	Ground heat exchanger	PCM thermal conductivity 1.09 W/m.K	COP increased to 4.2
[176]	Commercial salt hydrate (48 °C)	Coupled to heat pump for heating	PCM enhanced buffer tank	Thermal conductivity 0.45 W/m.K	COP reduced from 3.0 to 2.4
[48]	Sodium Acetate Trihydrate SAT (58°C)	Coupled to condenser for heating	Plate heat exchanger	Thermal conductivity 0.57 W/m.K	COP reported 4.5
[177]	SP24E, RT27, RT25 (24 °C - 25 °C)	Coupled to ventilation system for cooling	Plate heat exchanger	Thermal conductivity 0.60 W/m.K	Salt hydrate PCM had highest storage capacity

Table 10 Continued

[178]	FlatICE PCM (15 °C)	Coupled to chiller for space cooling and peak load shifting	Plate heat exchanger	Thermal conductivity 0.43 W/m.K	Chiller load reduced by 37%. PCM utilized 15% of its storage capacity

Heat Pump Integration

PCM-TES can be installed in building envelope, air distribution loops, or the vapor compression system itself. For an active PCM-TES to be installed in the building envelope, a heat exchanger is used and coupled to the air handling unit [136]. In the vapor compression system, either the PCM is directly installed in the condenser or evaporator or coupled via a stand-alone storage tank (Bruno et al., 2014; Real et al., 2014). Air distribution system has been the most commonly used configuration where the PCM is installed in the supply or return air ducts (Chaiyat, 2015; Hlanze et al., 2021).

Application and Configuration

Active HP-TES systems have been investigated for the demand response and load shifting potential. The literature reported in Table 11 and 12 show that the cooling applications are widely explored, and peak cooling demand is shifted to off peak hours using different control strategies.

A paraffin PCM was installed in a return air duct coupled with evaporator to enhance the cooling efficiency of air conditioning system (Chaiyat, 2015). The PCM was solidified during nighttime by the cold air from the heat pump. During the daytime, return air from the room was passed through the PCM, liquifying it and reducing the cooling load at the evaporator. The time-of-use TOU tarrif was used and 3-hour load was shifted to off-peak hours. 9% daily energy and cost savings were reported.

Bruno et al. (Bruno et al., 2014) used ice and two salt hydrates PCMs installed in a heat exchanger coupled to chillder. The cooling energy is provided through chiller to either the PCM for solidification, or to the building during off-peak hours. The charging time and duration was optimized depending on the outside temperature to minimize energy usage and the PCM with 10°C melting temperature could save 13% energy.

Table 11 and 12 below compare the energy savings and demand impact for Active TES systems integrated with heat pump via different configurations.

Table 11: Active HP-TES Configurations with Salt hydrate PCMS

Author	PCM material	Application	Configuration & HP integration	Charging Operation	Key Results
(Real et al., 2014)	S10 (10 °C) S27 (27 °C)	Both heating and cooling	In two storage tanks coupled to HVAC	Cooling energy is stored in cold tank at night using HVAC	18.97% energy saved
[48]	Sodium Acetate Trihydrate (SAT) (58 °C)	Space Heating	In storage tank coupled to condenser & electric heater	Heat pump condenser is used to charge PCM during off-peak hours	6 hours of peak load shifted
[40]	Salt Hydrate PCM 18T (18°C)	Space Cooling	In storage tank coupled to an air source heat pump	Return air from room passes through PCM before entering the evaporator to increase COP	Peak demand reduced by 32%
[44]	S27 (27°C) S25 (25°C)	Space Cooling	In storage tank coupled to vapor type compressor of heat pump	PCM is solidified using air-conditioner during off-peak hours	7-9% energy savings
(Bruno et al., 2014)	S4, S10 (4, 10 °C)	Space Cooling	In heat exchanger coupled to chiller	Chiller provides cooling to PCM during off-peak hours	Peak electric consumption reduced by 36.6%

Table 12: Active HP-TES Configurations with other PCMS

Author	PCM material	Application	Configuration & HP integration	Charging Operation	Key Results
[179]	35% paraffin GR25 composite (25°C)	Space Cooling	In supply air duct of a ventilation system	PCM is solidified during night using the cool air from AHU	Ventilation load reduced by 62.8%
[136]	Micro capsulate (25°C)	Space Cooling	In ceiling board coupled with AHU	PCM is charged overnight using AHU	9.4% load reduction
(Chaiyat, 2015)	RT20 Paraffin (20 °C)	Space Cooling	In return air duct coupled with the evaporator	Return air from room passes through PCM before entering the evaporator to increase COP	9% energy saved
[41]	RT11HC Paraffin (10-12°C)	Space Cooling	In storage tank coupled to heat pump	Heat pump directs cold water to solidify PCM	11.28% peak demand charges reduced
[38]	PureTemp 15T (15 °C)	Space Cooling	In supply air duct of air conditioning system	Cold supply air solidifies PCM during off-peak hours	Peak energy consumption reduced by 20-25%
[156]	ATS 30 (28 °C–33 °C)	Space Heating	In supply air system of heat pump	PCM is charged by heat pump at lower utility rates	6.7% energy consumption reduced

PCM melting point and charging operations are reported. Table 11 summarizes the salt hydrate PCMs while Table 12 reviews other PCMs used for HP-TES.

Results and Discussion

The demand impact reported in the tables 11 and 12 corresponds to peak load shifted, peak electricity consumption reduced, or heat pump cooling and heating loads reduced. This section would discuss the PCM melting temperature and heat pump TES configuration for maximum demand impact. There are still number of factors to be considered such as the ambient climate conditions, size of TES, and heat transfer coefficient. The scope of this paper is limited to PCM material, melting temperature, and heat pump configuration.

Melting Temperature

Figure 18 shows the range of PCM temperature corresponding to demand impact for space heating and cooling. The PCM materials with the melting temperature ranging from 15 to 27 °C showed the most savings and demand benefits. Majority of the HP-TES systems reported in literature for demand response have investigated a cooling system which shows that cooling demand dominates in the centrally air-conditioned residential homes. The PCM melting temperatures reported lie within the narrow range closer to room temperature except the Sodium Acetate Trihydrate (58 °C) which is used for space heating.

Configuration

PCM-TES has been integrated with heat pump in various different configurations. Heat exchanger or storage tank containing PCM is coupled to either building envelope or heat pump components. Heat pump components can be on the air-side or the refrigerant-side of the heat pump. The refrigerant-side is referred as vapor compression system components (condenser, evaporator, and compressor), and the air-side corresponds to the air distribution system (supply air duct and return loop). Figure 19 shows that the air-side configurations are the ones most commonly investigated and report maximum demand impact and energy savings.

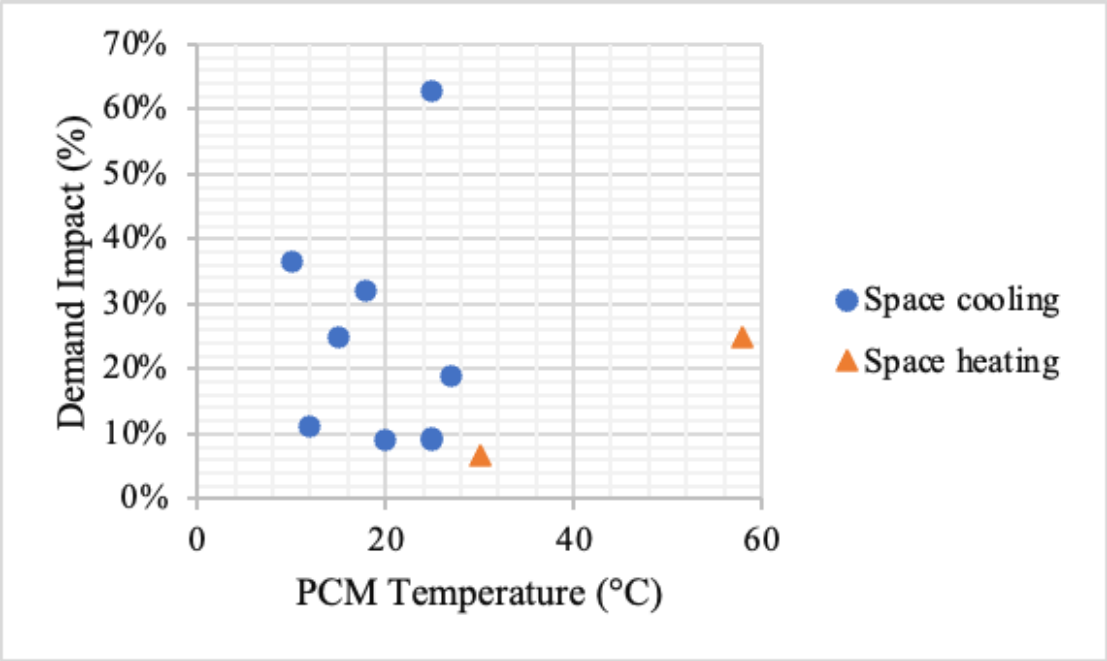


Figure 18: Demand Impact and PCM Temperature

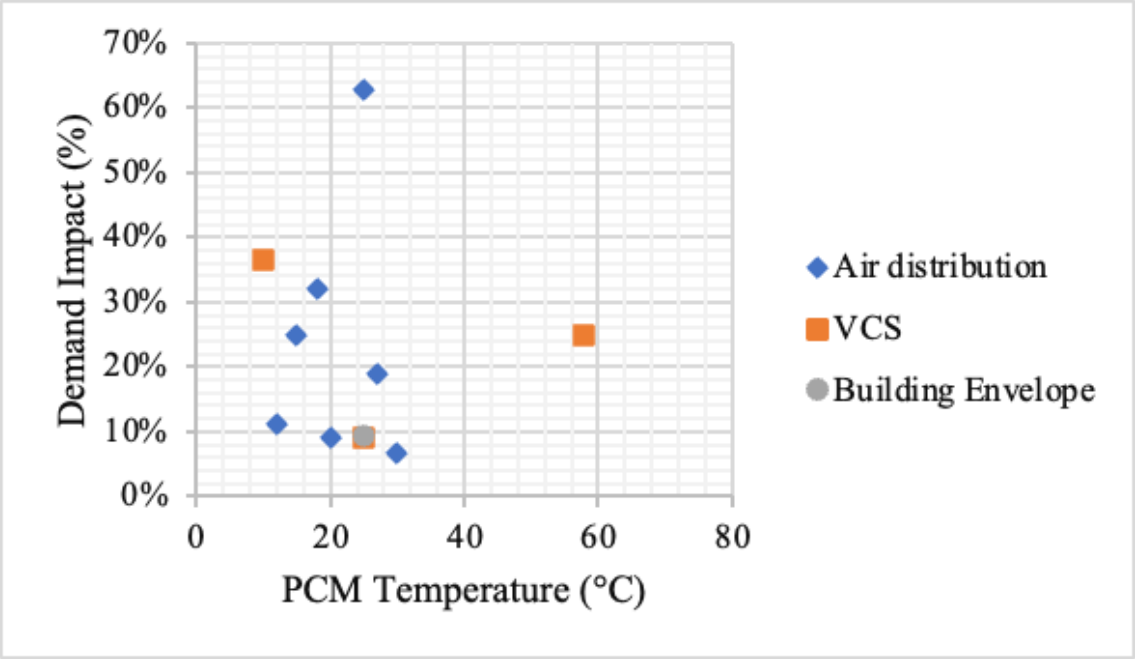


Figure 19: Demand Impact and heat pump configurations

CONCLUSIONS

Phase Change Material (PCM) based Thermal energy storage (TES) can provide economic and environmental benefits for grid-interactive residential buildings. The value and performance of TES vary greatly depending on the temperature range and storage capacity of the material, as well as the system configuration and ambient temperature. Active storage configurations allow real-time control of TES and are proven to be more effective than passive configurations, however, the active TES studies found in literature have utilized different materials for both heating and cooling.

This chapter reviewed the PCM materials, melting temperatures, and heat pump configurations to compare the energy savings and demand benefits of heat-pump integrated TES. The optimum demand impact and energy savings are reported for salt hydrate PCM with melting temperature between 15 and 27 °C integrated via air distribution system of the heat pump.

CHAPTER III

CASE STUDY – ECONOMIC IMPLICATIONS OF RESIDENTIAL BUILDINGS

A version of this chapter was originally published by S. Sultan *et al*:

Sultan, Sara; Hirschey, Jason; Gluesenkamp, Kyle R.; and Graham, Samuel, "Analysis of Residential Time- of-Use Utility Rate Structures and Economic Implications for Thermal Energy Storage" (2021). *International High Performance Buildings Conference*. Paper 370. https://docs.lib.purdue.edu/ihpbc/370

Model simulations and original manuscript draft was prepared by Sara Sultan and Jason Hirschey, Review and supervision by Samuel Graham, and Kyle R. Gluesenkamp.

Abstract

Thermal energy storage (TES) is an increasingly popular tool to level out the daily electrical demand and add stability to the electrical grid as more intermittent renewable energy sources are installed. TES systems can locally decouple high thermal loads from the operation of a heat pump or reduce the electrical energy demand of the heat pump by providing a more favorable temperature gradient. In addition, many policy makers and utility providers have introduced time-of-use (TOU) rate schedules for residential customers to better reflect the price of electricity generation and demand for specific times. TOU rate schedules price grid-provided electricity differently throughout the day depending on the region's climate, time of year, and electrical production portfolio. Large differences between on-peak and off-peak electrical prices may create an economic advantage for a residential customer to install a TES system. In this work, the economic and energy savings are calculated for a modeled 223 square foot residential building with water/ice-based TES using a TOU rate structure.

A southern California residential building's summertime cooling load during a week of extreme high temperatures is comparatively modeled with and without active TES. The TES is directly coupled to a vapor compression system and serves as the VCS condensing unit during peak hours rather than the ambient air. The PCM embedded in the TES for this analysis is ice/water with a phase change temperature of 0°C, and only interacts with VCS, not directly with the building. A residential TOU utility rate from a utility provider in

California, corresponding to the climate zone 3B, is used to assess the potential economic savings for the customer. The VCS was modeled using Engineering Equation Solver (EES). The simulation was carried out for cooling only during a week of extreme hot summer daytime temperature and the results showed that total energy consumption could be reduced by 14.5% with an 87.5% reduction in on-peak energy usage when the TES is installed. The cost of operating this system for space cooling was reduced by nearly 20% using the sample utility rate plan.

Research Question

How can PCM based Thermal Energy Storage be integrated into a heat pump for carbon mitigation, demand response, and reduced electric consumption of heat pumps in residential buildings?

Background

As of 2018, buildings in the United States accounted for about 40% of the total U.S. energy consumption and 75% of the total electricity consumption (U.S. Department of Energy, 2011; US EIA, 2020). Peak periods, generally, have the largest energy demand on the grid. Heating, ventilation, and air conditioning (HVAC) loads comprise 50% of building electricity consumption [53]. HVAC systems and the need for space cooling may exacerbate electrical demand issues during summer peak times, since as much as 50% of the grid electricity demand comes from homes mostly used for air conditioning [4].

Time-of-use (TOU), real-time-pricing (RTP), and other time-based utility rate structures are becoming more available to residential customers. TOU structures price electricity differently at specific hours during the day depending on the climate, time of year, the utility provider energy generation portfolio, and historical or predicted demand. On-peak hours are those where the electrical price is highest per unit energy for all electricity used from the grid in that time span. In summer months of warm climates, on-peak hours may be mid- to late-afternoon. In winter months of colder climates, on-peak hours may be early- to mid-morning. TOU rates vary wildly across the US. TOU rates are

predetermined and static during the contract period. The TOU analyzed here is an energy rate prized per kWh of energy used. Some TOU rates are demand based priced per average kW over short intervals. RTP rates reflect the instantaneous cost of bulk wholesale of electricity. Typically, prices are not disclosed to the customer more than a few days' notice but can be as short at three hours' notice the day prior. RTP rates are rare for residential customers due to this uncertainty. However, RTP rates generally do follow an hourly and monthly trend that may give the customer an economic advantage with proper controls and forecasting.

Researchers have investigated the impact of time-based utility pricing on residential electricity use with different load and energy demand control strategies. Findings suggest that electrical utility costs and peak hour energy demands associated with air conditioning can be reduced depending on utility rate structure, weather, building occupancy, and building thermal capacitance [181].

Yoon et al., (2016) demonstrated that depending on the size of house and utility price, up to 24.7% of HVAC loads can be reduced during peak times via demand response control and can provide up to 10.8% cost savings while maintaining occupant thermal comfort. Schibuola et al., (2015) simulated heat pump control based on RTP, with up to 30% of electricity consumption cost savings. Gottwalt et al., (2011) simulated the cumulative load profiles using TOU tariffs with smart appliances and concluded that the TOU tariffs could create new grid-level demand peaks which may not benefit the users economically, however, this practice may still benefit the utility providers by shifting more energy load to off-peak hours and effectively smoothing the demand curve.

TES is a popular energy storage solution to alleviate peak energy demand and may provide economic advantages to its users. TES can be realized by incorporating PCMs into HX either coupled to the existing HVAC system or interfacing directly with the space to be conditioned, thus creating a high-performance demand response energy storage system [3]. TES systems allow conventional air conditioning machinery to operate during off-peak hours, but leverage the isothermal storage properties of PCM to provide cooling during on-

peak hours [182]. PCMs may be incorporated as passive or active TES. Passive systems have no coupling to HVAC systems and do not respond to control schemes, but still may reduce building energy consumption [70], [75], [183]–[185].

Active TES systems, the focus of this paper, couple the TES to the HVAC system to respond to pricing and thermal signals. Active systems offer a high level of control of the TES and can improve energy storage efficiency [103], [118] evaluated residential HVAC loads' demand response potential, suggesting that value can be added by using even a small TES system. Table 13 summarizes studies on the energy and cost savings with PCM-based TES active storage.

The literature in Table 13 confirm that the cooling energy demand can be significantly shifted to off-peak times by using PCM-based active TES system integrated with building equipment such as HVAC [3], [30]. In addition, some studies have concluded that using PCM-based active TES to offset the peak load is more financially viable in the regions having higher electricity prices for on-peak hours and where the cooling systems dominate the demand [30], [186].

The literature survey shows that previous work on demand side management to off-set peak load using time-based utility pricing is mostly based on a demand response control without a TES. Some studies investigate an active PCM storage with heat pump, HVAC, or air conditioning system but most of them have focused on energy savings by shifting the load from high demand periods to low demand periods without considering the time-based utility pricing and a direct use of conventional VCS to accomplish heat transfer with TES.

In this work, a southern California residential building's summertime cooling load during a week of extreme high temperatures is comparatively modeled with and without active TES. The TES is directly coupled to a vapor compression system and serves as the VCS condensing unit during peak hours rather than the ambient air.

Table 13: PCM-based active TES for load shifting.

Author	Location	System Configuration	Energy savings	Cost savings
Bruno et al., 2014	Adelaide, Australia	PCM storage with chiller	13% energy savings	Not reported
Sehar et al., 2012	Various USA locations	Ice storage coupled with chiller	Peak time savings	35% annual cost savings
Mosaffa et al., 2016	Tehran, Iran	PCM slabs coupled with vapor type compressor	7-9% energy savings	Not reported
Jaber et al., 2012	Amman, Jordan	PCM coupled with indirect evaporative cooling system	80% less cooling load	7-8-year payback
Zhu et al., 2011	Beijing, and Hong Kong	PCM layers in air conditioning system	20% peak load reduction	11% cost reduced
Real et al., 2014	Madrid, Spain	PCM storage tanks with HVAC	18.97% energy saved	Not reported
Chaiyat, 2015	Chiang Mai, Thailand	PCM integrated in conventional HVAC system	Load decreased by 3.09 kWh/d	9.1% cost saved, 4.15 yr payback
Pop et al., 2018	Variable (12 global climates)	PCM integrated in fresh air-cooling system	7-41% energy saved	Not reported
Hirmiz et al., 2019	UK	Heat pump integrated PCM	Load shift of 6 hr., COP increased	Not reported
Dong et al., 2019	Knoxville, TN, USA	PCM integrated with electrical Heat Pump	13% less power consumed	Electricity cost saved 19%

The PCM embedded in the TES for this analysis is ice/water with a phase change temperature of 0°C, and only interacts with VCS, not directly with the building. A residential TOU utility rate from a utility provider in California, corresponding to the climate zone 3B, is used to assess the potential economic savings for the customer. The VCS was modeled using Engineering Equation Solver (EES).

Methodology

The complete modeled system is modular with several models converging including a simplified building, an R410A vapor compression system (VCS), TES with embedded PCM and heat exchanger, thermostatic controls, and a TES control strategy. The thermostat monitors the building indoor temperature and dispatches a call for cooling to the VCS system. The TES control strategy determines if the cooling is provided from the TES or by traditional VCS operation coupled to the ambient based on the time of day and utility electrical rate. The TES control strategy uses this same data to recharge the TES system using the same VCS, coupling the TES to the ambient when appropriate. The PCM used in this study is water/ice. The ambient weather data and TOU utility rate structure are from the same geographic region, ASHRAE climate zone 3B. The system is simulated for one week with a time step of one minute.

System Overview

A basic vapor compression system (VCS) is coupled to the water/ice-embedded TES. The TES heat exchanger is assumed to have infinite heat transfer coefficient and is at 0°C at all times. The PCM heat exchanger can serve as either evaporator or condenser in the VCS, depending on the mode of operation.

The coefficient of performance (COP) of a VCS is a measure of the desired heat moved to the electrical energy expended and is written as Equation 1 where Q is the heat removed for cooling as in refrigeration.

$$COP_c = \frac{Q_{evap}}{W_{comp}} \quad (1)$$

Figure 20a shows the baseline system whereby the building is cooled with VCS acting as a conventional air conditioning system. The building air is cooled by the VCS evaporator and heat expelled into the ambient at the condenser. The VCS moves heat from the building to the ambient across a positive temperature gradient. The increasing width of arrows represent added heat.

The building cooling performance can be improved with PCM-embedded TES, using negative temperature lift to introduce a more favorable gradient for which the VCS to operate, as illustrated in the Figure 20b. In this mode, the VCS condenser is coupled to the colder temperature of the PCM, 0°C in this system. Thus, the VCS has a negative temperature gradient to move the building thermal load. This allows the VCS to operate at a much higher performance as compared to the baseline. The TES can only operate when there exists some frozen PCM inside. Once all the PCM is melted, the TES can no longer absorb isothermal heat and the baseline VCS operation must be used to cool the building.

System Operating Modes and Controls

There are four operating modes (0,1,2,3, respectively) of the system as shown in Figure 21.

- In standby mode (0), the VCS is off the building responds to ambient thermal loads and solar heat gains.
- In the normal operating mode (1), the building is cooled by conventional VCS refrigeration with no TES involvement. The condenser heat, $Q_{cond,}$ is the heat being dumped to the ambient and the evaporator heat, $Q_{evap,}$ is the heat removed from the building and directed to the heat pump.
- In charging mode (2), the PCM HX operates as the evaporator and the latent heat of freezing is removed from the PCM. The VCS condenser heat is rejected to the ambient.

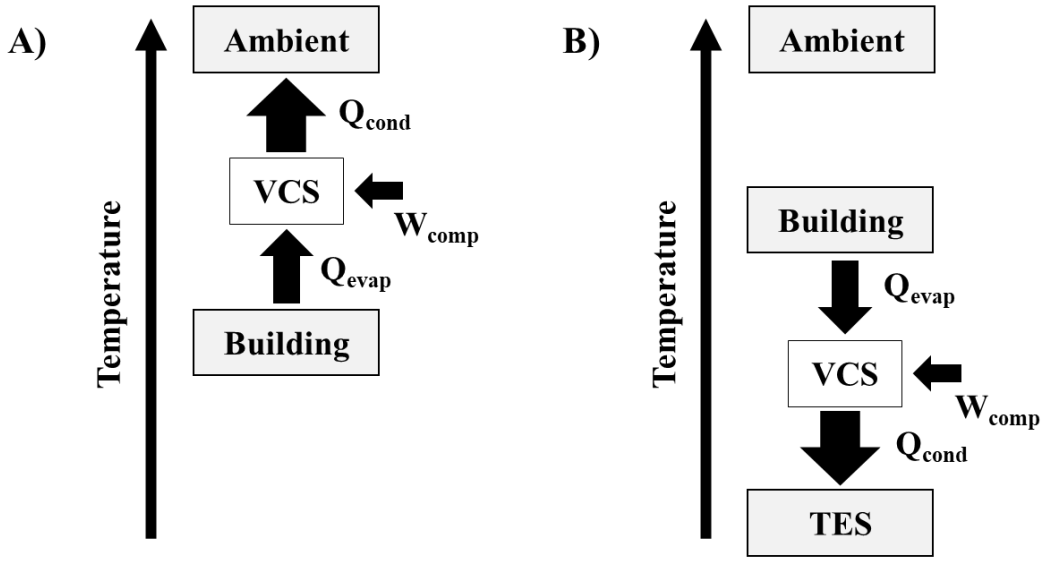


Figure 20: Comparison of temperature gradients for a) normal VCS operation and b) TES-assisted cooling

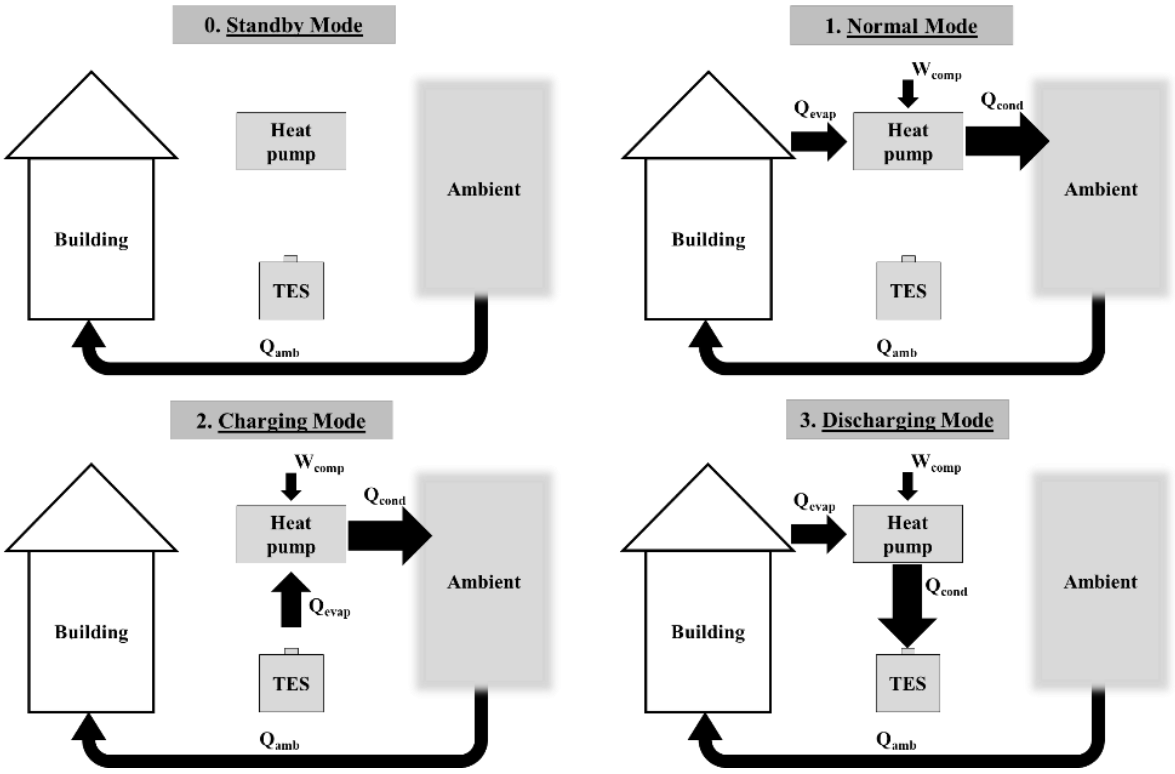


Figure 21: Energy flows in the four operating modes for summer (cooling only)

- In discharging mode (3), the PCM HX is the condenser and the heat, Q_{cond}, is absorbed by the PCM through the latent heat of melting. In this mode, the COP is higher than in normal operation.

The operating mode of VCS-TES system is selected by the controls decision tree shown in Figure 22. The selection depends on the on-peak/off-peak time, the need to cool the building, and PCM state of charge (SOC). When the thermostat calls for cooling during off-peak times, the VCS will enter normal mode operation. Normal mode is conventional HVAC operation. Charging mode restores the energy stored in the TES by refreezing any melted PCM and is only activated during off-peak times when the thermostat is not calling for building cooling to take advantage of the lower electrical cost and, incidentally, usually lower ambient temperatures. Charging mode can be interrupted by the thermostat if the building requires cooling and the system will enter normal mode, maintaining building indoor comfort. During on-peak time, when the thermostat calls for cooling, discharging mode will activate which cools the building with the TES. During discharging, the PCM in the TES is being melted and the latent heat associated with melting maintains a constant cold TES temperature. The TES can only operate when there exists some frozen PCM inside. Once all the PCM is melted, the TES can no longer absorb isothermal heat and the normal mode must be used to cool the building. All other times the VCS is in standby mode.

The overall flow of information in the model is depicted in Figure 23. The decision tree works as the main control to coordinate all these components. The feedback arrows represent the updated (i+1) values being fed back to the main models.

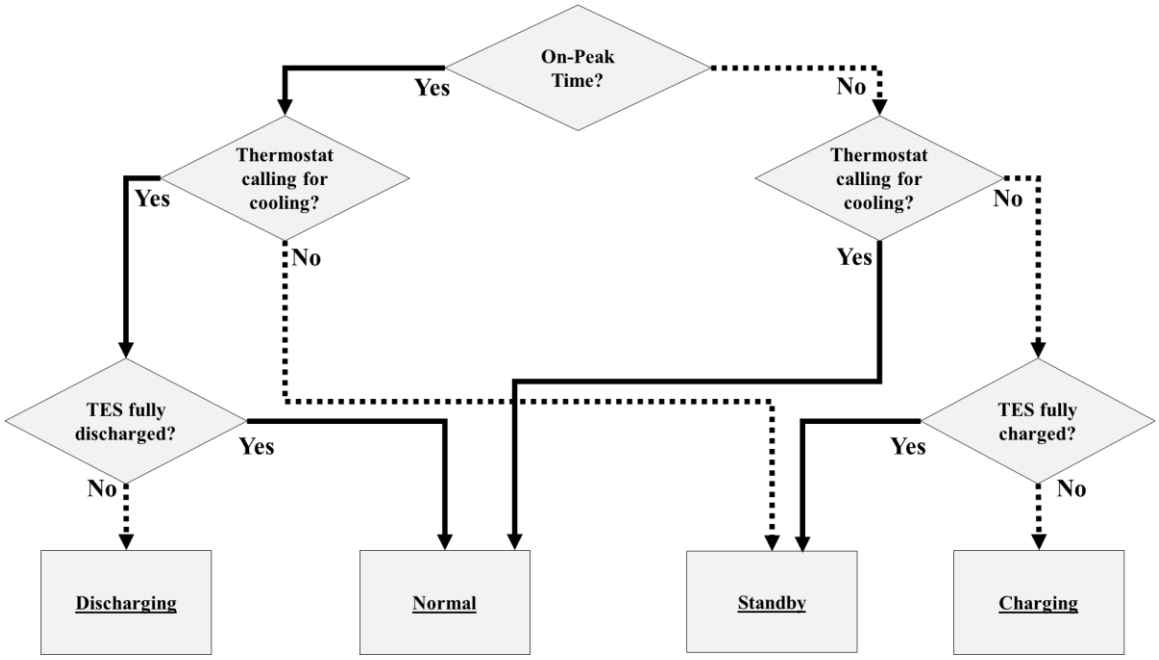


Figure 22: Controls decision tree

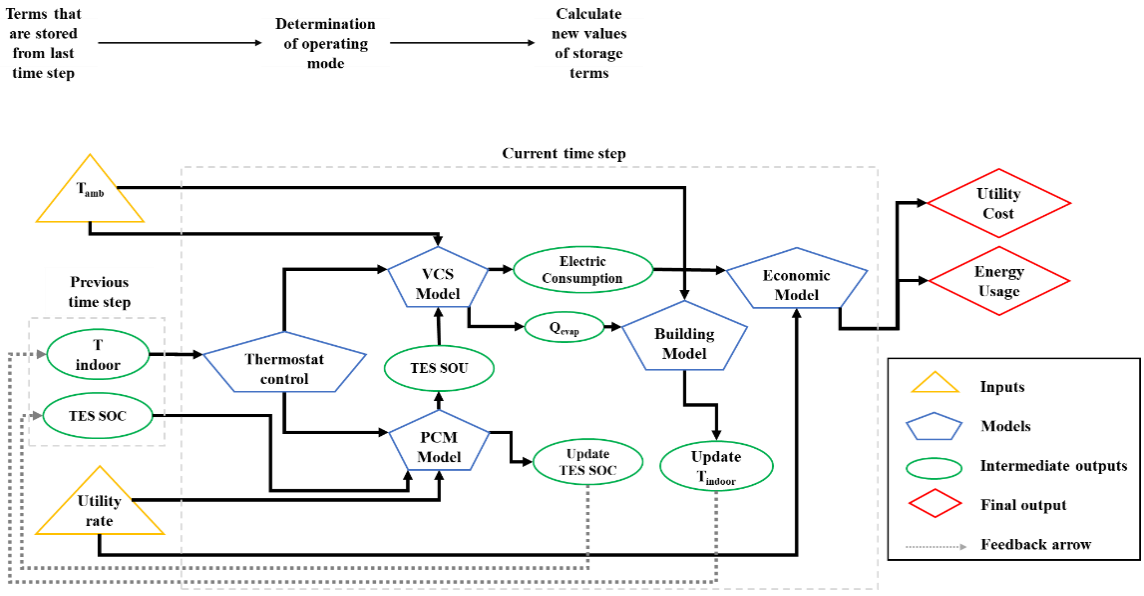


Figure 23: Total system information flow and relation between sub-models

Component Models

Weather Data

The system's performance is evaluated for a hot week in a dry climate of southern California, ASHRAE climate zone 3B, June 24-30, 1994. TMY 3 weather data for Fresno County, CA was used. The location correlates to the utility pricing. The dry bulb temperature is shown in Figure 24 with the indoor comfort temperature range shown for reference.

Building Model

A simplified building model is used to simulate the thermal response of the building. The simplified model calculates the indoor temperature depending on the ambient heat load, VCS heat load, and the building thermal capacitance. The ambient heat load is modeled by using an assumed building balance point temperature of 18°C with the heat exchange from the ambient proportional to the difference between the outdoor ambient temperature and the point balance temperature, as shown in Equation (2). The effective heat transfer coefficient, *U*, was estimated to be 0.21 kW-K^{-1}.

$$Q_{amb} = U * (T_{amb} - T_{bal}) \quad (2)$$

The indoor temperature is determined based on the heat balance according to Equation (3) where Q_{VCS} is the cooling load provided from the VCS in either normal or discharging modes dependent on the controls in Figure 4. The time step, dt, in this simulation is one minute. An overall effective building thermal capacitance, C, of 16459 J/K was chosen to represent a typical single-family house with 223 m^2 (2400 ft^2) area [3].

$$T_{indoor,i+1} = \frac{-(Q_{VCS} - Q_{amb}) * dt}{C} + T_{indoor,i} \quad (3)$$

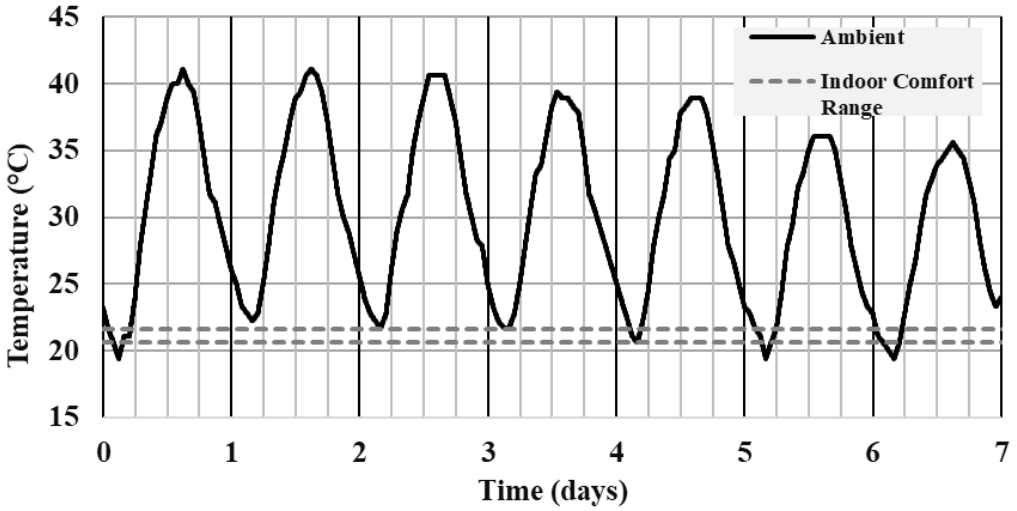


Figure 24: Ambient dry bulb temperature for the simulated week

Building Thermostat Model

The thermostat control has a constant setpoint of 21.1°C (70°F) and a deadband of ±0.5°C (±1.8°F). When the building temperature rises above the setpoint temperature plus the deadband, the VCS will be activated to cool the building in either normal or discharging mode dependent on the decision tree of Figure 22. The building will cool until the temperature falls below the setpoint temperature minus the deadband where the VCS will be shut off for direct building cooling.

VCS Model

The VCS was modeled in Engineering Equation Solver [187] to model a 2-ton HVAC system and couple it with PCM TES. The VCS uses R410a as the refrigerant with a constant volumetric flow through the compressor. The VCS modeled is ideal: the compressor undergoes isentropic compression, the expansion valve sees isenthalpic expansion, and there is no pressure drop across either the condenser or evaporator. In normal operation, the dry bulb temperature is taken as evaporator temperature. An approach temperature of 5 deg was fixed. The discharging, charging, and normal modes were modeled independently, and lookup tables developed.

For all modes the compressor has the same constant volumetric flow rate, 2.5e-6 m^3. In the normal and discharging modes, the VCS interfaces with the building with an evaporator at a near constant 15°C temperature. In the normal mode the condenser is coupled to the ambient, thus the ambient temperature, as shown in Figure 5, was used as an input. In discharging mode, the condenser is coupled to the TES, kept at a constant 0°C. Fans with a power draw of 0.585 kW are present only in the building air handling unit and the outdoor condensing unit and are activated when the operating mode dictates. The TES does not have a fan. While in charging mode, the VCS evaporator interfaces with the TES and the condenser to the ambient. Thus, the TES heat exchanger must be able to be switched from a condensing mode to evaporating mode. For a real system of this type, controllable valves, check valves, switches, and other special components may be

necessary for the TES system to make this switch. The simplicity of this model assumes these challenges can be met.

The work and heat for all modes was calculated and called upon by the building and thermostat models as determined by the decision tree of Figure 22 and the information flow of Figure 23. The values of work and heat are shown in Figure 25 plotted against the ambient temperature where applicable. The discharging mode has no external temperature dependence and thus its operating parameters are constant.

TES Model

The VCS is coupled to the TES system; the TES does not interact with the building directly and is insulated from ambient exposure. The PCM embedded in the TES is water/ice with a melting temperature of 0°C, in an assumed 80-gallon tank, which provides nearly 27.8 kWh of cooling capacity. The necessary heat exchanger in the TES is assumed to have near infinite heat transfer rate such that the temperature within the TES is constant at 0°C. The state of charge (SOC) is the percentage of maximum energy stored within the TES. When the TES is operated in the discharging or charging modes, the energy contained and SOC are reduced or increased, respectively, by the amount of heat determined by the VCS model.

This model only charges the TES between the hours of 1am and 7am. Different time controls or schedules may be utilized in real systems to avoid off-peak power demand spikes as predicted by Gottwalt et al., (2011) or to take advantage of abundant energy on the grid from daytime solar or heavy wind periods, depending on the energy portfolio of the utility provider or any off-grid energy sources a customer may have.

Utility Rate Analysis

The TOU utility tariff used in this analysis is Pacific Gas and Electric (PG&E) Electric Schedule E-TOU-B (Pacific Gas and Electric, 2020).

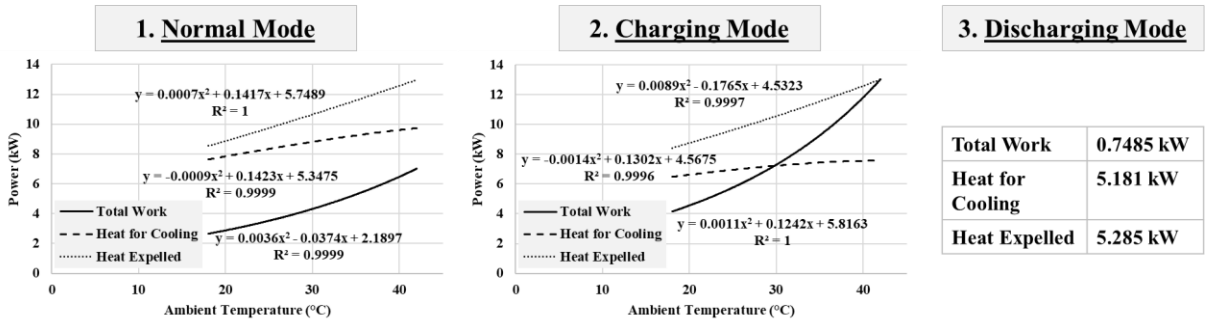


Figure 25: VCS operating power for normal, charging, and discharging modes.

This is a legacy tariff as of May 1, 2020, no longer accepting new customers, but the pricing structure is representative of the difference between on-peak and off-peak prices for current tariffs in the region (California Public Utilities Commission, 2019). The tariff is priced as follows: from June 1 to Sep 30, peak hours are 4pm to 9pm, Monday through Friday with a rate of $0.39689/kWh; all other hours, including all weekend hours, are off peak rates of $0.29383/kWh. Winter rates (Oct 1 – May 31) differ.

Ambient dry bulb temperature is plotted against utility rate in figure 26. Peak time also occurs when cooling demand is higher, so the control strategy is designed to shift the load from high demand period at extreme ambient temperatures.

Results and Discussion

For the simulated 7-day period, the electric consumption of the HVAC system and the total utility cost are compared for systems with and without water/ice-based TES. Figure 27 shows the total electric consumption as well as the on-peak hour consumption. Note that only the first five days (weekdays) have on-peak pricing; weekends are considered off-peak. The baseline system without TES used 353.2 kWh total with 98.1 kWh used during on-peak hours: weekdays, 4pm – 9pm. With the TES system, the total electrical usage was reduced 14.5% to 302.1 kWh including an 87.5% reduction of on-peak usage to 12.3 kWh.

The utility cost to run the VCS on a hot summer day increases as a function of outdoor dry bulb temperature. During the utility rate peak hours, 4 PM to 9 PM on weekdays, the cost spikes in the base case. The utility cost to cool the building is shown in Figure 28. The baseline model without the TES resulted in $112.52 but use of the TES system cost nearly 20% less at $90.04 for this simulated week. It should be noted that California has some of the highest utility costs in the US and this week simulated has particularly hot temperatures. These results should neither be extrapolated to yearly savings nor may be representative of other climates or regions. However, this does show that during extreme heat events, TES will be a crucial energy saving mechanism, reduce on-peak energy demand, and may be economically beneficial for the customer.

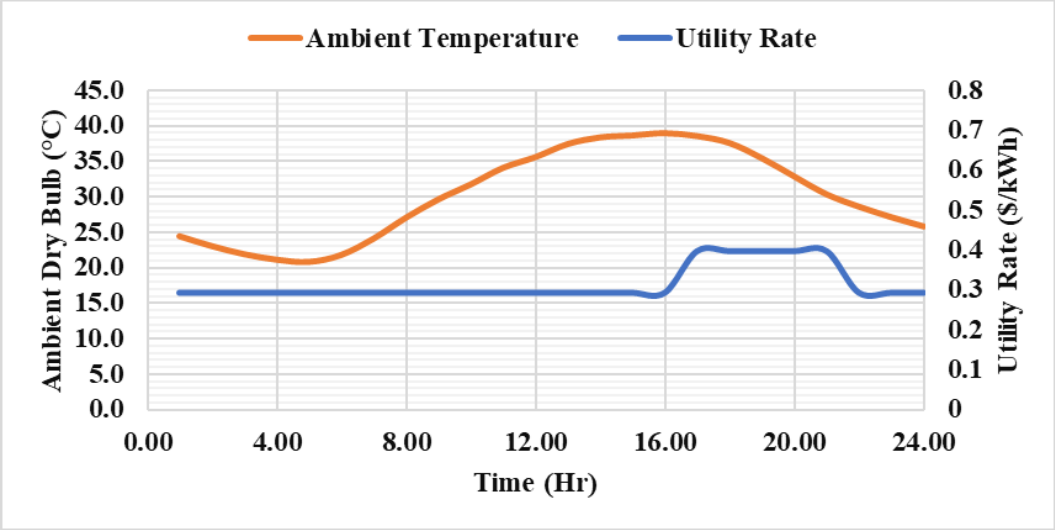


Figure 26: Ambient Temperature and Utility Data

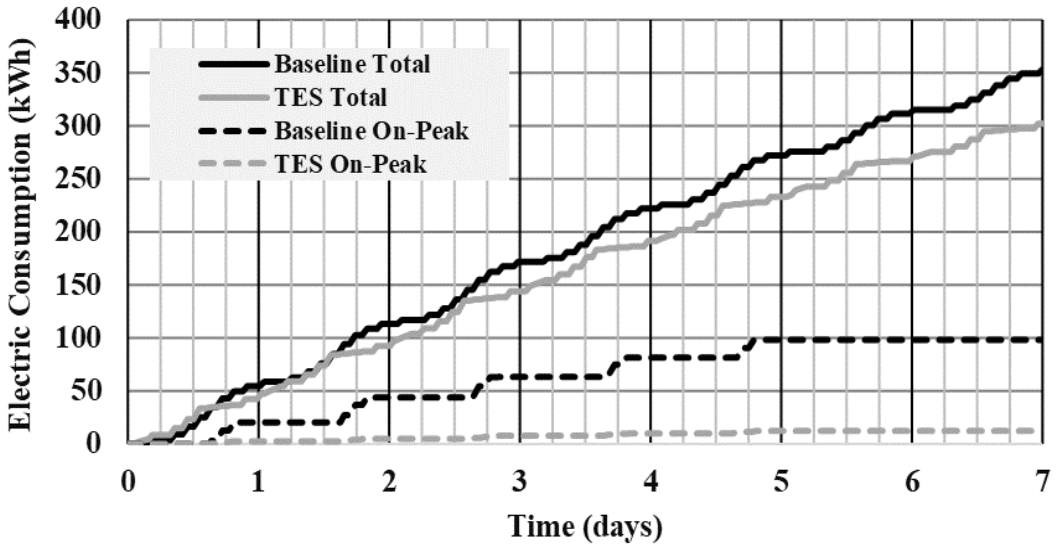


Figure 27: Electric Consumption comparison with and without TES

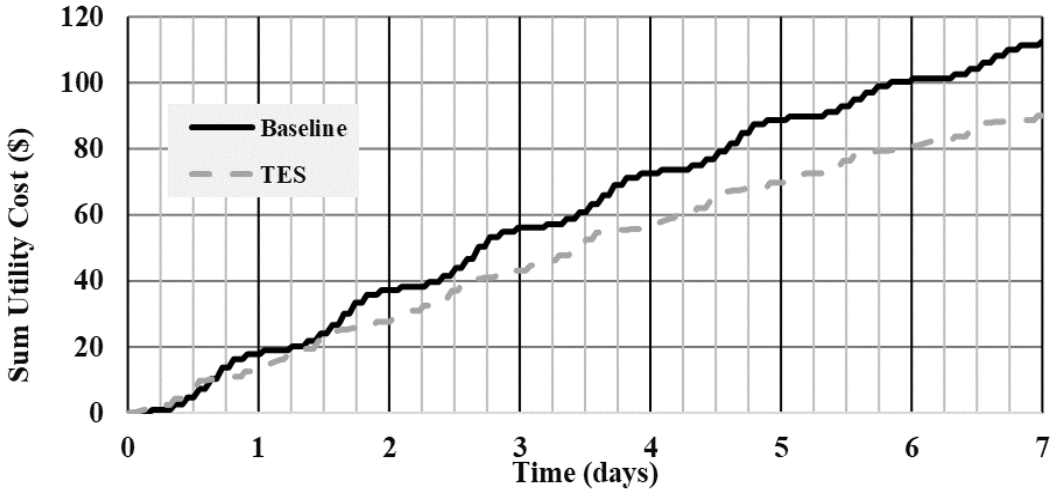


Figure 28: Total electrical utility cost with and without TES

Figure 29 shows the PCM state of charge (SOC) during the modeled time. The PCM is fully charged during off-peak hours and is discharged during peak times. Only on two days does the PCM fully discharge causing the VCS to revert to normal mode operation during peak hours. Despite this, the 100 gallon ice PCM is able to provide adequate energy for cooling for peak utility rate hours on a typical summer day in this climate.

Figure 30 shows indoor temperature profile with and without PCM. It can be seen that the occupant comfort was successfully maintained at 20°C for all the operating modes.

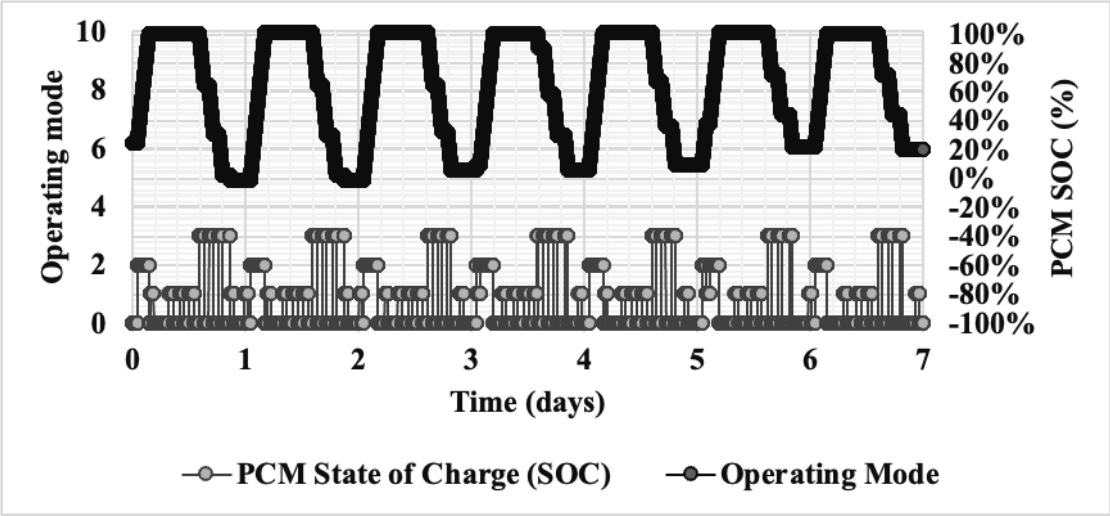


Figure 29: PCM SOC

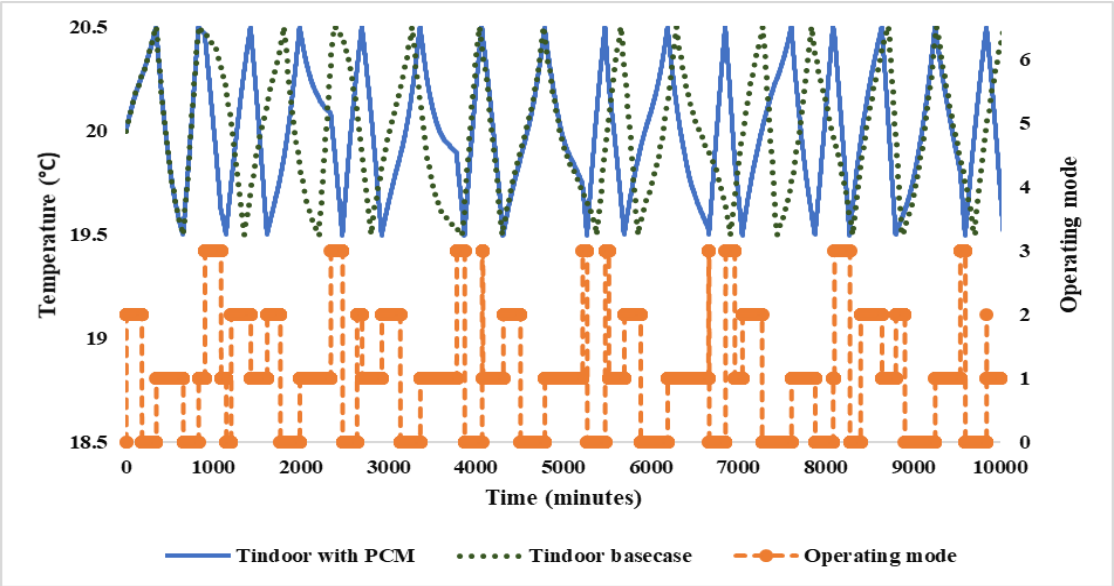


Figure 30: Indoor Temperature Profile

CONCLUSIONS

A residential building was modeled with PCM-based TES and the economic and energy savings were estimated under a TOU rate structure with a rate difference of 0.103$/kWh between on-peak and off-peak. The TMY3 weather data was used for ASHRAE climate zone 3B. The analysis showed that the total energy used to cool the space was reduced from 353.2 kWh without TES to 302.1 kWh with TES, a 14.5% reduction. The on-peak energy usage was reduced by 87.5%, from 98.1 kWh without TES to 12.3 kWh with TES. In addition, the cost to the customer was reduced by nearly 20%, from $112.52 without TES to $90.04 with TES.

Since only 7 days were simulated, the results should not be extrapolated for annual savings, but highlights the potential for reducing peak energy demand during weather extremes. This work also suggests that the demand side management systems, including TES, with on time-based electricity prices may create an economic advantage for residential customers to shift peak energy loads without compromising comfort. TES are a valuable tool to level out electrical grid demand and add stability to the grid.

CHAPTER IV

OPTIMISING PHASE CHANGE TEMPERATURE FOR HEAT PUMP INTEGRATED WITH TES

A version of this chapter is submitted for publication by S. Sultan *et al*:

Sultan, S., Hirschey J., Kumar N., Cui B., Liu X., LaClair T., & Gluesenkamp, K. R. (2023). "Techno-Economic Assessment of Residential Heat Pump Integrated with Thermal Energy Storage." *Energies*

Conceptualization, data collection, methodology and original manuscript draft was prepared by Sara Sultan, Jason Hirschey, and Navin Kumar. Borui Cui, Tim LaClair, and Xiaobing Liu provided help with editing and analysis. Review and supervision by Kyle R. Gluesenkamp.

Abstract

Phase change material (PCM)-based thermal energy storage (TES) can provide energy and cost savings and peak demand reduction benefits for grid-interactive residential buildings. Researchers established that these benefits vary greatly depending on the PCM phase change temperature (PCT), total TES storage capacity, system configuration and location and climate of the building. In this study, preliminary techno-economic performance is reported for a novel heat pump (HP)-integrated TES system using idealized approach. A simplified HP-TES was modeled for 1 year of space heating and cooling loads for a residential building in three different climates in the United States. The vapor compression system of the HP was modified to integrate with TES, and all heat transfer to and from the TES was mediated by the HP. A single PCM was used for heating and cooling, and the PCT and TES capacity were varied to observe their effects on the building's energy consumption, peak load shifting and cost savings. The maximum reduction in electric consumption, utility cost and peak electric demand were achieved at a PCT of 30°C for New York City and 20°C for Houston and Birmingham. Peak energy consumption in Houston, New York City, and Birmingham was reduced by 47%, 53%, and 70%, respectively, by shifting peak load using a time-of-use utility schedule. TES with 170 MJ storage capacity allowed for maximum demand shift from on-peak to off-peak hours, with

diminishing returns once the TES capacity equalled the daily building thermal loads experienced during the most extreme ambient conditions.

Research Question

What is the optimum PCM temperature and heat pump configuration for maximum economic and grid benefits of heat pump integrated TES?

Background

Buildings are responsible for about 40% of the total energy consumed in the United States [1], accounting for 75% of the total electricity consumption and 78% of the 2:00–8:00 p.m. peak period of electricity use [2, 3]. As of 2020, 75% of the homes in the United States use central air conditioning [190]. Since space conditioning loads comprise about half of the total building's load [188], residential buildings present an opportunity to reduce peak energy demands by managing building's heating and cooling demand and can relieve stress on the electric grid during peak times by shifting the peak loads [5, 6, 7, 8].

Thermal energy storage (TES) has been identified as a key enabler for reducing peak demand and providing resilience for reliable operation during power outages, as described in the US Department of Energy's *Grid-interactive Efficient Buildings* report [188]. According to the report [188], consumers who pay demand charges or time-of-use (TOU) rates are generally the most financially driven to adopt the technology because TES is beneficial for shifting predictable daily loads for demand response.

The US Census Bureau reports that more than 44% of US houses were built before 1970 and were constructed according to outdated standards [191]. As a result, oversized heat pumps (HPs) are essential for regulating humidity and temperature inside the house. Although renovating the house or fully upgrading the conventional HVAC equipment can be costly, heat pump (HP) systems are adaptable because they are able to respond smartly to the fluctuations in peak demand. The capabilities of HPs and TES can be combined by integrating these technologies. This integration allows the use of already-established

technology and resources with minimal equipment to reduce the installation complexity and TES footprint [2, 10]

Many possibilities exist for packaging phase change material (PCM)-TES in various configurations. Passive TES configurations, in which TES charging and discharging occur according to an uncontrolled independent variable such as ambient temperature and PCM melting temperature, are more common in literature. Passive TES may provide energy and cost saving benefits, but they pose challenges such as complex installation, material encapsulation, space constraints, and additional controls and components. Furthermore, passive TES are not ideal for peak demand reduction because they do not have control over TES operation [11, 12, 13, 14, 15, 16]. In active TES configurations, the decision of when to charge and discharge is determined by controller hardware. The major benefit of active TES configurations is the flexibility to be installed in an existing building infrastructure without needing a significant construction—the TES may be separate and removed from the space and simply integrated into existing HP equipment. The heat transfer is mediated by the HP in active HP–integrated TES (HP-TES) configurations, and the user can control the charging and discharging process based on cooling or heating demand because HP-TES is programable with the thermostat [23].

State of the art

Researchers have installed PCM via passive TES configurations in walls, ceilings, windows, or embedded directly into building materials such as concrete [17, 18, 19, 20, 21, 22]. HP-integrated active TES, where TES has been coupled to or installed in HP components such as an evaporator or condenser [23, 24, 25, 26, 27, 28] is the focus of this paper. The techno-economic value for each configuration varies by charging and discharging operation, storage capacity and the material used. A previous review [23] pointed out that researchers have shown energy savings of 9%–62% when using TES, but the PCM temperature and storage varies in each study [23].

A particularly promising active HP-TES configuration by Dong et al. [3] offers large performance improvement with minimum modification while reducing the TES footprint. The ice-based TES system simulated for 100 residential buildings in Tennessee was mediated by HP and absorbs the air conditioner's condenser heat during peak hours. Peak load of 12.7% was shifted, saving 19% of winter electricity cost and 13% of electric consumption for space heating on a winter day in Nashville.

The selection of PCM, phase change temperature (PCT) and storage capacity are important to design the appropriate TES [192]. Various approaches can be found in literature that choose the PCT to maximize their performance for space conditioning in buildings. Waqas et al. [192] argued that PCM temperature selection should be close to the comfort temperature of the chosen climate location. Medved and Arkar [121] studied passive cooling for continental climates and found the PCM with a melting point equal to the average temperature of hottest month was the most appropriate choice (i.e., 20°C–22°C). Waqas and Kumar [160] demonstrated optimum PCM storage unit performance by selecting a PCM with the melting point equal to the comfort temperature of hottest month for free cooling.

A single PCM unit for heating and cooling was analysed for the subtropical humid climate of Islamabad, Pakistan, which observes large variations in summer and winter temperatures [193]. A commercial PCM (salt and paraffin blend) was used, and a parametric study was performed. The optimum melting point was approximately 29°C for summer and approximately 21°C for winter. Both seasons could have optimized performance at approximately 27.5°C, but the cooling capacity drastically drops below this point. The study concluded that to choose a single melting temperature for both applications, the PCM melting point that maximized summer cooling could be used for winter heating but not vice versa [193].

Passive PCM-TES is proven to be effective for space cooling in literature, but for the climates with less significant diurnal or annual temperature variations, passive systems may not be beneficial [29, 32].

PCM temperature optimization has been studied by various researchers and is briefly discussed in Table 14. The table summarizes the range of PCTs used in each paper, with the optimized PCT for respective application. Notably, PCM is mostly used passively and is integrated in the building envelope.

The literature survey on optimization studies suggests that only passive systems have been investigated to find optimum PCT, which is room temperature for the majority of cases. Different PCM materials and melting temperatures have been selected for heating and cooling applications for a given TES [33, 34, 35, 36, 37, 38, 39, 40, 41, 42].

For the configuration chosen for this study, PCM-TES was not directly used to cool or heat the building but was coupled to the HP to provide a heat sink/source. This type of system can be integrated with the existing HP via active configuration and is beneficial for residential buildings [23], where even small TES can provide peak energy savings.

Research Gap and Objectives

This study fills a gap in the literature by modeling a single PCM characterized by a single PCT in HP-TES configuration for heating and cooling. This study evaluated the economic and grid benefits of HP-TES using time-based utility rates in three climates and performed parametric analysis. The PCM was installed in a heat exchanger coupled to the HP, with heat transfer to and from the TES always mediated by the HP. The HP model, building model and PCM model were simplified to show the promise of such HP-TES configurations. The scope of this study was to determine the optimum PCT and storage capacity for maximum energy savings, cost savings and peak load shifting benefits of the said configuration of HP-integrated TES.

The novelty of this research is:

- Evaluating a novel configuration of HP-TES and determining economic value of the system.

Table 14: Literature review on PCM temperature optimization

References	PCM material & melting range	Optimized PCM temperature	Methodology (Simulation based studies)	Application and PCM integration
[161]	Honeycomb PCM (26°C–29°C)	29°C (cooling)	Numerical, EnergyPlus (E+)	PCM-enhanced envelopes
[162]	Bio PCM (20°C–25°C)	25°C (cooling) 20°C (heating)	ConFD in E+	In building envelope coupled to HVAC
[163]	n-Octadecane PCM (22°C–32°C)	28°C (cooling)	Temperature controlled, E+	In wall coupled to HVAC, Benchmark cubic model
[164]	30 wt % paraffin PCM (23°C–26°C)	26°C (cooling) 20°C (heating)	Optimization using h-T function in E+ and GenOpt	Microencapsulated PCM direct integration in building envelope (inner surface of the exterior walls and roof)
[194]	Various Bio PCMs (21°C–29°C)	25°C (cooling) 21°C (heating)	Optimized PCM performance in E+	Various configurations with integration in wall
[168]	Knauf PCM, 30% microencapsulated paraffin (23°C–26°C)	25°C–25.9 °C (cooling)	10 scenarios in 4 climates, E+, shifted peak demand	Building envelope coupled to HVAC with controlled ventilation for charging
[170]	Paraffin with EG and polyethylene 1.(20°C–45°C) 2.(5°C–30°C)	27.5°C (cooling) 16.5°C (heating)	TRNSYS heat transfer model and GenOpt optimization	Double layer PCM Trombe wall PCM1: heat insulation PCM2: preservation

- Using single PCM for both heating and cooling for an active HP-TES, and determining optimum phase change temperature and storage capacity.

Methodology

The modeled system was composed of several models that operate simultaneously, including a simplified building model, vapor compression HP model, TES with embedded PCM as a heat exchanger, and thermostat model that monitors the building's indoor temperature and implements rule-based controls based on a fixed TOU pricing schedule. The HP-TES system was modeled using MATLAB.

The TES consists of an arbitrary PCM; the PCT does not correspond to any specific PCMs. The TES only interacts with the HP, and no direct heat transfer occurred between the TES and building. In this configuration, the TES was coupled to the vapor compression system (VCS) and absorbed the condenser heat during summer peak hours; the TES provided the evaporator heat during winter peak hours.

The focus of this study was to evaluate the effect of HP-integrated PCM-TES using simple, rule-based controls with time-based, predefined utility rates. The effects on peak energy consumption, annual energy consumption, and energy cost were calculated. A simple building model and control strategy were used, and these can be further improved in future studies to achieve more accurate results.

The building and TES-integrated HP was modeled for 1 calendar year using a minute time step. For each minute, the thermal profile of the building, the operation of the HP, and the cumulative electrical energy usage of the HP were determined. The temperature and energy storage capacity of TES were parametrically varied. Three different climate locations within the United States were examined: Birmingham, Alabama (ASHRAE climate zone 3A, mixed humid); Houston, Texas (2A, hot humid); and New York City, New York (4A, mixed humid) [195]. Each of these geographical locations requires summertime cooling and wintertime heating, but the amount of each varies.

With this model, the TES temperature corresponding to the lowest annual HP energy consumption was determined, which helped identify which PCMs may be integrated into TES systems for each location. The model also identified the minimum TES energy storage capacity necessary to see these energy savings for the building size and type modeled. This informed the total system sizing, which can be used in future work to determine associated manufacturing and installation costs.

System Overview

Two cases were compared using TOU rates: baseline and TES. The baseline system did not include TES, and the heating or cooling was provided by air source HP via a vapor compression refrigeration system. The scope is limited to space conditioning only and this paper does not consider hot water preparation.

In the TES case, the basic VCS was modified to enhance its performance by coupling it to PCM-TES. The TES was assumed to have an infinite heat transfer coefficient and was always at a constant temperature. Depending on the mode of operation, the PCM heat exchanger can function either as an evaporator or condenser in the HP.

Figure 31 compares the temperature gradient for normal VCS operation (baseline system) for primary modes and TES-assisted cooling or heating. The baseline system for the primary cooling mode is shown in Figure 31a, where the building was cooled with VCS acting as conventional air conditioning system [154]. The VCS evaporator cooled the building air, and the condenser dispersed the heat into the ambient. A positive temperature gradient allowed the VCS to transfer heat between the building and the ambient. A similar positive gradient is illustrated in Figure 31c, representing a baseline system for the primary heating mode. The increasing width of arrows indicates added heat.

PCM-embedded TES can improve the building cooling and heating performance by introducing a more favorable temperature gradient for the operation of the VCS. Figure 31b shows the TES-assisted cooling, where the condenser was coupled to the colder temperature of the TES [154].

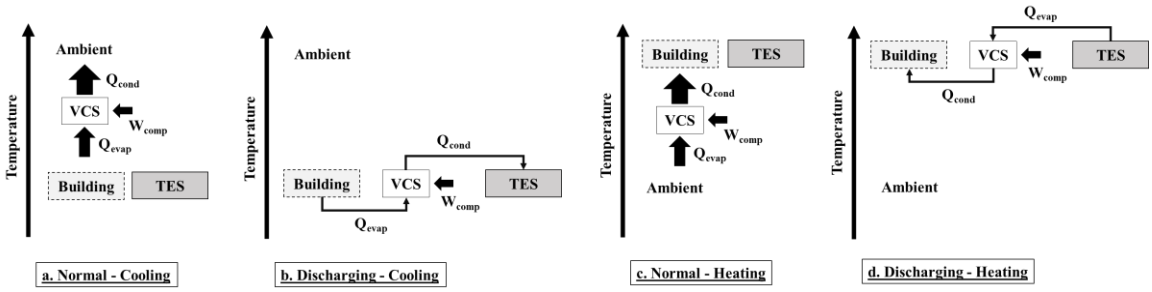


Figure 31: Comparison of temperature gradients for baseline and TES cases.

Therefore, to move the building's cooling load, the VCS had a negative temperature gradient. Similarly, for the TES-assisted heating, the evaporator was coupled to the hotter temperature of the PCM and moved the heating load using a negative gradient. This gradient enabled the VCS to operate at a much higher performance compared with the baseline.

Operating Modes

The system had two primary modes: a primary cooling mode and primary heating mode. Each primary mode had four operational modes: normal mode, charging mode, discharging mode, and standby. The TES was not involved in the standby and normal modes.

Standby mode is when the HP is off, and no cooling or heating is provided. The ambient thermal loads and solar heat is gained passively during the standby cooling mode. In the normal mode, the building is cooled or heated by conventional HP operation only. In the primary cooling mode, the vapor compression cycle operates such that the condenser moves heat (Q_{cond}) to the ambient, and the evaporator removes heat (Q_{evap}) from the building. In the primary heating mode, the vapor compression cycle is reversed; the evaporator extracts energy from the ambient, and the condenser delivers heat to the building.

For discharging operation in primary cooling mode, the evaporator is coupled to the building to provide space cooling, and the condenser is coupled to the TES. The heat, Q_{cond}, is absorbed by the PCM through latent heat of melting. Likewise, for discharging operation in primary heating mode, the HP condenser is coupled to the building to provide space heating, and the evaporator is coupled to the TES. The PCM releases heat, Q_{evap}. The coefficient of performance (COP) is higher than in the normal operation during discharging.

The PCM heat exchanger operates as the evaporator in the charging mode for cooling. The latent heat of freezing is removed from the PCM, and the condenser heat is rejected to

the ambient. In the charging heating mode, the PCM operates as the condenser and absorbs Q_{cond} through the latent heat of melting.

Figures 32 and 33 show the configurations in all operating modes.

Component Models

The total model was a collection of submodels that operated together to maintain indoor building temperature at comfortable levels at each 1-minute time step of the simulation. Figure 34 shows the general operating schematic of the total model and the exchange of information between submodels. All models were written in MATLAB. The following sections describe each submodel in detail.

Weather Data

Typical meteorological year (TMY3) data was used for this analysis [196]. This TMY3 data is hourly in its raw form with each temperature corresponding to the end of the hour. It was interpolated using a spline fit to expand to minute time step resolution. Only the ambient temperature was used. This model did not include solar irradiation or wind on the building. This information can be included in future model iterations. Considering the solar irradiation in building model would be expected to change the building loads. Specifically, solar gain in winters would decrease the winter daytime building load (with limited effect on the electricity demand during the morning grid peak time) while solar gain in summer would increase the summer peak load. This may increase the importance of summer load, and require larger cooling capacity. Potentially, our load shifting controls will then also generate higher benefits.

The climate locations studied were Birmingham, Houston, and New York City, corresponding to ASHRAE climate zones 3A (mixed humid), 2A (hot humid), and 4A (mixed humid), respectively [195]. These are the representative climate zones from both cooling and heating dominated regions and should have different performance affected by the weather.

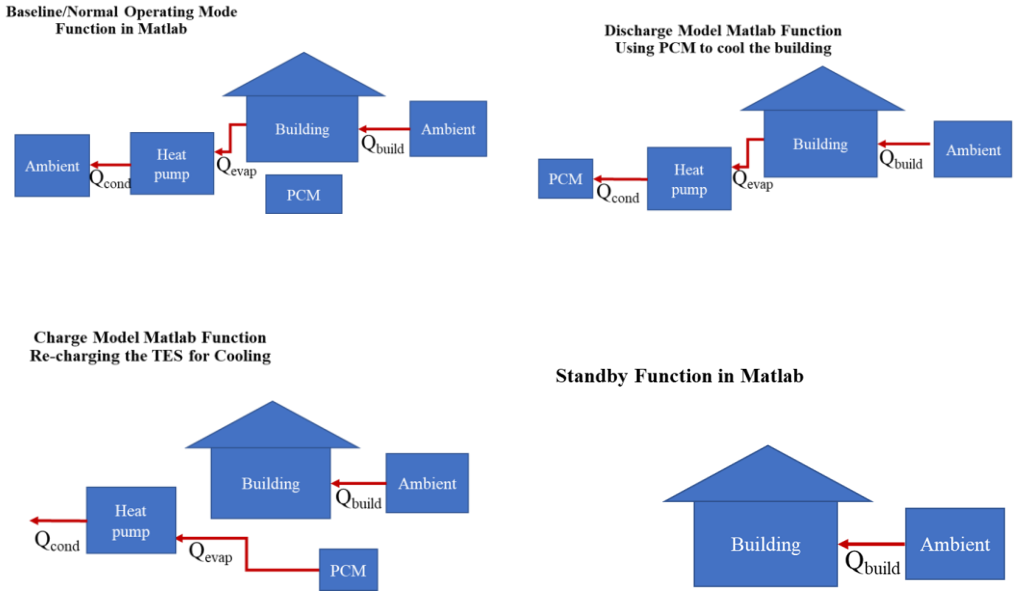


Figure 32: Cooling Operating modes with TES.

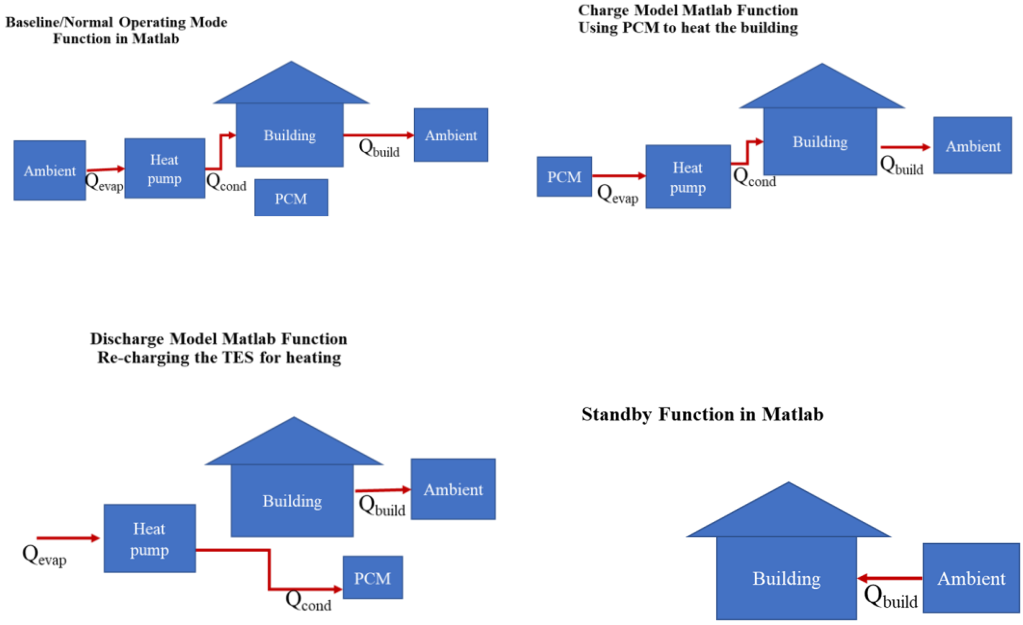


Figure 33: Heating Operating modes with TES.

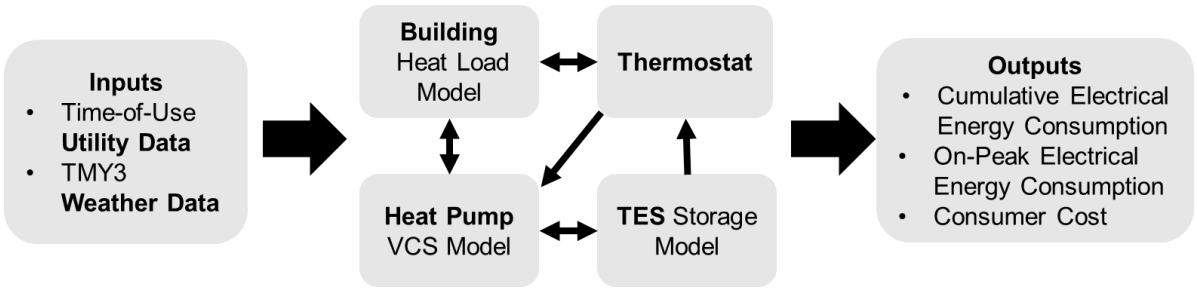


Figure 34: Operation flow chart showing the submodels and direction of information flow.

Figure 35 shows the average ambient dry-bulb temperature during each month for all three locations.

Utility Data

For this model, the on-peak periods were determined using TOU utility rates available to a residential consumer in each geographic location. TOU rates price the cost of electricity differently depending on the time of day and the month. In this analysis, only energy-based TOU rates were used—that is, the electricity is priced per kilowatt hour. Other TOU rates may have limitations on the instantaneous demand, but this factor was not considered here.

TOU rates were found for each location, and the model was run such that the on-peak times were determined when the cost of electricity was higher than the baseline. Table 15 shows the utility cost information during 2020 for all locations, which demonstrates the disparity in electrical pricing across the United States and highlights the different financial incentives that TES may offer.

TES Model

The TES model was simplified for ease in analysis with only energy balance performed; no considerations were made to the inner workings of the TES system. The TES was assumed to be a heat exchanger with embedded PCM, which enabled isothermal operation. In this analysis, the TES heat exchanger was considered to have an infinite heat transfer coefficient; thus, the TES was maintained at the PCM PCT, T_{TES}. The model was simplified to assume that T_{evap} and T_{cond} were equal to T_{TES} during charging and discharging modes, respectively, when TES was coupled to HP.

The PCM is idealized in this model, leading to more favorable results. Zero glid and zero super cooling were assumed [45, 46].

The TES stored the thermal energy desirable for the primary space conditioning mode, which defines the state of charge (SOC).

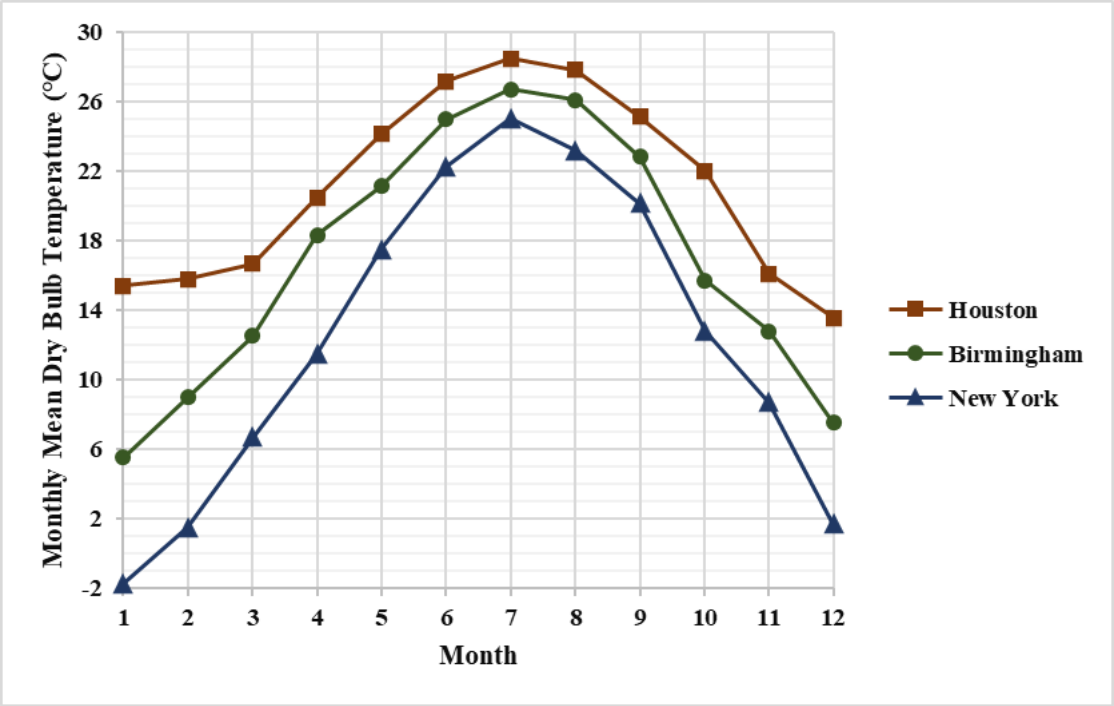


Figure 35: Average dry-bulb temperature.

Table 15: Electric utility rates

Location	Utility	TOU tariff			Non-TOU tariff	
		Tariff name	**On-peak rate (¢/kWh)**	**Off-peak rate (¢/kWh)**	**Tariff name**	**¢/kWh**
Birmingham, Alabama	Alabama Power	Residential Time Advantage	27.0 (summer[1]) 9.0 (winter[2])	7.0 (summer[1]) 7.0 (winter[2])	Standard Rate Plan	12.48 (summer[1]) 12.23 (winter[2])
Houston, Texas	Gexa Energy	Free Mornings & Nights 12	24.5 (year round)	0 (year round)	EveryDay | EveryNight 12	20.3
New York City, New York	ConEdison	Rate II - Residential and Religious - Voluntary Time-of-Day	40.1 (summer[1]) 14.5 (winter[2])	1.5 (summer[1]) 1.5 (winter[2])	Rate I - Residential and Religious	14.6 (summer[1]) 12.7 (winter[2])

At its full capacity, TES SOC is 0 in primary cooling mode and 1 in primary heating mode. TES SOC is defined as a thermal battery, where 0 refers to the PCM fully frozen (zero usable thermal energy), and 1 indicates that its fully melted (full of thermal energy).

Table 16 explains the SOC in different modes. During discharging cooling mode, the TES acts as a heat sink for the HP, and TES SOC increases, melting the PCM. During discharging heating mode, TES acts as a heat source for the HP, and TES SOC decreases, solidifying the PCM. During the use of TES, if energy storage capacity is reached, the system will default to normal mode operation.

Thermostat Controls

The thermostat is the core of the model and communicated information between all submodels. It determined which operating mode to use to run the TES system by monitoring the indoor temperature, TES SOC, and on-peak status. Thermostat controls are implemented in two steps. First, depending on the monthly average temperature, the thermostat determined if the building and HP were operating in primary heating mode or primary cooling mode for the given month. If the monthly average ambient temperature was greater than 2°C above indoor set point temperature, the system operated in primary cooling mode for that month. Otherwise, the system defaulted to primary heating mode. This step is only for convenience and does not impact the results. For the main controls to determine TES operating modes, daily values were considered, and indoor temperature is rewritten for each minutely time step.

The building set point temperature and dead band for the primary cooling mode was 23°C ± 0.5°C and 20°C ± 0.5°C for the primary heating mode, which correspond to typical occupant behavior and ASHRAE standards for indoor climate comfort (ASHRAE 55). In the primary cooling mode, the system primed itself to reduce energy only to cool. If the indoor space needed to be heated during this mode, the TES wouldn’t be used, and the system would only use the normal heating mode. The same is true in the primary heating

mode. Within these primary modes, the thermostat determined whether the heat pump or TES should be used for cooling or heating at a given time.

As shown in the control's decision tree in Figure 36, if cooling or heating was not needed during off-peak time, and the TES SOC < 1, charging mode was activated. During peak time, TES was discharged until SOC reached 0.

Table 16 shows the operating mode decisions based on indoor temperature, SOC and peak time (TOU) determination. Primary modes (column 1), as determined by monthly average temperature, had controls to determine operating modes (column 5). T_{indoor} and TOU were checked at each time step, but SOC was only checked for TES modes after the first two conditions were met. This decision was the first decision made in each time step, and the appropriate information was sent to each submodel.

Heat Pump Model

The R410A refrigerant HP was modeled first in Engineering Equation Solver (EES) for an array of evaporator and condenser temperatures. The EES model was the same as that in previous work [14]. HP electrical work and heat loads were calculated from the EES model and fit to the following equations.

$$Q_{\text{hc}} = a(T_{\text{evap}}) \times b \times c(T_{\text{evap}}, T_{\text{cond}}) \quad (4)$$

where the parameter *a* curve fits the density of saturated R410A vapor at the compressor suction.

$$a(T_{\text{evap}}) = (30.5571378 + (1.02160466 \times T_{\text{evap}}) + (0.0138446344 \times T_{\text{evap}}^2)) \quad (5)$$

Parameter *b* normalizes the operation of the HP such that 7.5 kW of cooling is achieved with T_{evap} = 0°C and T_{cond} = 35°C.

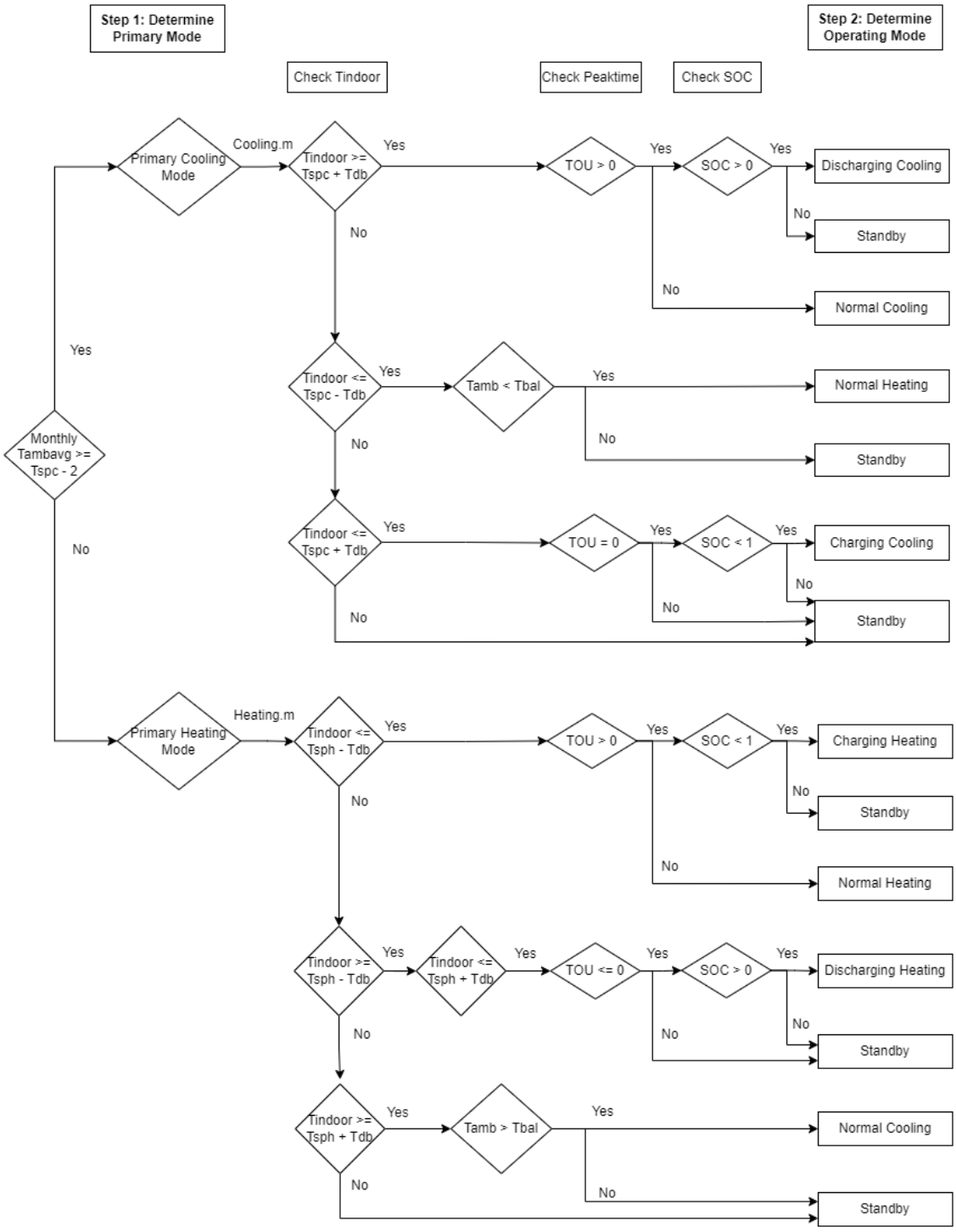


Figure 36: Controls decision tree.

Table 16: Operating mode examples

Primary Mode	Conditions to satisfy for operating mode			Operating mode
	$T_{indoor(i-1)}$	Peak time	SOC	
Primary Cooling	≥23.5 (thermostat calls for cooling)	Yes	>0	Discharging cooling $T_{evap} \equiv T_{indoor}$ $T_{cond} \equiv T_{TES}$
		No	Any	Normal cooling $T_{evap} \equiv T_{indoor}$ $T_{cond} \equiv T_{ambient}$
	≤23.5 (thermostat does not call for cooling)	No	<1	Charging cooling $T_{evap} \equiv T_{TES}$ $T_{cond} \equiv T_{ambient}$
	≤22.5 and $T_{bal} > T_{amb(i)}$ (thermostat calls for heating)	No	Any	Normal heating $T_{evap} \equiv T_{ambient}$ $T_{cond} \equiv T_{indoor}$
	All other times			Standby
Primary Heating	≤19.5 (thermostat doesn't call for heating)	No	<1	Charging heating $T_{evap} \equiv T_{ambient}$ $T_{cond} \equiv T_{TES}$
		No	Any	Normal heating $T_{evap} \equiv T_{ambient}$ $T_{cond} \equiv T_{indoor}$
	≥19.5 and ≤20.5 (thermostat calls for heating)	Yes	>0	Discharging heating $T_{evap} \equiv T_{TES}$ $T_{cond} \equiv T_{indoor}$
	≥20.5 and $T_{bal} < T_{amb(i)}$ (thermostat calls for cooling)	No	Any	Normal cooling $T_{evap} \equiv T_{indoor}$ $T_{cond} \equiv T_{ambient}$
	All other times			Standby

$$b = \frac{7.5}{30.58} \tag{6}$$

Parameter *c* accounts for the increase in vapor mass fraction quality entering the evaporator during isenthalpic expansion. The approximate specific heat, c_p, is 1.5 J/(g·K) and 220 is approximate enthalpy of vaporization, ΔH_g, for R410A used in Equation 4 to normalize parameter *c*.

$$c\left(T_{\text{evap}}, T_{\text{cond}}\right) = 1 - \frac{\left(1.5 \times \left(T_{\text{cond}} - T_{\text{evap}}\right)\right)}{220} \tag{7}$$

The coefficients of performance for heating and cooling were estimated using Carnot relationships and an assumed Carnot efficiency of 30%. In the case where the heat source was hotter than the heat sink, this study assumed a fixed COP. Paired with Equation 4, the heating and cooling capacity and electrical work were determined for given condensing and evaporating temperatures of the HP. During the total model run, the inputs to T_{cond} and T_{evap} were either the indoor temperature, TES temperature, or ambient temperature decided by the thermostat model and the operating mode.

Figure 37 shows T-s diagram for cooling cycle with PCM. This assumption causes high approach temperature on the condenser.

Building Model

The building model was simplified to focus on HP-TES configuration. A simple, single resistor and single capacitance (1R-1C) building system was used for calculating the thermal loads on the building [154], [199]. The heating and cooling of the building was based on daily TMY data of the individual climate regions. The resistance values were calculated based on building loads by analysing prebuilt building models in each climate zone from EnergyPlus [200]. The values for a typical 2,500 ft^2 detached single family home in the United States were assumed as overall heat transfer coefficient; UA = 0.11 kW/K. The building capacitance; C_{build} was calculated using Equation 10 with the balance temperature of 15°C.

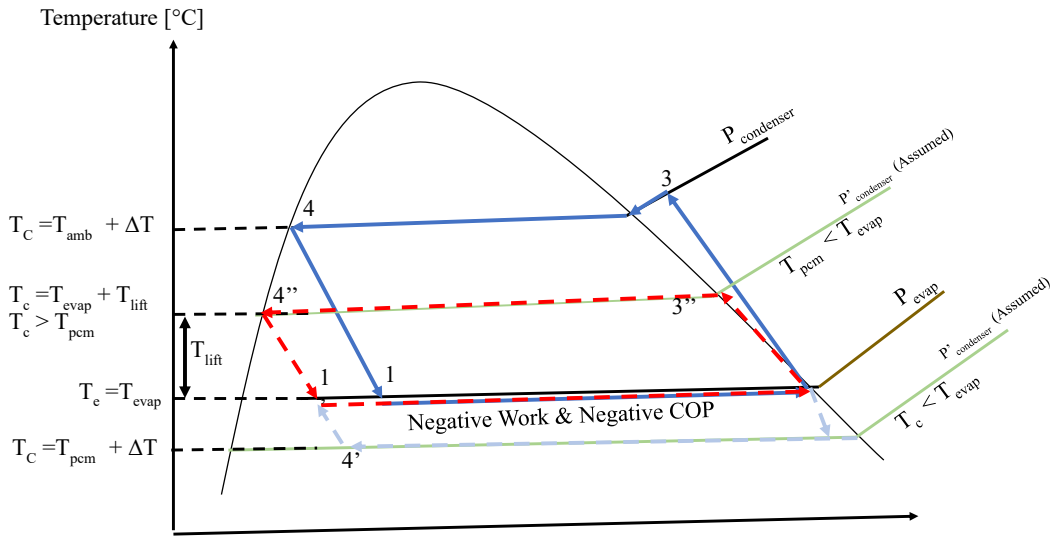


Figure 37: T-s diagram for cooling cycle

The heat load on the building from the ambient was calculated simply using the building UA and the difference between balance point temperature and ambient temperature at time *i*.

$$Q_{\text{building},i} = UA \times \left(T_{\text{amb},i} - T_{\text{balance}}\right) \tag{8}$$

The building indoor temperature was set at the set point temperature at the initial time step, and at the next time step $i + 1$, it was found by Equation 6. This equation sums the heat load from the ambient and the heat load from the HP submodel.

$$T_{b\text{building},i+1} = T_{\text{building},i} - \frac{\left(Q_{\text{heat,pump}} - Q_{\text{building},i}\right)}{C_{\text{build}}} \times dt \tag{9}$$

$$C_{b\text{uild}} = m^{*}\, C_p \times dt \tag{10}$$

Humidity was not considered in this model. Future iterations of this analysis may improve on the building model.

Results

The PCT and TES storage capacity (E_{PCM}) were varied parametrically to evaluate their effect on utility cost, electric consumption and peak consumption for a year. PCT was varied from 5°C to 45°C and E_{PCM} from 5.56 to 47.2 kWh (20 to 170 MJ). Three locations in the United States were simulated.

In the following sections, results are presented for each location for annual electricity energy consumption, annual electricity consumed during peak hours and annual electric utility cost. Note that the scale on the vertical axis changes for each location. Each line in a figure corresponds to a different energy storage capacity of the TES, and winter and summer seasons were plotted separately. Baseline is the case where no TES was present, and the system operated as a conventional air source HP system.

For utility cost analysis, the TES case used the TOU tariff, and there were two baseline cases. The primary baseline was the no-TES case, where a standard utility tariff (non-TOU) was implemented; the additional baseline was the no-TES case with a TOU tariff. For each location, TOU and non-TOU tariffs are mentioned in Table 15. The utility costs were the only energy consumption charges associated with space conditioning. This study excluded connection and base service charges.

Birmingham, Alabama

Birmingham is in ASHRAE climate zone 3A (warm and humid climate). Figure 35 shows the results for electricity consumption during peak times for winter and summer (as defined by utility tariff). The winter months simulated were those in which a winter TOU tariff was active for the local utility (October–May), and the summer months simulated were the months in which a summer TOU tariff was active (June–September).

The TES with a larger storage capacity allowed for more demand shift from on-peak to off-peak hours, with diminishing returns once the TES capacity equalled the daily building thermal loads experienced during the most extreme ambient conditions.

At PCT below 20°C for cooling, the peak energy consumption was consistent. This consistency was because the study assumed a constant COP when the source was hotter than the sink. Above 20°C shows decreasing benefits as the PCM temperature increased, and as it approached 35°C, the TES consumed more energy than the baseline. This increase was because the control strategy only depended on peak time, which was defined by the TOU rate; it did not depend on ambient weather. At 35°C, the peak energy consumption was the same regardless of the size. This lack of change was because 32°C–35°C was the average ambient temperature during summer peak hours, and discharging TES for cooling at 32°C–35°C was expected to be equivalent to or worse than the baseline. As PCT further increases, there was a penalty to discharge the system when TES becomes even hotter than the ambient; the TES consumed more energy than the baseline. Hence, TES was not

effective if PCT was closer to or hotter than the ambient. PCT of 20°C saved maximum energy for the cooling season, and 35°C was ideal for heating.

Figure 38 shows seasonal results. Throughout the year, using a single PCM with 20°C PCT and TES with 47.2 kWh (170 MJ) storage capacity, the annual reduction in energy consumption during on-peak hours was 70.5% (517 kWh/year baseline vs. 152 kWh/year with TES). In the TES case, the cumulative energy consumption during on-peak hours was 152 kWh/year (not shown in figure). Compared with the baseline, 365 kWh/year energy consumption was shifted from on-peak to off-peak hours.

Figure 39 shows summer and winter energy consumption associated with space conditioning as a function of PCT for different TES sizes. Percent cooling energy savings were highest with a PCT of 20°C and energy storage capacity of 33.3 kWh (120 MJ). During summers, at 20°C, the smallest TES consumed more energy than the baseline. This increase was because of the suboptimal rule-based control strategy, which did not account for ambient temperature in charging decision-making. TES was charging even when it was hot outside, and that hurt the charging-discharging cycle efficiency of the TES, resulting in more energy consumption. This effect was less prominent in a larger TES because it took longer for the larger TES to charge. For the cooling season, a larger TES experienced the charging process further into the evening when the ambient temperature naturally dropped. Cooling energy savings were observed only when the PCT was between 15°C and 25°C. It is unfavorable to use TES at temperatures far from the indoor temperature. The smallest 5.56 kWh (20 MJ) TES consumed less energy than the larger TES at extreme temperatures because the smallest did not get used as much.

The heating results are more consistent and do not deviate as much at extreme temperatures because Birmingham is a cooling-dominated climate. The ambient temperatures were not that extreme for frequent unfavorable charging, and even 70 MJ TES in this case could fulfil the heating demand at 35°C PCT.

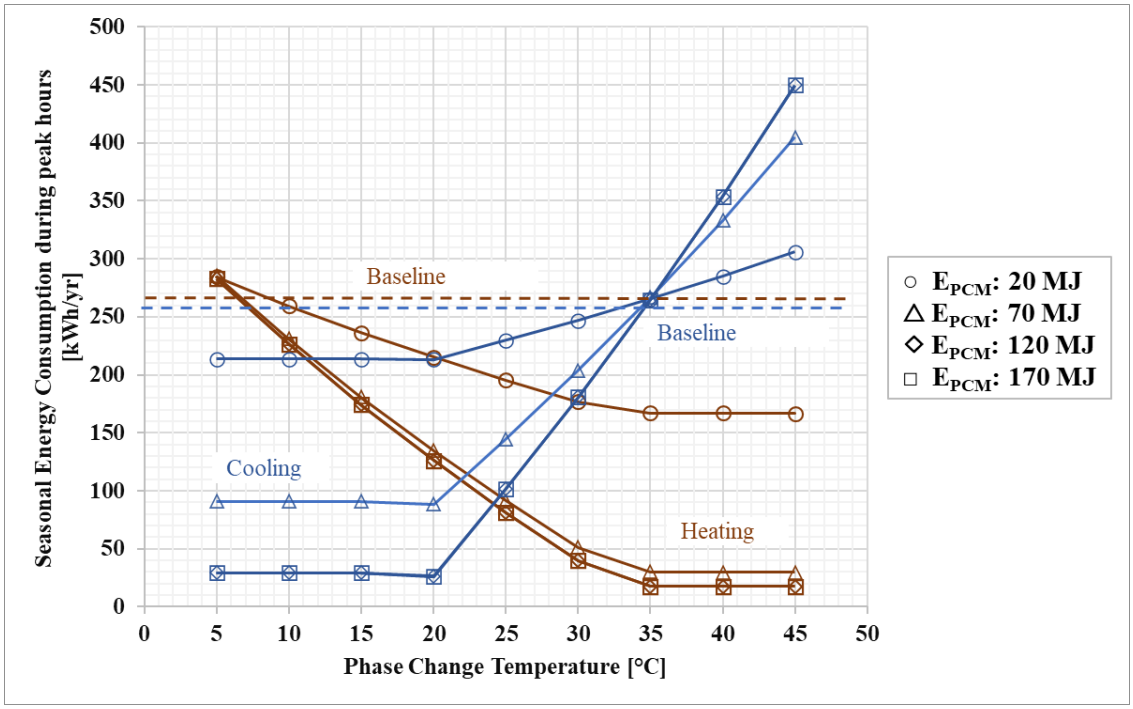


Figure 38: Birmingham results for peak energy consumption.

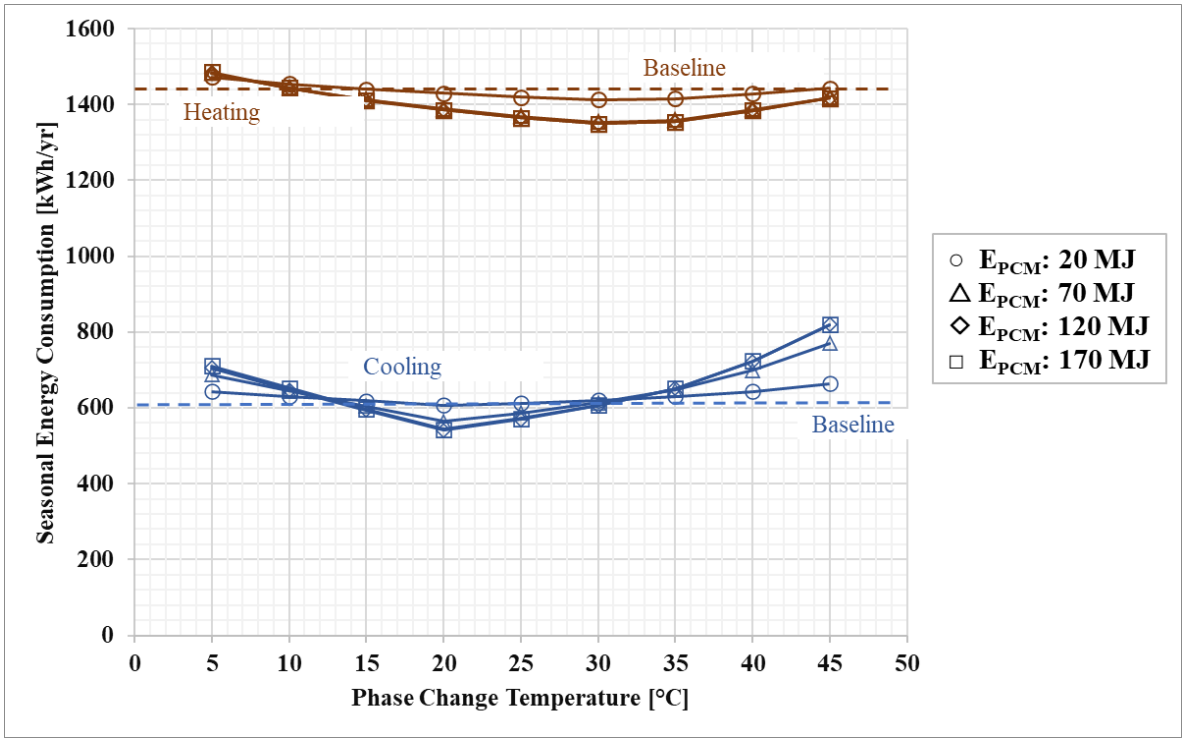


Figure 39: Birmingham results for energy consumption.

Annual energy savings (not shown in figure) for a single PCM with a PCT of 20°C at an energy storage capacity of 33.3 kWh (120 MJ) was 5.4% (2,036 kWh/year baseline vs. 1,925 kWh/year with TES). Annual energy savings in general were much less than peak savings because of the increased energy consumption during off-peak times required to recharge the TES. This result is consistent with previous works.

The heating and cooling cost of the integrated HP and TES system in Birmingham is shown in Figure 40. TES used the TOU rate and was compared against TOU and non-TOU baselines. The trend for TES is similar to the peak energy consumption for summers, except the cost slightly rose again below 20°C. This increase was because more off-peak energy below 20°C means an increase in utility payment. For winters, the off-peak price was greater than in summers; thus, the savings were more significant.

Figure 40 shows that TOU baselines were already saving cost as compared with non-TOU baselines. For the winter baseline case, more cost was saved using a TOU tariff. The difference between the primary baseline and TOU baseline is huge because on-peak and off-peak TOU rates were less than the standard rate (non-TOU) in winters. For summer, the primary baseline saved more cost than the TOU baseline because the on-peak TOU rate was much higher than the standard non-TOU rate (difference of 15.48 ¢/kWh).

Figure 40 shows seasonal results. Total annual results are not shown. The annual TES cost was $141/year (a savings of $111/year compared with the baseline). The 43.9% cost savings were achieved by using TES at 20°C PCT and 33.3 kWh (120 MJ) energy storage capacity under the TOU rate structure with $0.2/kWh price differential between on-peak and off-peak times during summers and $0.02/kWh during winters. For the baseline system, the annual energy cost would have been $252.7/year.

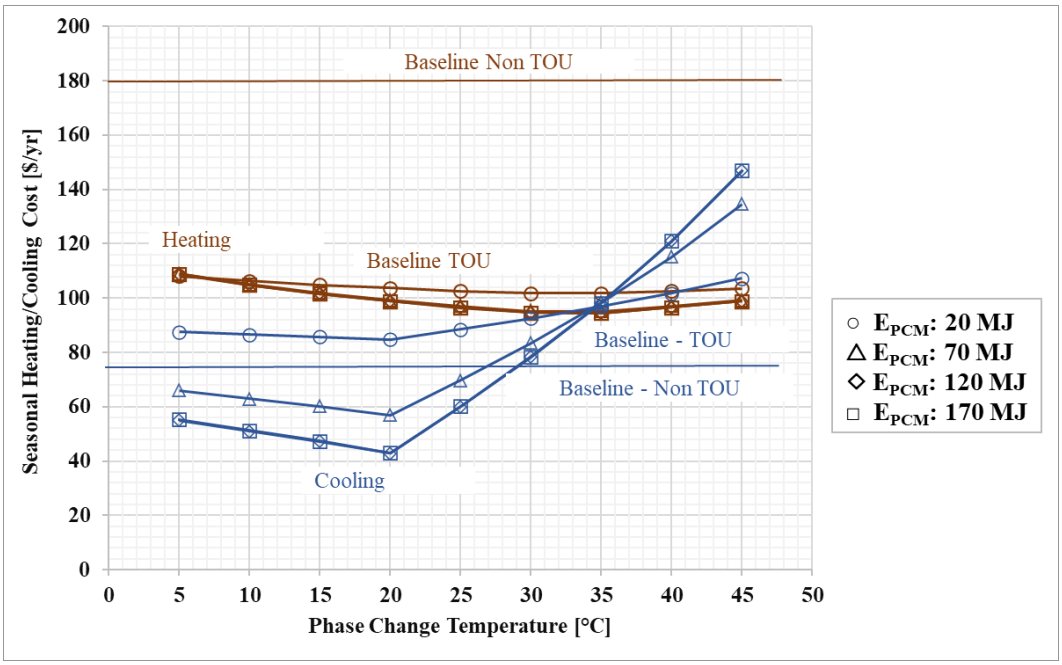


Figure 40: Birmingham results for utility cost.

New York City, New York

New York City is in ASHRAE climate zone 4A, a mixed humid climate. It is considered a subtropical continental climate with large variations between summer and winter.

Figure 41 shows the results for electricity consumption during peak times for winter and summer (as defined by utility tariff). Winter months were when the winter TOU tariff was active (October–May), and summer is the months in which the summer TOU tariff was active (June–September). The trend is similar to peak energy results in Birmingham. Maximum savings are observed at PCT 20°C for the summer season and 35°C for heating, with a 170 MJ storage capacity for both cases. TES was not effective when PCT was far from these values.

Figure 41 shows seasonal results optimized at different PCT and E_{PCM} for winter and summers. The annual results were calculated by performing parametric analysis for the whole year and finding the PCT and E_{PCM} that delivered maximum annual reduction in the cumulative energy consumption during on-peak hours. Peak energy consumption of 53% was reported, achieved by using a TES with 47.2 kWh (170 MJ) storage capacity and 30°C PCT under the TOU tariff. The on-peak TOU rates in New York are much higher than others. The cumulative energy consumption during on-peak hours was 627 kWh, and for the baseline, the minimum on-peak annual energy consumed was 1,344 kWh/year. Compared to the baseline, 717 kWh/year energy consumption was shifted from on-peak to off-peak hours.

Figure 42 shows seasonal energy consumption associated with space conditioning against PCT for different TES sizes. Cooling energy savings were insignificant—0.98%—achieved only with a PCT of 20°C, and heating savings (6.9%) were achieved with PCT 30°C, both at an energy storage capacity of 170 MJ. For heating, TES energy savings were observed when the PCT was between 25°C and 35°C. It is unfavorable to use TES otherwise.

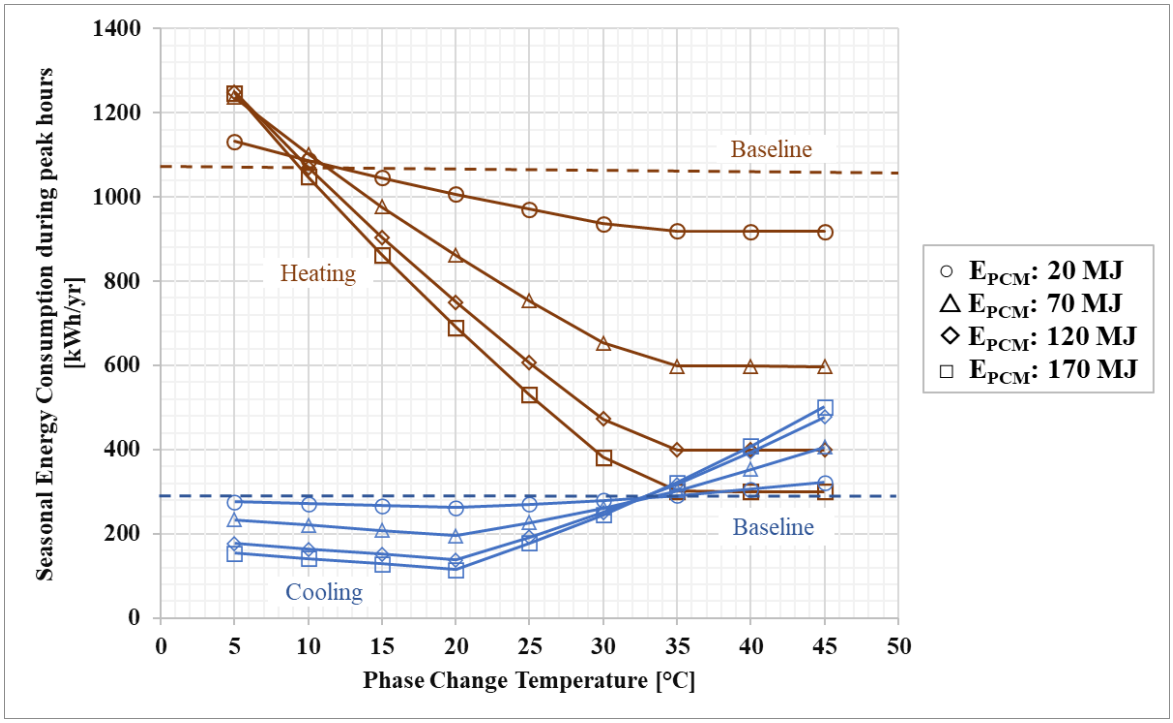


Figure 41: New York City results for peak energy consumption.

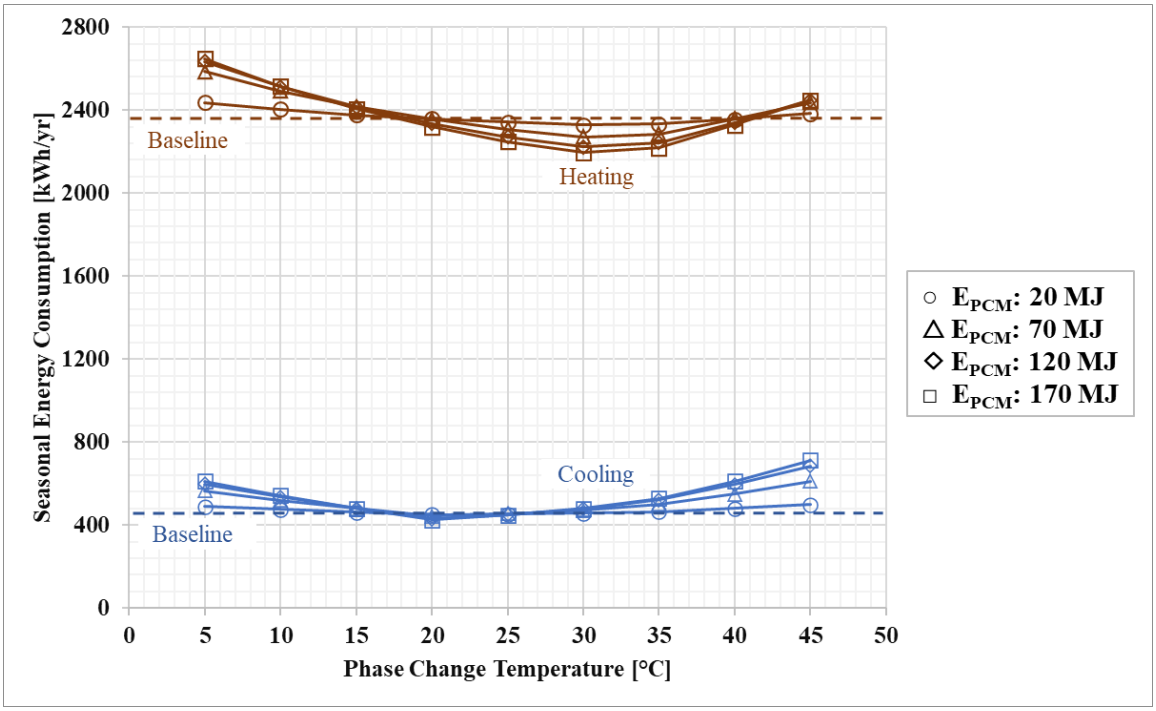


Figure 42: New York City results for energy consumption.

The maximum annual energy savings (not shown in figure) for New York City were approximately 3.9% (2,675 kWh/year vs. 2,785 kWh/year) with a PCT of 30°C and energy storage capacity of 47.2 kWh (170 MJ).

Figure 43 shows the seasonal heating and cooling cost of the integrated HP and TES system in New York City. Maximum TES savings were achieved using 170 MJ E_{PCM} at 35°C in winters and 20°C in summers. TES and TOU baselines meet at 32°C in summers and 10°C in winters, which indicates that discharging TES at these PCTs is the same as normal HP operation, yielding no savings.

For winters, TOU baselines saved more cost compared with non-TOU baselines. The TOU off-peak rate was very cheap, and it was almost free electricity at 1.5¢/kWh (Table 2). For summer, the primary baseline saved more cost than the TOU baseline because the on-peak TOU rate was much higher (40.1¢/kWh) than the standard non-TOU rate (14.6¢/kWh).

Annual savings of 35% were achieved at 30°C PCT and 170 MJ E_{PCM}. TES cost was $185/year under the TOU rate structure. Without the TOU rate structure, the minimum peak annual energy cost was $287.5/year.

Houston, Texas

Houston is a hot, humid climate zone, categorized in 2A. In these plots, winter was November through March, and summer was April through October, as defined by historical average climate in Houston [201].

Figure 44 shows peak energy consumption during winter and summer for Houston. The notable cooling energy savings were observed at PCT 20°C and E_{PCM} of 170 MJ. For the winter season, even a 70 MJ storage capacity was enough to meet the load, and maximum savings were achieved at PCT 35°C. Baseline heating and TES met at 20°C, which means that discharging TES for heating at 20°C would be the same as using an HP in normal mode. This was also the case for cooling at 35°C. The TES consumption increased at PCT far from these values.

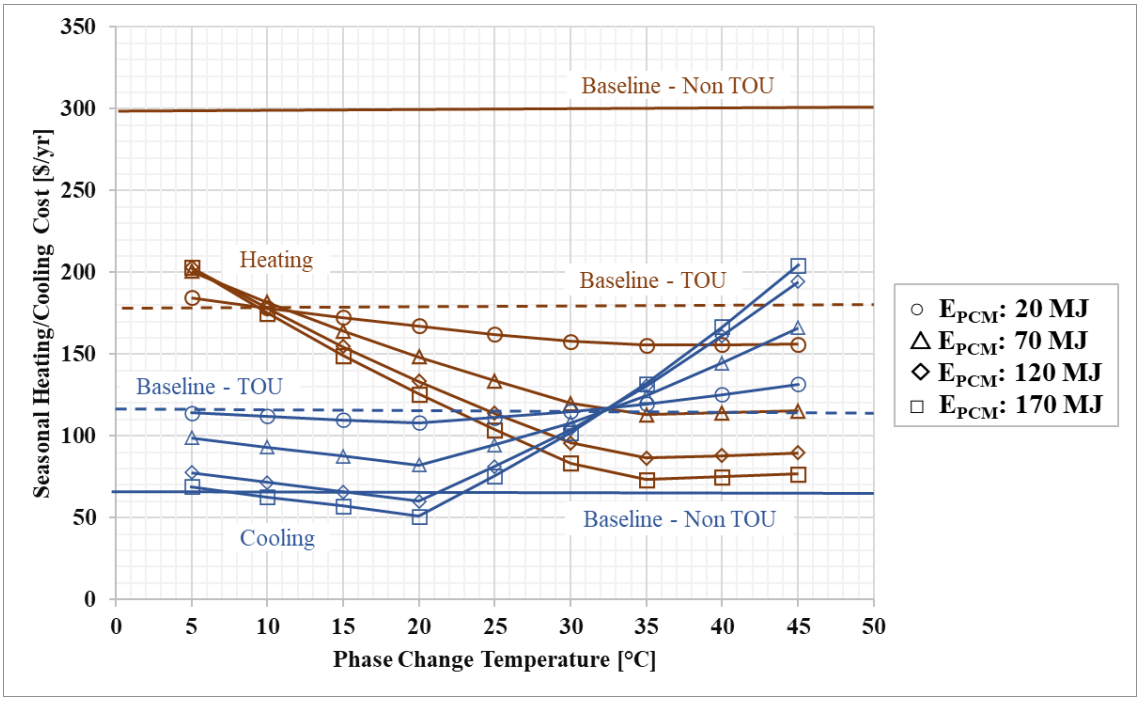


Figure 43: New York City results for utility cost.

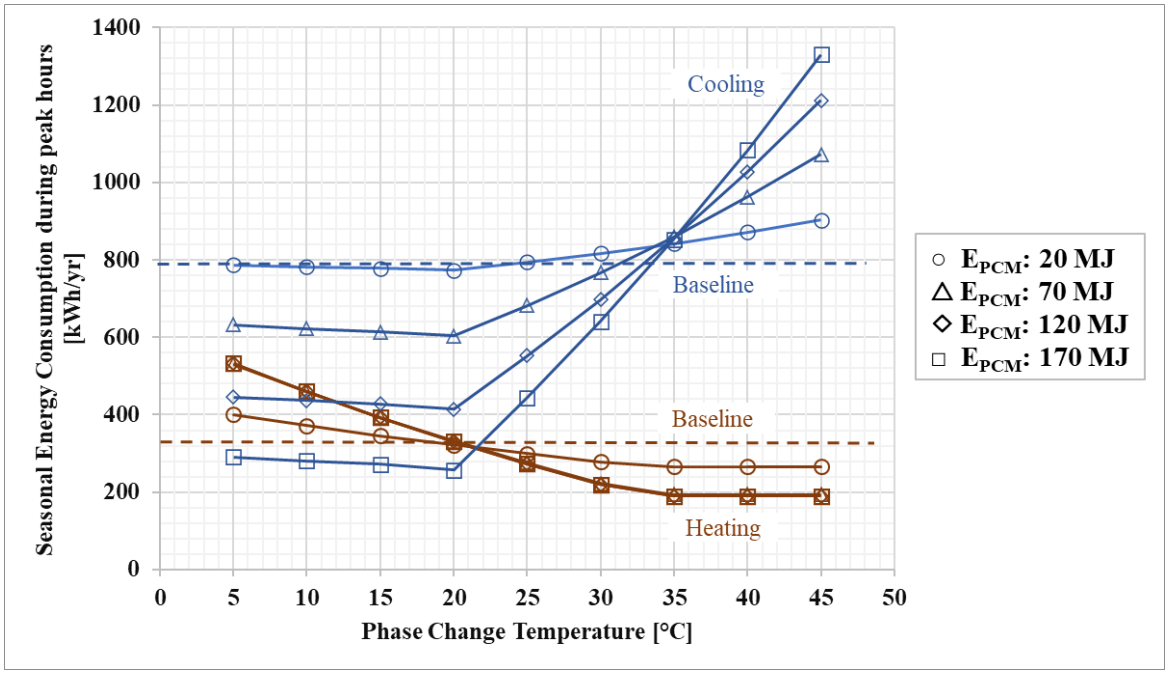


Figure 44: Houston results for peak energy consumption.

The maximum annual reduction (not shown in figure) in the cumulative energy consumption during on-peak hours was 47%, achieved by using a TES with 47.2 kWh (170 MJ) storage capacity and 20°C PCT under the TOU tariff. The cumulative energy consumption during on-peak hours was 588 kWh. For the baseline system, the minimum on-peak annual energy consumed was 1,120 kWh/year without the TOU tariff. Energy consumption of 531.9 kWh/year was shifted from on-peak to off-peak hours.

Figure 45 shows seasonal results optimized at different PCT and E_{PCM} for winter and summer. The minimum annual energy consumption (not shown in figure) was 1,816 kWh/year with a PCT of 20°C and energy storage capacity of 47.2 kWh (170 MJ). For the baseline case, energy consumption was 1,848 kWh/year. Annual energy savings were observed only when the PCT was between 20°C and 35°C. The energy savings were 1.75%, which is lower than the savings at other locations. Heating energy savings during winters in the New York City case made a huge difference to the results. Houston, on the other hand, is a cooling-dominated, humid climate with very short and mild winters, yielding less significant heating energy savings.

Figure 46 shows the seasonal heating and cooling cost of the integrated HP and TES system in Houston. Maximum TES savings were achieved using 170 MJ EPCM at 35°C in winters and 20°C in summers. TES and TOU baselines met at 35°C in summers and 20°C in winters, which indicates that discharging TES at these PCTs was same as normal heat pump operation, yielding no savings.

For both seasons, TOU baselines saved more cost compared with non-TOU baselines because off-peak energy was free in Houston under the TOU tariff by Gexa Energy (Table 15).

Figure 46 shows seasonal results. The annual minimum on-peak annual energy cost of the integrated HP and TES system in Houston was $144/year with 20°C PCT under the TOU rate structure. Without the TOU rate structure, the minimum peak annual energy cost was $274.6/year, corresponding to 47% savings.

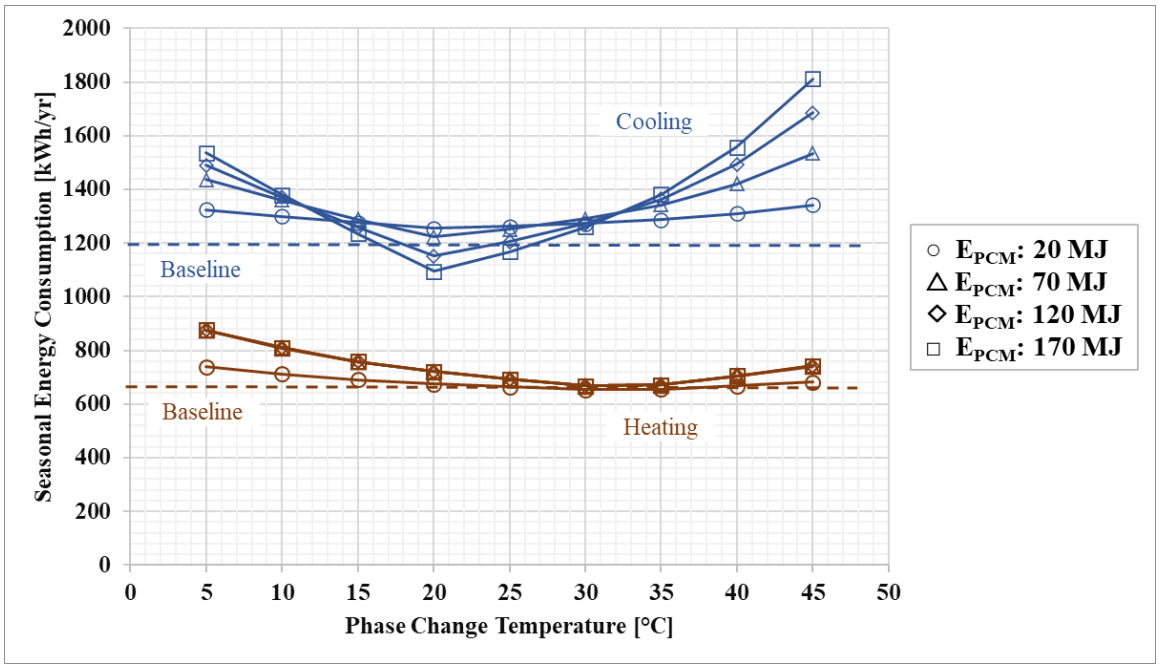


Figure 45: Houston results for energy consumption.

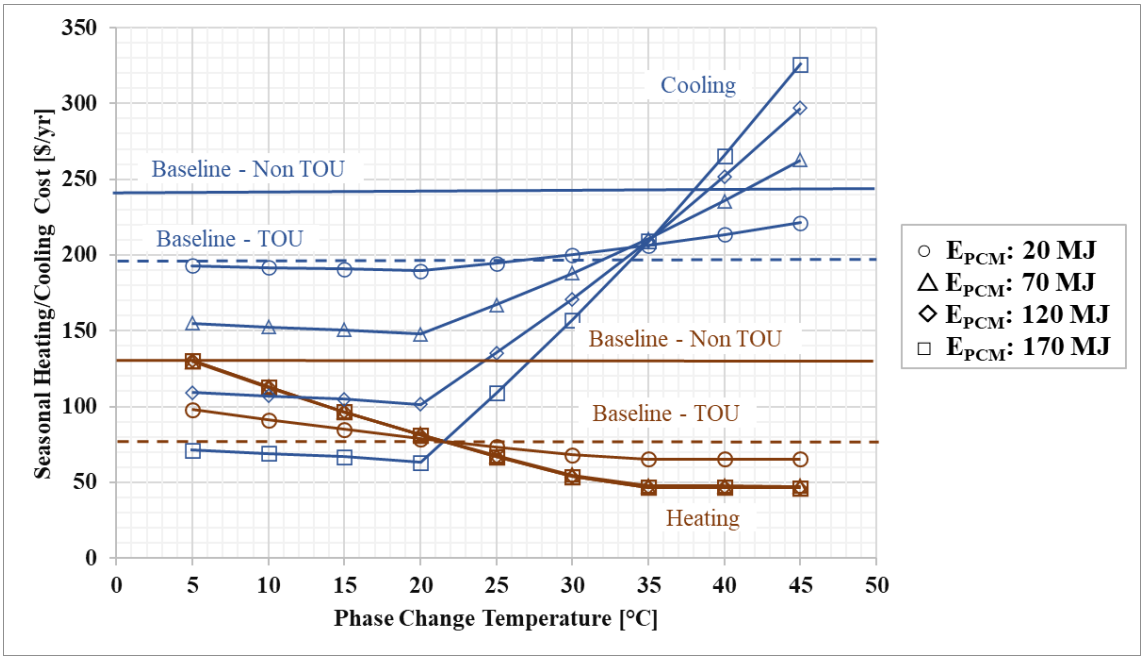


Figure 46: Houston results for utility cost.

Discussion

This study focused on evaluating the indirect HP-TES configuration using simple, rule-based controls with time-based, predefined utility rates. For that reason, the building model and control strategy were simplified.

Figure 47 shows monthly total energy consumption for all three locations. The minimum refers to the values obtained at optimum PCTs (20°C for summers and 30°C for winters). The maximum values refer to those found at extreme PCTs (45°C for summers and 5°C for winters). The consumption is highest for New York during winters and for Houston during summers. Even though cooling loads for Birmingham are higher than the heating loads, they are comparatively moderate.

In a previous study [154], 20% energy savings were achieved by using the similar control strategies and configuration for an ice storage system in Fresno, California (ASHRAE climate zone 3B). The TES in the previous study was simulated for 1 week, and only the cooling mode was studied. The total energy consumption savings were smaller in the current study. One reason for this decrease is that the week simulated in Fresno in the previous study [154] had particularly large diurnal temperature swings, and the year-long simulations in this study had smaller average diurnal swings. TES can provide more energy savings for climate locations where daily diurnal temperature swing is larger than the difference between indoor and PCM temperature.

The annual results are shown in Table 17 and Figure 48. To meet the high cooling demand in Birmingham and Houston, the optimized PCT was 20°C for maximum annual cost savings and peak electric demand reduction. For the New York City case, the optimum PCT was 30°C because of high heating load.

Energy savings highly depend on the ambient temperature and diurnal swing, while the cost savings and peak load shifted were driven by the peak time and heating and cooling demand for each climate location studied. It can be concluded that higher savings are expected in warmer areas where cooling demands dominate.

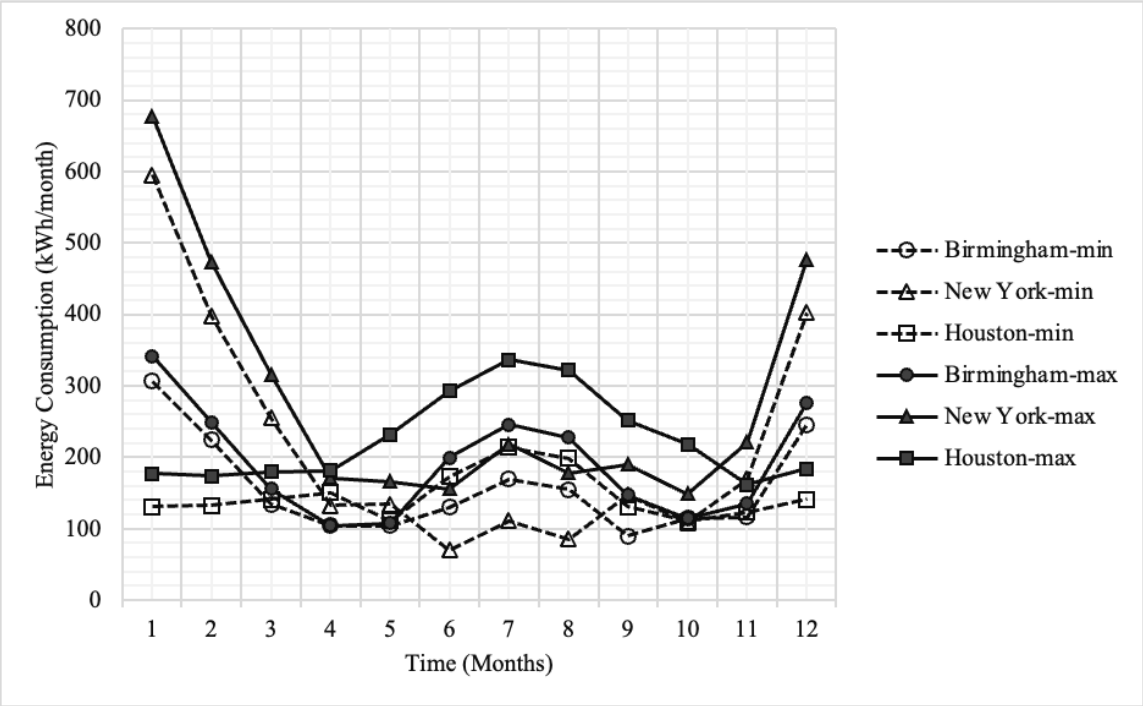


Figure 47: Electric Consumption.

Table 17: Annual results summary

Location	PCT	E_{PCM}	Total annual energy consumption reduced		Total annual utility cost saved		Total annual on-peak energy shifted	
	(°C)	*(MJ)*	*(kWh/year)*	*(%)*	*($/year)*	*(%)*	*(kWh/year)*	*(%)*
Birmingham, AL	20°C	120 MJ	110.5	5.4	111.0	43.9	365.2	70.5
New York, NY	30°C	170 MJ	109.6	3.93	177.4	48.9	717.5	53.3
Houston, TX	20°C	170 MJ	32.3	1.75	231.1	47.4	531.9	47.4

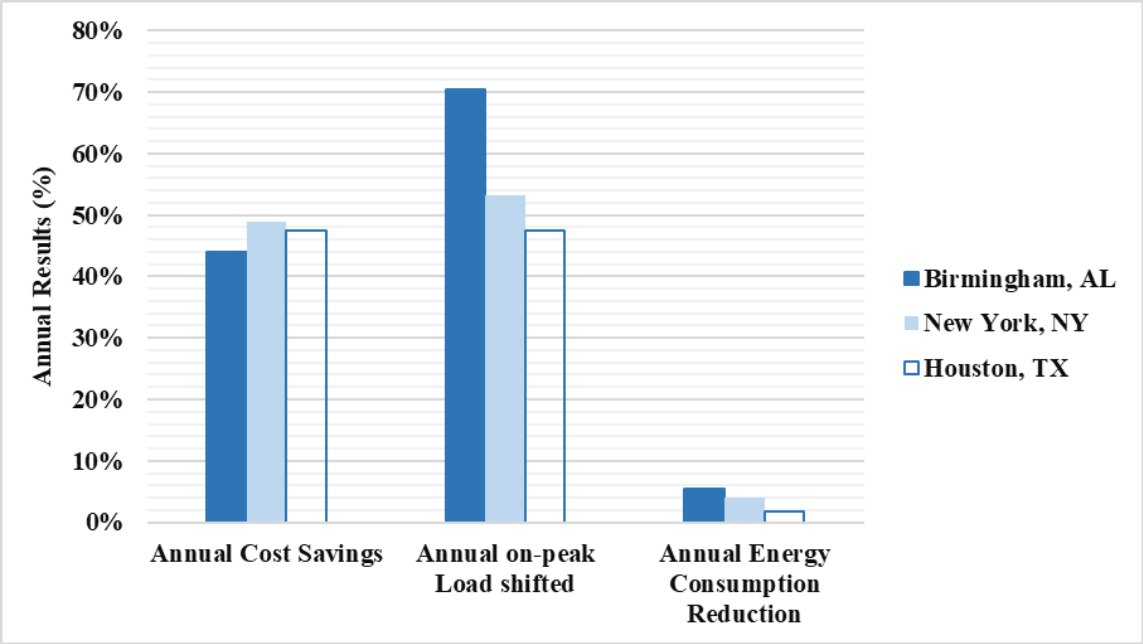


Figure 48: Summary of annual results for all three locations.

We only analysed PCT from 0°C to 45°C with a resolution of 5 C which is a limitation of this study. If the optimum lies in between 20 and 25 for example, that won't show up in our assessment.

An important controls shortcoming was identified in this study. PCM was used for discharging even if the ambient temperature was not favorable. For instance, if the PCT was lower than the ambient temperature, extracting heat from the TES resulted in more electricity consumption to meet the heating load as compared with the normal mode (i.e., extracting heat from warmer ambient air). Thus, predictive weather data should be included in control strategies for future work to optimize TES operation.

TES systems with larger storage capacities were shown to have a narrower acceptable PCT range because the adverse effects of this suboptimal control strategy became more pronounced at extreme PCTs. In future work, the control strategy should be improved to take advantage of the daily ambient temperature swing.

CONCLUSIONS

An HP-integrated TES was modeled in a simple configuration to determine the PCT and storage capacity that maximized energy savings, cost savings, and peak shifting for select residential building types. Three TES systems were modeled and compared with a baseline for different climate zones in the United States: Birmingham, Houston, and New York City. The simple, rule-based TES controls were designed to shift the load from on-peak to off-peak hours based on TOU utility tariffs available to residential customers in these locations. Very simple models of the HP, TES, and building were used to focus on evaluating the potential energy and cost savings and grid benefits of this HP-TES configuration. The best TES storage capacity and melting temperature were calculated for each case.

Birmingham and Houston are cooling-dominated climates, and 20°C was found to be the best melting temperature for annual energy and cost savings, as well as demand shift. New York City saw the largest energy savings and demand shift at 30°C because the system needed to meet a high heating demand. The highest energy savings of 5.4% and maximum peak load shifting of 70% compared with the baseline HP were observed in the Birmingham case. Maximum energy cost savings of 48.9% compared with the baseline ASHP were achieved in New York City. The energy cost savings and peak load shifted were driven by the peak time and heating and cooling demand for each climate location studied. TES with larger storage capacity allowed for more demand shift, with diminishing returns once the TES capacity equalled the daily building thermal loads experienced during the most extreme ambient conditions.

The scope of this work is limited to space conditioning in typical single-family residential buildings of U.S. and the building model is simplified. A more sophisticated model will be implemented in future iterations of this work and is expected to change the building loads. Three climate zones have been analysed in this work, but for future, a comprehensive analysis will be performed on more locations to represent more variations in climates and to generalize expected results. For the TES model, an arbitrary idealized

PCM is used and a range of PCTs is analysed with a difference of 5°C only. Future work will consider more values in between for optimization and a more robust TES model. Future models will also improve the control strategy and consider more variables like ambient temperature and diurnal swing.

CHAPTER V

ANALYSIS ON HP-TES IN VARIOUS CLIMATE ZONES IN U.S. AND EXPERIMENTAL VALIDATION

A version of this chapter is accepted for publication:

Sultan, S., Hirschey J., Li Z., Shen B., Graham S., & Gluesenkamp, K. R. (2023). "Carbon Mitigation Potential of Heat Pump Integrated with Thermal Storage for Grid-Interactive Residential Buildings." *14th IEA Heat Pump Conference*

Conceptualization, data collection, methodology and original manuscript draft was prepared by Sara Sultan, Jason Hirschey, and Navin Kumar. Borui Cui, Tim LaClair, and Xiaobing Liu provided help with editing and analysis. Review and supervision by Kyle R. Gluesenkamp.

A version of this chapter is in preparation for publication.

Abstract

Past work on TES integrated with heat pumps (HP) has demonstrated significant load shifting and economic benefits. However, the potential for TES to reduce carbon emissions has not been widely explored. This study evaluates carbon mitigation potential of HP-TES based on a simple rule-based control strategy accounting for electric grid emissions data.

The objective of this work is to shift the peak load while also reducing the emissions by designing controls using both utility and grid data. Marginal grid emissions data is obtained to determine if the emissions are relatively higher than the average of the previous day. The controls are then designed for the heat pump and TES operation, and emissions are reported. MATLAB is used to model the system controls and integrated sub-models. The modeled HP-TES system for single-family residential building demonstrates decreased carbon emissions with reduced peak utility cost.

Research Questions

How much reduction in cost of electricity and carbon emissions is possible by shifting the load from peak to off-peak hours for residential buildings in various climates?

How can PCM based Thermal Energy Storage be integrated into a heat pump for carbon mitigation, demand response, and reduced electric consumption of heat pumps in residential buildings?

Background and Literature Review

Heating, cooling, and ventilation loads in residential buildings account for about 10% of energy consumption and CO_2 emissions worldwide and comprises 50% of the building electricity consumption [1]–[3]. The potential of onsite thermal energy storage (TES) has mostly been underestimated even though its significance for decarbonization and demand reduction has been established by researchers [2].

Studies can be found in literature that investigate the demand response potential of TES. Peak thermal loads have been shifted to off peak time using utility pricing and demand-based controls [2], [137], [154], [202]. However, only a handful of research works reported in literature have investigated TES for carbon emissions reduction accounting for HP loads. The Table 18 below summarizes the literature investigating TES potential for demand management and carbon mitigation. Noticeably, gas consumption for furnace as a base case is compared against electric HP in most papers.

As shown in Table 18, the papers reported in literature are either passive or hybrid TES systems. Most researchers either employed passive cooling or heating by using PCM in building envelope or in case of active system, integrated TES with an additional energy production sources like PV systems. There is a large disparity in savings reported. Majority of the works evaluate the electric heat pump CO_2 emission reduction in comparison to gas furnaces as a reference, which yields more than 40% reduction [34]–[36]. Other studies compared PCMs with various insulations and passive configurations [203], [204]. In optimization studies, different PCMs and their melting points have been investigated to optimize the savings [205], [206].

Table 18: Load shifting, and carbon mitigation reported in literature using PCM-TES

Author	Location	System Description	Demand Impact	Carbon Mitigation
[33]	Turkey, Spain	PCM in buildings using passive TES and Active Aquifer TES	Loads reduced by 7% for cooling and 10% for heating	~26%* CO_2 emission reduction
[34]	Ithaca, NY	Borehole TES coupled to heat pump	Not reported	64% CO_2 emission reduction
[208]	Spain	Passive PCM in buildings	HVAC loads reduced by 20%	5.5% CO_2 emission reduction
[35]	Italy	TES with Photo Voltaic system and heat pump	41% energy cost reduced by peak load shifting	50% CO_2 emission reduction
[194]	Iran	Bio PCM integrated in wall and construction material of building	4% annual cooling and heating load reduction	2-5% CO_2 emission reduction
[203]	Saudi Arabia	3 different PCMs (18, 23, 25°C) in building envelope	Not reported	6.8-56.9% CO_2 emission reduction
[36]	UK	PCM in floor, coupled to air source HP	50% annual load reduction	36% CO_2 emission reduction
[206]	Saudi Arabia	PCMs (18, 21, 24, 25, 28°C) in wall, coupled to HVAC	Not reported	9.4-61% CO_2 emission reduction
[204]	Mexico	PCM (25°C) in building envelope	11-58% annual load reduction	~25%* CO_2 emission reduction
[205]	Turkey	PCM in wall, configuration and temperature optimized	17.2% annual energy savings	18.4% CO_2 emission reduction

*Calculated from the data given in the paper

Figure 49 shows the reduced carbon emissions in literature for different regions. Passive TES have varying benefits but for all regions, heat pump coupled systems consistently report more than 35% reduction.

HP-TES has especially garnered attention for its demand response potential, flexible configurations, and less space requirements. Active HP-TES systems were reviewed to establish that peak loads and cost associated with HVAC loads can be successfully reduced [23]. Many researchers have used demand response control strategies to shift the peak load, but very few papers have investigated the decarbonization potential of TES. Peak load was shifted using various controls and configurations for residential HP-TES, and corresponding emissions were reported [207]. The emissions have been calculated by deriving relations to the energy consumption and power usage. Abu Hamdeh *et al.* (2022) multiplied the power usage by the amount of greenhouse gases emission per kWh [203]. Arce *et al.* (2011) used European Commission emission factors, load reduction and energy savings to calculate the carbon emissions reduced [208]. Cabeza *et al.* (2015) defined CO_2 factor as a corelation between CO_2 emissions (g) and energy consumption (kWh). The CO_2 footprint (g/kWh) is 0.08 times energy consumption [33].

Table 19 shows the gap in literature and scope of this work. No studies were found that utilize emissions data into the control strategy of HP-TES systems.

Marginal Grid Emissions

The electricity sector has seen a shift from traditional centralized system to a smart grid device. This phenomenon has been ushered in by the increased integration of renewable energies. The rapid proliferation of the 'Internet of Things' (IoT) [59], allow major loads, such as HP, to be controlled with the goal of reducing peak power consumption on the electrical grid. In a smart grid, HP can be considered part of the demand side that can be actively managed to stabilize voltage fluctuations caused by high demand or high penetration of renewable energy [209].

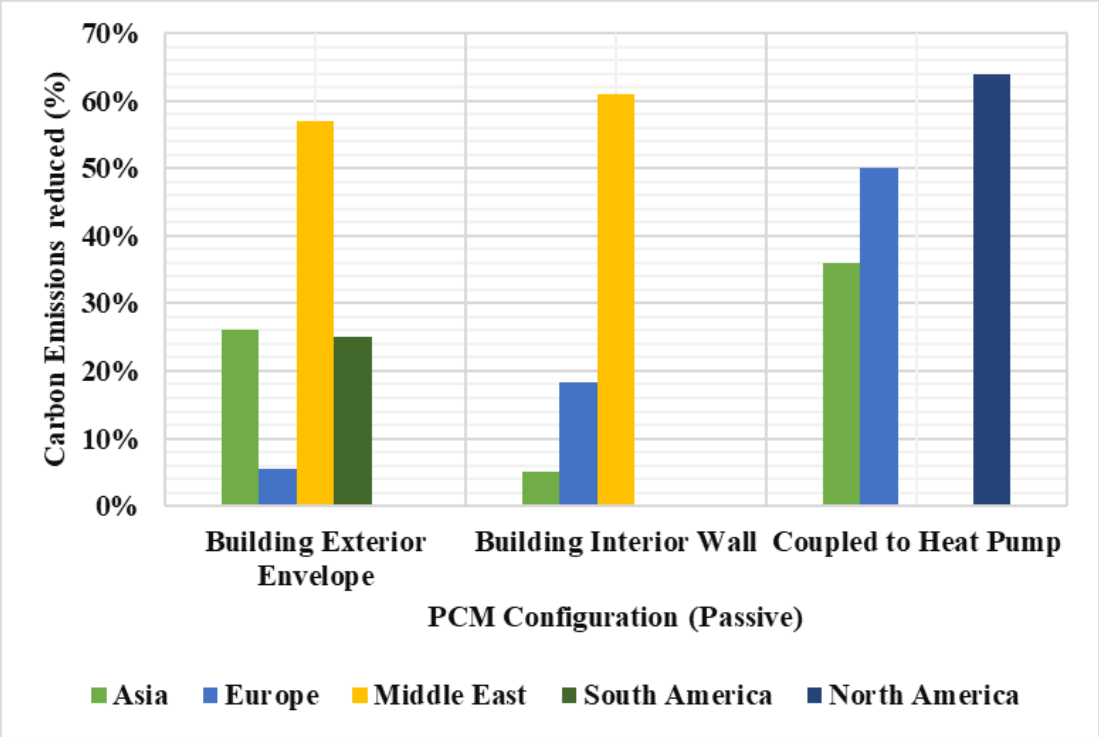


Figure 49: One representative reference reporting emission reduction by using PCM in various locations and configurations.

Table 19: Table showing gap in literature and scope of this work.

Reference	Active HP-TES mediated by heat pump	Carbon Emission controls for HP-TES	CO_2 emissions reported	Electric heat pump baseline vs PCM	Utility based controls for peak load shifting
[33]	×	×	■	×	×
[34]	×	×	■	×	■
[208]	×	×	■	×	×
[35]	×	×	■	×	■
[207]	×	×	■	×	■
[194]	×	×	■	■	×
[203]	×	×	■	■	×
[36]	×	×	■	×	■
[3]	■	×	×	■	■
This work	■	■	■	■	■

With smart control of HP-TES, the system can switch between charging and discharging mode depending on the outdoor temperature, electricity price, desired indoor temperature, renewable energy generation, and COP of HP [59]. It is important to describe how to incorporate a grid's GHG (greenhouse gases) condition into a site-specific MPC. The grid system-wide emission rate in a specific grid region depends on the total power production rate from grid power generators, and other factors that affect system operating conditions, such as weather. The marginal operating emissions rate (MOER) is the partial derivative of the systemwide emission rate with respect to the total production rate [210]. It means the change of the emission rate in the grid region with respect to the last megawatt produced by dispatchable generators having the unit of metric Ton CO_2-equivalent per MWh [mTonCO_2/MWh]. Intuitively, this indicates how much carbon emission rate increases/decreases in a grid region when one consumes one megawatt more/less. Therefore, MOER allows for associating the power usage at a specific site with the carbon emission rate in the grid region by simply multiplying the on-site power consumption with the MOER signal. In this work, we used the MOER signal, based on a proprietary model [210], but adapted for real-time use [211].

Case Study

The focus of this case study is to evaluate the carbon mitigation potential of TES assisted heat pumps against the normal heat pump operation, to compare the emissions with and without TES using a rule-based control strategy.

In our previous work, we used time-based pricing to determine the economic value of residential TES system [154]. The PCM was incorporated into the conventional HVAC and time-of-use (TOU) utility rate schedule was analysed to evaluate the demand impact and energy savings. The objective of this present work is to evaluate the simple control strategy to reduce grid emissions while shifting the peak load, accounting for both grid and utility data. Marginal grid emissions data is used to determine if the emissions are relatively

higher than the average of the previous day. The controls are then applied for the heat pump and TES operation, and emissions are reported.

A simple building thermal energy model and HP model is evaluated with an active configuration implying direct use of TES for the building cooling during the discharge. The TES is based on water/ice PCM with 0°C storage temperature. TES is not directly conditioning the building but interacts with HP to mediate the heat transfer. The potential reduction in grid emissions is assessed using marginal grid emissions data and peak load is shifted using residential TOU utility tariff. Both correspond to the ASHRAE climate zone 3B, in California. For modelling, Engineering Equation Solver (EES) and Microsoft Excel are used. System overview and decision controls are explained in the Methodology.

Methodology

The model comprises of various components connected to the building and HP using R410-a refrigerant. A TES heat exchanger with embedded PCM is integrated into HP to modify the vapor compression system and is transferring energy to and from the ambient. Thermostat controls monitor the building indoor temperature. The ambient weather data, TOU utility data, and marginal grid emissions data obtained for the same climate location, ASHRAE climate zone 3B. Marginal grid emissions data and electric utility schedule controls the heat pump to cool the building, and charge and discharge the ice-based TES. The analysis is performed for cooling only during the hottest week of June. The building energy consumption, HP work, and emissions are calculated in Microsoft Excel according to the rule-based control strategy in the minutely time steps.

1. *System Overview and Configuration*

The conventional vapor compression cycle of HP is modified by coupling TES to the system. TES is integrated with HP via active configuration and assists the HP cooling. TES does not cool the building directly, but heat transfer occurs through HP, as shown in Figure 50.

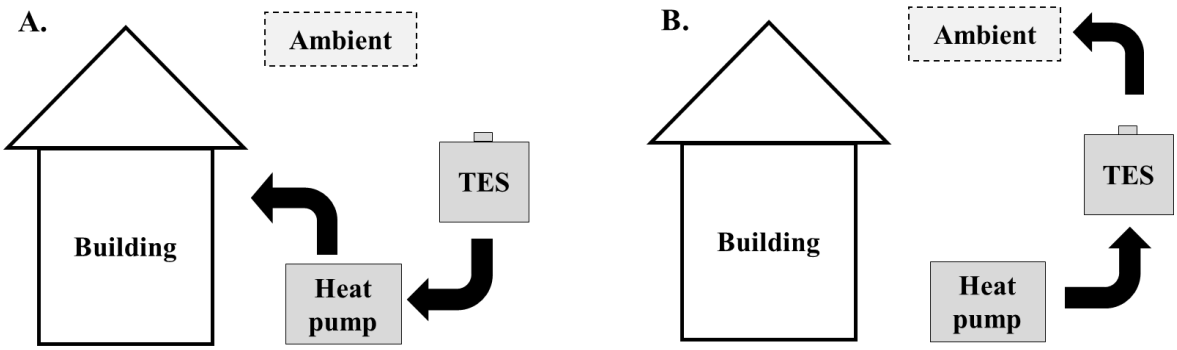


Figure 50: HP-TES configuration in cooling mode (A. TES Discharging B. TES Charging)

PCM-TES can function either as a condenser or an evaporator, dependent upon the mode of operation. It is assumed that TES has an infinite coefficient of heat transfer and is always at constant temperature of 0°C.

HP has four modes of operation. HP is turned off in the standby mode and only thermal energy from outdoors is being transferred to the building. HP is turned on to cool the building through refrigeration cycle in normal mode, and no TES is involved. During charging mode, TES stores the energy from HP as Q_{PCM} to be used at later time. During discharging mode, TES releases the already stored energy into the building via HP. This mode has increased COP than the normal mode due to favourable temperature gradient. TES, which is at a colder temperature, is coupled to HP condenser and creates a negative temperature lift to move the condenser heat from building to TES.

2. Cooling Mode

Operating modes for cooling and respective energy flows are shown in Figure 51. Ambient is at a higher temperature than the building. During cooling normal operation, the condenser heat, Q_{cond}, is discarded to the ambient while the heat of the evaporator, Q_{evap}, is removed from the building and directed to the heat pump.

TES behaves as condenser or evaporator depending on the mode of operation. Evaporator is assumed to be the TES during charging. So, the TES is being cooled directly. The heat, Q_{evap}, is removed from the TES though latent heat of freezing. TES solidifies as the heat stored from the TES is discarded to the ambient via heat pump. In the discharging mode, the TES is defined as the condenser and the evaporator was tied to the building. The Q_{cond} is now being stored to the TES instead of ambient and the PCM within the TES is being liquified.

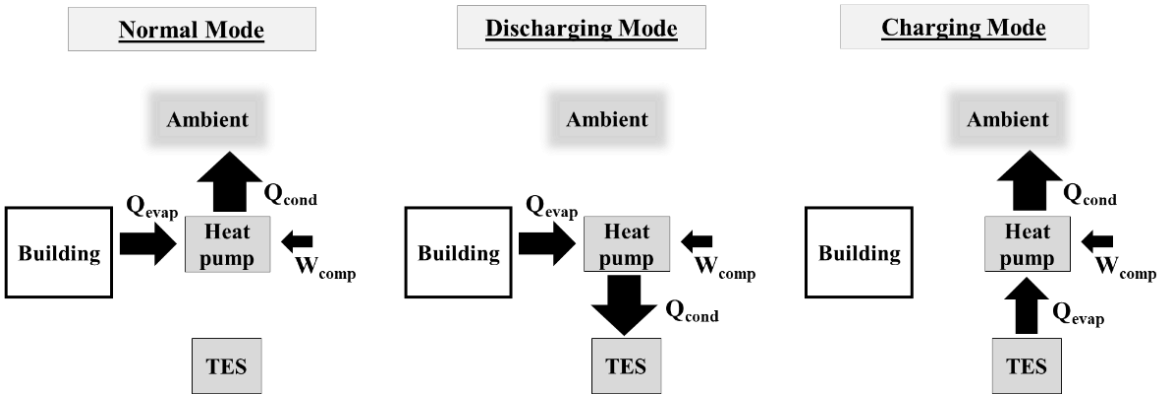


Figure 51: Operating modes in cooling.

3. System Controls

The operating mode of HP-TES is determined by the thermostat decision whether the building needs to be cooled or not, utility off-peak and on-peak time, state of charge of PCM (SOC), and grid emissions. The control strategy of HP-TES model is regulated based on four decision variables: 'Thermostat call', 'Utility Peak', 'Emissions Peak' and 'State of Charge'.

The thermostat model regulates the indoor temperature and determines if cooling is needed at a given time to call for cooling. A cooling temperature setpoint is fixed at 21°C, and the need is determined when the indoor temperature is higher than the cooling setpoint. The utility model determines the utility peak time. The emissions are obtained from the grid emissions model while the TES model determines the PCM state of charge.

The operating modes are shown in the decision tree diagram (Figure 52). Assuming the initial PCM SOC as 50%, if the thermostat is calling for cooling during the utility peak time defined by TOU tariff, PCM discharging mode will turn on. But during utility off peak, the emissions peak will determine if the discharging mode should be on. Charging mode is only activated during off-peak times to take advantage of the lower electrical cost and emissions, while thermostat is not calling for cooling, and PCM is not already charged. If during utility off-peak time, thermostat is calling for cooling, the HP goes into normal operation depending on emissions peak. Emissions peak is determined by average of grid emissions in the past 24 hours, if emissions are greater than the average of last 24 hours at a given point, it's emissions peak. In previous work [6], emissions were not included, and controls were based only on utility data.

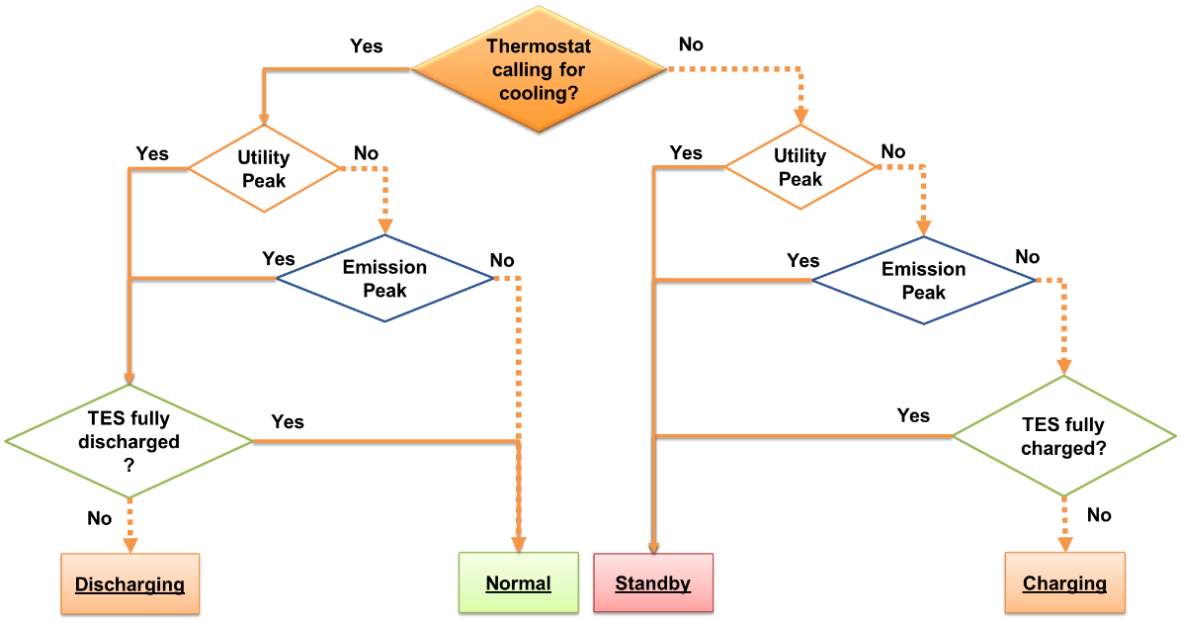


Figure 52: Controls decision tree used in this work.

4. Information Flow

The overall system flow is depicted in Figure 53, which depends on the component models to analyze the weather, utility and emissions data. All the components are mainly coordinated by the decision tree as a main control to maximize the system efficiency. Some values are updated to use as intermediate inputs in the model, represented by feedback arrows. The building model, HP model, and TES model are used from the previous work [154].

Component Models

1. Weather and Utility Data

The TMY 3 weather data used is of Fresno, CA which corresponds to ASHRAE climate zone 3B. The location correlates to marginal grid emissions and utility tariff. The Time of Use (TOU) utility data is a fixed utility rate schedule from Pacific Gas and Electric (PG&E) Electric Schedule E-TOU-B. The analysis for cooling is performed considering both peak and off-peak hours for a hot week of June 24-30, 1994. The peak hours vary by season. For cooling season defined from June till September, on-peak hours are observed from 4pm to 9pm on weekdays, and the utility rate is $0. 39689/kWh. At other times, including the weekends, the off-peak rate is $0. 29383/kWh. The difference between on-peak and off-peak utility rate is $0.103/kWh.

Figure 54 shows ambient temperature versus utility rate for cooling season. The cost for cooling increases when the demand increases as a function of outdoor dry bulb temperature. The design objective is to take advantage of the low rates and assist heat pump operation using TES when the cost is high during peak hours.

2. Building Model

Building's thermal response is simulated by a simple building model that calculates indoor temperature. The model takes into account the heat pump load, building's thermal capacitance, and ambient load.

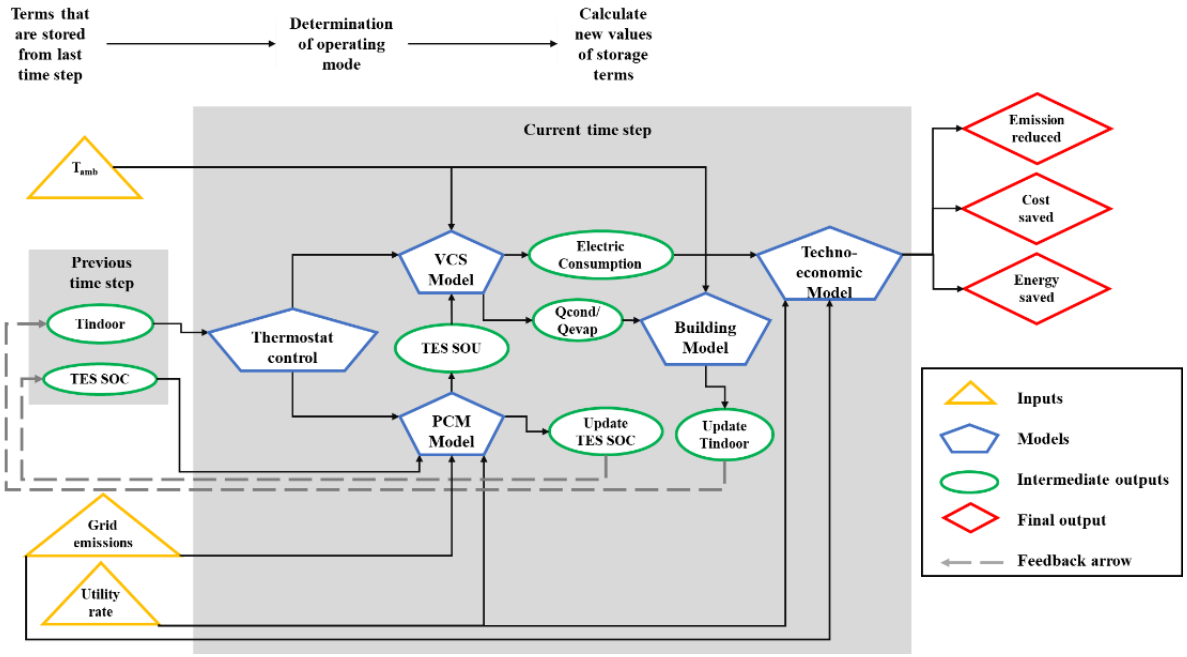


Figure 53: Information Flow Diagram

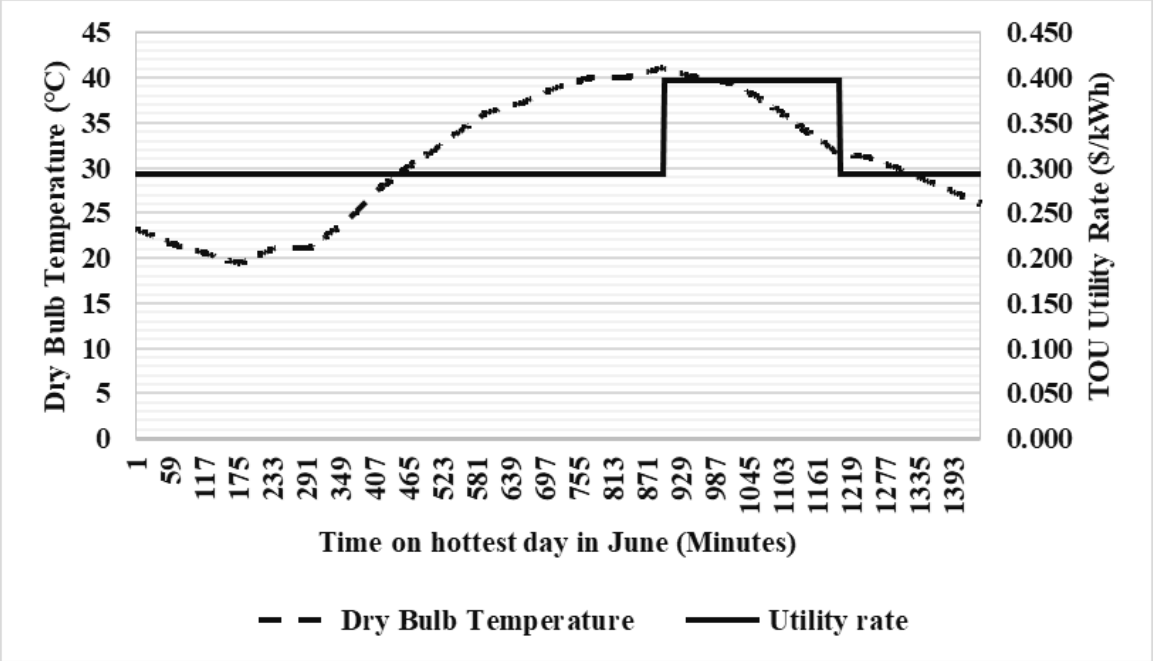


Figure 54: Ambient Temperature and Utility data for cooling day

A balance point temperature of 18℃ is assumed to model the ambient load, as shown in Equation 12. An overall heat transfer coefficient of 0.25 kW/K is estimated based on cooling design day.

$$Q_{amb} = U * (T_{amb} - T_{bal}) \quad (11)$$

Indoor temperature is determined by the energy balance where Q_{VCS} is the cooling or heating load output from the heat pump model in either normal or discharging modes, in one minute time step. A single-family house with 223 m^2 (2400 ft^2) area was selected and the building capacitance was estimated to be 16459 J/K [154]. It was chosen to result in a reasonable rate of change of building.

$$T_{indoor,i+1} = \frac{-(Q_{VCS} - Q_{amb}) * dt}{C} + T_{indoor,i} \quad (12)$$

3. Thermostat Model

The thermostat model tracks the indoor temperature and calculates the variable 'thermostat call'. It uses a constant setpoint temperature to turn on cooling mode. Due to thermal loading from the ambient temperature, when the building indoor temperature exceeds the setpoint cooling temperature of 21°C (with a dead band of +/- 0.5°C), the thermostat calls for cooling. Depending on other conditions (time of day, emissions, and outdoor temperature), the HP will enter into either discharging mode where TES will be used, or normal mode where HP cools the building without TES.

4. Heat Pump Model

A heat pump model was simulated in EES and the operating modes with TES were modelled separately. The vapor compression model calculates the COP for cooling from the evaporator output and electric consumption by compressor [6]. The compressor has a constant volumetric flow rate of $2.5e^{-6}$ m^3. Equation 13 defines the cooling COP.

$$COP_c = \frac{Q_{evap}}{W_{comp}} \quad (13)$$

The outputs of heat pump model, Q_{evap} from the evaporator and Q_{cond} from the condenser are called into Excel, where they are coupled to the PCM-TES or ambient depending on the operating mode. The condenser is tied to the ambient in normal mode, thus the dry bulb temperature was used as an input. The condenser is paired to the TES in the discharging mode. Where TES is kept at a constant 0°C. The discharging mode does not depend on ambient temperature and thus its operating parameters are constant. Because the temperature gradient is more favourable, total work during discharging is 0.748 kW, much lower than the normal mode which varies between 2.65 and 7 kW depending on the ambient temperature. The condenser is coupled to the ambient in charging mode, and now the evaporator interacts with the TES. The decision tree (Figure 52) and thermostat model was used to control the HP and PCM state of use.

5. TES Model

The HP vapor compression system is coupled to PCM via heat exchanger in such a way that TES does not interact directly with the building and is not affected by the ambient temperature. An ice/water based PCM with phase change temperature of 0°C is embedded in the TES. TES heat exchanger is assumed to have an indefinite heat transfer rate at a constant temperature maintained at 0°C. TES is modelled as an 80-gallon tank, which can provide up to 27.8 kWh of cooling capacity. The operating modes are controlled by the PCM state of charge which is a function of peak time, and indoor temperature.

The fraction of maximum energy that can be stored by TES is defined as state of charge of PCM (PCM SOC). The PCM SOC is increased during charging to store the energy and reduced during discharging mode when it is consumed. For charging mode, the state of use of PCM (SOU) is -1, for discharging it is +1, and PCM SOU is 0 when it is not being used.

6. Grid Emissions Model

Marginal grid emissions schedule is obtained for Fresno, CA from a data driven tool that uses an empirical model. The tool generates emissions schedule based on continuous emissions and electricity generation data from major fossil fuel plants in the U.S.

Figure 55 shows the hourly emissions data for the year of 2022 obtained on November 15. The data from January until November 15 is real time, and rest is projected based on historical data. Controls are designed based on average of the last 24 hours and variable called 'Emission Peak' is defined. If at any given point, the emissions exceed the average of last 24 hours, it will be considered emission peak. Discharging mode will be turned on if cooling is needed at that time. This strategy avoids using HP during both utility and emission peak times, to assess the maximum grid emission savings.

Results and Discussion

The analysis is performed for one week of cooling season to report utility cost, electric consumption, and carbon emission reduction. The indoor temperature was maintained at 20℃ for cooling. For the simulated 7-day period, the grid emissions corresponding to the HP electric consumption are compared for the cases with and without PCM TES. The baseline system is defined as the case without TES.

1. Carbon Emissions

Figure 56 shows the grid emissions for both baseline and TES systems. The no-TES baseline case resulted in 181.78 kg of CO_2 over the simulated week, while using the TES system, emissions were 160.1 kgCO_2, reducing 11.92% grid emissions for the simulated week. These savings were achieved by using TES to discharge during emission peak and utility peak.

2. Electric Consumption

Figure 57 shows the HVAC electric consumption and the peak electric consumption for both baseline and TES systems. TOU tariff for Fresno, CA is used for this study and the on-peak pricing applies from Monday through Friday only, excluding weekends. For the baseline system, where no TES was used, total electric consumption was 353.2 kWh, and on-peak consumption was 98.1 kWh.

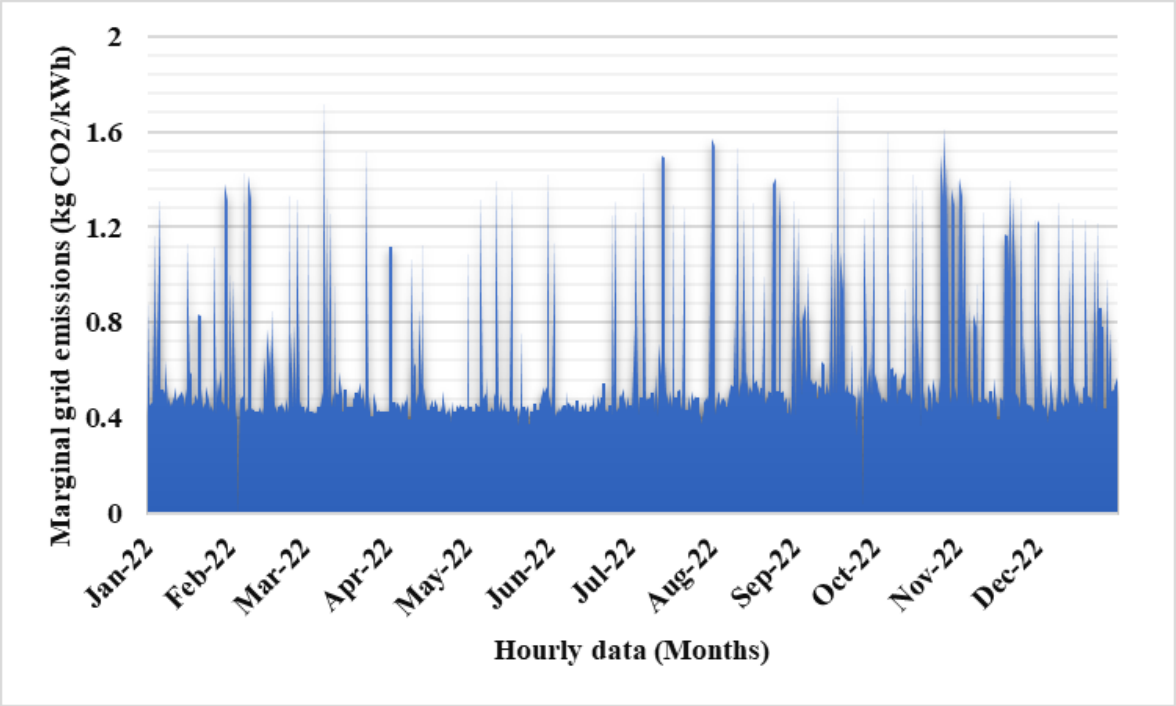


Figure 55: Fresno annual grid emissions during 2022

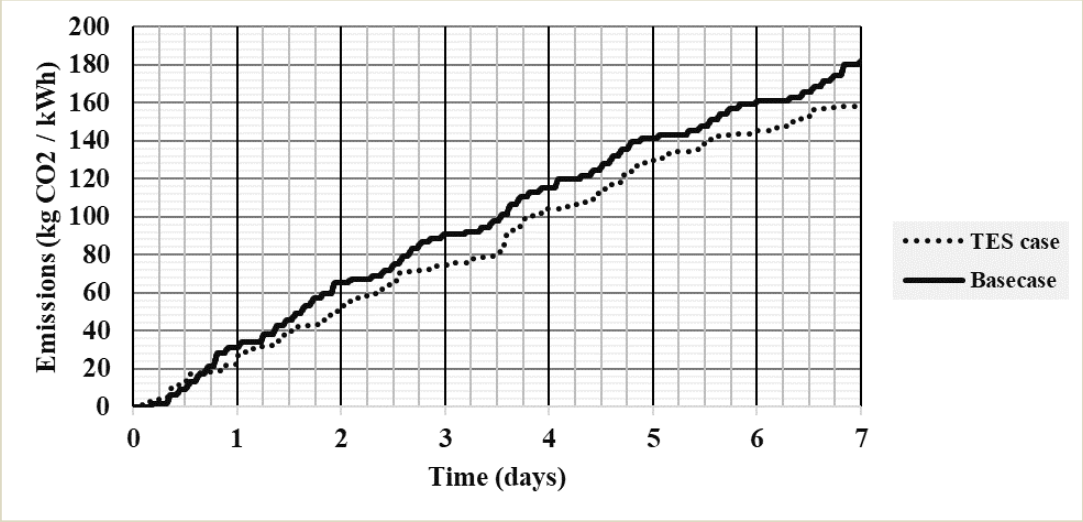


Figure 56: Emissions reduced using TES

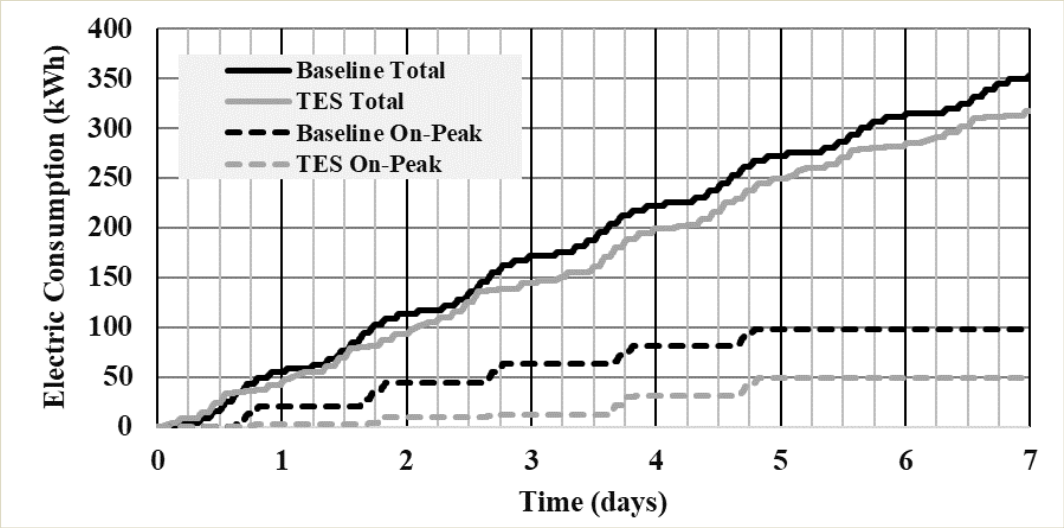


Figure 57: Electric Consumption with and without TES.

For the system with TES, the total electric consumption was reduced by 10.19% to 317.2 kWh. TES on-peak usage was 48.8 kWh, which means 50.2% of peak load was shifted. In our previous study [6], 87% of peak load was shifted to off-peak hours using TES under TOU tariff. The present study also implements grid emissions-based controls and TES is more frequently used in discharging mode than in previous study.

3. Operating Cost

The utility cost to cool the building is shown in Figure 58. Compared to baseline, 12.68% of system operating cost was saved using TES. The baseline system without TES accumulated $112.52 for cooling during the simulated week, while TES accounted for $98.25. In the previous study [6], 20% utility cost was saved using TES. The cost for the present system has increased when additional emission-based controls were introduced. In the control strategy, the emissions peak has precedent over the utility peak. Therefore, cost savings are not as significant as was seen in the previous study when only cost peak was considered.

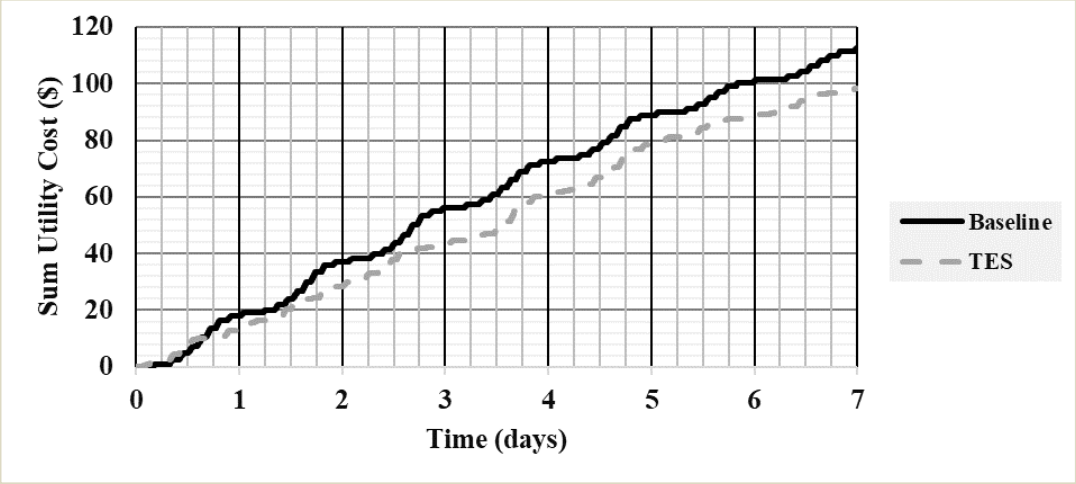


FIGURE 58: UTILITY COST REDUCED USING TES.

CONCLUSIONS

The objective of this case study is to assess the carbon emissions reduction potential of HP-TES using a rule-based strategy accounting for marginal grid emissions data and time-of-use utility tariff. An HP-TES configuration was evaluated with an ice/water based PCM coupled to the HP. A vapor compression model was developed using EES, and Excel was used to compute results for the integrated HP-TES system. The analysis was performed for one week of cooling season. The utility cost for cooling was reduced by 12.68% using TES while also maintaining occupant comfort. The total electric consumption was also reduced by 10.19% and 50.2% of peak electric load was shifted to off-peak time. 11.92% of grid emissions were reduced by using TES during emissions and utility peak times defined in the control strategy. The study concluded that while this configuration can still create some economic advantage with a simple control strategy, controls should be further optimized to reduce peak energy consumption. The analysis was performed for 7 days only, and the results should not be extrapolated for annual savings. This work highlights the potential for reducing grid emissions using a rule-based strategy.

Annual Simulations

The focus of this work is on developing controls of TES integrated with HP, and modeling the behavior of TES with HP. The preliminary work used a simplified heat pump and building model to evaluate the HP-TES configuration, and reported preliminary results based on a sub-optimal control strategy. The new model improves improve the controls, and sub-models.

Overview

The model comprises of various components connected to the building and R-410a vapor compression system (VCS). A PCM heat exchanger is integrated into the heat pump to modify the vapor compression system and is transferring energy to and from the ambient. Thermostat controls monitor the building indoor temperature. The marginal grid emissions data and electric utility schedule controls the heat pump to heat or cool the building, and charge and discharge the PCM. TMY 3 weather data is used corresponding to the respective ASHRAE climate zone.

MATLAB flow chart

The building, Vapor Compression Heat Pump (VCHP), PCM-TES, and all the operating modes are modular functions to be integrated in the MAIN file. The thermostat controls are in MAIN file.

Figure 59 shows a simplified MATLAB flow diagram. The red arrows that are fed back to the MAIN, refer to updated i+1 values. Tindoor and thermostat determine if the system should call Cooling.m for primary cooling mode or Heating.m for primary heating mode. A detailed flow chart is also shown in Figure 60.

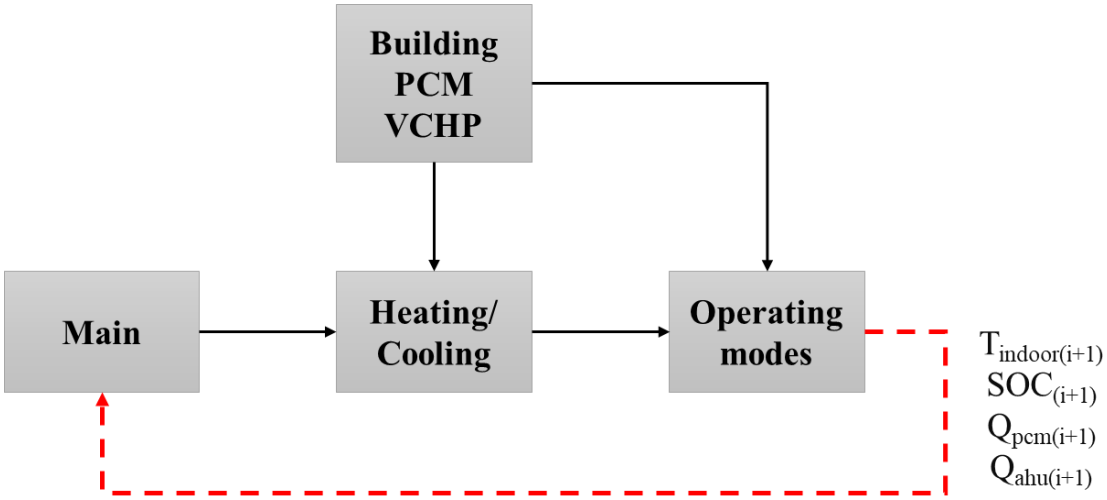


Figure 59: Simplified information flow

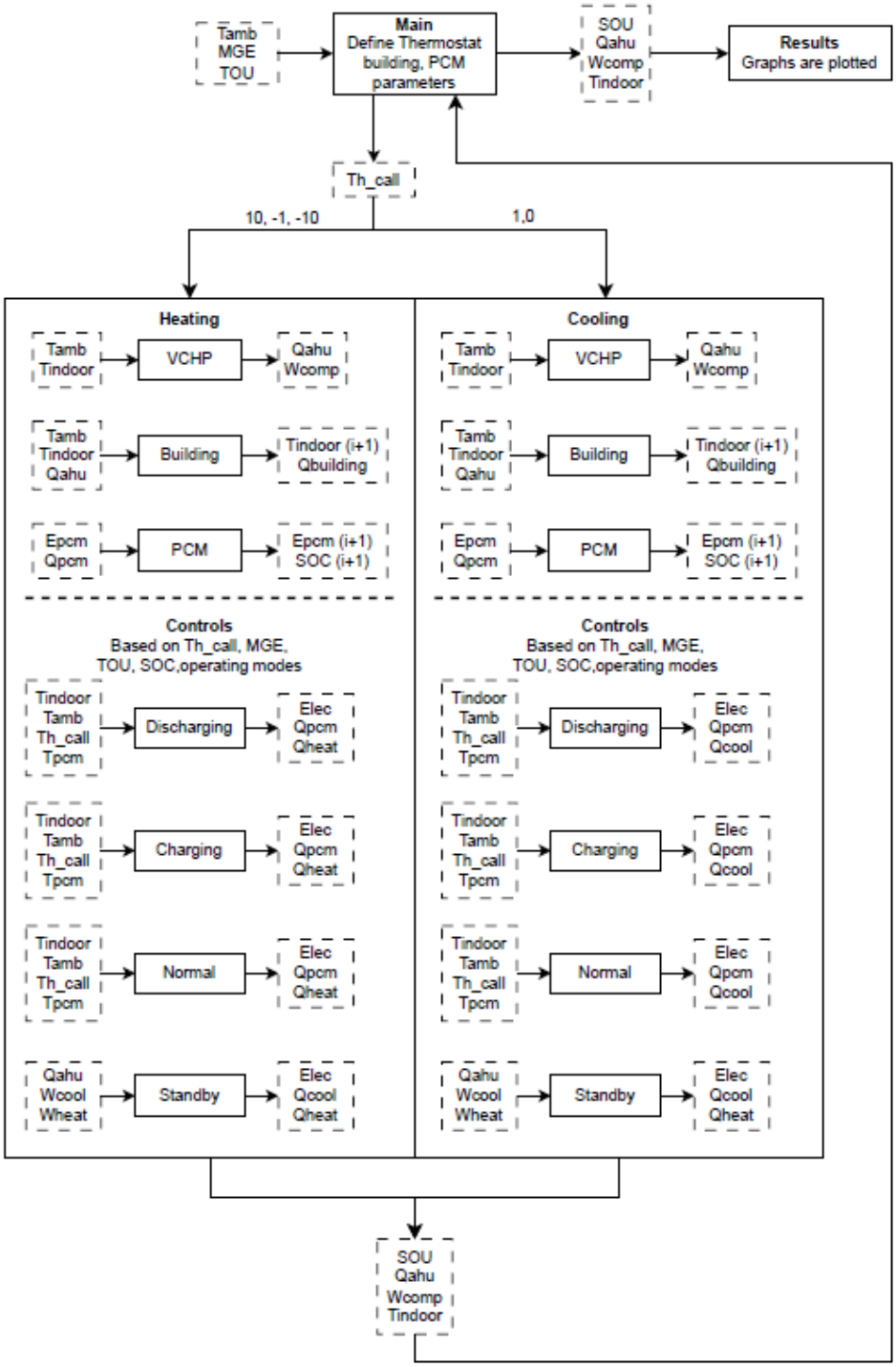


Figure 60: MATLAB Model flow

Thermostat model

Table 20 and Figure 61 shows the main indoor setpoint temperatures and respective modes. We use a variable named Th-call that refers to thermostat call, i.e., whether the thermostat is calling for heating or cooling. Th-call has 5 values,

- Th-call = 0 means cooling not needed
- Th-call = 1 means cooling is needed
- Th-call = -1 means heating is needed
- Th-call = 10 means heating is not needed
- Th-call = -10 means auxiliary heating is needed

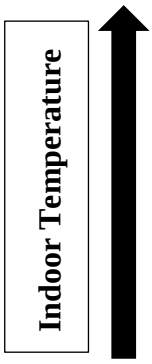
Th-call is determined by indoor temperature, T_{indoor}, and set point temperatures for both heating and cooling modes. The operating modes for both heating and cooling are separate functions and are determined by controls logic.

Figure 62 shows the models that were integrated into MATLAB for HP-TES analysis. An existing validated building model provided by Cui et al. [212]–[214] as a python code was integrated into the developed model as a MATLAB function. The HP and PCM model functions were written in MATLAB.

Building Model

The preliminary model used a simplified building model to simulate the thermal response of the building by calculating the indoor temperature. The reason for using simplified model was to report the preliminary results by analyzing the HP-TES configuration and developing control strategies for maximized cost savings and demand reduction. The new model used equations from a validated RC building model by Cui et al. [212]–[214] and implemented in MATLAB. The values for model were taken from Jason et al. [215] and same values were used for all climate zones for the sake of simplicity (shown in Table 21). Table 22 shows the buildings selected for this analysis.

Table 20: Thermostat logic to trigger actions at T_{indoor}, setpoint, and deadband.



Thermostat	Action
+Cooling Deadband **Cooling Setpoint**	Cool until indoor temperature reaches cooling Deadband
23°C **−Cooling Deadband**	
22.5°C	Cooling not needed
22°C	Repeat action from previous time step
21°C **+Heating Deadband**	Heating not needed
20.5°C **Heating Setpoint**	Heat until indoor temperature reaches heating Deadband
20°C **−Heating Deadband**	

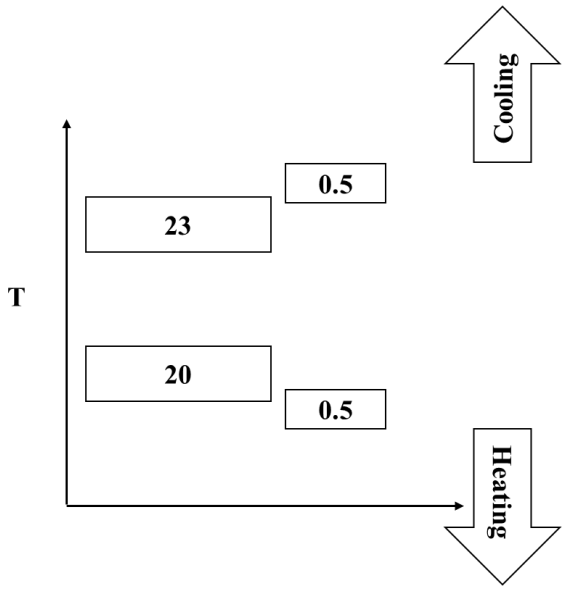


Figure 61: Indoor temperature setpoints.

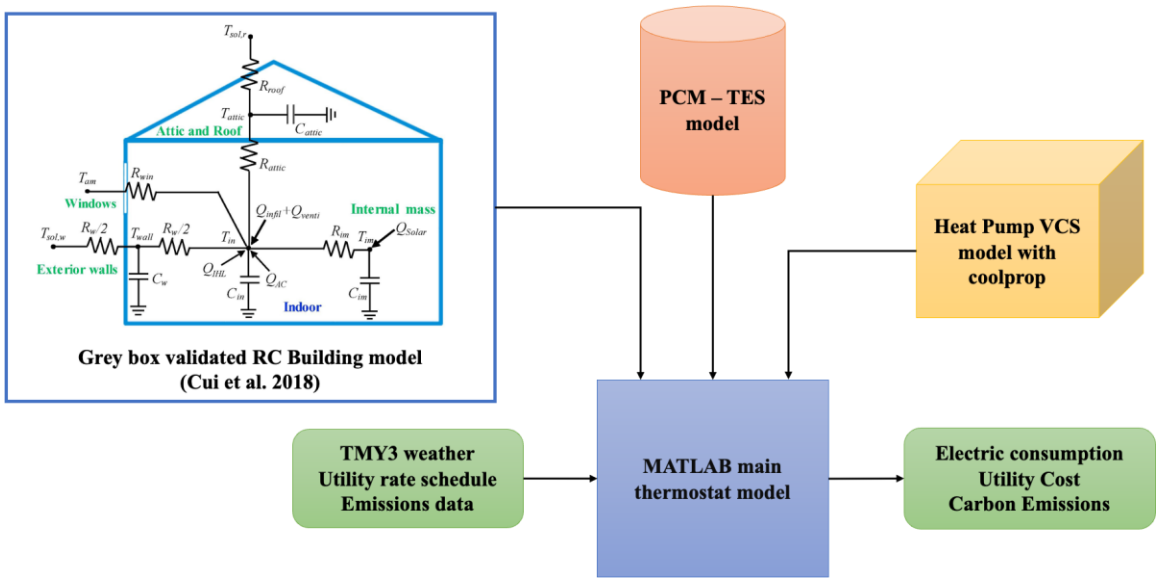


Figure 62: Models integration for HP-TES in MATLAB.

Table 21: Building Thermal Energy Simulation Model Parameters

Simulation RC Variables					
Variable	**Value [K/W]**	**Variable**	**Value [J/K]**	**Variable**	**[J/K]**
R_{wall}	0.0046	C_{wall}	57142857	C_1	0.666
R_{attic}	0.0114	C_{attic}	285714	C_2	0.673
R_{roof}	0.0017	C_{im}	11428571	C_3	0.1
R_{im}	0.0034	C_{in}	4285714		
Physical Building Characteristics					
Variable	**Value**	**Variable**	**Value**	**Variable**	**Value**
F_{window}	0.25 [-]	A_{window}	10 [m^2]	SHGC	0.25 [-]
F_{wall}	0.25 [-]	α_{wall}	0.5 [-]	Q_{IHL}	2000 [W]
F_{roof}	0.5 [-]	α_{roof}	0.65 [-]		

Table 22: Buildings selected for analysis.

Building Details	Location (IECC Zone)	Characteristics
Honda Smart Home	Davis, CA (3B)	Two story SF 1944 ft^2
NREL Habitat for Humanity	Wheat Ridge, CO (5B)	SF residential 1280 ft^2
NIST (Net-Zero Energy Residential Test Facility)	Gaithersburg, MD (4A)	SF residential 4165 ft^2

HP Model

A 2-ton HP is simulated in MATLAB using Coolprop. The basic vapor compression model calculates the COP for cooling and heating from the evaporator and condenser outputs and electric consumption by compressor. Equation 14 and 15 define cooling and heating COP, respectively.

$$COP_c = Q_{evap}/W_{comp} \quad (14)$$

$$COP_h = Q_{cond}/W_{comp} \quad (15)$$

The outputs of HP model, Q_{evap} from the evaporator and Q_{cond} from the condenser are called into the cooling and heating functions in MATLAB, where they are coupled to PCM-TES depending on the operating mode. The thermostat model is used to control the VCS and PCM state of use.

Operating modes

TES is integrated with HP in such a way that heat transfer is only mediated by HP and TES does not have a direct interaction with building. In other words, TES aids HP operation and is used as heat source or sink instead of directly conditioning the building. This configuration can be referred as indirect HP-TES configuration.

Operating modes are illustrated with examples in Figure 63 and 64. There are total eight operating modes (four in heating and cooling each) for our HP-TES system; Normal operation, Standby operation, HP-TES Charging, and HP-TES Discharging. For comparison, direct charging and discharging operations are shown as well.

Figure 63 shows HP-TES cooling operating modes. In the normal operation, HP extracts the heat from building and rejects it to the ambient via VCC. In the HP-TES discharging operation, HP rejects the building heat into TES instead of ambient. It improves the HP's coefficient of performance since TES is at lower temperature than the ambient.

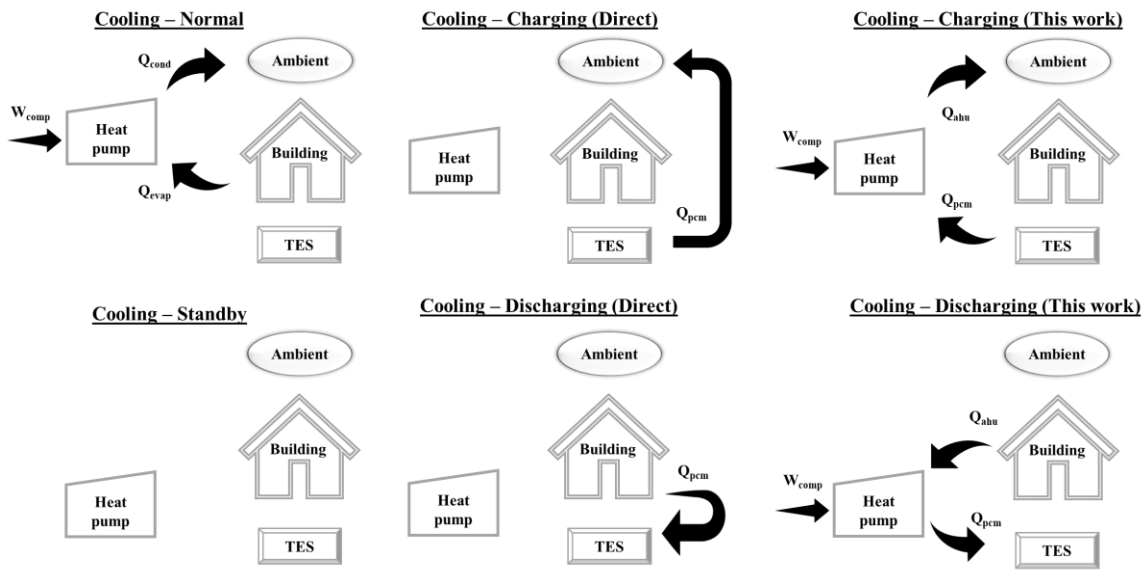


Figure 63: HP-TES cooling operating modes.

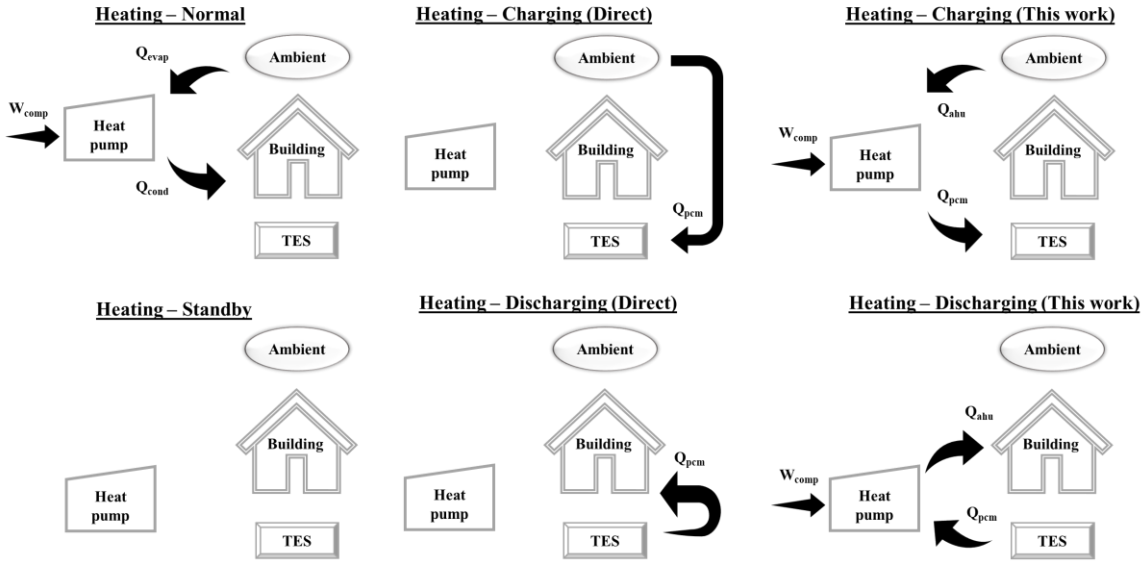


Figure 64: HP-TES heating operating modes.

The charging mode is activated when the cooling is not needed, often when the ambient temperature is lower, the heat is removed from TES and rejected to the ambient. Figure 64 shows HP-TES heating operating modes. The operating mode vapor compression cycle is reversed to heat the building. Now the TES assists HP for adding heat to the building from ambient.

The energy flow is different in direct TES modes where TES is used to heat or cool the building. Additional equipment is required to use TES. Indirectly coupling HP with TES (as in this work), avoids the cost and complexity of adding new equipment for heat transfer between the building and TES.

Configurations

Detailed configurations with vapor compression cycle (VCC) are shown for operating modes with and without TES. In the normal cooling mode, building is the heat source and ambient is heat sink (Figure 65). The building heat is removed through evaporator as Q_{evap} and rejected to ambient as Q_{cond} via condenser. The cycle is reversed in normal heating mode, as shown in Figure 66.

The vapor compression cycle is modified to integrate TES. PCM-TES behaves as evaporator or condenser. For charging cooling mode (Figure 67), evaporator is coupled to PCM. Building is not involved in this mode, ambient is heat sink while PCM is the heat source. For discharging mode (Figure 68), ambient is not involved, and PCM is the heat sink.

TES Model

The HP vapor compression system is coupled to PCM via HX. An arbitrary salt hydrate with melting temperature of 20°C is used as the PCM. The operating modes are controlled by the PCM state of charge (SOC) which is a function of peak time, and indoor temperature. The PCM operating modes are charging, discharging, and standby, and are selected by control logic (upcoming section).

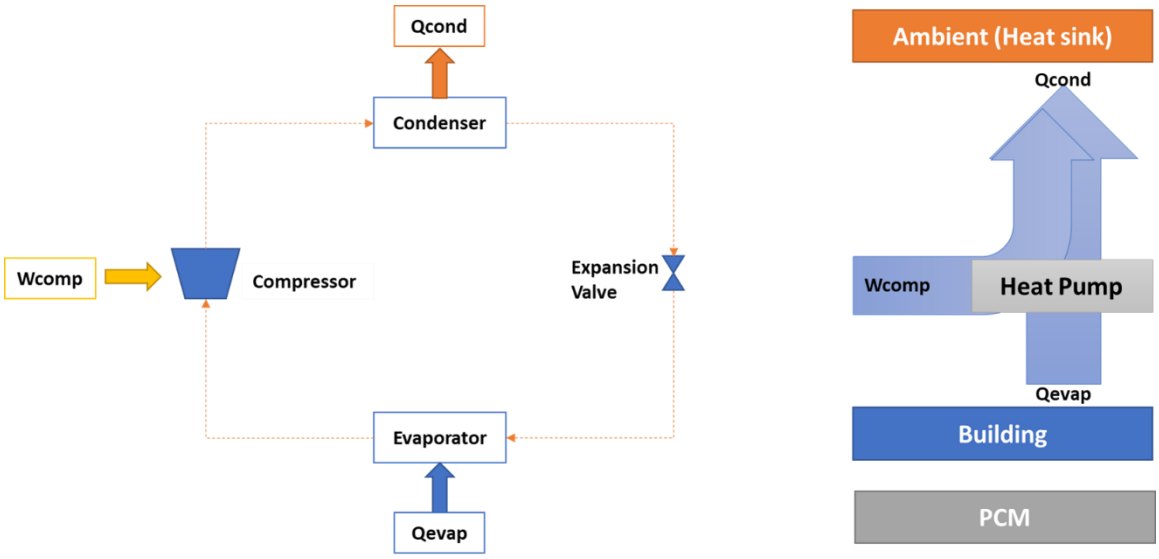


Figure 65: Vapor Compression Cycle for Normal Cooling.

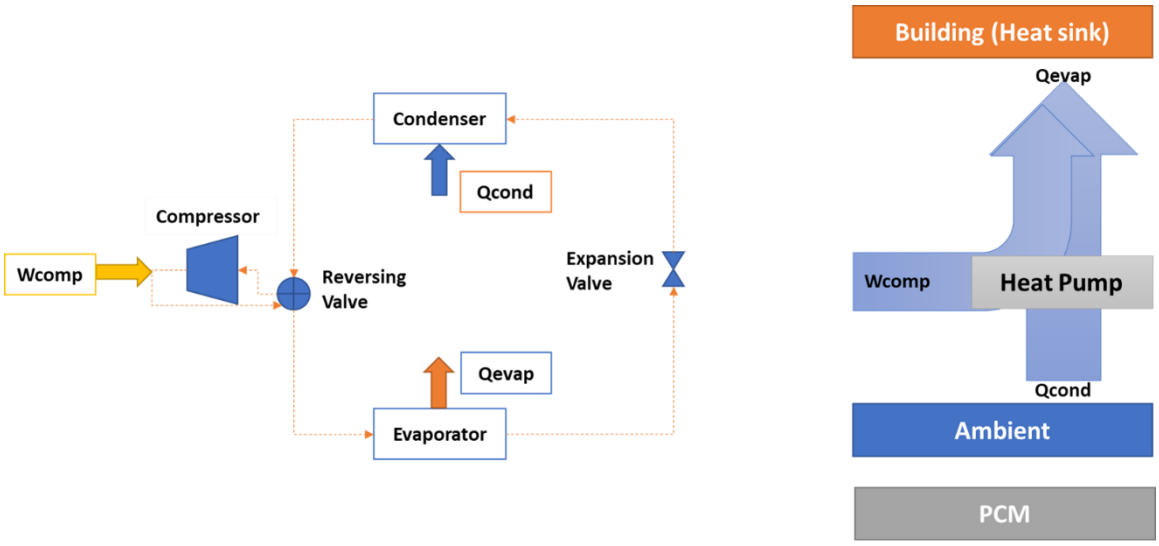


Figure 66: Vapor Compression Cycle for Normal Heating.

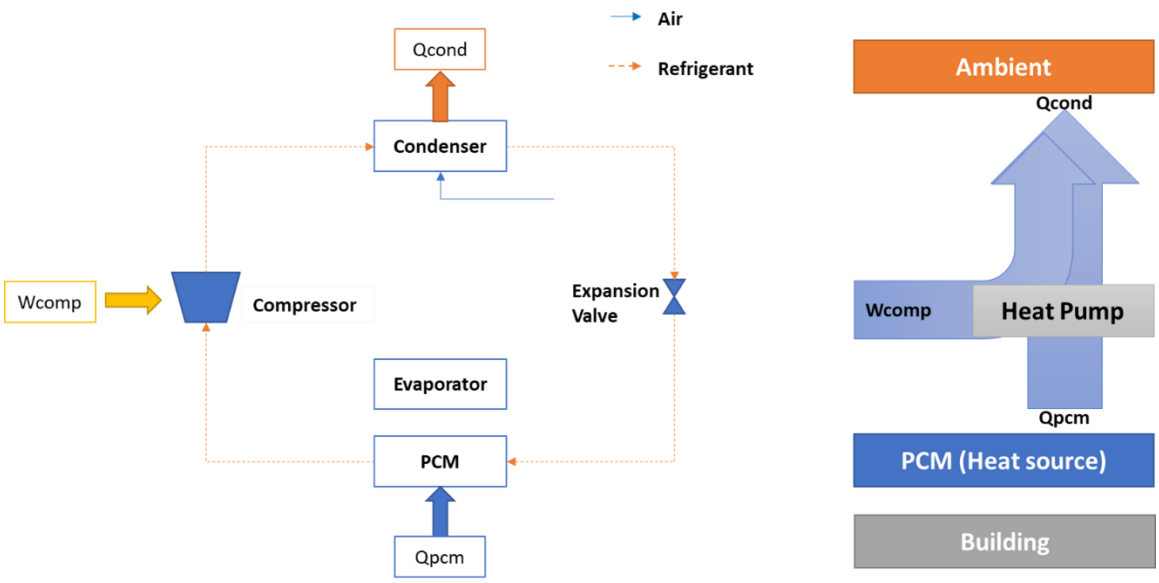


Figure 67: Vapor Compression Cycle for Charging Cooling

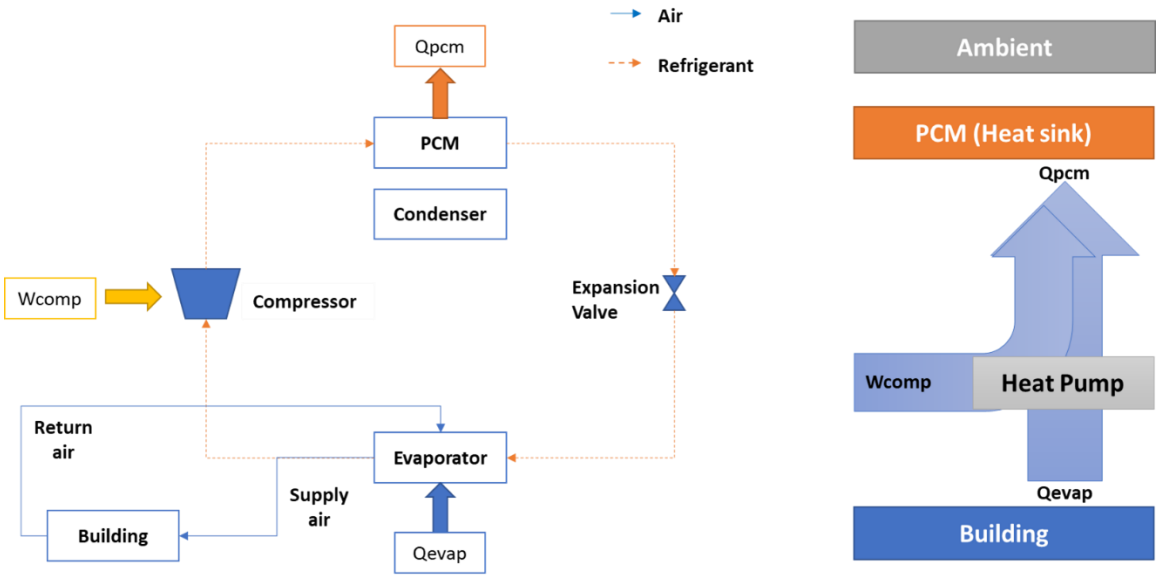


Figure 68: Vapor Compression Cycle for Discharging Cooling

The definitions of SOC for both heating and cooling modes are consistent with utility perspective on electrochemical batteries behind the meter and are shown in Table 23.

Figure 69 shows the energy flow for each operating mode. The equations were driven from this schematic for each mode and integrated into MATLAB functions.

A comparative analysis is performed for three cases as shown in Table 24. Base case does not use any controls. Rule based control strategies for peak time are defined for the other two cases.

For case 1, time-of-use utility data is obtained for each climate zone evaluated.

For case 2, in addition to time-of-use utility data, marginal grid emissions data is also obtained, and both are implemented in the control strategy.

The utility data and grid emissions data corresponding to each climate zones will be described in analysis section.

Electric consumption is calculated from each operating mode using equation 16,

$$P_{electric} = Q_{ahu}/COP \quad (16)$$

Where, Q_{ahu} is the HP capacity, and COP of HP for all modes is defined as,

$$COP = Q_{ahu}/W_{comp} \quad (17)$$

In normal cooling mode, evaporator is coupled to building and the condenser is coupled to ambient. Since TES is not used in this case, Q_{pcm} is 0.

$$T_{evap} = T_{indoor} - AT \quad (18)$$

$$T_{cond} = T_{amb} + AT \quad (19)$$

$$Q_{ahu} = Q_{evap} \quad (20)$$

$$Q_{pcm} = 0 \quad (21)$$

Table 23: Definitions of SOC

Mode	SOC	Meaning
Cooling	0	Fully discharged, i.e., full of energy (PCM liquified)
Cooling	1	Fully charged, i.e., empty of energy (PCM solidified)
Cooling	<1	Charging
Cooling	>0	Discharging
Heating	1	Fully discharged, i.e., empty of energy (PCM solidified)
Heating	0	Fully charged, i.e., full of energy (PCM liquified)
Heating	<1	Discharging
Heating	>0	Charging

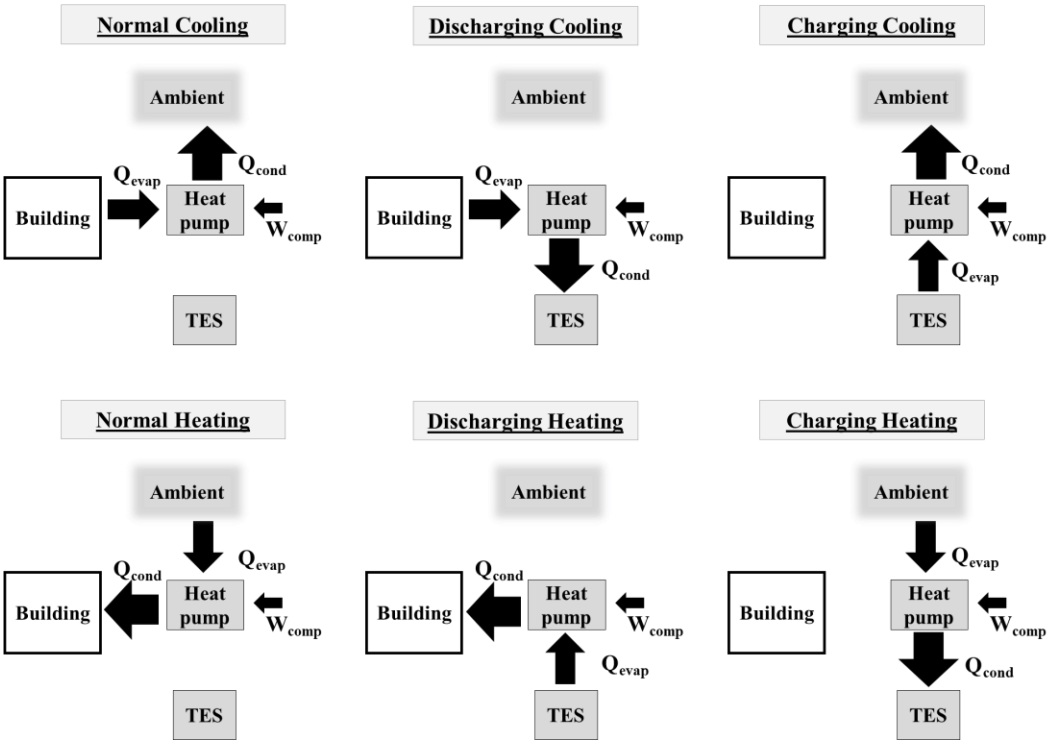


Figure 69: HP-TES integration and energy flow

Table 24: Cases for comparative analysis

Base case	**Case 1**	**Case 2**
Without any controls	Utility peak time controls	Both utility peak time and Emissions peak time controls

The HP is off for cooling standby mode.

$$Q_{ahu} = 0 \quad (22)$$

$$Q_{pcm} = 0 \quad (23)$$

In the cooling charging mode, TES is recharged and evaporator heat is removed from TES. Condenser is coupled to ambient and evaporator is coupled to PCM-TES. State of charge and PCM storage capacity are defined and rewritten at each time step.

$$T_{evap} = T_{pcm} - AT \quad (24)$$

$$T_{cond} = T_{amb} + AT \quad (25)$$

$$Q_{ahu} = 0 \quad (26)$$

$$Q_{pcm} = Q_{evap} \quad (27)$$

$$SOC_{@t=i+1} = SOC_{@t=i} - Q_{evap_{@t=i}} * (\Delta T) \quad (28)$$

$$E_{pcm} = E_{pcm(i-1)} + Q_{pcm} \quad (29)$$

In the cooling discharging mode, TES is used to cool the building via HP and condenser heat is added to TES. Evaporator is coupled to building and condenser is coupled to PCM-TES in this case.

$$T_{evap} = T_{indoor} - AT \quad (30)$$

$$T_{cond} = T_{pcm} + AT \quad (31)$$

$$Q_{ahu} = Q_{evap} \quad (32)$$

$$Q_{pcm} = -Q_{cond} \quad (33)$$

$$SOC_{@t=i+1} = SOC_{@t=i} + Q_{cond_{@t=i}} * (\Delta T) \quad (34)$$

$$E_{pcm}(t) = E_{pcm(t-1)} - Q_{pcm} \quad (35)$$

In normal heating mode, evaporator is coupled to ambient and the condenser is coupled to building. Since TES is not used in this case, Q_{pcm} is 0.

$$T_{evap} = T_{amb} - AT \quad (36)$$

$$T_{cond} = T_{indoor} + AT \quad (37)$$

$$Q_{ahu} = Q_{cond} \quad (38)$$

$$Q_{pcm} = 0 \quad (39)$$

The HP is off for heating standby mode.

$$Q_{ahu} = 0 \quad (40)$$

$$Q_{pcm} = 0 \quad (41)$$

In the heating charging mode, TES is recharged and condenser heat is added to TES. Evaporator is coupled to ambient and condenser is coupled to PCM-TES. State of charge and PCM storage capacity are defined and rewritten at each time step.

$$T_{evap} = T_{amb} - AT \quad (42)$$

$$T_{cond} = T_{pcm} + AT \quad (43)$$

$$Q_{ahu} = 0 \quad (44)$$

$$Q_{pcm} = Q_{cond} \quad (45)$$

$$SOC_{@t=i+1} = SOC_{@t=i} + Q_{cond_{@t=i}} * (\Delta T) \quad (46)$$

$$E_{pcm}(t) = E_{pcm(t-1)} + Q_{pcm} \quad (47)$$

In the heating discharging mode, TES is used to heat the building via HP and evaporator heat is removed from TES. Evaporator is coupled to PCM-TES and condenser is coupled to building in this case.

$$T_{evap} = T_{pcm} - AT \quad (48)$$

$$T_{cond} = T_{indoor} + AT \quad (49)$$

$$Q_{ahu} = Q_{cond} \quad (50)$$

$$Q_{pcm} = -Q_{evap} \quad (51)$$

$$SOC_{@t=i+1} = SOC_{@t=i} - Q_{evap_{@t=i}} * (\Delta T) \quad (52)$$

$$E_{pcm} = E_{pcm(i-1)} - Q_{pcm} \quad (53)$$

Controls logic

For simplicity, controls logic is implemented in two steps. First, thermostat call is determined for each mode in all three cases (Figure 70 and 71). Then State of Use of PCM (SOU) is defined and operating modes are determined based on SOU. Base case controls are simple since no PCM is involved. For the other two cases, utility and emissions peak time are used to determined SOU (Figure 72 and 73).

Utility peak times are pre-defined in TOU rate schedule for both winter and summer in each climate zone. Emissions peak is defined at each time step based on marginal grid emissions (MGE) data. If the MGE value at a given time step exceeds the average of emissions in past 24 hours, it is defined as peak.

Experimental Validation

We developed an experimental setup for HP-TES using the low-cost salt hydrate PCM prepared at ORNL. The technology integrates phase change material with heat pump (PCM-HP) to reduce demand in peak hours. It enables year-round demand flexibility, energy savings and shortens payback period. A single PCM storage tank is used for both heating and cooling modes in dual-mode heat pumps. TES is directly coupled with heat pump and does not interact with building. PCM tank is used as either condenser or evaporator depending on operating modes, and heat transfer is mediated by heat pump, as shown in Figure 74. PCM is charged during off-peak hours, and it is discharged during peak hours. The charge and discharge operations are automatically achieved by system control.

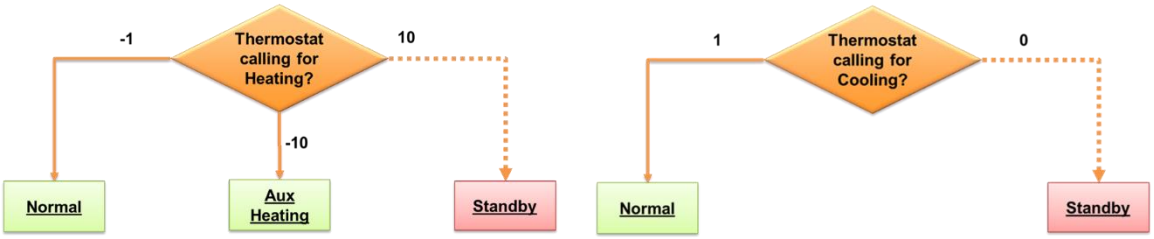


Figure 70: Operating mode controls for base case

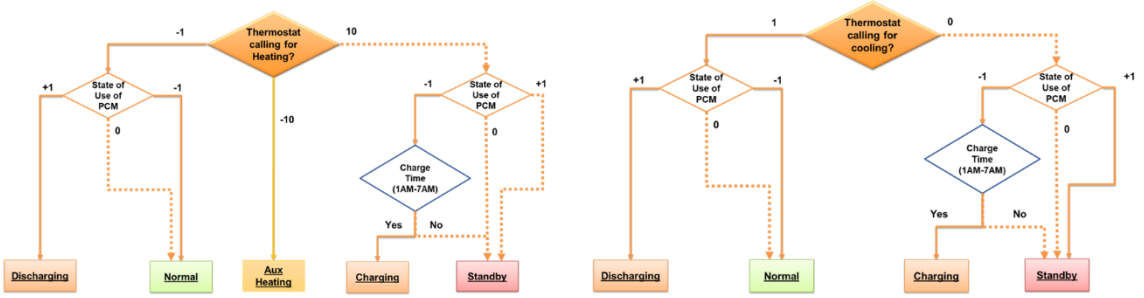


Figure 71: Operating mode controls for case 1 and 2

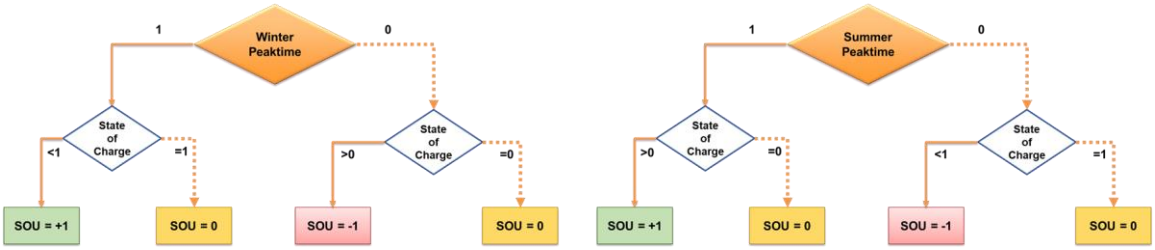


Figure 72: SOU controls for case 1

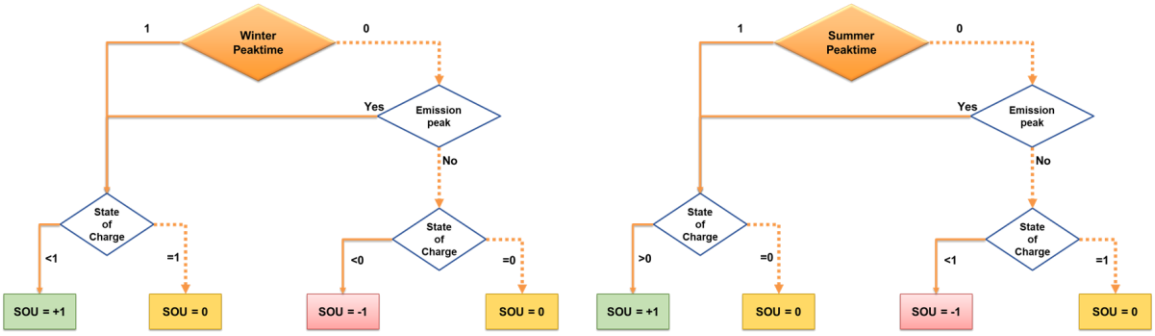


Figure 73: SOU controls for case 2

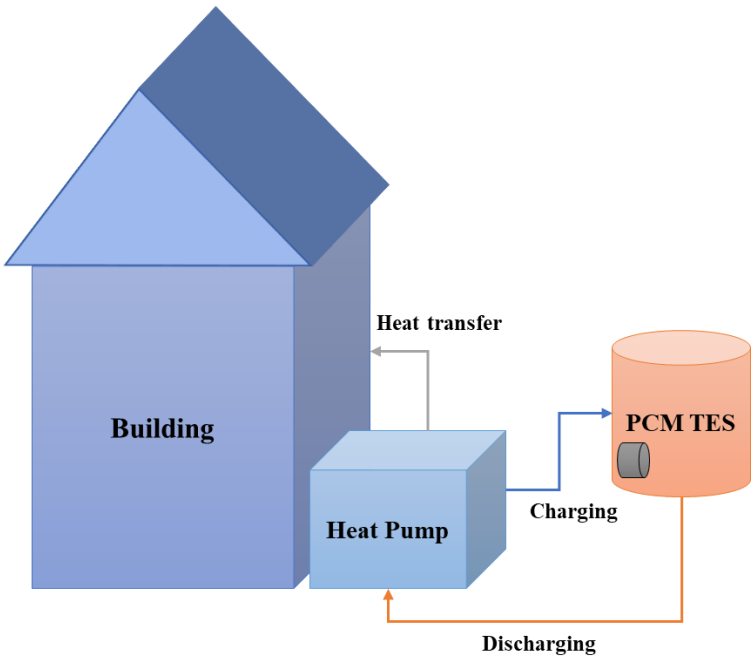


Figure 74: Conceptual figure of HP-TES with building

The proposed HP-TES can provide load shifting and improve system efficiency in both cooling (summer) and heating (winter) modes. It is expected to achieve 50% demand reduction for up to 4 hours in heating mode, a 35% demand reduction for 2 hours in cooling mode and a 10% year-round efficiency improvement by favorably exploiting diurnal ambient temperature swings.

Building RC Model

Multiple different structures exist for modeling the thermal dynamics of a building zone. Among them, the resistance and capacitance (RC) network is a common and popular subclass [216]. A RC model is a typical control-oriented grey-box model that can capture adequate thermal behaviors of the system to keep its robustness under different operation conditions [217], and it has been proven to be quite effective in predicting the thermal response of buildings [218]. Many studies have identified the thermal parameters of an RC network model for commercial [219] and residential buildings [220]. RC models have been widely used for MPCs [219] since they can be developed in first-order differential equations containing undetermined parameters and that can be easily transformed to a discretized state-space model (SSM).

In this study, a control-oriented RC model was developed for room 104 in FRP building. The schematic of the model is shown in Figure 75. This gray-box model is used to predict the mean indoor air temperature (T_{in}). The model consists of four states: mean indoor air temperature (T_{in}), mean north exterior wall temperature (T_{wall_N}), mean west exterior wall temperature (T_{wall_W}) and mean internal thermal mass temperature (T_{mass}).

Exterior walls should be considered respectively according to their orientations because the dynamic models of exterior walls at different orientations have different forcing functions (differential equations) due to the changing position of the sun [221]. Therefore, the exterior building envelope was split into two parts based on their orientations.

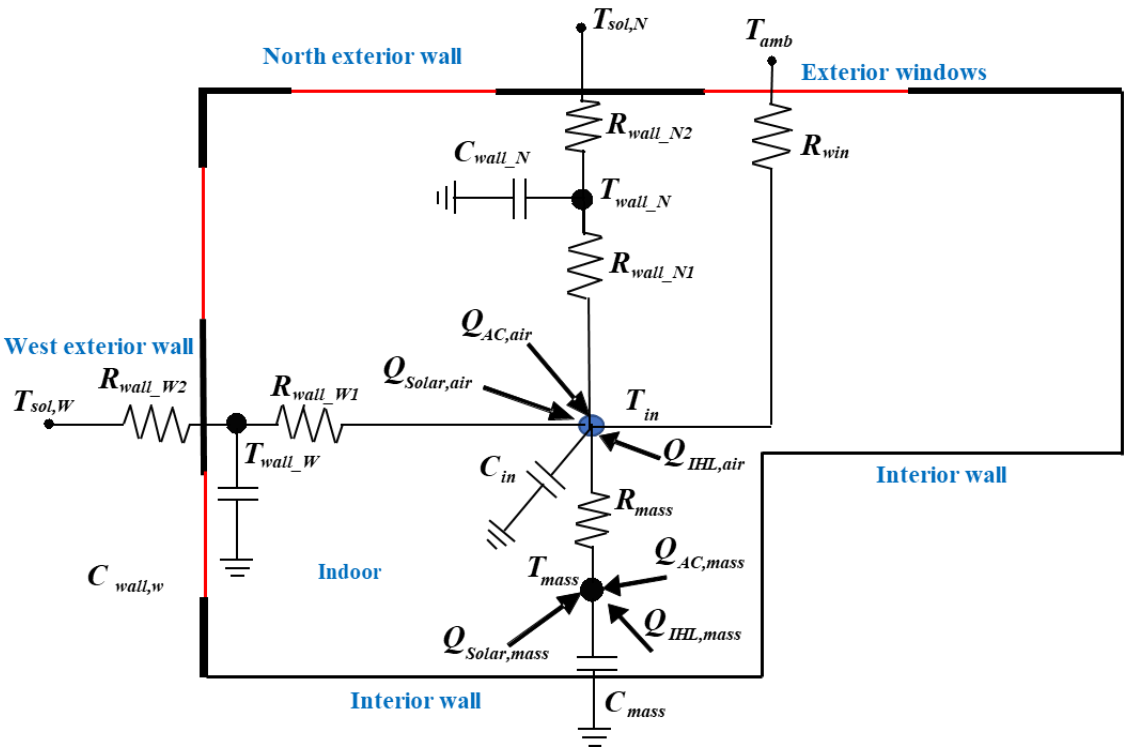


Figure 75: Schematic of the simplified building thermal network model

The heat transfer in the building model is described using the following set of first-order differential equations:

$$C_{in}\frac{dT_{in}(t)}{dt} = \frac{T_{wall\_N}(t)-T_{in}(t)}{R_{wall\_N}} + \frac{T_{wall\_W}(t)-T_{in}(t)}{R_{wall\_W}} + \frac{T_{mass}(t)-T_{in}(t)}{R_{mass}} + \frac{T_{amb}(t)-T_{in}(t)}{R_{win}} + Q_{AC,air} * C_{AC,air} + Q_{IHL,air} * C_{IHL,air} + Q_{solar,air} * C_{solar,air} \quad (54)$$

$$C_{wall\_N}\frac{dT_{wall\_N}(t)}{dt} = \frac{T_{sol,N}(t)-T_{wall\_N}(t)}{R_{wall\_N2}} - \frac{T_{wall\_N}(t)-T_{in}(t)}{R_{wall\_N1}} \quad (55)$$

$$C_{wall\_W}\frac{dT_{wall\_W}(t)}{dt} = \frac{T_{sol,W}(t)-T_{wall\_W}(t)}{R_{wall\_W2}} - \frac{T_{wall\_W}(t)-T_{in}(t)}{R_{wall\_W1}} \quad (56)$$

$$C_{mass}\frac{dT_{mass}(t)}{dt} = -\frac{T_{mass}(t)-T_{in}(t)}{R_{mass}} + Q_{AC,mass} * C_{AC,mass} + Q_{IHL,mass} * C_{IHL,mass} + Q_{solar,mass} * C_{solar,mass} \quad (57)$$

where, C_{in}, C_{wall_N}, C_{wall_W}, and C_{im} are the equivalent overall thermal capacitances of indoor air, north external wall (opaque wall), west external wall (opaque wall), and internal thermal mass, respectively (J/K). R_{wall_N1}, R_{wall_N2}, R_{wall_W1}, R_{wall_W2}, R_{win}, and R_{mass} are the equivalent overall thermal resistances of north external wall (opaque wall) part 1, north exterior wall (opaque wall) part 2, west exterior wall (opaque wall) part 1, west exterior wall (opaque wall) part 2, windows, and internal thermal mass, respectively (K/W).

Building internal mass includes interior partitions, furniture, and so on, and was included in the models because it absorbs solar radiation passing through the windows [222]. The building internal mass must be considered since its effect on cooling/heating energy consumption and indoor temperature is significant. The total area of the internal mass was assumed to be equal to the floor area, although the actual area of internal mass may be larger.

Q_{IHL} is the sensible heat gain from indoor heat sources (W). Q_{cool} is the sensible cooling supply from the HVAC (W). Q_{solar} is the total solar radiation rate (W) transmitted through the windows into the zone. These values were the measurements from the reference room (i.e., room 104). Partial Q_{IHL}, Q_{cool} and Q_{solar} were transferred to indoor air directly, as $Q_{IHL,air}$, $Q_{cool,air}$ and $Q_{solar,air}$. The left part of Q_{IHL}, Q_{cool} and Q_{solar} were adsorbed by the internal mass through radiation, as $Q_{IHL,mass}$, $Q_{cool,mass}$ and $Q_{solar,mass}$. $C_{AC,air}$, $C_{IHL,air}$, $C_{solar,air}$, $C_{AC,mass}$, $C_{IHL,mass}$, and $C_{solar,mass}$ are the coefficients which are assumed to be unknown and need to be identified by the search algorithm illustrated in the next sub-section.

The effects of solar radiation on external walls (i.e., north and west walls) were considered by calculating $T_{sol,W}$ and $T_{sol,N}$ respectively, which are the sol-air temperatures, shown in the following equations:

$$T_{sol,W} = \frac{I_W(t)}{h_W(t)} + T_{amb} \tag{58}$$

$$T_{sol,N} = \frac{I_N(t)}{h_N(t)} + T_{amb} \tag{59}$$

where T_{amb} is the outdoor dry bulb temperature (°C); h_W and h_N are the convective heat transfer coefficients of the exterior surfaces of west and north external walls, respectively (W/m^2·K); and I_W and I_N are the effective solar radiation absorbed on the exterior surfaces of west and north external walls, respectively (W/m^2) with absorption coefficients already incorporated.

Two assumptions were made in the model: only sensible loads were considered, and all the *R* and *C* parameters were assumed to be time-invariant.

Please note that, for simplification, the heat transfer effect from surrounding rooms/zones (i.e., rooms 102, 103 and 105) were not considered initially and the indoor air temperature values in those room were assumed to be unknown.

1. Parameter identification

The searching process for the optimal values of the undetermined parameters (i.e., C_{wall_N}, C_{wall_W}, C_{air}, C_{mass}, R_{wall_N1}, R_{wall_N2}, R_{wall_W1}, R_{wall_W2}, R_{win}, R_{mass}, $C_{AC,air}$, $C_{IHL,air}$, $C_{solar,air}$, $C_{AC,mass}$, $C_{IHL,mass}$, and $C_{solar,mass}$) in the RC model is a nonlinear optimization process. Given a set of parameters, the gray-box model can predict a T_{in} profile. An objective function is used to evaluate the fitness between the results predicted by the RC model and the measured indoor time temperature during the training period; details on the training period are provided in a later section. The objective function $J_{Benchmark}$ of such optimization is to minimize the root mean squared error (*RMSE*) as defined in Equation 60.

$$J_{Benchmark}(C_{wall_N}, C_{wall_W}, C_{air}, C_{mass}, R_{wall_{N1}}, R_{wall_{N2}}, R_{wall_{W1}}, R_{wall_{W2}}, R_{win}, R_{mass}, C_{AC,air}, C_{IHL,air}, C_{solar,air}, C_{AC,mass}, C_{IHL,mass}, C_{solar,mass}) = \sqrt{\frac{\sum_{i=1}^{N}(T_{in,real}-T_{in,RC})^2}{N-1}} \quad (60)$$

where $T_{in,real}$ is the measured mean indoor air temperature from the reference room, and $T_{in,RC}$ is the mean indoor air temperature predicted by the developed RC model.

The model development was written in Python. The parameters were identified using the particle swarm optimization (PSO) method. PSO is a computational method that optimizes a problem by iteratively trying to improve a candidate solution with regard to a given measure of quality [214]. It solves a problem by having a population of candidate solutions and moving these particles around in the search space according to simple mathematical formulae over the particle's position and velocity [223].

The model development was written and the PSO package was imported in Spyder [224], which is a free and open-source integrated development environment for Python.

Experimental setup with HP in FRP-2

The heat pump is a dual source (air source and ground source) heat pump (DSHP). The cooling capacity of the HP is 2 ton. Hot or chilled water is produced through a brazed plate heat exchanger for storing energy in the PCM HX. A fan coil in the hydraulic lines is used for discharging stored energy in the PCM HX for space cooling or heating.

Various sensors are installed in the HP to measure the temperature, pressure, and flow rates of air, water, and refrigerant.

Table 25 below shows the heat pump capacity and COP during heating mode or cooling mode. DX means the heat pump only provides spacing heating or cooling, Hydronic means the heat pump only provides chilled water or hot water for the PCM HX.

During the charging and discharging tests, the heat pump storage capacity varied with time for each cycle, as shown in Figure 76 below. The discharging rate is 1-2 ton, the average discharging rate is around 1.2 ton. The measured phase change temperature is around 26-32℃ for melting and 24℃ for freezing (Figure 77). Figure 78 shows the complete setup at ORNL.

PCM Heat exchanger and HP-TES integration

The PCM HX consists of a tank filled with the PCM and a plastic tubing network that serves to transfer heat to the PCM. Hot or chilled water is produced through a brazed plate heat exchanger for storing energy in the PCM HX. The coil of the tubing network is 23” round by 30” tall. Total length of tubing is between 670-675 meters. Figure 79 shows the dimensions of PCM-HX integrated with HP. Hydronic piping and setup is shown in Figure 80.

Total PCM volume in the PCM HX is 48 gal. The discharging rate of the PCM HX is 1-2 ton, the average discharging rate is around 1.2 ton. An SSD-SPDD salt hydrate PCM was developed in lab. 34.2 w% sodium sulfate decahydrate [SSD], 60.8 w% sodium phosphate dibasic dodecahydrate [SPDD], and 5 w% borax.

Table 25: HP capacity and COP

H/C	Compressor Speed	Mode	Source Temperature (F)	Entering air conditions	Heat Capacity (kW)	Power (kW)	COP
Heating	High	DX	50	73F, 30-35% RH	9.0	1.6	5.7
Heating	Low	DX	50	73F, 30-35% RH	6.5	1.1	5.8
Heating	High	Hydronic	51	73F, 30-35% RH	5.8	1.5	3.8
Heating	Low	Hydronic	50	73F, 30-35% RH	4.4	1.1	4.1
Cooling	High	DX	50	70F, 30-35% RH	6.0	0.9	7.0
Cooling	Low	DX	50	70F, 30-35% RH	4.6	0.6	8.0
Cooling	High	Hydronic	49	70F, 30-35% RH	6.7	0.9	7.5
Cooling	Low	Hydronic	49	70F, 30-35% RH	5.3	0.5	10.3

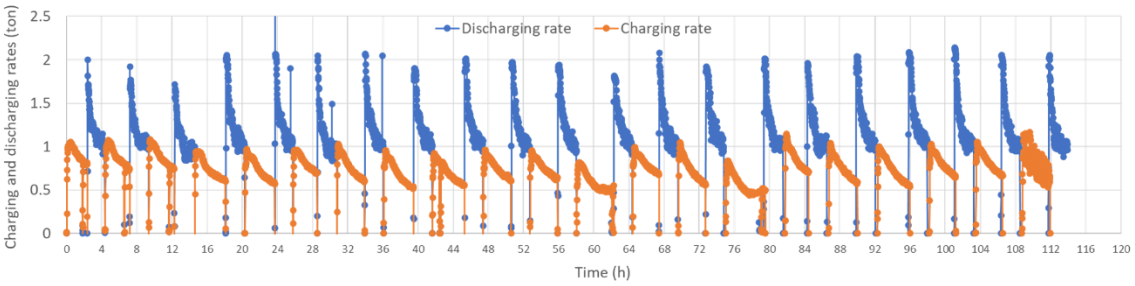


Figure 76: HP Charging and Discharging rate.

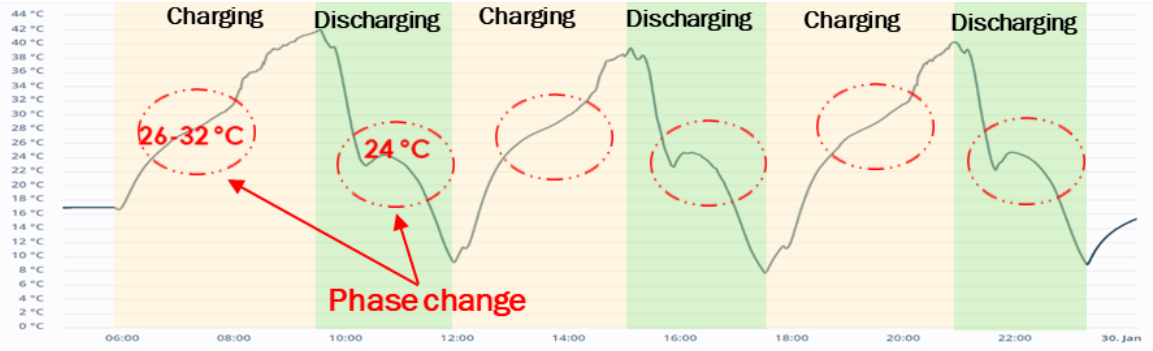


Figure 77: Measured PCT using sensors.

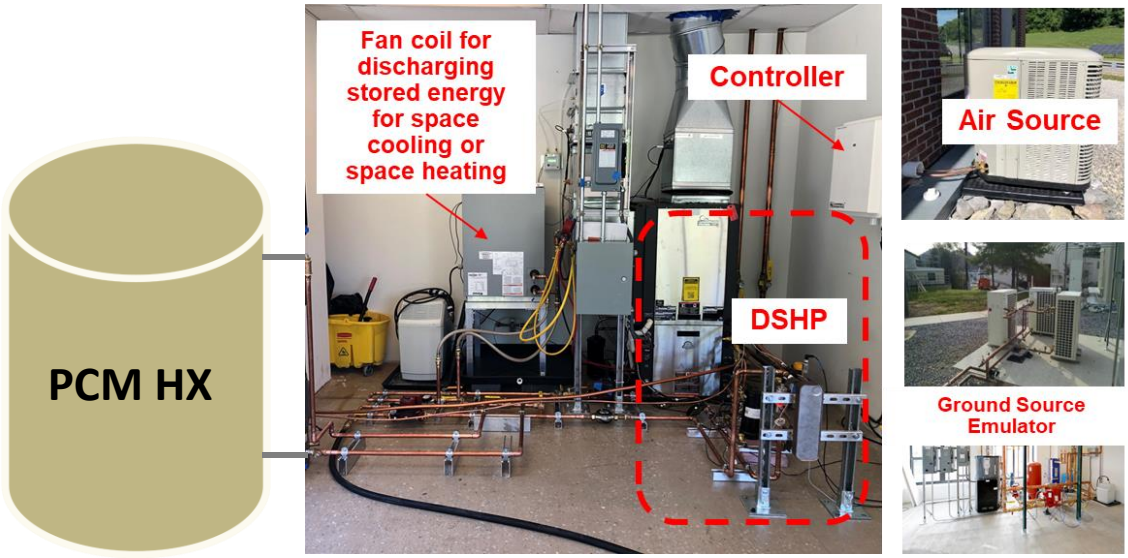


Figure 78: Experimental setup at ORNL.

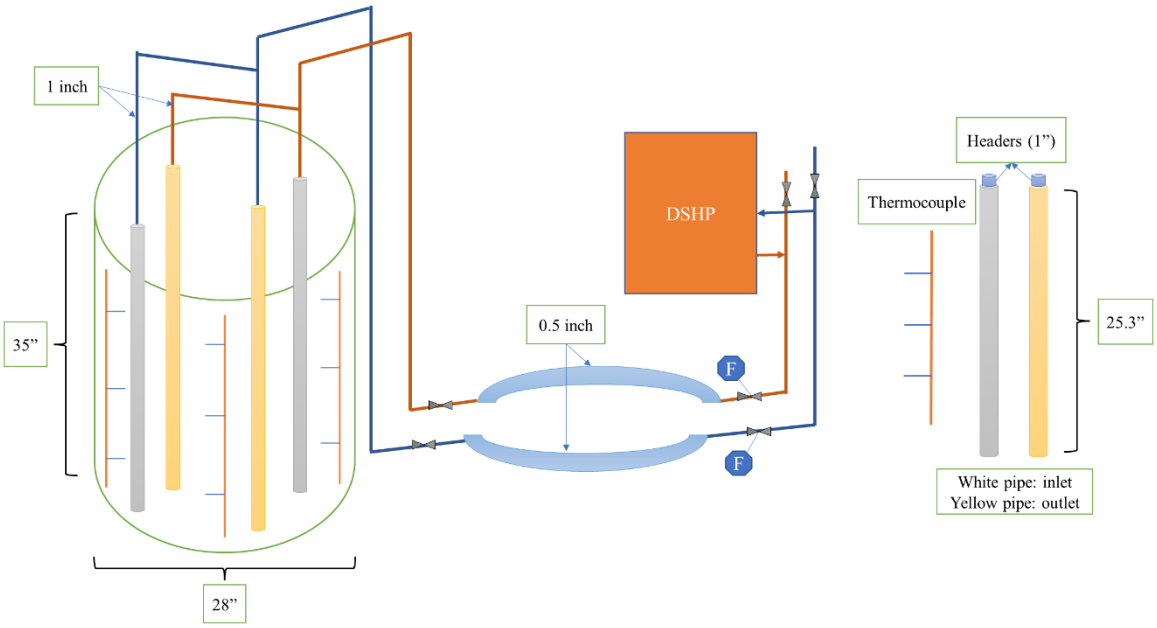


Figure 79: PCM-HX integrated with DSHP.

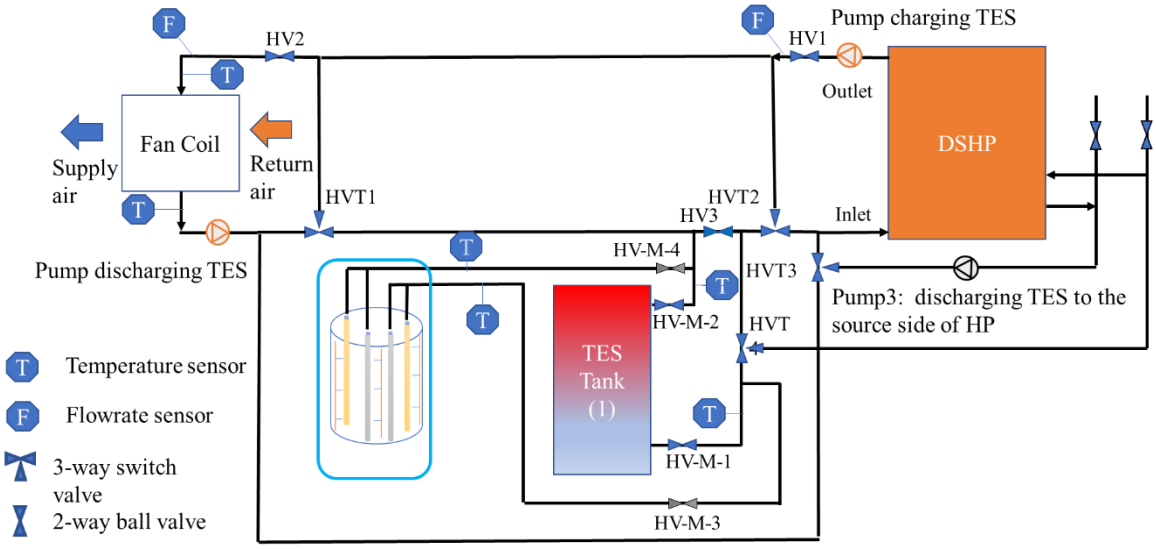


Figure 80: Hydronic piping and data points.

Analysis

The analysis is performed on three climate zones for electric consumption, utility cost, and grid emissions. Physical buildings for each climate are selected and hot and cold weeks are analyzed. Three cases are analyzed using both utility and grid emissions data. Base case does not include any controls. Case 1 is rule-based strategy defined by TOU utility schedule only, while Case 2 is rule-based strategy defined by both TOU utility schedule and marginal grid emissions data. Pareto charts are developed to compare controls. The charts show percent decrease in peak utility cost and peak emissions in both cases.

Climate Zone and Input Data

Three climate zones were selected for analysis based on the data availability of physical buildings. The building information was collected from Benchmark building database by U.S. DOE [225].

TMY 3 weather data was used for all three buildings,

1. Honda Smart Home, Davis, CA.
2. NREL Habitat for Humanity, Wheat Ridge, CO.
3. NIST building (Net-Zero Energy Residential Test Facility, Gaithersburg, MD)

TOU utility rates were obtained corresponding to each location and are shown in Table 26. Marginal grid emissions data was collected from Watt Time for all three locations.

Figure 81 and 82 show grid emissions during winter and summer, respectively, for all three locations. Figure 83 through 88 show ambient dry bulb temperature and utility rate trend. Hottest and coldest day for each climate zone was plotted against utility rate. For a hottest day in Baltimore, MD, utility peak also occurs when the ambient temperature is high, and vice versa for the coldest day. However, in Sacramento, CA, utility peaks do not correspond with the ambient temperature peak. This is a limitation of this study that controls do not consider ambient temperature extremes while deciding when to charge or discharge TES.

Table 26: TOU Utility Schedule

Location	Utility	TOU tariff		
		Tariff name	**On-peak rate (¢/kWh)**	**Off-peak rate (¢/kWh)**
Sacramento, California	Sacramento Municipal Utility District	Time-of-Day (5-8 p.m.) Rate	32.79 (summer[1]) 15.47 (winter[2])	13.50 (summer[1]) 11.20 (winter[2])
Golden, Colorado	Xcel Energy	Time-of-Use (TOU)	28 (summer[1]) 18 (winter[2])	11 (year-round)
Baltimore, Maryland	Baltimore Gas and Electric Company	Residential delivery and energy time-of-use - electric schedule RD	13.31 (Year around)	2.58 (year-round)

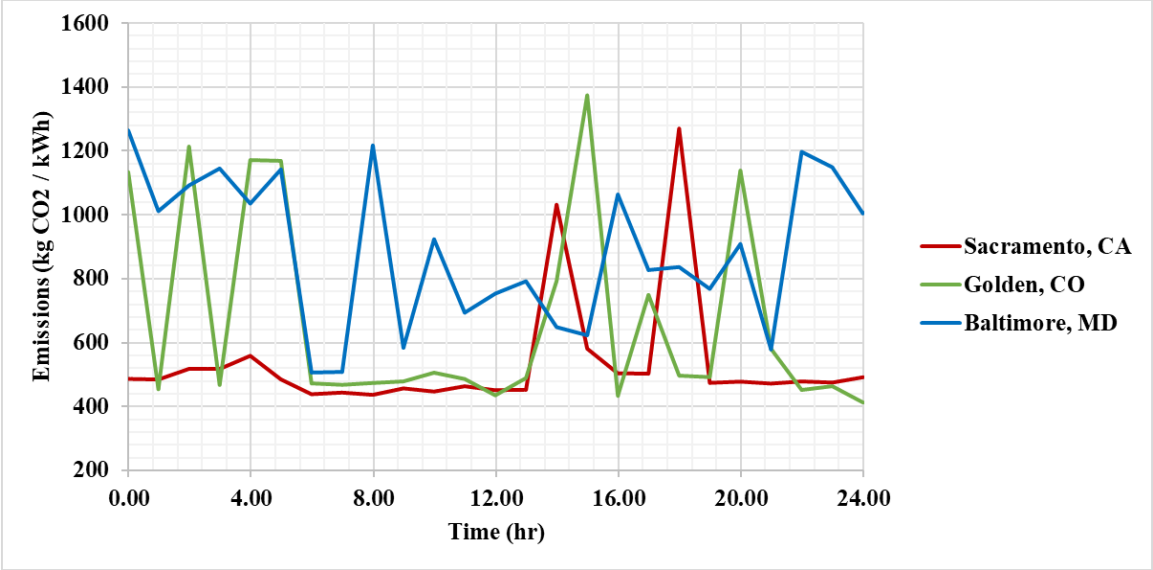


Figure 81: Representative MGE Data for Summer in all locations.

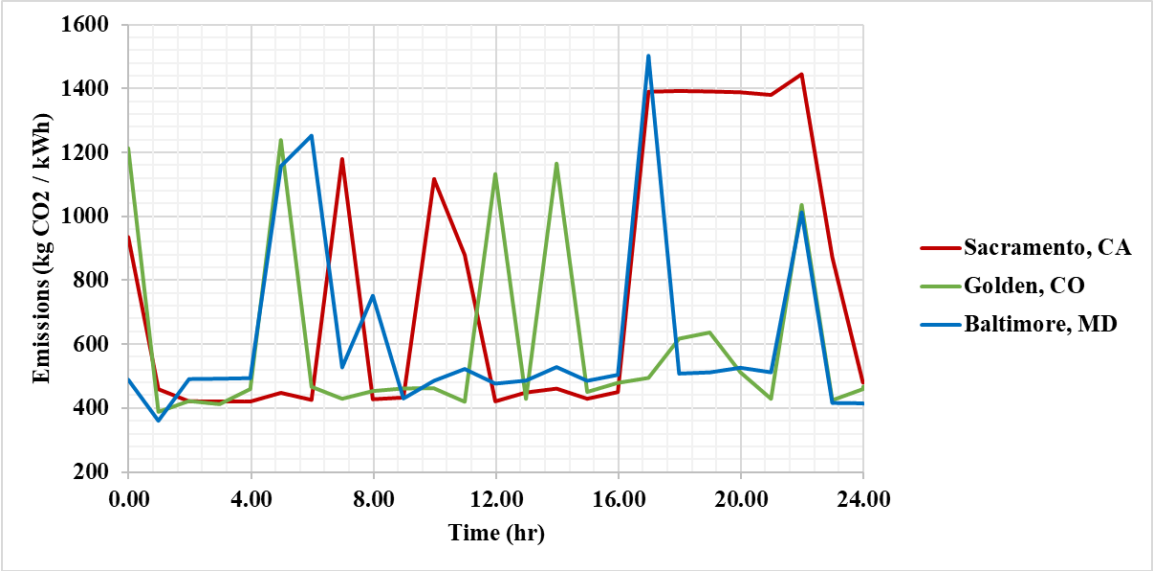


Figure 82: Representative MGE Data for Winter in all locations.

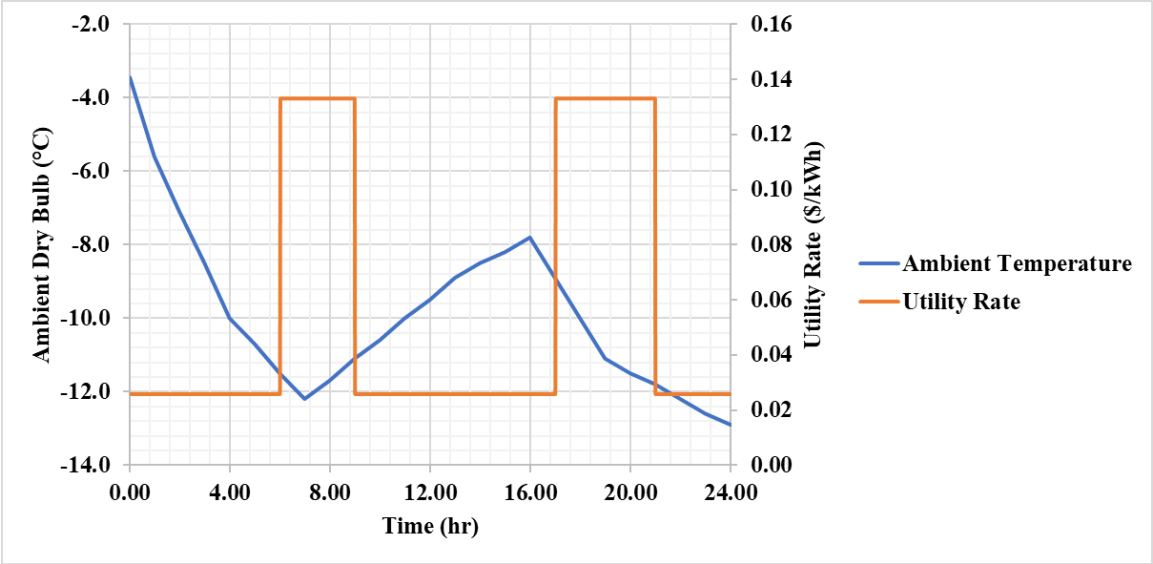


Figure 83: Ambient Weather and Utility Rate on the coldest day in Baltimore

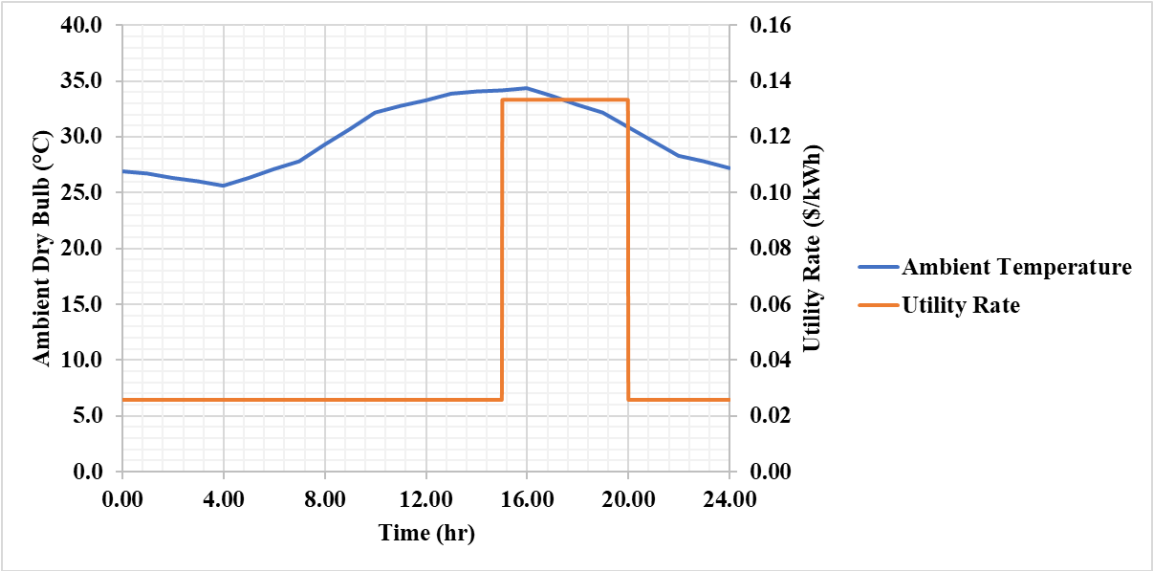


Figure 84: Ambient Weather and Utility Rate on the hottest day in Baltimore

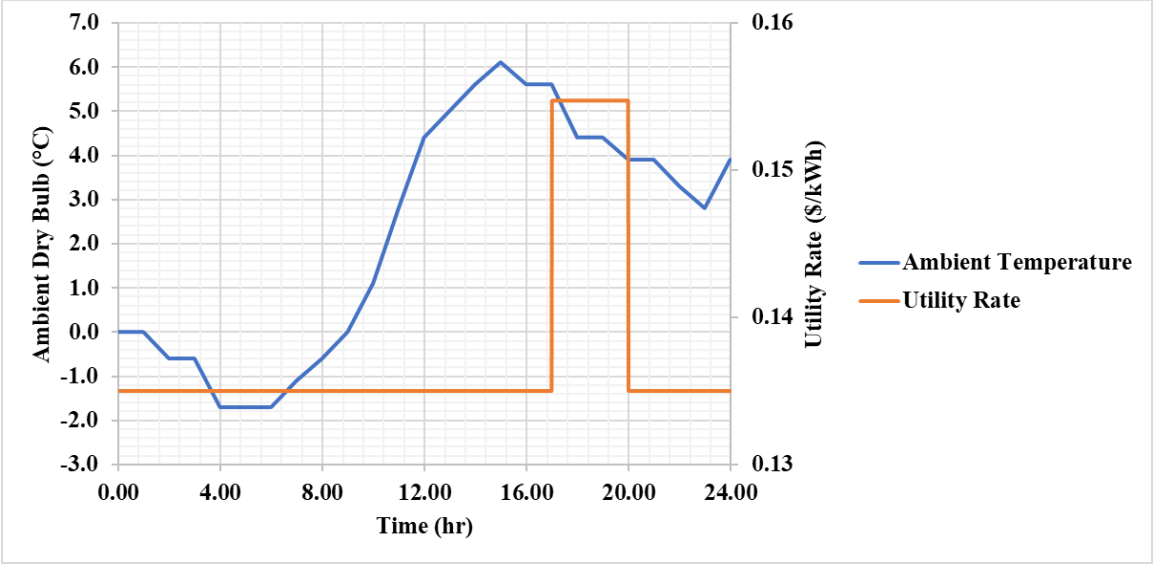


Figure 85: Ambient Weather and Utility Rate on the coldest day in Sacramento

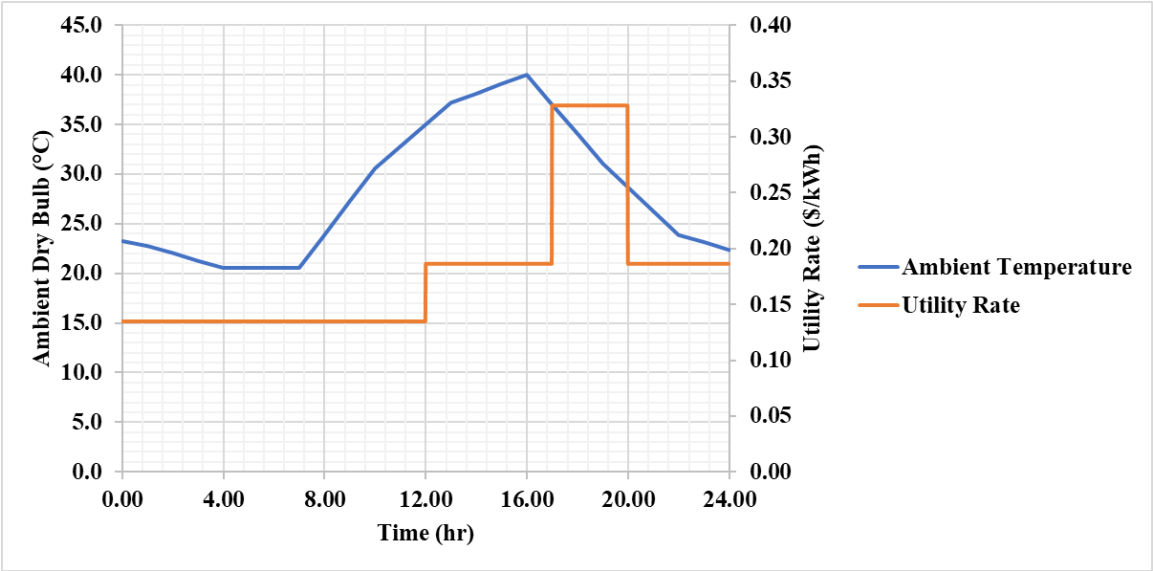


Figure 86: Ambient Weather and Utility Rate on the hottest day in Sacramento

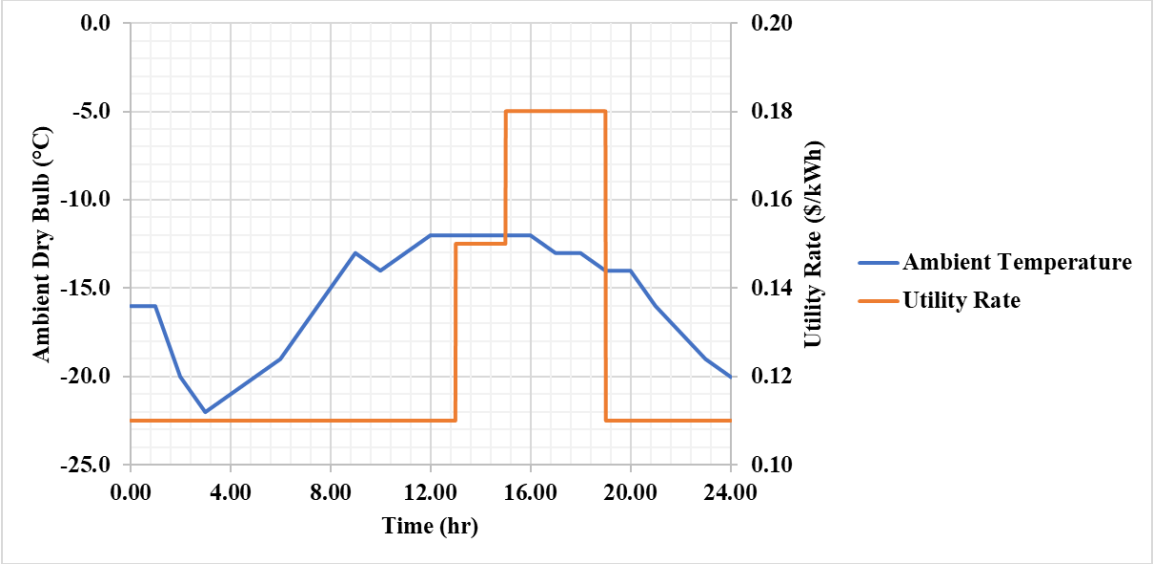


Figure 87: Ambient Weather and Utility Rate on the coldest day in Golden

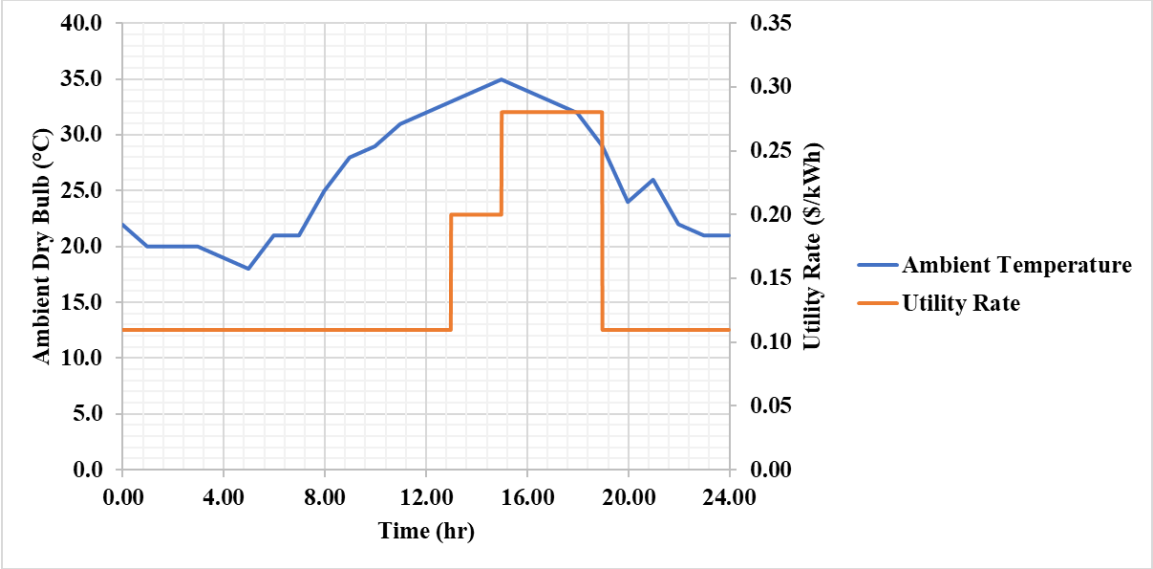


Figure 88: Ambient Weather and Utility Rate on the hottest day in Golden

Analysis on Baltimore, MD

Baltimore is a heating dominated climate. The analysis was performed for winter typical and winter extreme weeks for both cases. The charts show average percent decrease in peak utility cost and peak emissions in both cases. Figures 89 and 90 show the results for winter typical and winter extreme respectively. For typical week, the case with both MGE and TOU controls was promising as it decreased maximum emissions by 33% and cost by 58% (only average values shown in chart). The TOU only case saves cost at similar percentage, but emission savings are much lower.

Analysis on Golden, CO

Golden is also a heating dominated climate. The analysis was performed for winter typical and winter extreme weeks for both cases. Figures 91 and 92 show percent decrease in peak utility cost and peak emissions for winter typical and winter extreme respectively, in both cases. For winter typical week, the case with both MGE and TOU controls saved emissions (35%) by a huge margin as compared to the case with TOU controls only (10%).

Analysis on Sacramento, CA

Sacramento is a mild climate zone and analysis is performed for both winter and summer extremes. Figures 93 and 94 show comparison for peak utility cost and peak emissions during extreme week of summer and winter in Sacramento, respectively. Since the utility peaks and ambient weather extremes do not align in this case, TES may be used for charging during the times when cooling or heating demand is high. This leads to increased electric consumption as compared to base case. Emissions were increased as compared to base case for summer.

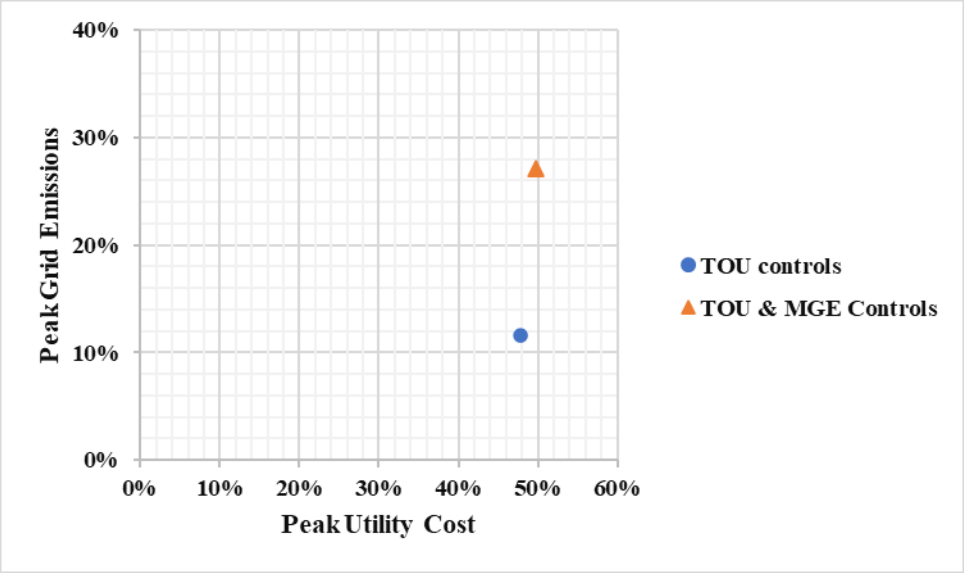


Figure 89: Control Strategy Comparison for Winter Typical week in Baltimore

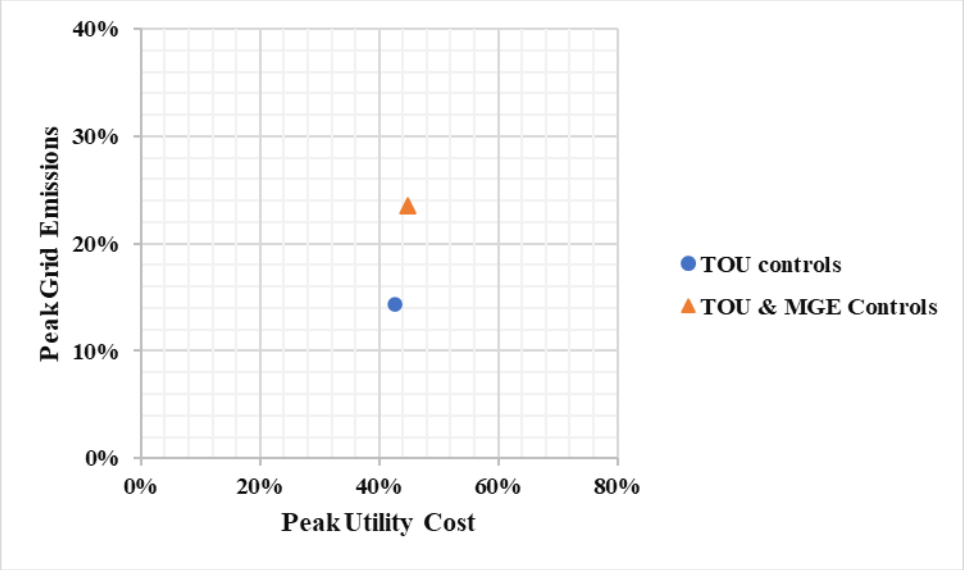


Figure 90: Control Strategy Comparison for Winter Extreme week in Baltimore

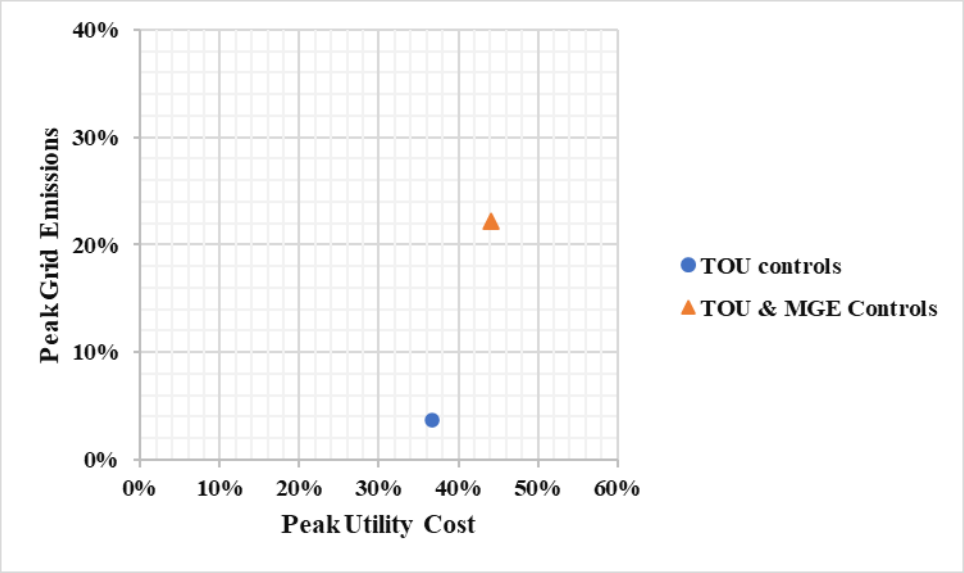


Figure 91: Control Strategy Comparison for Winter Typical week in Golden

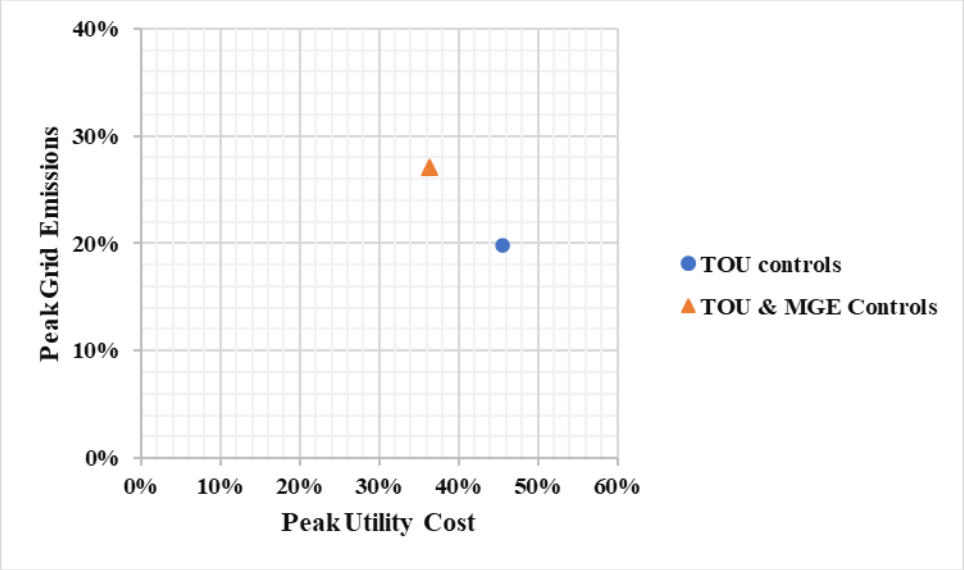


Figure 92: Control Strategy Comparison for Winter Extreme week in Golden

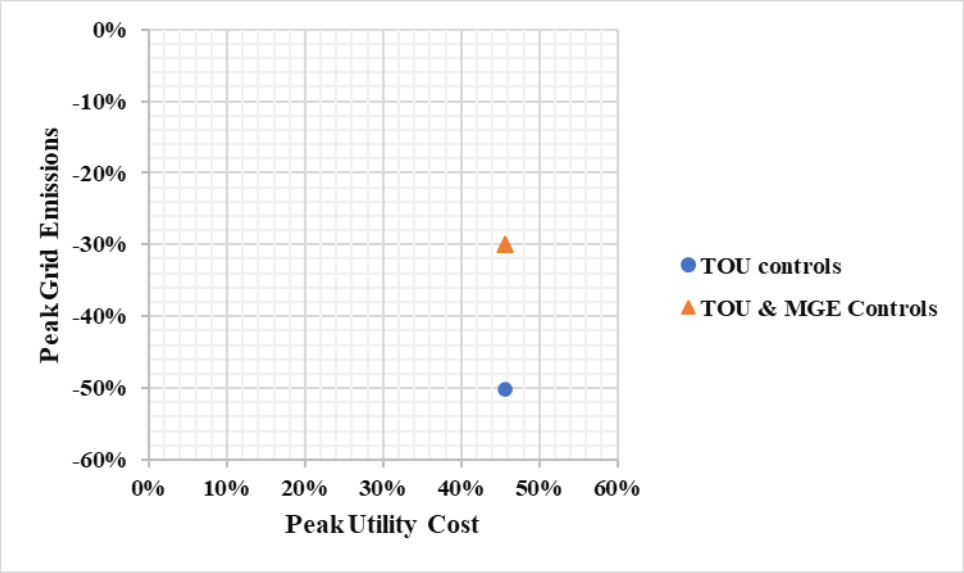


Figure 93: Control Strategy Comparison for Summer Extreme week in Sacramento

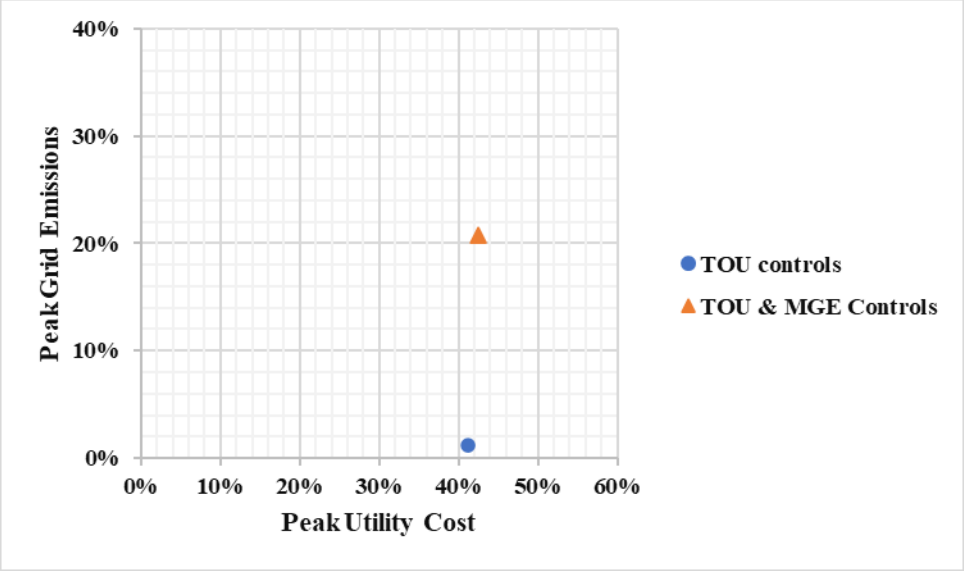


Figure 94: Control Strategy Comparison for Winter Extreme week in Sacramento

Conclusions

This work developed a full-scale HP-TES prototype and bridged the experimental gap in HP-TES research. The prototype validated the MATLAB model and demonstrated the cost, energy and grid benefits for selected phase change temperature (PCT) and storage capacity. The demand, energy and cost analysis were compared to the reported results from HP-TES simulation for optimized PCT and storage capacity.

The PCM-integrated heat pump was designed to achieve the targeted load shift capabilities. An existing high efficiency heat pump was selected and sized based on the building load and performance. Off-the-shelf PCM was used in the TES tank. The PCM heat exchanger was sized based on the shifted load to achieve required demand reduction and coupled to heat pump.

Discussions

HP-TES research has only garnered attention in the past decade. The reason that HP-TES integration is not widely adopted is that it's still difficult to quantify the technology cost and benefits without global metrics and standards for TES selection, design, and evaluation. Furthermore, the research already conducted on HP-TES is mostly based on simulations and very few works present an experimental analysis on both heating and cooling systems.

Ermel et al. [226] highlighted the complexity of integrating TES with HP in their systematic review on performance of air source heat pumps integrated TES. Integrating PCM-TES with HP can be challenging as energy storage materials are manifold and depend on application. It is important to select a suitable material, packaged in an optimized container and configuration to manage the thermal loads and heat transfer, and to overcome the low thermal conductivity of PCMs. Furthermore, controls strategies are needed to develop and optimized for grid-interactive buildings, and heat pumps' demand response.

This work focused on evaluating configuration and controls for HP-TES. Developing controls for a new technology is challenging especially when the literature is

not sufficient, and data is not readily available. The configuration we studied for HP-TES was new and there were not many systems available to compare it against.

HP-TES provides degree of freedom as compared to conventional HVAC system in both hardware design and controls choices. But exploring all these possibilities to model HP-TES becomes challenging and complex as all these decisions need to be made.

There are number of possibilities that can be explored to couple TES with existing hardware components, avoiding the installation of new equipment which can be costly and takes up more space. We provided a review on configurations to focus on HP component integration and configuration choice was a major portion of this research. Furthermore, choices were made for HX size, PCM size, and phase change temperature.

For the control choices, decision to charge and discharge TES could depend on number of factors such as weather forecast, utility rate forecast, and grid emissions forecast. We explored rule-based strategies with different data sets and climate zones which led to divergent result scenarios. A more comprehensive review on controls optimization could be included in future studies.

Finally, thermostat was main part of the model, and all the controls were integrated with thermostat to avoid additional equipment and to mediate the heat transfer via HP. There are number of possibilities to model thermostat behavior as well.

DISSERTATION CONCLUSIONS

A novel TES system is integrated with an existing residential air source HP. Research focuses on controls and configurations to reduce residential building's energy consumption, consumer cost, carbon emissions, and peak energy consumption associated with HP heating and cooling applications. Since HP space conditioning contributes to half of the buildings' energy consumption, it exacerbates demand issues. This work will contribute to the development of a framework for commercialized HP-TES and policies to reduce peak energy demand and carbon emissions of utility grids.

We used active configuration where HP is integrated with PCM-TES to mediate the heat transfer. TES is not directly coupled to the building to provide air conditioning but coupled to VCS, behaving as heat sink or source for HP. Rule-based control strategies were used to shift the peak loads and emissions. A single TES is used for both space heating and cooling of system and parametric analysis showed that 20℃ was the best PCT for most climates, yielding up to 70% peak demand reduction.

A limited number of studies have been conducted on HP-TES and no standards have been developed for comparing them. No comprehensive experimental system has been investigated in literature that addresses all aspects of HP-TES, including controls, configurations, and performance. In addition, no simulations have compared different climate zones. A simulation-based system is developed and experimentally validated for a single-family residential building to fill this gap. We investigate the impact of control settings and configuration on performance in different climate zones in the US.

This work aligns with DOE's goals to decarbonize and reduce demand by 2030. Commercialized HP-TES are expected to have a much broader impact on the research community as well as consumers. Residential homeowners will benefit from HP-TES' flexible installation, enabling them to use existing HP equipment for controls with a minimal footprint, while reducing installation and consumer costs.

Summary

This work presents an HP-TES system with a focus on configurations, controls, and coupling of HP-TES using single PCM for both heating and cooling in different climates. An analysis is performed to compare the utility cost, electric consumption, carbon emissions, and peak demand savings.

A review on HP-TES configurations showed that Active HP-TES improves energy storage and can provide up to 80% demand reduction through real-time charging and discharging. The utility cost savings for active HP-TES depend on the type and size of TES, TES location within an HP, and utility tariff, and energy savings highly depend on the climate and TES application. The financial viability of active HP-TES is higher in cooling-dominated climates with higher peak electricity prices.

We reviewed suitable PCMs for HP-TES system. The optimum demand impact and energy savings were reported for salt hydrate PCMs with phase change temperature between 15 and 27 °C integrated via air distribution system of the heat pump.

Economic implications case study showed the potential of ice-based HP-TES. For a case study where hottest week analysis was performed on Fresno, CA, the total energy used to cool the space was reduced 14.5% when TES was used. The on-peak energy usage was reduced by 87.5%, and the cost to the customer was reduced by nearly 20%.

Preliminary annual simulations were performed on HP-TES MATLAB model and optimized PCT of 20°C and EPCM of 170 MJ was determined through a parametric analysis. Those optimized parameters were used further in detailed simulation model which was validated through experimental prototype. Controls were compared for demand reduction and decarbonization. The analysis showed that the emissions and peak utility cost reduction was more promising for the control strategy where both MGE and TOU peak time controls were implemented.

Broader Impact

This work presents an active HP-TES for buildings using a novel indirect configuration. Active HP-TES allow use of already established equipment and provide configuration flexibility. The indirect configuration provides control flexibility and user can decide when to charge or discharge TES depending on factors like ambient weather, utility peak time, and indoor temperature.

This work aligns with DOE's 2023 goals of demand reduction and decarbonizing buildings. HP-TES is gaining popularity among researchers and overall research trends are improving. This work will get more visibility in research community and will contribute significantly to the literature since not much work has been accomplished in this area.

The broader impact of this work has been estimated via policy and entrepreneurship projects. A summary is illustrated in the Figure 95. The impact and benefits are reported in three categories, economic, technical and non-economic. The benefits are in comparison to the baseline which is a conventional heat pump or air conditioning system with no TES and no DR controls.

An initial market analysis was conducted through ICORPS program for customer discovery. The findings also dictated some of the research plan for this work. Some of the key findings are summarized here:

- Design/Consulting Engineers are critical influencers for the uptake of storage. As more research is being done in TES, with better demonstration of improved results and performance, people will be more likely to adapt the up-to-date technology with more reliability.
- Value proposition is relatively higher for customers with extended periods of off-peak energy load. Residential customers living in relatively extreme weather locations tend to benefit more from TES.

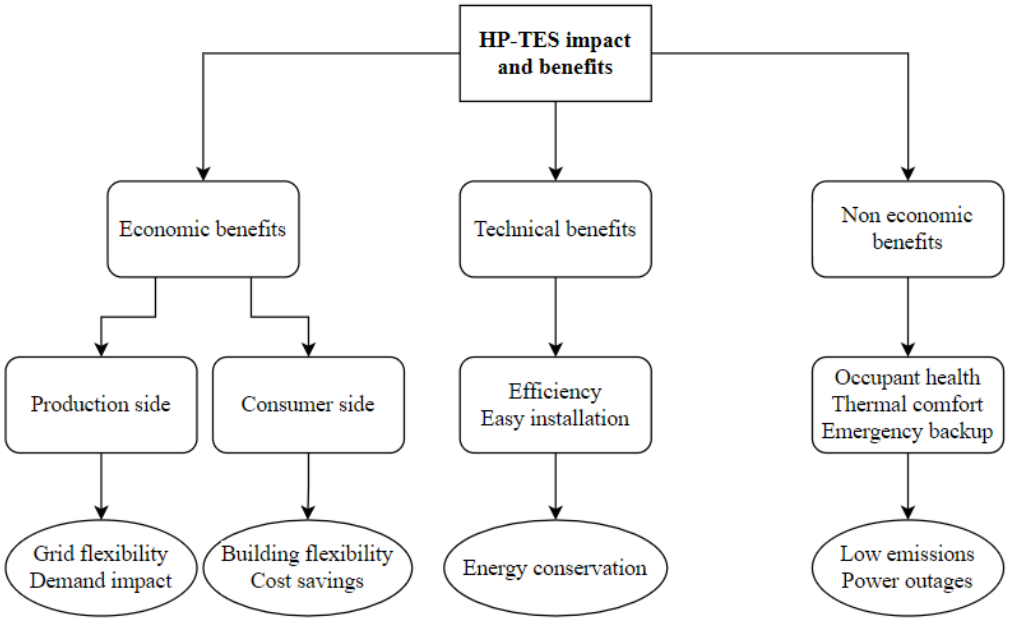


Figure 95: Broader Impacts of research.

- Daily demand and cost benefits are predominant in mixed humid and dry climates due to large fluctuations in diurnal temperature.
- Regions with high energy demands and higher electricity prices can offer higher cost savings by taking advantage of time-based utility tariff.
- Consumers are more inclined towards TES in regions where utility providers offer rebates on investments and generation compensations.
- Payback period and system size are important factors to consider. Some of the TES systems are costly to install and require complex programing for controls.
- TES configurations and materials' temperature can be optimized to maximize savings.
- Many customers may consider other cooling options in the near future as the phase out of ozone-depleting refrigerants intensifies. A grid emissions analysis can play a role for better environmental policies implementation.

Being a selected innovator in the 2022 cohort for IMPEL (Incubating Market-Propelled Entrepreneurial-Mindset at the Labs and Beyond) program by Lawrence Berkeley National Laboratory (Figure 96), business model was developed for this work. A market adaptation plan was also developed by participating in DOE Jump into STEM program by Oak Ridge National Laboratory (Figure 97). Both programs concluded that commercializing such systems will benefit both consumers and utilities.



Figure 96: Business model development.

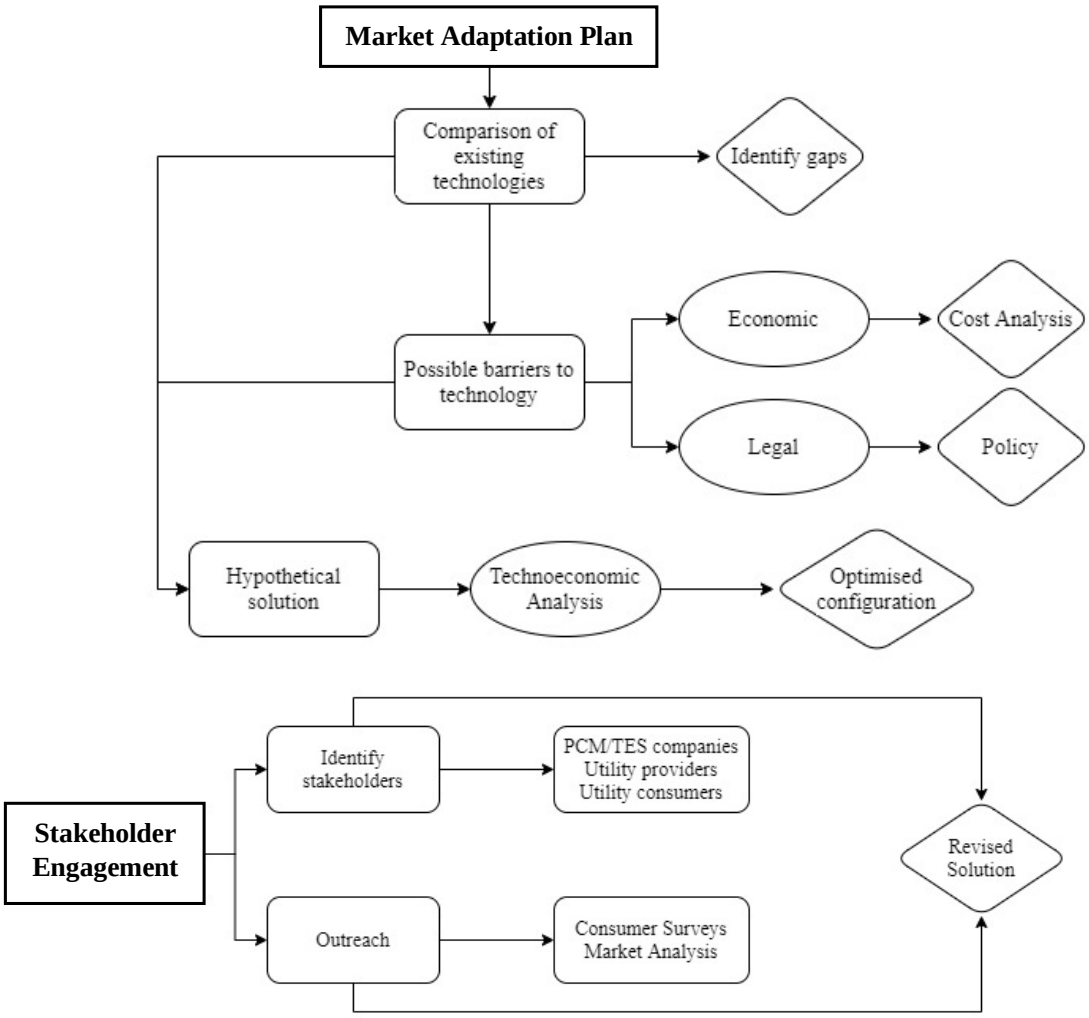


Figure 97: Market adaptation framework.

Future Work

HP-TES are gaining popularity among researchers; however, much work remains to be investigated. HP-TES technology with greater flexibility presents research opportunities in materials, configurations, and controls: novel TES materials can be developed to increase energy storage density, many configurations can be explored to reduce installation complexities and TES footprint, and TES operation can be optimized through controls for demand response in grid-interactive buildings to offer greater energy and demand reduction potential.

Retrofit technologies are needed for a rapid transition to HP-TES. Integrating TES with HP can be challenging from design and control optimization perspective. TES with suitable properties is needed to accommodate the building's thermal load and is packaged in a suitable HX for heat transfer optimization. The PCT of the material and storage capacity needs to be optimized for maximum energy, cost, and DR benefits. Furthermore, control strategies need to be developed for smart integration with the grid.

This work evaluated a novel configuration to use TES indirectly for space conditioning in residential buildings. There are many possible configurations to explore and analyze, as well as the controls need to be more sophisticated.

This work numerically investigated only rule based control strategies for single family residential buildings using air source HP. More detailed simulations are needed that evaluate different building types, and different HP with variable speed compressor.

A salt hydrate PCM with 20°C phase change temperature has been used in this study and the experiments are performed for single climate zone. For future work, PCM model and HX can be improved.

More comprehensive review papers are needed for HP-TES to compare controls, HP, and building types in different climate zones.

REFERENCES

[1] U.S. Energy Information Administration - EIA, “Annual Energy Outlook 2020,” 2020. Accessed: Apr. 19, 2020. [Online]. Available: https://www.eia.gov/outlooks/aeo/

[2] A. Odukomaiya *et al.*, “Addressing energy storage needs at lower cost via on-site thermal energy storage in buildings,” *Energy Environ Sci*, vol. 14, no. 10, pp. 5315–5329, Oct. 2021, doi: 10.1039/D1EE01992A.

[3] J. Dong, B. Shen, J. Munk, K. R. Gluesenkamp, T. Laclair, and T. Kuruganti, “Novel PCM Integration with Electrical Heat Pump for Demand Response,” in *IEEE Power and Energy Society General Meeting*, 2019. doi: 10.1109/PESGM40551.2019.8973936.

[4] B. Cui, J. Munk, R. Jackson, D. Fugate, and M. Starke, “Building thermal model development of typical house in U.S. for virtual storage control of aggregated building loads based on limited available information,” in *30th International Conference on Efficiency, Cost, Optimization, Simulation and Environmental Impact of Energy Systems, ECOS 2017*, 2017.

[5] A. Sepehri, “Introduction and Literature Review of Building Components with Passive Thermal Energy Storage Systems,” *Green Energy and Technology*, pp. 1–18, 2022, doi: 10.1007/978-3-031-08732-5_1/FIGURES/11.

[6] A. Behzadi, S. Holmberg, C. Duwig, F. Haghighat, R. Ooka, and S. Sadrizadeh, “Smart design and control of thermal energy storage in low-temperature heating and high-temperature cooling systems: A comprehensive review,” *Renewable and Sustainable Energy Reviews*, vol. 166, p. 112625, Sep. 2022, doi: 10.1016/J.RSER.2022.112625.

[7] S. Chavan, R. Rudrapati, and S. Manickam, “A comprehensive review on current advances of thermal energy storage and its applications,” *Alexandria Engineering Journal*, vol. 61, no. 7, pp. 5455–5463, Jul. 2022, doi: 10.1016/J.AEJ.2021.11.003.

[8] A. Kurdi, N. Almoatham, M. Mirza, T. Ballweg, and B. Alkahlan, “Potential Phase Change Materials in Building Wall Construction—A Review,” *Materials 2021, Vol. 14, Page 5328*, vol. 14, no. 18, p. 5328, Sep. 2021, doi: 10.3390/MA14185328.

[9] T. Amberkar and P. Mahanwar, “Thermal energy management in buildings and constructions with phase change material-epoxy composites: a review,” *https://doi.org/10.1080/15567036.2023.2171514*, vol. 45, no. 1, pp. 727–761, Dec. 2023, doi: 10.1080/15567036.2023.2171514.

[10] M. M. Rahman and M. A. Habib, “Energy storage using phase change materials - Challenges and opportunities for power savings in residential buildings,” *AIP Conf Proc*, vol. 2681, no. 1, p. 020054, Nov. 2022, doi: 10.1063/5.0117296.

[11] F. Hassan *et al.*, “Recent advancements in latent heat phase change materials and their applications for thermal energy storage and buildings: A state of the art review,” *Sustainable Energy Technologies and Assessments*, vol. 49, p. 101646, Feb. 2022, doi: 10.1016/J.SETA.2021.101646.

[12] K. Jon Chua, L. Pompei, F. Nardecchia, and A. Miliozzi, “Current, Projected Performance and Costs of Thermal Energy Storage,” *Processes 2023, Vol. 11, Page 729*, vol. 11, no. 3, p. 729, Feb. 2023, doi: 10.3390/PR11030729.

[13] S. Barbi *et al.*, “Phase Change Material Evolution in Thermal Energy Storage Systems for the Building Sector, with a Focus on Ground-Coupled Heat Pumps,” *Polymers 2022, Vol. 14, Page 620*, vol. 14, no. 3, p. 620, Feb. 2022, doi: 10.3390/POLYM14030620.

[14] P. Deka, A. Szlęk, P. Deka, and A. Szlęk, “Thermal energy storage in buildings: opportunities and challenges,” *journals.pan.pl*, vol. 43, no. 4, pp. 21–61, 2022, doi: 10.24425/ather.2022.144405.

[15] L. Wang *et al.*, "Experimental performance analysis of a dual source heat pump integrated with thermal energy storage," Dec. 2022, doi: 10.22488/OKSTATE.22.000036.

[16] L. Shi, X. Liu, M. Qu, and B. Shen, "Performance analysis of novel thermal storage integrated heat pump system in a residential building at the hot climate for demand flexibility," 2022, Accessed: Mar. 13, 2023. [Online]. Available: https://www.osti.gov/biblio/1877462

[17] J. Da, M. Li, G. Li, Y. Wang, and Y. Zhang, "Simulation and experiment of a photovoltaic—air source heat pump system with thermal energy storage for heating and domestic hot water supply," *Build Simul*, pp. 1–17, Jan. 2023, doi: 10.1007/S12273-022-0960-6/METRICS.

[18] M. G. Gado and H. Hassan, "Energy-saving potential of compression heat pump using thermal energy storage of phase change materials for cooling and heating applications," *Energy*, vol. 263, p. 126046, Jan. 2023, doi: 10.1016/J.ENERGY.2022.126046.

[19] J. Hirschey, R. Simmons, T. Laclair, and K. Gluesenkamp, "A Framework for Analyzing Widespread Grid Intervening Technologies: A Case Study of Heat Pump-Integrated Thermal Energy Storage Systems in Buildings," 2022, Accessed: Mar. 13, 2023. [Online]. Available: https://www.osti.gov/servlets/purl/1876256

[20] S. Sultan *et al.*, "PCM Material Selection For Heat Pump Integrated With Thermal Energy Storage For Demand Response in Residential Buildings," *International High Performance Buildings Conference*, Jul. 2022, Accessed: Jan. 19, 2023. [Online]. Available: https://docs.lib.purdue.edu/ihpbc/427

[21] B. Shen, J. Munk, and K. Gluesenkamp, "Cold Climate Integrated Heat Pump," 2022, Accessed: Mar. 13, 2023. [Online]. Available: https://www.osti.gov/biblio/1879942

[22] S. Mumme, F. Brown, B. Bass, B. Shen, and S. Shrestha, “Implications of Electrifying Residential Space Heating in Cold Climates with Heat Pumps, Envelope Improvements, and Thermal Storage,” 2022, Accessed: Mar. 13, 2023. [Online]. Available: https://www.osti.gov/servlets/purl/1885299

[23] S. Sultan, K. R. Gluesenkamp, and U. States, “The State of Art of Heat-Pump integrated Thermal Energy Storage for Demand Response,” *IEA Heat Pump Technologies Magazine*, vol. 40, no. 2, pp. 27–30, 2021. doi: https://doi.org/10.23697/62tr-nt79.

[24] L. Shi, M. Qu, X. Liu, J. Dong, B. Cui, and L. Wang, “Model Predictive Control for a Grid-interactive Efficiency Thermal-storage-integrated Heat Pump System,” 2022, Accessed: Mar. 13, 2023. [Online]. Available: https://docs.lib.purdue.edu/cgi/viewcontent.cgi?article=1414&context=ihpbc

[25] J. Hirschey, Z. Li, K. R. Gluesenkamp, T. J. LaClair, and S. Graham, “Demand Reduction and Energy Saving Potential of Thermal Energy Storage Integrated Heat Pumps,” *International Journal of Refrigeration*, Feb. 2023, doi: 10.1016/J.IJREFRIG.2023.01.026.

[26] A. C. Nunna, Y. Zong, L. Georges, and S. You, “Demand response with active phase change material based thermal energy storage in buildings,” *Energy Reports*, vol. 9, pp. 227–235, May 2023, doi: 10.1016/J.EGYR.2022.12.131.

[27] X. Jin, S. Zheng, G. Huang, and A. CK Lai, “Energy and economic performance of the heat pump integrated with latent heat thermal energy storage for peak demand shifting,” *Appl Therm Eng*, vol. 218, p. 119337, Jan. 2023, doi: 10.1016/J.APPLTHERMALENG.2022.119337.

[28] P. Hlanze, Z. Jiang, J. Cai, and B. Shen, “Model-based predictive control of multi-stage air-source heat pumps integrated with phase change material-embedded ceilings,” *Appl Energy*, vol. 336, p. 120796, Apr. 2023, doi: 10.1016/J.APENERGY.2023.120796.

[29] K. K. Ibrahim Alghamdi Christian Bach Jeffrey D Spitler, K. Ibrahim, K. I. Alghamdi, C. K. Bach, and J. D. Spitler, "Water-Based Thermal Energy Storage for Heating and Air-Conditioning Applications in Residential Buildings: Review and Preliminary Study," 2022, Accessed: Mar. 13, 2023. [Online]. Available: https://docs.lib.purdue.edu/cgi/viewcontent.cgi?article=3344&context=iracc

[30] A. Waqas, J. Ji, M. Ali, and J. Z. Alvi, "Effectiveness of the phase change material-based thermal energy storage integrated with the conventional cooling systems of the buildings – A review," *Proceedings of the Institution of Mechanical Engineers, Part A: Journal of Power and Energy*, vol. 232, no. 6, pp. 735–766, Sep. 2018, doi: 10.1177/0957650917754033.

[31] L. Pérez-Lombard, J. Ortiz, and C. Pout, "A review on buildings energy consumption information," *Energy Build*, vol. 40, no. 3, pp. 394–398, Jan. 2008, doi: 10.1016/j.enbuild.2007.03.007.

[32] C. Li and J. Zhao, "Experimental Study on Indoor Air Temperature Distribution of Gravity Air-Conditioning for Cooling," *Energy Procedia*, vol. 17, pp. 961–967, Jan. 2012, doi: 10.1016/J.EGYPRO.2012.02.194.

[33] L. F. Cabeza *et al.*, "CO2 mitigation accounting for Thermal Energy Storage (TES) case studies," *Appl Energy*, vol. 155, pp. 365–377, Oct. 2015, doi: 10.1016/J.APENERGY.2015.05.121.

[34] S. Durga, K. F. Beckers, M. Taam, F. Horowitz, L. M. Cathles, and J. W. Tester, "Techno-economic analysis of decarbonizing building heating in Upstate New York using seasonal borehole thermal energy storage," *Energy Build*, vol. 241, p. 110890, Jun. 2021, doi: 10.1016/J.ENBUILD.2021.110890.

[35] A. L. Facci, V. K. Krastev, G. Falcucci, and S. Ubertini, "Smart integration of photovoltaic production, heat pump and thermal energy storage in residential applications," *Solar Energy*, vol. 192, pp. 133–143, Nov. 2019, doi: 10.1016/J.SOLENER.2018.06.017.

[36] L. Cabrol and P. Rowley, “Towards low carbon homes – A simulation analysis of building-integrated air-source heat pump systems,” *Energy Build*, vol. 48, pp. 127–136, May 2012, doi: 10.1016/J.ENBUILD.2012.01.019.

[37] G. Gholamibozanjani and M. Farid, “Peak load shifting using a price-based control in PCM-enhanced buildings,” *Solar Energy*, vol. 211, pp. 661–673, Nov. 2020, doi: 10.1016/j.solener.2020.09.016.

[38] P. Hlanze, A. Elhefny, Z. Jiang, J. Cai, and H. Shabgard, “Integration of Phase Change Material-Based Storage in Air Distribution Systems to Increase Building Power Flexibility,” 2021, Accessed: Aug. 31, 2021. [Online]. Available: https://docs.lib.purdue.edu/cgi/viewcontent.cgi?article=1365&context=ihpbc

[39] J. Ling *et al.*, “Energy savings and thermal comfort evaluation of a novel personal conditioning device,” *Energy Build*, vol. 241, p. 110917, Jun. 2021, doi: 10.1016/j.enbuild.2021.110917.

[40] S. Farah, M. Liu, and W. Saman, “Numerical investigation of phase change material thermal storage for space cooling,” *Appl Energy*, vol. 239, pp. 526–535, Apr. 2019, doi: 10.1016/j.apenergy.2019.01.197.

[41] X. Chen, Q. Zhang, Z. (John) Zhai, and J. Qiu, “Performance of a cold storage air-cooled heat pump system with phase change materials for space cooling,” *Energy Build*, vol. 228, p. 110405, Dec. 2020, doi: 10.1016/j.enbuild.2020.110405.

[42] F. Bruno, N. H. S. Tay, and M. Belusko, “Minimising energy usage for domestic cooling with off-peak PCM storage,” *Energy Build*, vol. 76, pp. 347–353, Jun. 2014, doi: 10.1016/j.enbuild.2014.02.069.

[43] N. Chaiyat, “Energy and economic analysis of a building air-conditioner with a phase change material (PCM),” *Energy Convers Manag*, vol. 94, pp. 150–158, 2015, doi: 10.1016/j.enconman.2015.01.068.

[44] A. H. Mosaffa and L. Garousi Farshi, “Exergoeconomic and environmental analyses of an air conditioning system using thermal energy storage,” *Appl Energy*, vol. 162, pp. 515–526, 2016, doi: 10.1016/j.apenergy.2015.10.122.

[45] A. Maccarini, G. Hultmark, N. C. Bergsøe, and A. Afshari, “Free cooling potential of a PCM-based heat exchanger coupled with a novel HVAC system for simultaneous heating and cooling of buildings,” *Sustain Cities Soc*, vol. 42, pp. 384–395, Oct. 2018, doi: 10.1016/j.scs.2018.06.016.

[46] J. Mazo, M. Delgado, J. M. Marin, and B. Zalba, “Modeling a radiant floor system with Phase Change Material (PCM) integrated into a building simulation tool: Analysis of a case study of a floor heating system coupled to a heat pump,” *Energy Build*, vol. 47, pp. 458–466, Apr. 2012, doi: 10.1016/j.enbuild.2011.12.022.

[47] R. Hirmiz, H. M. Teamah, M. F. Lightstone, and J. S. Cotton, “Performance of heat pump integrated phase change material thermal storage for electric load shifting in building demand side management,” *Energy Build*, vol. 190, pp. 103–118, May 2019, doi: 10.1016/j.enbuild.2019.02.026.

[48] T. Xu, E. N. Humire, J. N. Chiu, and S. Sawalha, “Latent heat storage integration into heat pump based heating systems for energy-efficient load shifting,” *Energy Convers Manag*, vol. 236, p. 114042, May 2021, doi: 10.1016/j.enconman.2021.114042.

[49] U.S. Energy Information Administration EIA, “‘Use of Energy in the United States Explained.’ US Energy Information Administration.,” *EIA*, 2019. https://www.eia.gov/energyexplained/index.php?page=us_energy_homes (accessed Jul. 13, 2019).

[50] U.S. Department of Energy, “2011 Buildings Energy Data Book,” 2011.

[51] U.S. Energy Information Administration, “Air conditioning accounts for about 12% of U.S. home energy expenditures,” *Today in Energy*, 2018. https://www.eia.gov/todayinenergy/detail.php?id=36692 (accessed Jul. 14, 2019).

[52] U.S. Energy Information Administration EIA, “Residential Energy Consumption Survey (RECS) 2015 Consumption and Expenditures Technical Documentation Summary,” Washington, DC, 2015. Accessed: Jul. 13, 2019. [Online]. Available: https://www.eia.gov/consumption/residential/reports/2015/methodology_c&e/

[53] B. Goetzler, M. Guernsey, and T. Kassuga, “Grid-interactive Efficient Buildings Technical Report Series: Heating, Ventilation, and Air Conditioning (HVAC); Water Heating; Appliances; and Refrigeration,” 2019.

[54] A. Arteconi, A. Mugnini, and F. Polonara, “Energy flexible buildings: A methodology for rating the flexibility performance of buildings with electric heating and cooling systems,” *Appl Energy*, vol. 251, no. May, p. 113387, 2019, doi: 10.1016/j.apenergy.2019.113387.

[55] R. G. Junker *et al.*, “Characterizing the energy flexibility of buildings and districts,” *Appl Energy*, vol. 225, no. April, pp. 175–182, 2018, doi: 10.1016/j.apenergy.2018.05.037.

[56] Y. Chen, P. Xu, J. Gu, F. Schmidt, and W. Li, “Measures to improve energy demand flexibility in buildings for demand response (DR): A review,” *Energy and Buildings*, vol. 177. Elsevier Ltd, pp. 125–139, Oct. 15, 2018. doi: 10.1016/j.enbuild.2018.08.003.

[57] S. Ø. Jensen *et al.*, “IEA EBC Annex 67 Energy Flexible Buildings,” *Energy Build*, vol. 155, pp. 25–34, Nov. 2017, doi: 10.1016/j.enbuild.2017.08.044.

[58] H. Tang, S. Wang, and H. Li, “Flexibility categorization, sources, capabilities and technologies for energy-flexible and grid-responsive buildings: State-of-the-art and future perspective,” *Energy*, vol. 219, p. 119598, Mar. 2021, doi: 10.1016/J.ENERGY.2020.119598.

[59] P. Siano, “Demand response and smart grids—A survey,” *Renewable and Sustainable Energy Reviews*, vol. 30, pp. 461–478, Feb. 2014, doi: 10.1016/J.RSER.2013.10.022.

[60] Y. Chen, P. Xu, J. Gu, F. Schmidt, and W. Li, “Measures to improve energy demand flexibility in buildings for demand response (DR): A review,” *Energy Build*, vol. 177, pp. 125–139, Oct. 2018, doi: 10.1016/J.ENBUILD.2018.08.003.

[61] F. Pallonetto, M. De Rosa, F. D’Ettorre, and D. P. Finn, “On the assessment and control optimisation of demand response programs in residential buildings,” *Renewable and Sustainable Energy Reviews*, vol. 127, p. 109861, Jul. 2020, doi: 10.1016/J.RSER.2020.109861.

[62] J. Wang, H. Zhong, Z. Ma, Q. Xia, and C. Kang, “Review and prospect of integrated demand response in the multi-energy system,” *Appl Energy*, vol. 202, pp. 772–782, Sep. 2017, doi: 10.1016/J.APENERGY.2017.05.150.

[63] K. Shan, S. Wang, C. Yan, and F. Xiao, “Building demand response and control methods for smart grids: A review,” *https://doi.org/10.1080/23744731.2016.1192878*, vol. 22, no. 6, pp. 692–704, Aug. 2016, doi: 10.1080/23744731.2016.1192878.

[64] D. Fischer and H. Madani, “On heat pumps in smart grids: A review,” *Renewable and Sustainable Energy Reviews*, vol. 70, pp. 342–357, Apr. 2017, doi: 10.1016/J.RSER.2016.11.182.

[65] M. Majidi, B. Mohammadi-Ivatloo, and A. Anvari-Moghaddam, “Optimal robust operation of combined heat and power systems with demand response programs,” *Appl Therm Eng*, vol. 149, pp. 1359–1369, Feb. 2019, doi: 10.1016/J.APPLTHERMALENG.2018.12.088.

[66] Y. Zhang, G. Zhou, K. Lin, Q. Zhang, and H. Di, “Application of latent heat thermal energy storage in buildings: State-of-the-art and outlook,” *Build Environ*, vol. 42, no. 6, pp. 2197–2209, 2007, doi: 10.1016/j.buildenv.2006.07.023.

[67] J. Heier, C. Bales, and V. Martin, “Combining thermal energy storage with buildings - A review,” *Renewable and Sustainable Energy Reviews*, vol. 42, pp. 1305–1325, 2015, doi: 10.1016/j.rser.2014.11.031.

[68] D. Zhou, C. Y. Zhao, and Y. Tian, “Review on thermal energy storage with phase change materials (PCMs) in building applications,” *Applied Energy*, vol. 92. Elsevier Ltd, pp. 593–605, 2012. doi: 10.1016/j.apenergy.2011.08.025.

[69] M. Pomianowski, P. Heiselberg, and Y. Zhang, “Review of thermal energy storage technologies based on PCM application in buildings,” *Energy Build*, vol. 67, pp. 56–69, 2013, doi: 10.1016/j.enbuild.2013.08.006.

[70] A. De Gracia and L. F. Cabeza, “Phase change materials and thermal energy storage for buildings,” *Energy Build*, vol. 103, pp. 414–419, 2015, doi: 10.1016/j.enbuild.2015.06.007.

[71] K. Pielichowska and K. Pielichowski, “Phase change materials for thermal energy storage,” *Prog Mater Sci*, vol. 65, pp. 67–123, 2014, doi: 10.1016/j.pmatsci.2014.03.005.

[72] L. Navarro *et al.*, “Thermal energy storage in building integrated thermal systems: A review. Part 2. Integration as passive system,” *Renew Energy*, vol. 85, pp. 1334–1356, 2016, doi: 10.1016/j.renene.2015.06.064.

[73] S. B. Sadineni, S. Madala, and R. F. Boehm, “Passive building energy savings: A review of building envelope components,” *Renewable and Sustainable Energy Reviews*, vol. 15, no. 8, pp. 3617–3631, 2011, doi: 10.1016/j.rser.2011.07.014.

[74] S. A. Memon, “Phase change materials integrated in building walls: A state of the art review,” *Renewable and Sustainable Energy Reviews*, vol. 31, pp. 870–906, 2014, doi: 10.1016/j.rser.2013.12.042.

[75] H. Akeiber *et al.*, “A review on phase change material (PCM) for sustainable passive cooling in building envelopes,” *Renewable and Sustainable Energy Reviews*, vol. 60, pp. 1470–1497, 2016, doi: 10.1016/j.rser.2016.03.036.

[76] Q. Al-Yasiri and M. Szabó, “Incorporation of phase change materials into building envelope for thermal comfort and energy saving: A comprehensive analysis,”

Journal of Building Engineering, vol. 36. Elsevier, p. 102122, Apr. 01, 2021. doi: 10.1016/j.jobe.2020.102122.

[77] A. Waqas and Z. Ud Din, "Phase change material (PCM) storage for free cooling of buildings - A review," *Renewable and Sustainable Energy Reviews*, vol. 18, pp. 607–625, 2013, doi: 10.1016/j.rser.2012.10.034.

[78] M. Iten, S. Liu, and A. Shukla, "A review on the air-PCM-TES application for free cooling and heating in the buildings," *Renewable and Sustainable Energy Reviews*, vol. 61, pp. 175–186, 2016, doi: 10.1016/j.rser.2016.03.007.

[79] F. Souayfane, F. Fardoun, and P. H. Biwole, "Phase change materials (PCM) for cooling applications in buildings: A review," *Energy Build*, vol. 129, pp. 396–431, 2016, doi: 10.1016/j.enbuild.2016.04.006.

[80] M. A. Wahid, S. E. Hosseini, H. M. Hussen, H. J. Akeiber, S. N. Saud, and A. T. Mohammad, "An overview of phase change materials for construction architecture thermal management in hot and dry climate region," *Appl Therm Eng*, vol. 112, pp. 1240–1259, 2017, doi: 10.1016/j.applthermaleng.2016.07.032.

[81] A. Pasupathy, R. Velraj, and R. V. Seeniraj, "Phase change material-based building architecture for thermal management in residential and commercial establishments," *Renewable and Sustainable Energy Reviews*, vol. 12, no. 1, pp. 39–64, 2008, doi: 10.1016/j.rser.2006.05.010.

[82] G. Alva, Y. Lin, and G. Fang, "An overview of thermal energy storage systems," *Energy*, vol. 144, pp. 341–378, 2018, doi: 10.1016/j.energy.2017.12.037.

[83] D. Yang, N. Wang, J. Xie, and J. Wang, "Review on active building energy conservation using phase change materials," in *E3S Web of Conferences*, EDP Sciences, Feb. 2021, p. 05007. doi: 10.1051/e3sconf/202123605007.

[84] V. Vakiloroaya, B. Samali, A. Fakhar, and K. Pishghadam, “A review of different strategies for HVAC energy saving,” *Energy Convers Manag*, vol. 77, pp. 738–754, 2014, doi: 10.1016/j.enconman.2013.10.023.

[85] Z. Afroz, G. M. Shafiullah, T. Urmee, and G. Higgins, “Modeling techniques used in building HVAC control systems: A review,” *Renewable and Sustainable Energy Reviews*, vol. 83, pp. 64–84, Mar. 2018, doi: 10.1016/j.rser.2017.10.044.

[86] N. J. Hewitt, “Heat pumps and energy storage - The challenges of implementation,” *Appl Energy*, vol. 89, no. 1, pp. 37–44, 2012, doi: 10.1016/j.apenergy.2010.12.028.

[87] S. Rashidi, H. Shamsabadi, J. A. Esfahani, and S. Harmand, “A review on potentials of coupling PCM storage modules to heat pipes and heat pumps,” *Journal of Thermal Analysis and Calorimetry*, vol. 140, no. 4. Springer Netherlands, pp. 1655–1713, May 01, 2020. doi: 10.1007/s10973-019-08930-1.

[88] E. Osterman and U. Stritih, “Review on compression heat pump systems with thermal energy storage for heating and cooling of buildings,” *Journal of Energy Storage*, vol. 39. Elsevier, p. 102569, Jul. 01, 2021. doi: 10.1016/j.est.2021.102569.

[89] A. Takudzwa Muzhanje, M. A. Hassan, and H. Hassan, “Phase change material based thermal energy storage applications for air conditioning: Review,” *Appl Therm Eng*, vol. 214, p. 118832, Sep. 2022, doi: 10.1016/J.APPLTHERMALENG.2022.118832.

[90] C. Ermel, M. V. A. Bianchi, A. P. Cardoso, and P. S. Schneider, “Thermal storage integrated into air-source heat pumps to leverage building electrification: A systematic literature review,” *Appl Therm Eng*, vol. 215, p. 118975, Oct. 2022, doi: 10.1016/J.APPLTHERMALENG.2022.118975.

[91] H. Gu, Y. Chen, X. Yao, L. Huang, and D. Zou, “Review on heat pump (HP) coupled with phase change material (PCM) for thermal energy storage,” *Chemical Engineering Journal*, p. 140701, Dec. 2022, doi: 10.1016/J.CEJ.2022.140701.

[92] D. H. Blum, “Improving the Use of Commercial Building HVAC Systems for Electric Grid Ancillary Services,” 2016.

[93] C. W. Gellings, “The Concept of Demand-Side Management for Electric Utilities,” *Proceedings of the IEEE*, vol. 73, no. 10, pp. 1468–1470, 1985, doi: 10.1109/PROC.1985.13318.

[94] A. Arteconi, N. J. Hewitt, and F. Polonara, “Domestic demand-side management (DSM): Role of heat pumps and thermal energy storage (TES) systems,” *Appl Therm Eng*, vol. 51, no. 1–2, pp. 155–165, Mar. 2013, doi: 10.1016/j.applthermaleng.2012.09.023.

[95] T. Q. Péan, J. Salom, and R. Costa-Castelló, “Review of control strategies for improving the energy flexibility provided by heat pump systems in buildings,” *J Process Control*, vol. 74, pp. 35–49, Feb. 2019, doi: 10.1016/J.JPROCONT.2018.03.006.

[96] B. Neenan, “Quantifying the Impacts of Time-Based Rates, Enabling Technology, and Other Treatments in Consumer Behavior Studies,” *EPRI Technical Report*, no. July, p. 142, 2013.

[97] G. Krasimiroy, “Building Thermal Energy Storage,” Technical University of Denmark, Department of Civil Engineering., 2014.

[98] B. Cui, S. Wang, and Y. Sun, “Life-cycle cost benefit analysis and optimal design of small scale active storage system for building demand limiting,” *Energy*, vol. 73, pp. 787–800, Aug. 2014, doi: 10.1016/j.energy.2014.06.084.

[99] I. Dincer, “Renewable energy and sustainable development: a crucial review,” *Renewable and Sustainable Energy Reviews*, vol. 4, no. 2, pp. 157–175, 2000, doi: 10.1016/S1364-0321(99)00011-8.

[100] N. Takham and N. Tippayawong, “Experimental Investigation of hot Water Generation from Small CaO/Ca(OH)2 Thermochemical Energy Storage System,”

IOP Conf Ser Earth Environ Sci, vol. 159, no. 1, p. 012002, Jun. 2018, doi: 10.1088/1755-1315/159/1/012002.

[101] I. Dincer, A. Midilli, and H. Kucuk, Eds., *Progress in Sustainable Energy Technologies: Generating Renewable Energy*. Cham: Springer International Publishing, 2014. doi: 10.1007/978-3-319-07896-0.

[102] A. S. Fleischer, *Thermal Energy Storage Using Phase Change Materials*. in SpringerBriefs in Applied Sciences and Technology. Cham: Springer International Publishing, 2015. doi: 10.1007/978-3-319-20922-7.

[103] I. Sarbu and C. Sebarchievici, "A comprehensive review of thermal energy storage," *Sustainability (Switzerland)*, vol. 10, no. 1, 2018, doi: 10.3390/su10010191.

[104] X. Wang, Y. Zhang, W. Xiao, R. Zeng, Q. Zhang, and H. Di, "Review on thermal performance of phase change energy storage building envelope," *Chinese Science Bulletin*, vol. 54, no. 6, pp. 920–928, Mar. 2009, doi: 10.1007/s11434-009-0120-8.

[105] M. Thambidurai, K. Panchabikesan, N. Krishna Mohan, and V. Ramalingam, "Review on phase change material based free cooling of buildings-The way toward sustainability," *J Energy Storage*, vol. 4, pp. 74–88, 2015, doi: 10.1016/j.est.2015.09.003.

[106] G. R. Newsham and B. G. Bowker, "The effect of utility time-varying pricing and load control strategies on residential summer peak electricity use: A review," *Energy Policy*, vol. 38, no. 7, pp. 3289–3296, Jul. 2010, doi: 10.1016/j.enpol.2010.01.027.

[107] J. E. Braun, "Reducing energy costs and peak electrical demand through optimal control of building thermal storage," in *ASHRAE Transactions*, 1990, pp. 876–888.

[108] A. Rabl and L. K. Norford, "Peak load reduction by preconditioning buildings at night," *Int J Energy Res*, vol. 15, no. 9, pp. 781–798, Dec. 1991, doi: 10.1002/er.4440150909.

[109] S. Gottwalt, W. Ketter, C. Block, J. Collins, and C. Weinhardt, “Demand side management-A simulation of household behavior under variable prices,” *Energy Policy*, vol. 39, no. 12, pp. 8163–8174, Dec. 2011, doi: 10.1016/j.enpol.2011.10.016.

[110] E. Vrettos, K. Lai, F. Oldewurtel, and G. Andersson, “Predictive Control of buildings for Demand Response with dynamic day-ahead and real-time prices,” in *2013 European Control Conference, ECC 2013*, 2013, pp. 2527–2534. doi: 10.23919/ecc.2013.6669762.

[111] J. H. Yoon, R. Bladick, and A. Novoselac, “Demand response for residential buildings based on dynamic price of electricity,” *Energy Build*, vol. 80, pp. 531–541, Sep. 2014, doi: 10.1016/j.enbuild.2014.05.002.

[112] J. H. Yoon, R. Baldick, and A. Novoselac, “Demand response control of residential HVAC loads based on dynamic electricity prices and economic analysis,” *Sci Technol Built Environ*, vol. 22, no. 6, pp. 705–719, Aug. 2016, doi: 10.1080/23744731.2016.1195659.

[113] L. Schibuola, M. Scarpa, and C. Tambani, “Demand response management by means of heat pumps controlled via real time pricing,” *Energy Build*, vol. 90, pp. 15–28, Mar. 2015, doi: 10.1016/j.enbuild.2014.12.047.

[114] M. Farrokhifar, F. Momayyezi, N. Sadoogi, and A. Safari, “Real-time based approach for intelligent building energy management using dynamic price policies,” *Sustain Cities Soc*, vol. 37, pp. 85–92, Feb. 2018, doi: 10.1016/j.scs.2017.11.011.

[115] L. Romero Rodríguez, J. Sánchez Ramos, S. Álvarez Domínguez, and U. Eicker, “Contributions of heat pumps to demand response: A case study of a plus-energy dwelling,” *Appl Energy*, vol. 214, pp. 191–204, Mar. 2018, doi: 10.1016/j.apenergy.2018.01.086.

[116] V. Arabzadeh, B. Alimohammadisagvand, J. Jokisalo, and K. Siren, “A novel cost-optimizing demand response control for a heat pump heated residential building,”

Build Simul, vol. 11, no. 3, pp. 533–547, Jun. 2018, doi: 10.1007/s12273-017-0425-5.

[117] W. J. N. Turner, I. S. Walker, and J. Roux, "Peak load reductions: Electric load shifting with mechanical pre-cooling of residential buildings with low thermal mass," *Energy*, vol. 82, pp. 1057–1067, Mar. 2015, doi: 10.1016/j.energy.2015.02.011.

[118] M. Ali, A. Safdarian, and M. Lehtonen, "Demand response potential of residential HVAC loads considering users preferences," in *IEEE PES Innovative Smart Grid Technologies Conference Europe*, IEEE Computer Society, Jan. 2015. doi: 10.1109/ISGTEurope.2014.7028883.

[119] B. Alimohammadisagvand, S. Alam, M. Ali, M. Degefa, J. Jokisalo, and K. Sirén, "Influence of energy demand response actions on thermal comfort and energy cost in electrically heated residential houses," *Indoor and Built Environment*, vol. 26, no. 3, pp. 298–316, Sep. 2017, doi: 10.1177/1420326X15608514.

[120] B. Alimohammadisagvand, J. Jokisalo, S. Kilpeläinen, M. Ali, and K. Sirén, "Cost-optimal thermal energy storage system for a residential building with heat pump heating and demand response control," *Appl Energy*, vol. 174, pp. 275–287, Jul. 2016, doi: 10.1016/j.apenergy.2016.04.013.

[121] C. Arkar and S. Medved, "Free cooling of a building using PCM heat storage integrated into the ventilation system," *Solar Energy*, vol. 81, no. 9, pp. 1078–1087, Sep. 2007, doi: 10.1016/j.solener.2007.01.010.

[122] F. Ahmed, M. Mahmood, A. Waqas, N. Ahmad, and M. Ali, "Thermal analysis of macro-encapsulated phase change material coupled with domestic gas heater for building heating," *Sustainable Energy Technologies and Assessments*, vol. 47, p. 101533, Oct. 2021, doi: 10.1016/j.seta.2021.101533.

[123] X. Chen, Q. Zhang, Z. J. Zhai, and X. Ma, “Potential of ventilation systems with thermal energy storage using PCMs applied to air conditioned buildings,” *Renew Energy*, vol. 138, pp. 39–53, Aug. 2019, doi: 10.1016/j.renene.2019.01.026.

[124] C. K. Halford and R. F. Boehm, “Modeling of phase change material peak load shifting,” *Energy Build*, vol. 39, no. 3, pp. 298–305, Mar. 2007, doi: 10.1016/j.enbuild.2006.07.005.

[125] J. Kośny, A. Fallahi, N. Shukla, E. Kossecka, and R. Ahbari, “Thermal load mitigation and passive cooling in residential attics containing PCM-enhanced insulations,” *Solar Energy*, vol. 108, pp. 164–177, Oct. 2014, doi: 10.1016/j.solener.2014.05.007.

[126] R. Barzin, J. J. J. Chen, B. R. Young, and M. M. Farid, “Application of PCM underfloor heating in combination with PCM wallboards for space heating using price based control system,” *Appl Energy*, vol. 148, pp. 39–48, Jun. 2015, doi: 10.1016/j.apenergy.2015.03.027.

[127] M. T. Plytaria, C. Tzivanidis, E. Bellos, and K. A. Antonopoulos, “Energetic investigation of solar assisted heat pump underfloor heating systems with and without phase change materials,” *Energy Convers Manag*, vol. 173, pp. 626–639, Oct. 2018, doi: 10.1016/j.enconman.2018.08.010.

[128] K. Muruganantham, P. Phelan, P. Horwath, D. Ludlam, and T. McDonald, “Experimental investigation of a bio-based phase-change material to improve building energy performance,” in *ASME 2010 4th International Conference on Energy Sustainability, ES 2010*, American Society of Mechanical Engineers Digital Collection, Dec. 2010, pp. 979–984. doi: 10.1115/ES2010-90035.

[129] F. Ascione, N. Bianco, R. F. De Masi, M. Mastellone, and G. Peter Vanoli, “Phase change materials for reducing cooling energy demand and improving indoor comfort: A step-by-step retrofit of a Mediterranean educational building,” *Energies (Basel)*, vol. 12, no. 19, p. 3661, Sep. 2019, doi: 10.3390/en12193661.

[130] K. Peippo, P. Kauranen, and P. D. Lund, “A multicomponent PCM wall optimized for passive solar heating,” *Energy Build*, vol. 17, no. 4, pp. 259–270, Jan. 1991, doi: 10.1016/0378-7788(91)90009-R.

[131] R. Barzin, J. J. J. Chen, B. R. Young, and M. M. Farid, “Peak load shifting with energy storage and price-based control system,” *Energy*, vol. 92, pp. 505–514, Dec. 2015, doi: 10.1016/j.energy.2015.05.144.

[132] N. H. Abu-Hamdeh, A. A. Melaibari, T. S. Alquthami, A. Khoshaim, H. F. Oztop, and A. Karimipour, “Efficacy of incorporating PCM into the building envelope on the energy saving and AHU power usage in winter,” *Sustainable Energy Technologies and Assessments*, vol. 43, p. 100969, Feb. 2021, doi: 10.1016/j.seta.2020.100969.

[133] Y. Hu, P. K. Heiselberg, and T. S. Larsen, “Demand control strategies of a pcm enhanced ventilation system for residential buildings,” *Applied Sciences (Switzerland)*, vol. 10, no. 12, p. 4336, Jun. 2020, doi: 10.3390/app10124336.

[134] P. Devaux and M. M. Farid, “Benefits of PCM underfloor heating with PCM wallboards for space heating in winter,” *Appl Energy*, vol. 191, pp. 593–602, 2017, doi: 10.1016/j.apenergy.2017.01.060.

[135] M. Zhang, M. A. Medina, and J. B. King, “Development of a thermally enhanced frame wall with phase-change materials for on-peak air conditioning demand reduction and energy savings in residential buildings,” *Int J Energy Res*, vol. 29, no. 9, pp. 795–809, Jul. 2005, doi: 10.1002/er.1082.

[136] T. Kondo and T. Ibamoto, “Research on thermal storage using rock wool phase-change material ceiling board,” in *ASHRAE Transactions*, 2006, pp. 526–531.

[137] N. Zhu, S. Wang, Z. Ma, and Y. Sun, “Energy performance and optimal control of air-conditioned buildings with envelopes enhanced by phase change materials,” *Energy Convers Manag*, vol. 52, no. 10, pp. 3197–3205, Sep. 2011, doi: 10.1016/j.enconman.2011.05.011.

[138] M. Yamaha and S. Misaki, “The evaluation of peak shaving by a thermal storage system using phase-change materials in air distribution systems,” *HVAC and R Research*, vol. 12, pp. 861–869, 2006, doi: 10.1080/10789669.2006.10391213.

[139] V. V. Tyagi, A. K. Pandey, D. Buddhi, and R. Kothari, “Thermal performance assessment of encapsulated PCM based thermal management system to reduce peak energy demand in buildings,” *Energy Build*, vol. 117, pp. 44–52, 2016, doi: 10.1016/j.enbuild.2016.01.042.

[140] N. Chaiyat, “Energy and economic analysis of a building air-conditioner with a phase change material (PCM),” *Energy Convers Manag*, vol. 94, pp. 150–158, 2015, doi: 10.1016/j.enconman.2015.01.068.

[141] N. Chaiyat and T. Kiatsiriroat, “Energy reduction of building air-conditioner with phase change material in Thailand,” *Case Studies in Thermal Engineering*, vol. 4, pp. 175–186, 2014, doi: 10.1016/j.csite.2014.09.006.

[142] F. Bruno, N. H. S. Tay, and M. Belusko, “Minimising energy usage for domestic cooling with off-peak PCM storage,” *Energy Build*, vol. 76, pp. 347–353, Jun. 2014, doi: 10.1016/j.enbuild.2014.02.069.

[143] A. Real, V. García, L. Domenech, J. Renau, N. Montés, and F. Sánchez, “Improvement of a heat pump based HVAC system with PCM thermal storage for cold accumulation and heat dissipation,” *Energy Build*, vol. 83, pp. 108–116, 2014, doi: 10.1016/j.enbuild.2014.04.029.

[144] S. Jaber and S. Ajib, “Novel cooling unit using PCM for residential application,” *International Journal of Refrigeration*, 2012, doi: 10.1016/j.ijrefrig.2012.03.023.

[145] J. Y. Long and D. S. Zhu, “Numerical and experimental study on heat pump water heater with PCM for thermal storage,” *Energy Build*, vol. 40, no. 4, pp. 666–672, Jan. 2008, doi: 10.1016/j.enbuild.2007.05.001.

[146] D. Zou *et al.*, “Experimental research of an air-source heat pump water heater using water-PCM for heat storage,” *Appl Energy*, vol. 206, pp. 784–792, Nov. 2017, doi: 10.1016/j.apenergy.2017.08.209.

[147] P. Moreno, C. Solé, A. Castell, and L. F. Cabeza, “The use of phase change materials in domestic heat pump and air-conditioning systems for short term storage: A review,” *Renewable and Sustainable Energy Reviews*, vol. 39, pp. 1–13, 2014, doi: 10.1016/j.rser.2014.07.062.

[148] G. Gholamibozanjani and M. Farid, “A comparison between passive and active PCM systems applied to buildings,” *Renew Energy*, vol. 162, pp. 112–123, Dec. 2020, doi: 10.1016/j.renene.2020.08.007.

[149] S. Takeda, K. Nagano, T. Mochida, and K. Shimakura, “Development of a ventilation system utilizing thermal energy storage for granules containing phase change material,” *Solar Energy*, vol. 77, no. 3, pp. 329–338, Sep. 2004, doi: 10.1016/j.solener.2004.04.014.

[150] K. Nagano, S. Takeda, T. Mochida, K. Shimakura, and T. Nakamura, “Study of a floor supply air conditioning system using granular phase change material to augment building mass thermal storage - Heat response in small scale experiments,” *Energy Build*, vol. 38, no. 5, pp. 436–446, May 2006, doi: 10.1016/j.enbuild.2005.07.010.

[151] F. Sehar, S. Rahman, and M. Pipattanasomporn, “Impacts of ice storage on electrical energy consumptions in office buildings,” *Energy Build*, vol. 51, pp. 255–262, Aug. 2012, doi: 10.1016/j.enbuild.2012.05.002.

[152] S. Sanaye and A. Shirazi, “Thermo-economic optimization of an ice thermal energy storage system for air-conditioning applications,” *Energy Build*, vol. 60, pp. 100–109, May 2013, doi: 10.1016/j.enbuild.2012.12.040.

[153] O. G. Pop, L. Fechete Tutunaru, F. Bode, A. C. Abrudan, and M. C. Balan, “Energy efficiency of PCM integrated in fresh air cooling systems in different climatic

conditions," *Appl Energy*, vol. 212, pp. 976–996, Feb. 2018, doi: 10.1016/j.apenergy.2017.12.122.

[154] S. Sultan, J. Hirschey, K. Gluesenkamp, and S. Graham, "Analysis of Residential Time-of-Use Utility Rate Structures and Economic Implications for Thermal Energy Storage," 2021, pp. 1–10. Accessed: Aug. 31, 2021. [Online]. Available: https://docs.lib.purdue.edu/cgi/viewcontent.cgi?article=1369&context=ihpbc

[155] K. Kaygusuz and T. Ayhan, "Experimental and theoretical investigation of combined solar heat pump system for residential heating," *Energy Convers Manag*, 1999, doi: 10.1016/S0196-8904(99)00026-6.

[156] Y. Hu, P. K. Heiselberg, C. Drivsholm, A. S. Søvsø, P. J. C. Vogler-Finck, and K. Kronby, "Experimental and numerical study of PCM storage integrated with HVAC system for energy flexibility," *Energy Build*, p. 111651, Nov. 2021, doi: 10.1016/j.enbuild.2021.111651.

[157] G. Gholamibozanjani and M. Farid, "Application of an active PCM storage system into a building for heating/cooling load reduction," *Energy*, vol. 210, p. 118572, Nov. 2020, doi: 10.1016/j.energy.2020.118572.

[158] A. Real, V. García, L. Domenech, J. Renau, N. Montés, and F. Sánchez, "Improvement of a heat pump based HVAC system with PCM thermal storage for cold accumulation and heat dissipation," *Energy Build*, vol. 83, pp. 108–116, 2014, doi: 10.1016/j.enbuild.2014.04.029.

[159] U.S. Energy Information Administration - EIA, "U.S. Energy Information Administration - EIA - Independent Statistics and Analysis." https://www.eia.gov/todayinenergy/detail.php?id=44556 (accessed Apr. 25, 2022).

[160] A. Waqas and S. Kumar, "Utilization of latent heat storage unit for comfort ventilation of buildings in hot and dry climates," *Int J Green Energy*, vol. 8, no. 1, pp. 1–24, 2011, doi: 10.1080/15435075.2010.529406.

[161] G. Evola, L. Marletta, and F. Sicurella, “A methodology for investigating the effectiveness of PCM wallboards for summer thermal comfort in buildings,” *Build Environ*, vol. 59, pp. 517–527, Jan. 2013, doi: 10.1016/j.buildenv.2012.09.021.

[162] M. Alam, H. Jamil, J. Sanjayan, and J. Wilson, “Energy saving potential of phase change materials in major Australian cities,” *Energy Build*, vol. 78, pp. 192–201, Aug. 2014, doi: 10.1016/j.enbuild.2014.04.027.

[163] J. Lei, J. Yang, and E. H. Yang, “Energy performance of building envelopes integrated with phase change materials for cooling load reduction in tropical Singapore,” *Appl Energy*, vol. 162, pp. 207–217, Jan. 2016, doi: 10.1016/j.apenergy.2015.10.031.

[164] M. Saffari, A. de Gracia, C. Fernández, and L. F. Cabeza, “Simulation-based optimization of PCM melting temperature to improve the energy performance in buildings,” *Appl Energy*, vol. 202, pp. 420–434, Sep. 2017, doi: 10.1016/j.apenergy.2017.05.107.

[165] E. Markarian and F. Fazelpour, “Multi-objective optimization of energy performance of a building considering different configurations and types of PCM,” *Solar Energy*, vol. 191, pp. 481–496, Oct. 2019, doi: 10.1016/j.solener.2019.09.003.

[166] U. Berardi and S. Soudian, “Experimental investigation of latent heat thermal energy storage using PCMs with different melting temperatures for building retrofit,” *Energy Build*, vol. 185, pp. 180–195, Feb. 2019, doi: 10.1016/j.enbuild.2018.12.016.

[167] M. Prabhakar, M. Saffari, A. de Gracia, and L. F. Cabeza, “Improving the energy efficiency of passive PCM system using controlled natural ventilation,” *Energy Build*, vol. 228, p. 110483, Dec. 2020, doi: 10.1016/j.enbuild.2020.110483.

[168] C. Piselli, M. Prabhakar, A. de Gracia, M. Saffari, A. L. Pisello, and L. F. Cabeza, “Optimal control of natural ventilation as passive cooling strategy for improving the

energy performance of building envelope with PCM integration," *Renew Energy*, vol. 162, pp. 171–181, Dec. 2020, doi: 10.1016/j.renene.2020.07.043.

[169] M. Arıcı, F. Bilgin, S. Nižetić, and H. Karabay, "PCM integrated to external building walls: An optimization study on maximum activation of latent heat," *Appl Therm Eng*, vol. 165, p. 114560, Jan. 2020, doi: 10.1016/j.applthermaleng.2019.114560.

[170] N. Zhu, R. Deng, P. Hu, F. Lei, L. Xu, and Z. Jiang, "Coupling optimization study of key influencing factors on PCM trombe wall for year thermal management," *Energy*, vol. 236, p. 121470, Dec. 2021, doi: 10.1016/j.energy.2021.121470.

[171] A. Alkhwildi, R. Elhashmi, and A. Chiasson, "Parametric modeling and simulation of Low temperature energy storage for cold-climate multi-family residences using a geothermal heat pump system with integrated phase change material storage tank," *Geothermics*, vol. 86, p. 101864, Jul. 2020, doi: 10.1016/j.geothermics.2020.101864.

[172] X. Jin *et al.*, "Experimental investigation of the novel melting point modified Phase–Change material for heat pump latent heat thermal energy storage application," *Energy*, vol. 216, p. 119191, Feb. 2021, doi: 10.1016/j.energy.2020.119191.

[173] Z. Han, M. Zheng, F. Kong, F. Wang, Z. Li, and T. Bai, "Numerical simulation of solar assisted ground-source heat pump heating system with latent heat energy storage in severely cold area," *Appl Therm Eng*, vol. 28, no. 11–12, pp. 1427–1436, Aug. 2008, doi: 10.1016/j.applthermaleng.2007.09.013.

[174] M. Yamaguchi *et al.*, "Heat Storage-Type Floor Heating System with Heat Pump Driven by Discount Electricity Supplied at Night," *KAGAKU KOGAKU RONBUNSHU*, vol. 21, no. 5, pp. 853–858, 1995, doi: 10.1252/kakoronbunshu.21.853.

[175] H. Benli, "Energetic performance analysis of a ground-source heat pump system with latent heat storage for a greenhouse heating," in *Energy Conversion and*

Management, Pergamon, Jan. 2011, pp. 581–589. doi: 10.1016/j.enconman.2010.07.033.

[176] N. J. Kelly, P. G. Tuohy, and A. D. Hawkes, "Performance assessment of tariff-based air source heat pump load shifting in a UK detached dwelling featuring phase change-enhanced buffering," *Appl Therm Eng*, vol. 71, no. 2, pp. 809–820, Oct. 2014, doi: 10.1016/j.applthermaleng.2013.12.019.

[177] T. Kumirai, J. Dirker, and J. Meyer, "Experimental analysis for thermal storage performance of three types of plate encapsulated phase change materials in air heat exchangers for ventilation applications," *Journal of Building Engineering*, vol. 22, pp. 75–89, Mar. 2019, doi: 10.1016/J.JOBE.2018.11.016.

[178] M. Alam, P. X. W. Zou, J. Sanjayan, and S. Ramakrishnan, "Energy saving performance assessment and lessons learned from the operation of an active phase change materials system in a multi-storey building in Melbourne," *Appl Energy*, vol. 238, pp. 1582–1595, Mar. 2019, doi: 10.1016/j.apenergy.2019.01.116.

[179] S. Takeda, K. Nagano, T. Mochida, and K. Shimakura, "Development of a ventilation system utilizing thermal energy storage for granules containing phase change material," *Solar Energy*, vol. 77, no. 3, pp. 329–338, Sep. 2004, doi: 10.1016/j.solener.2004.04.014.

[180] S. Koebrich, E. Chen, T. Bowen, S. Forrester, and T. Tian, "2017 Renewable Energy Data Book Including Data and Trends for Energy Storage and Electric Vehicles," 2017. doi: DOE/GO-102019-5113.

[181] G. R. Newsham and B. G. Bowker, "The effect of utility time-varying pricing and load control strategies on residential summer peak electricity use: A review," *Energy Policy*, vol. 38, no. 7, pp. 3289–3296, Jul. 2010, doi: 10.1016/j.enpol.2010.01.027.

[182] I. Dincer, S. Dost, and X. Li, "Thermal energy storage applications from an energy saving perspective," *International Journal of Global Energy Issues*, vol. 9, no. 4, pp. 351–364, 1997, doi: 10.1504/IJGEI.1997.063347.

[183] N. Soares, J. J. Costa, A. R. Gaspar, and P. Santos, “Review of passive PCM latent heat thermal energy storage systems towards buildings’ energy efficiency,” *Energy Build*, vol. 59, pp. 82–103, 2013, doi: 10.1016/j.enbuild.2012.12.042.

[184] S. Sonnick *et al.*, “Passive room conditioning using phase change materials—Demonstration of a long-term real size experiment,” *Int J Energy Res*, Apr. 2020, doi: 10.1002/er.5406.

[185] R. Arivazhagan *et al.*, “Review on performance assessment of phase change materials in buildings for thermal management through passive approach,” *Mater Today Proc*, vol. 22, pp. 419–431, Jan. 2020, doi: 10.1016/j.matpr.2019.07.616.

[186] M. Liu, W. Saman, and F. Bruno, “Review on storage materials and thermal performance enhancement techniques for high temperature phase change thermal storage systems,” *Renewable and Sustainable Energy Reviews*, vol. 16, no. 4. Pergamon, pp. 2118–2132, May 2012. doi: 10.1016/j.rser.2012.01.020.

[187] “F-Chart Software: Engineering Equation Solver.”

[188] B. Goetzler, M. Guernsey, and T. Kassuga, “Grid-Interactive Efficient Buildings Technical Report Series: HVAC; Water Heating; Appliances; and Refrigeration,” 2019. Accessed: May 19, 2021. [Online]. Available: http://www.osti.gov/servlets/purl/1577966/%0Ahttp://files/87/Neukomm et al. - 2019 - Grid-Interactive Efficient Buildings Technical Rep.pdf

[189] Center for Sustainable Systems, “Residential Buildings Factsheet,” 2021. Accessed: Jun. 16, 2022. [Online]. Available: https://css.umich.edu/publications/factsheets/built-environment/residential-buildings-factsheet

[190] U.S. Energy Information Administration - EIA, “Nearly 90% of U.S. households used air conditioning in 2020,” *Residential Energy Consumption Survey*. https://www.eia.gov/todayinenergy/detail.php?id=52558&src=%E2%80%B9%20

Consumption%20%20%20%20%20%20Residential%20Energy%20Consumption%20Survey%20(RECS)-b1 (accessed Jun. 16, 2022).

[191] M. Sarkar, “How American Homes Vary By the Year They Were Built; How American Homes Vary By the Year They Were Built,” Washington, DC, 2011. Accessed: May 19, 2021. [Online]. Available: http://www.census.gov/const/www/charindex.html

[192] A. Waqas and S. Kumar, “Phase change material (Pcm)-based solar air heating system for residential space heating in winter,” *Int J Green Energy*, vol. 10, no. 4, pp. 402–426, 2013, doi: 10.1080/15435075.2012.673518.

[193] A. Waqas, M. Ali, and Z. Ud Din, “Performance analysis of phase-change material storage unit for both heating and cooling of buildings,” *International Journal of Sustainable Energy*, vol. 36, no. 4, pp. 379–397, Apr. 2017, doi: 10.1080/14786451.2015.1018832.

[194] E. Markarian and F. Fazelpour, “Multi-objective optimization of energy performance of a building considering different configurations and types of PCM,” *Solar Energy*, vol. 191, pp. 481–496, Oct. 2019, doi: 10.1016/J.SOLENER.2019.09.003.

[195] M. C. Baecheler, J. Williamson, T. Gilbride, P. Cole, M. Hefty, and P. M. Love, “Guide to determining climate regions by county,” 2010. Accessed: Jan. 12, 2022. [Online]. Available: www.buildingamerica.gov

[196] “NSRDB | TMY.” https://nsrdb.nrel.gov/data-sets/tmy (accessed Aug. 09, 2022).

[197] X. X. Zhang, Y. F. Fan, X. M. Tao, and K. L. Yick, “Crystallization and prevention of supercooling of microencapsulated n-alkanes,” *J Colloid Interface Sci*, vol. 281, no. 2, pp. 299–306, Jan. 2005, doi: 10.1016/J.JCIS.2004.08.046.

[198] K. El Omari, Y. Le Guer, and P. Bruel, “Analysis of micro-dispersed PCM-composite boards behavior in a building’s wall for different seasons,” *Journal of*

Building Engineering, vol. 7, pp. 361–371, Sep. 2016, doi: 10.1016/J.JOBE.2016.07.013.

[199] B. Cui, J. Dong, J. Munk, N. Mao, and T. Kuruganti, "A simplified regression building thermal model of detached two-floor house in U.S. for virtual energy storage control," *International High Performance Buildings Conference*, Jul. 2018, Accessed: Mar. 07, 2023. [Online]. Available: https://docs.lib.purdue.edu/ihpbc/284

[200] "Prototype Building Models | Building Energy Codes Program." https://www.energycodes.gov/prototype-building-models#Residential (accessed Mar. 07, 2023).

[201] "Climate and Average Weather Year Round in Houston, Texas, United States." https://weatherspark.com/y/9247/Average-Weather-in-Houston-Texas-United-States-Year-Round (accessed Jan. 24, 2023).

[202] F. Li, B. Sun, C. Zhang, and C. Liu, "A hybrid optimization-based scheduling strategy for combined cooling, heating, and power system with thermal energy storage," *Energy*, vol. 188, p. 115948, Dec. 2019, doi: 10.1016/J.ENERGY.2019.115948.

[203] N. H. Abu-Hamdeh, R. A. R. Bantan, and R. I. Hatamleh, "Carbon dioxide reduction using passive technique of incorporating phase change materials into envelopes: A case study of climate data from Saudi Arabia," *J Energy Storage*, vol. 49, p. 104153, May 2022, doi: 10.1016/J.EST.2022.104153.

[204] S. Mousavi, M. Gijón-Rivera, C. I. Rivera-Solorio, and C. Godoy Rangel, "Energy, comfort, and environmental assessment of passive techniques integrated into low-energy residential buildings in semi-arid climate," *Energy Build*, vol. 263, p. 112053, May 2022, doi: 10.1016/J.ENBUILD.2022.112053.

[205] M. Arıcı, F. Bilgin, M. Krajčík, S. Nižetić, and H. Karabay, "Energy saving and CO2 reduction potential of external building walls containing two layers of phase

change material," *Energy*, p. 124010, Apr. 2022, doi: 10.1016/J.ENERGY.2022.124010.

[206] N. Farouk, M. A. El-Rahman, M. Sharifpur, and W. Guo, "Assessment of CO2 emissions associated with HVAC system in buildings equipped with phase change materials," *Journal of Building Engineering*, vol. 51, p. 104236, Jul. 2022, doi: 10.1016/J.JOBE.2022.104236.

[207] R. Renaldi, A. Kiprakis, and D. Friedrich, "An optimisation framework for thermal energy storage integration in a residential heat pump heating system," *Appl Energy*, vol. 186, pp. 520–529, Jan. 2017, doi: 10.1016/J.APENERGY.2016.02.067.

[208] P. Arce, M. Medrano, A. Gil, E. Oró, and L. F. Cabeza, "Overview of thermal energy storage (TES) potential energy savings and climate change mitigation in Spain and Europe," *Appl Energy*, vol. 88, no. 8, pp. 2764–2774, Aug. 2011, doi: 10.1016/J.APENERGY.2011.01.067.

[209] D. Fischer, H. M.-R. and S. E. Reviews, and undefined 2017, "On heat pumps in smart grids: A review," *Elsevier*, Accessed: Nov. 21, 2022. [Online]. Available: https://www.sciencedirect.com/science/article/pii/S1364032116309418?casa_token=Qh18EGJLZLwAAAAA:vpcm3J1pwdEV8U5QYm_IU7cE3i4I6Wuv_Zp3WoY2Sf95l1BAIPqXKo95rW9jIkSZs6zNmasuGQ

[210] K. Siler-Evans, I. L. Azevedo, M. G. Morgan, and J. Apt, "Regional variations in the health, environmental, and climate benefits of wind and solar generation," *Proc Natl Acad Sci U S A*, vol. 110, no. 29, pp. 11768–11773, Jul. 2013, doi: 10.1073/PNAS.1221978110.

[211] D. S. Callaway, M. Fowlie, and G. McCormick, "Location, location, location: The variable value of renewable energy and demand-side efficiency resources," *J Assoc Environ Resour Econ*, vol. 5, no. 1, pp. 39–75, Jan. 2018, doi: 10.1086/694179.

[212] B. Cui *et al.*, “A simplified regression building thermal modelling method for detached two- floor house in U.S.,” in *International High Performance Buildings Conference*, 2018. [Online]. Available: https://docs.lib.purdue.edu/ihpbc/284

[213] B. Cui, J. Munk, R. Jackson, D. Fugate, and M. Starke, “Building thermal model development of typical house in U.S. for virtual storage control of aggregated building loads based on limited available information,” in *PROCEEDINGS OF ECOS 2017 - THE 30TH INTERNATIONAL CONFERENCE ON EFFICIENCY, COST, OPTIMIZATION, SIMULATION AND ENVIRONMENTAL IMPACT OF ENERGY SYSTEMS*, 2012. [Online]. Available: http://energy.gov/downloads/doe-public-access-plan

[214] B. Cui *et al.*, “A hybrid building thermal modeling approach for predicting temperatures in typical, detached, two-story houses,” *Appl Energy*, vol. 236, pp. 101–116, Feb. 2019, doi: 10.1016/J.APENERGY.2018.11.077.

[215] J. Hirschey, “Investigation of Inorganic Salt Hydrate Phase Change Materials for Thermal Energy Storage Integrated into Heat Pump Systems,” 2022. Accessed: May 04, 2023. [Online]. Available: https://smartech.gatech.edu/handle/1853/70179

[216] C. Zhang, W. Gang, X. Xu, L. Li, and J. Wang, “Modelling, experimental test, and design of an active air permeable wall by utilizing the low-grade exhaust air,” *Appl Energy*, vol. 240, pp. 730–743, Apr. 2019, doi: 10.1016/J.APENERGY.2019.02.087.

[217] M. Hu, F. Xiao, J. B. Jørgensen, and R. Li, “Price-responsive model predictive control of floor heating systems for demand response using building thermal mass,” *Appl Therm Eng*, vol. 153, pp. 316–329, May 2019, doi: 10.1016/J.APPLTHERMALENG.2019.02.107.

[218] M. Hu, F. Xiao, J. B. Jørgensen, and S. Wang, “Frequency control of air conditioners in response to real-time dynamic electricity prices in smart grids,” *Appl Energy*, vol. 242, pp. 92–106, May 2019, doi: 10.1016/J.APENERGY.2019.03.127.

[219] B. Cui, D. ce Gao, F. Xiao, and S. Wang, “Model-based optimal design of active cool thermal energy storage for maximal life-cycle cost saving from demand management in commercial buildings,” *Appl Energy*, vol. 201, pp. 382–396, Sep. 2017, doi: 10.1016/J.APENERGY.2016.12.035.

[220] E. Di Giuseppe, M. D’Orazio, and C. Di Perna, “Thermal and Filtration Performance Assessment of a Dynamic Insulation System,” *Energy Procedia*, vol. 78, pp. 513–518, Nov. 2015, doi: 10.1016/J.EGYPRO.2015.11.721.

[221] S. Wang and X. Xu, “Parameter estimation of internal thermal mass of building dynamic models using genetic algorithm,” *Energy Convers Manag*, vol. 47, no. 13–14, pp. 1927–1941, Aug. 2006, doi: 10.1016/J.ENCONMAN.2005.09.011.

[222] X. Xu and S. Wang, “A simplified dynamic model for existing buildings using CTF and thermal network models,” *International Journal of Thermal Sciences*, vol. 47, no. 9, pp. 1249–1262, Sep. 2008, doi: 10.1016/J.IJTHERMALSCI.2007.10.011.

[223] A. Kusiak, M. Li, and F. Tang, “Modeling and optimization of HVAC energy consumption,” *Appl Energy*, vol. 87, no. 10, pp. 3092–3102, Oct. 2010, doi: 10.1016/J.APENERGY.2010.04.008.

[224] Spyder, “Spyder | The Scientific Python Development Environment,” 2022. https://www.spyder-ide.org (accessed May 04, 2023).

[225] “Benchmark Datasets for Buildings.” https://bbd.labworks.org/project/bbd (accessed May 05, 2023).

[226] C. Ermel, M. V. A. Bianchi, A. P. Cardoso, and P. S. Schneider, “Thermal storage integrated into air-source heat pumps to leverage building electrification: A systematic literature review,” *Appl Therm Eng*, vol. 215, p. 118975, Oct. 2022, doi: 10.1016/J.APPLTHERMALENG.2022.118975.

APPENDIX

Appendix A: HP-TES configurations review

Comparative Analysis

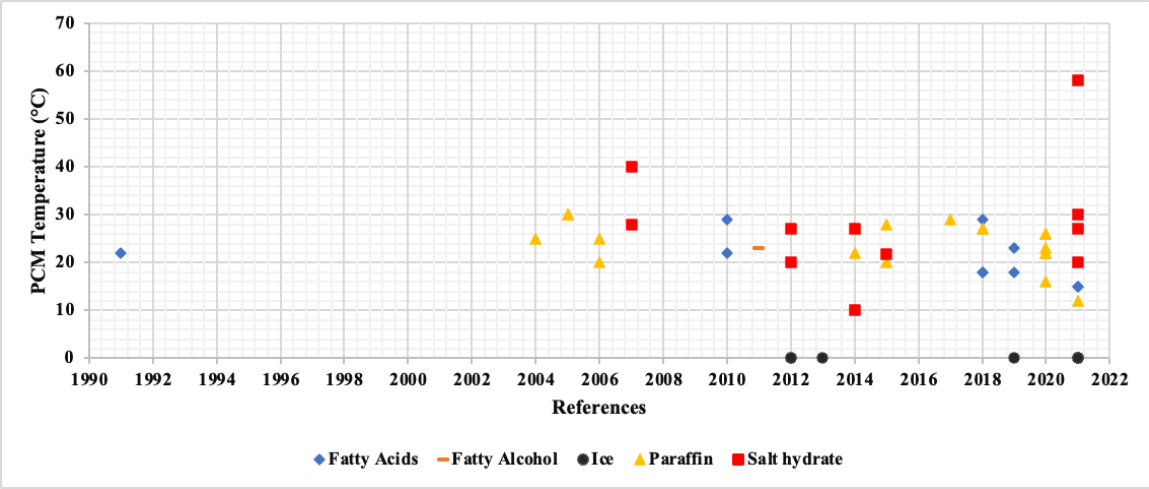


Figure 98: Historical trend of PCMs for HP-TES

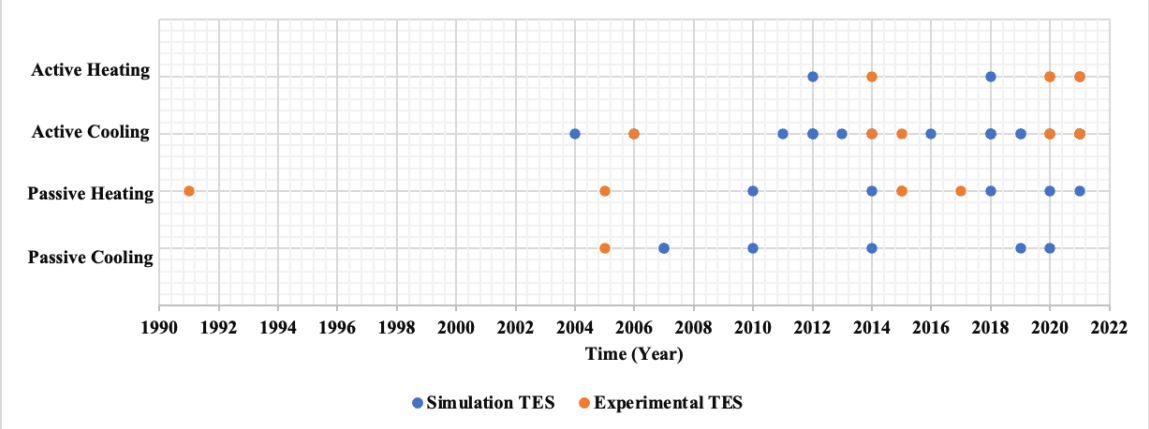


Figure 99: Historical trend of HP-TES research with TES type

Payback Period

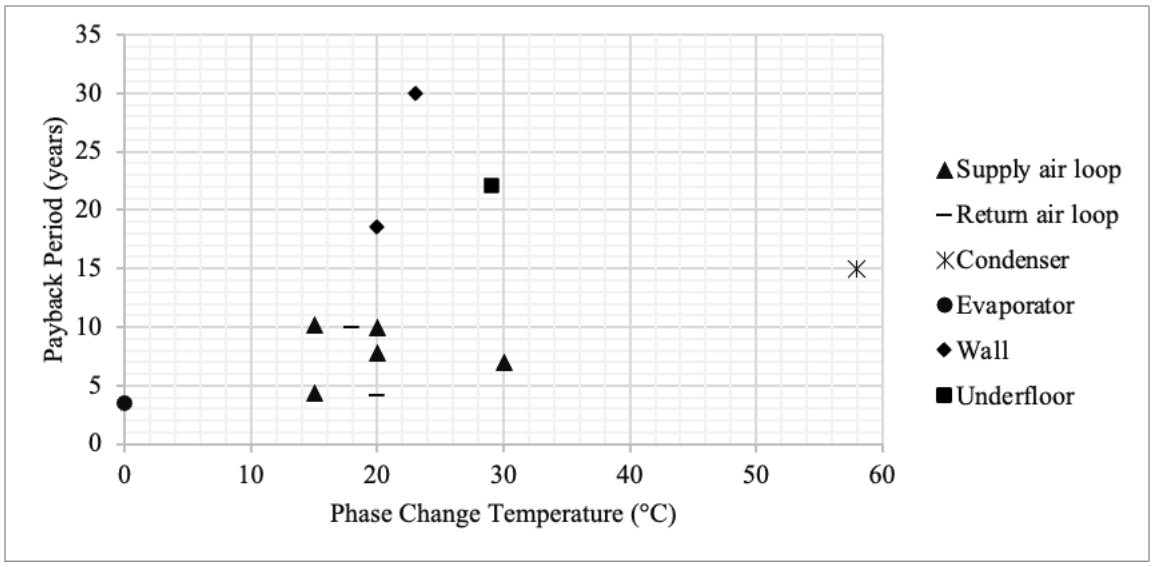


Figure 100: Payback period comparison against configurations

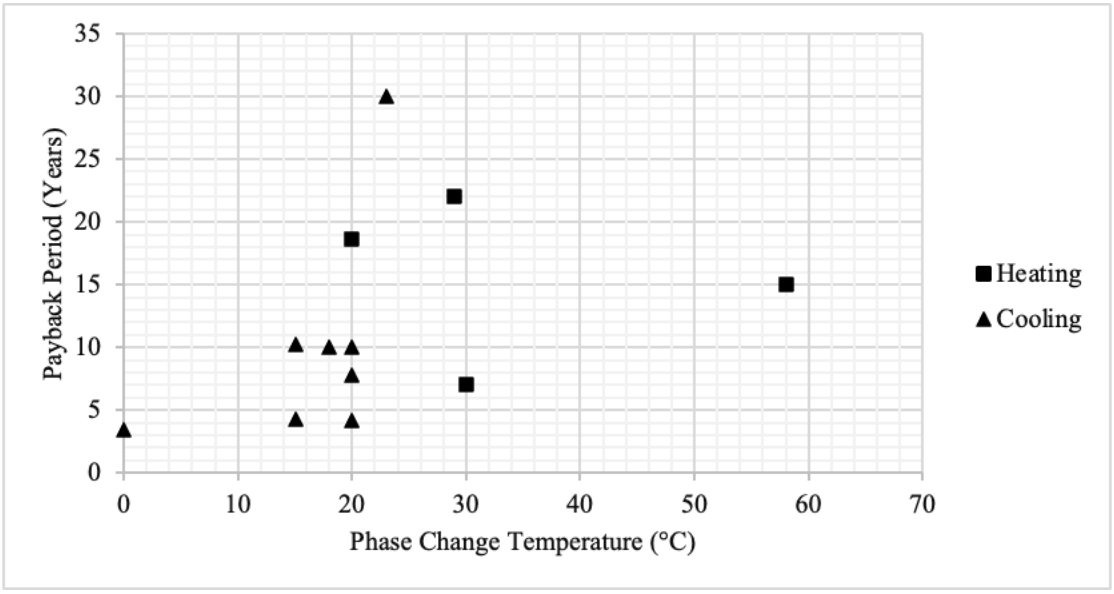


Figure 101: Payback period comparison against application

Load Shifting

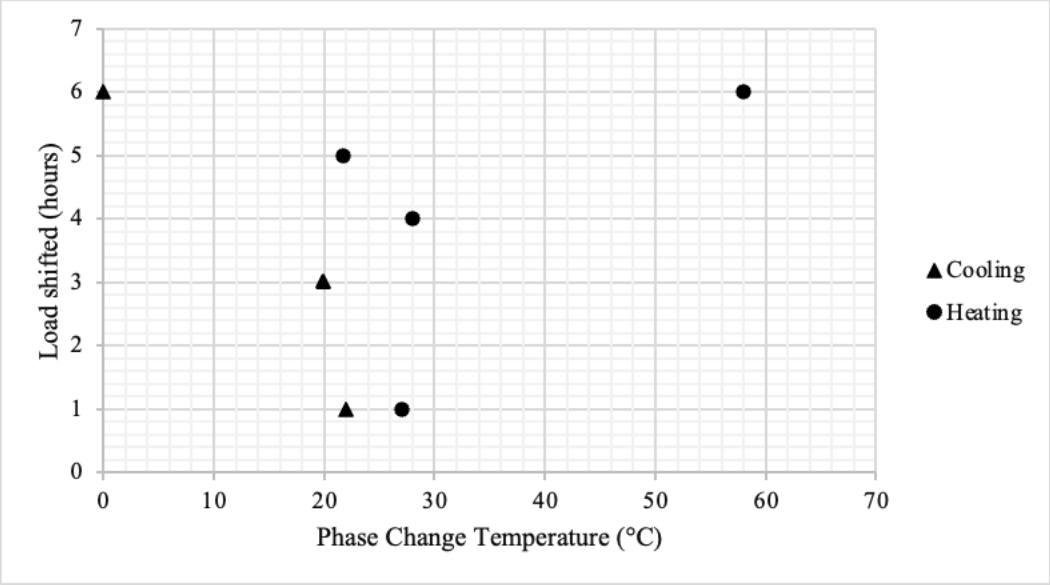


Figure 102: Load shifting comparison against application

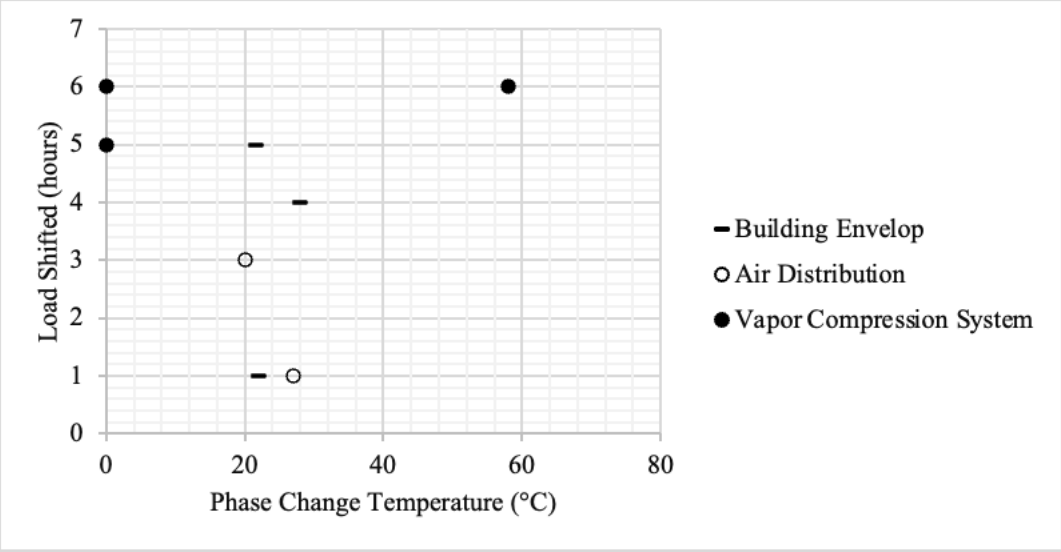


Figure 103: Load shifting comparison against configuration

Demand Impact

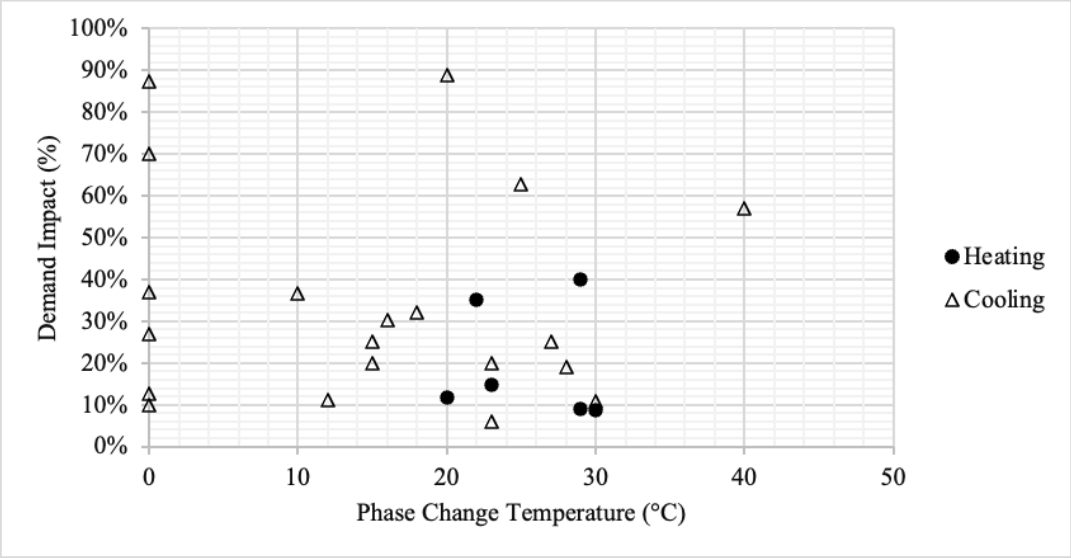


Figure 104: Demand Impact comparison against application

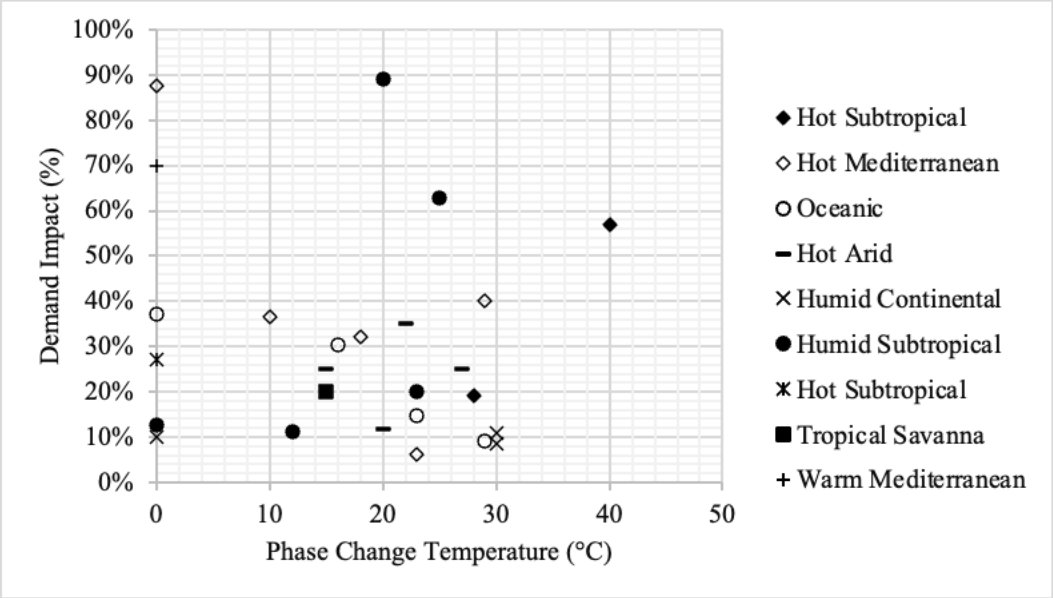


Figure 105: Demand Impact comparison against climate zone

Energy Savings

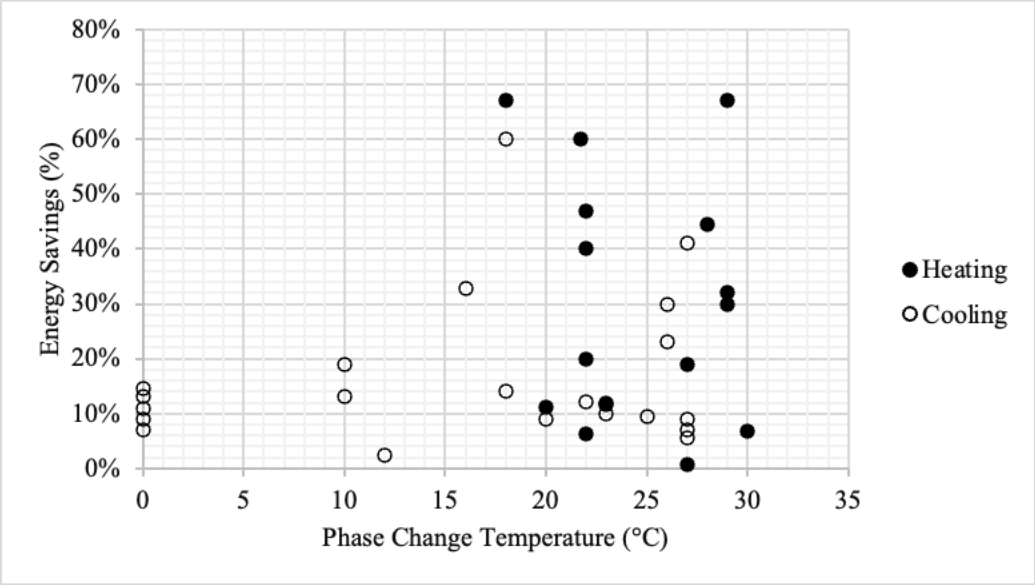


Figure 106: Energy savings comparison against application

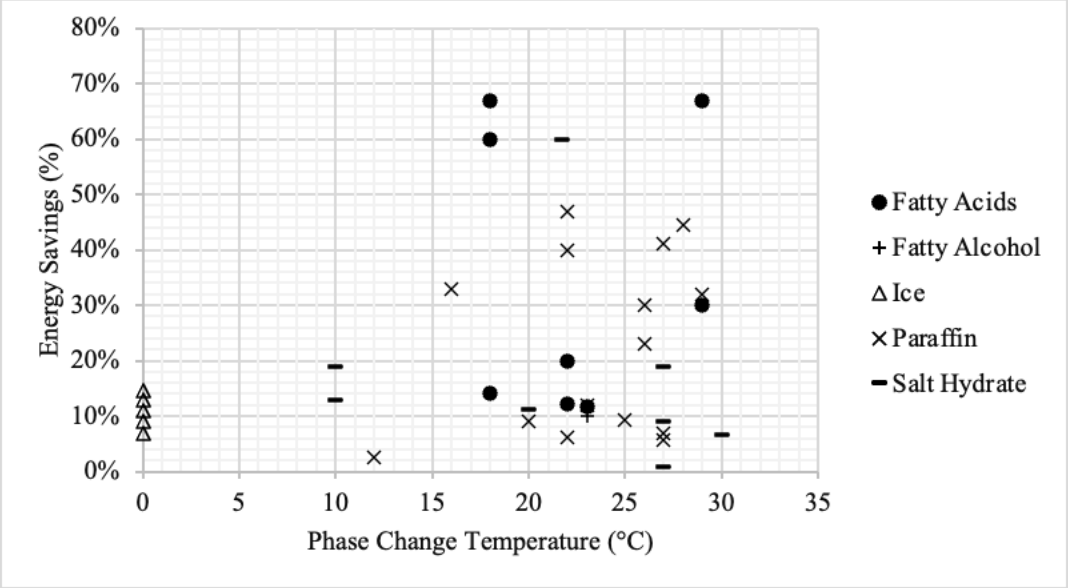


Figure 107: Energy savings comparison against PCM type

Utility Cost Savings

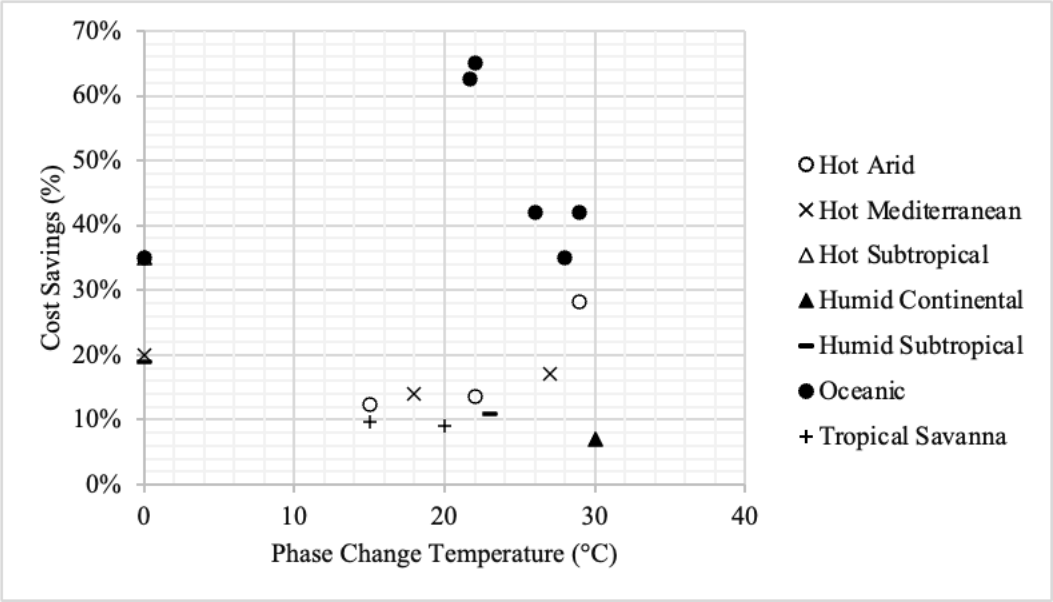


Figure 108: Utility cost comparison against climate zone

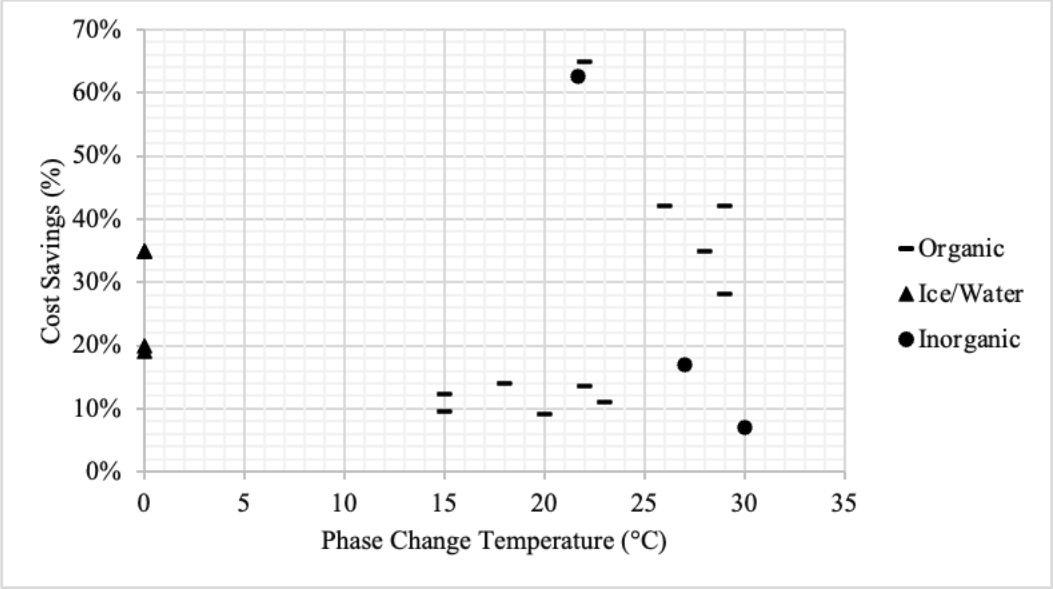


Figure 109: Utility cost comparison against TES type

Appendix B: Alabama case study analysis

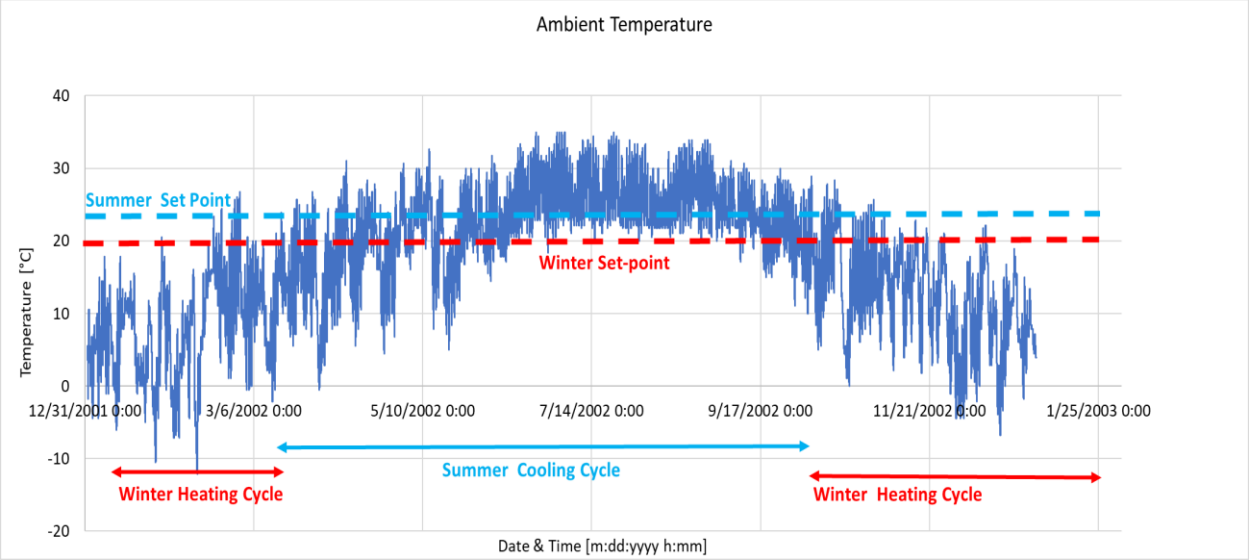


Figure 110: Alabama Ambient TMY

Payback Period

$$Cost\ of\ TES\ System = Payback\ year * \left[Year\ Saving_{Customer} + \frac{\$}{kWh_{year}} * Energy_{saving,year} + \frac{\$}{kWh_{peak,year}} * Peak_{reducation,year} \right]$$

$\frac{\$}{kWh}$ = The dollar value for reducing the total energy consumption

This will equate to the rebate's provided by the government.

$\frac{\$}{kWh_{peak}}$ = The dollar value benefit to utilities for reducing peak demand

Using monthly savings for utility customer only: The cost of TES system to have a 5 years payback period in Alabama should have a capital cost of *$840.75 for a 92 MJ unit.*

Appendix C: HP Analysis on California Case Study

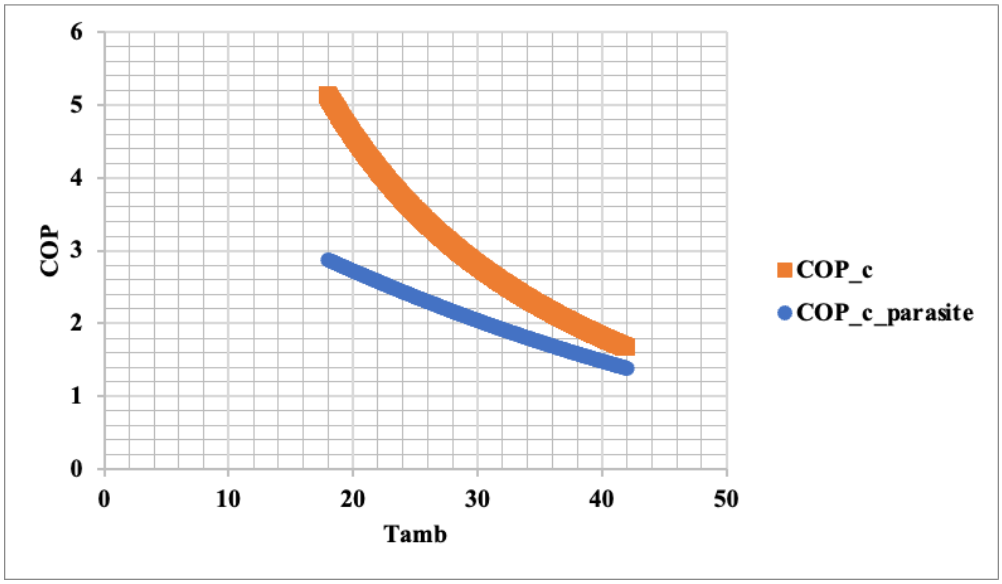


Figure 111: HP-TES Normal mode COP

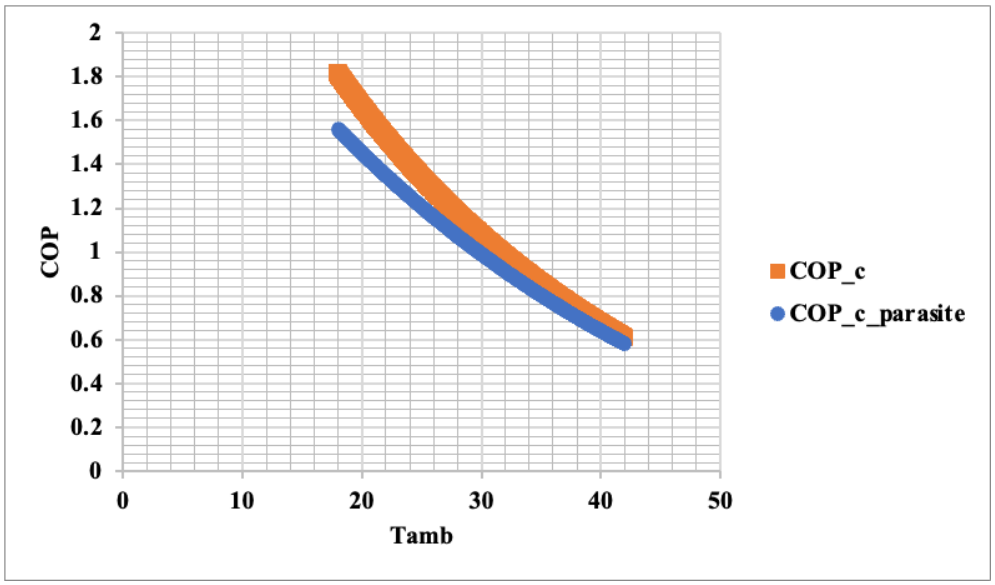


Figure 112: HP-TES Charging mode COP

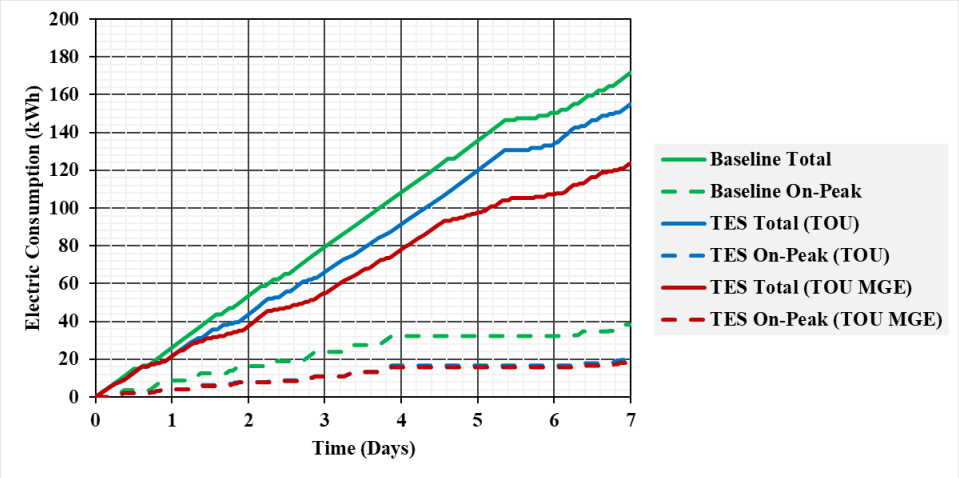


Figure 113: Electric Consumption of Winter Typical week in Baltimore, MD

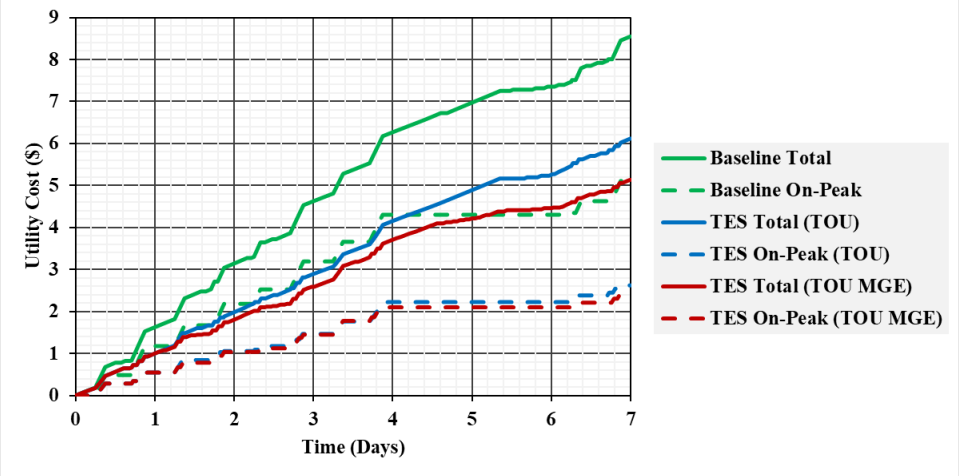


Figure 114: Utility Cost of Winter Typical week in Baltimore, MD

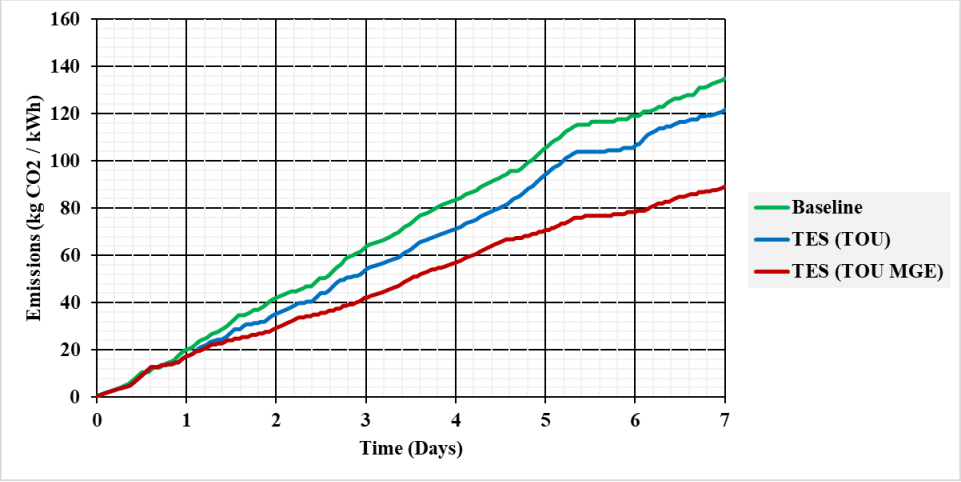


Figure 115: Grid Emissions of Winter Typical week in Baltimore, MD

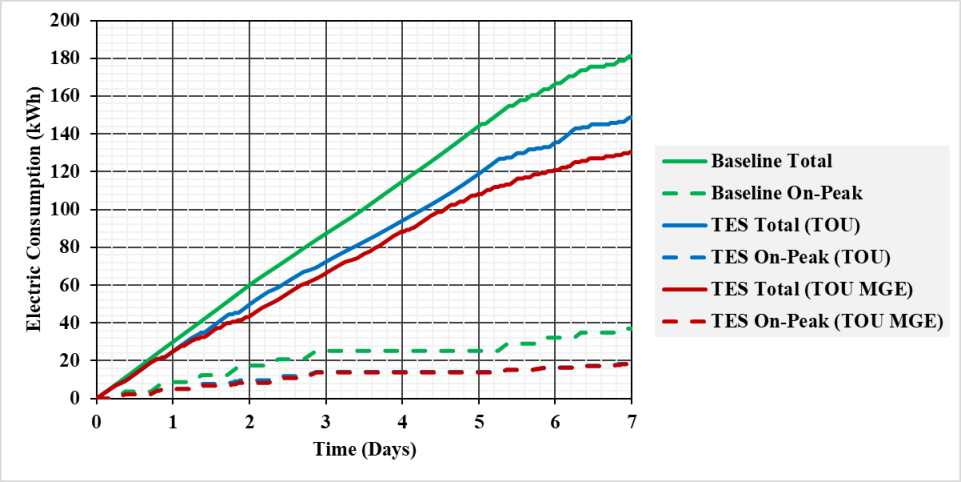


Figure 116: Electric Consumption of Winter Extreme week in Baltimore, MD

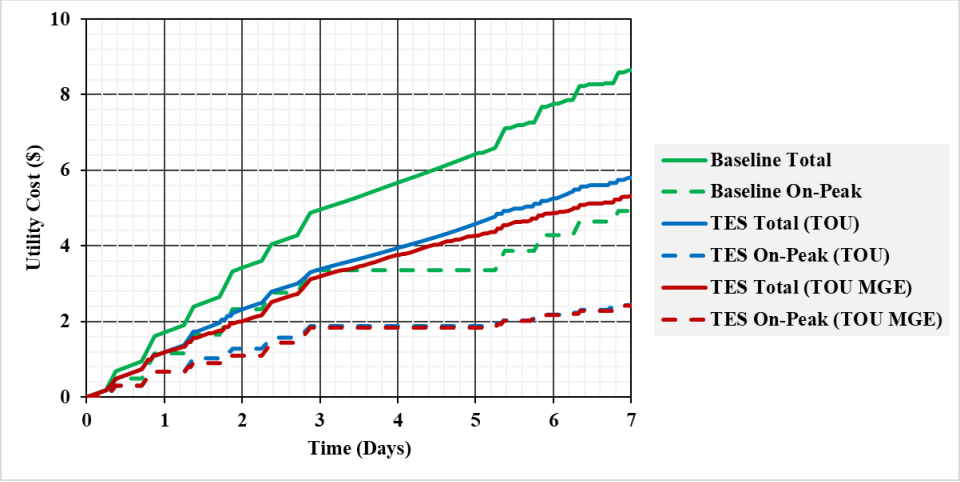


Figure 117: Utility Cost of Winter Extreme week in Baltimore, MD

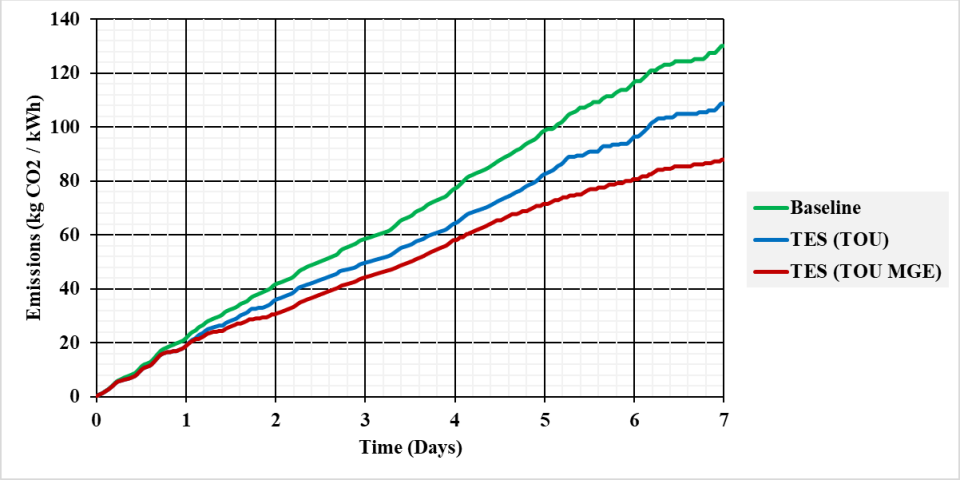


Figure 118: Grid Emissions of Winter Extreme week in Baltimore, MD

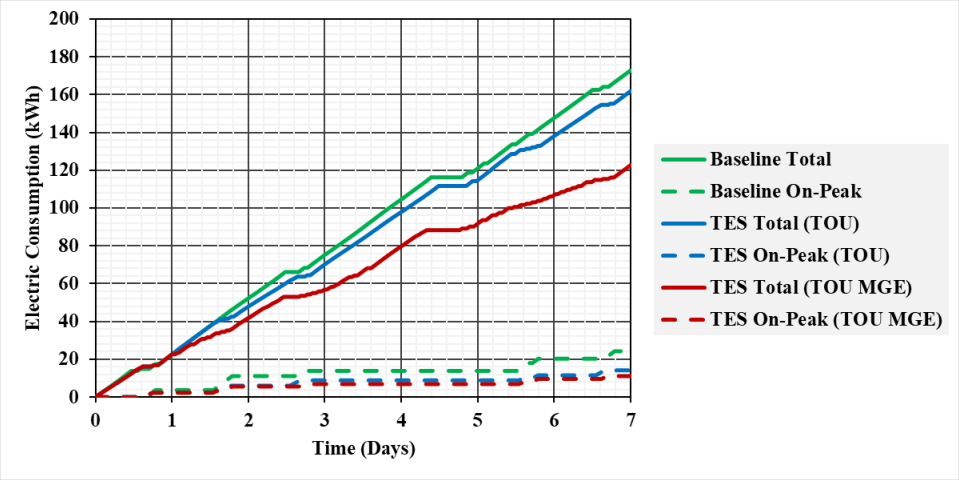


Figure 119: Electric Consumption of Winter Typical week in Golden, CO

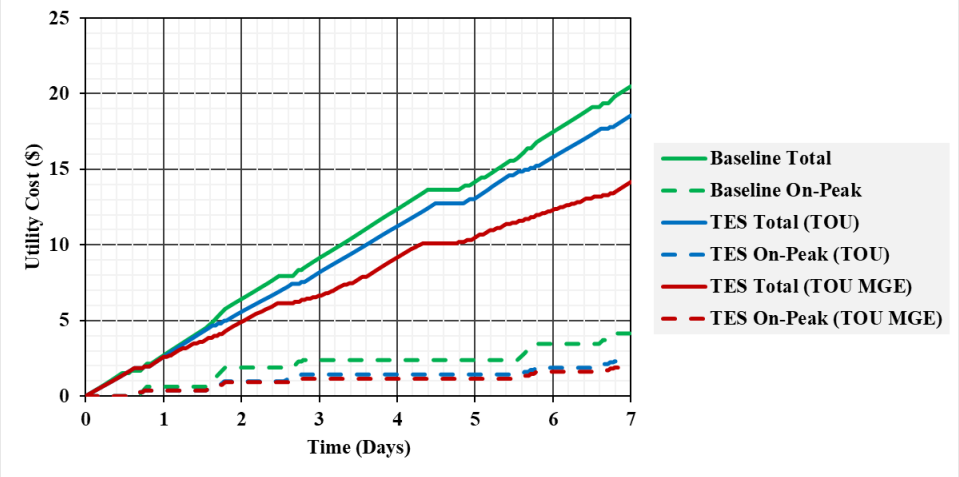


Figure 120: Utility Cost of Winter Typical week in Golden, CO

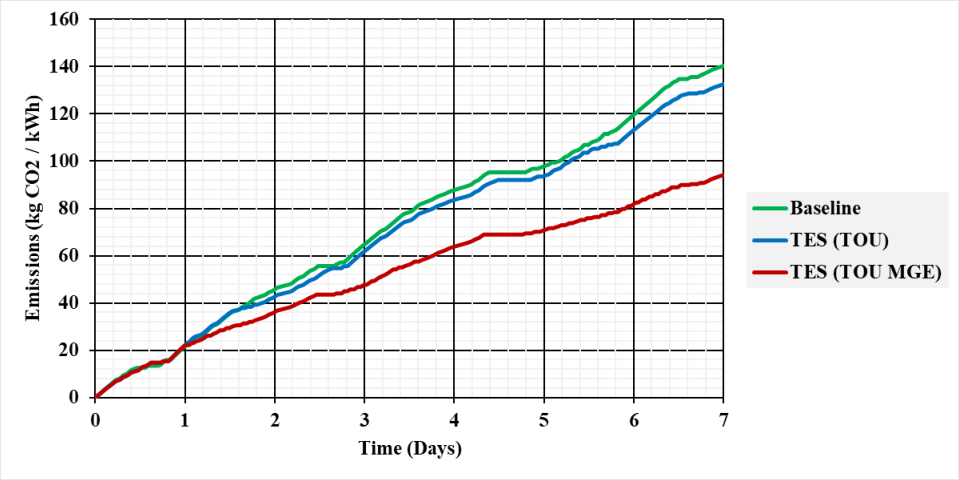


Figure 121: Grid Emissions of Winter Typical week in Golden, CO

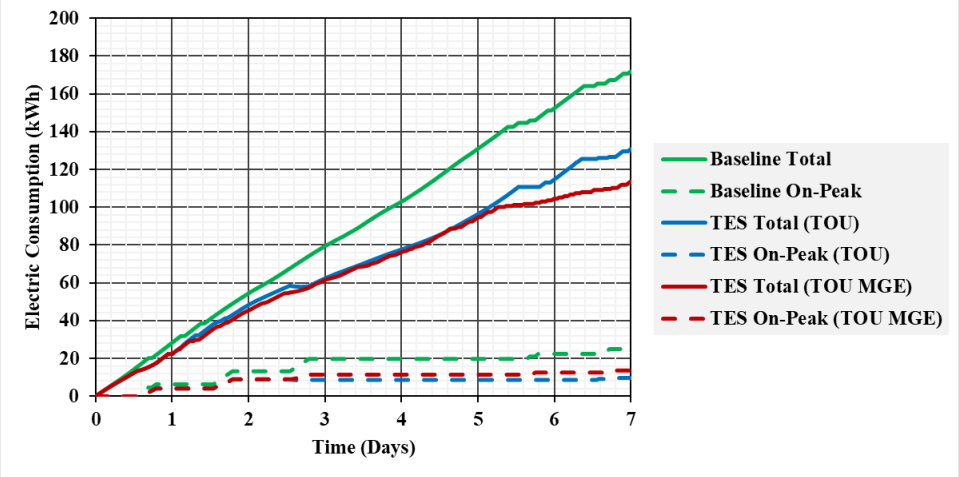


Figure 122: Electric Consumption of Winter Extreme week in Golden, CO

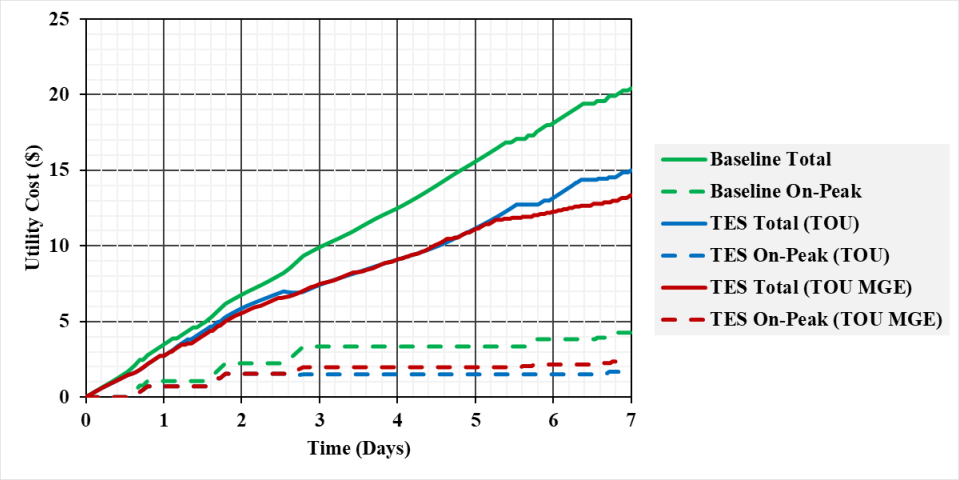


Figure 123: Utility Cost of Winter Extreme week in Golden, CO

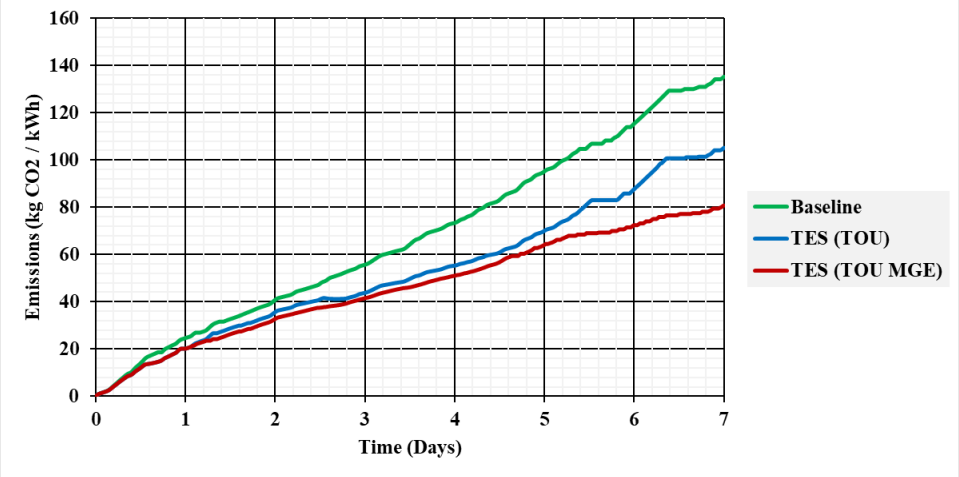


Figure 124: Grid Emissions of Winter Extreme week in Golden, CO

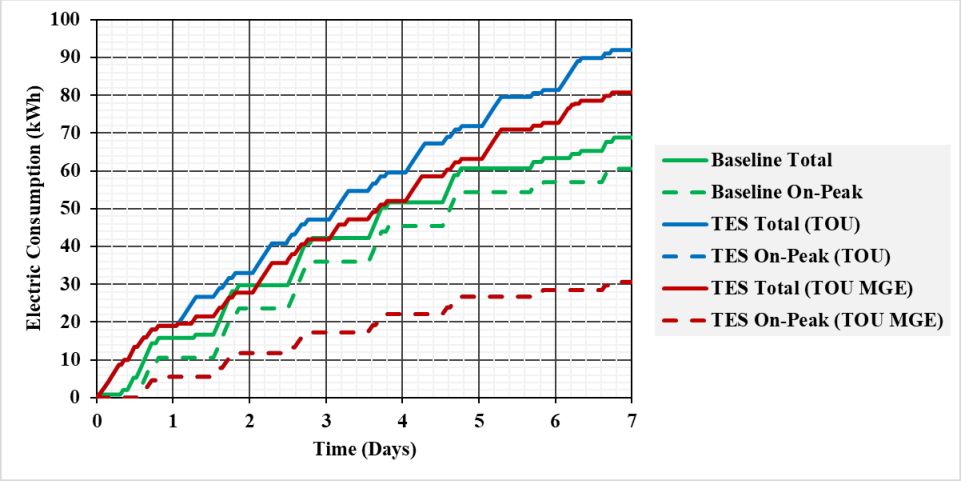


Figure 125: Electric Consumption of Summer Extreme week in Sacramento, CA

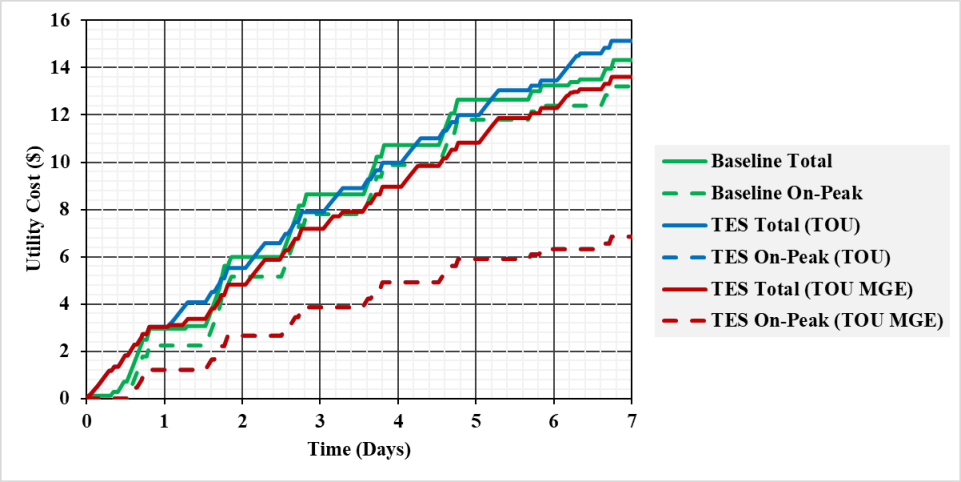


Figure 126: Utility Cost of Summer Extreme week in Sacramento, CA

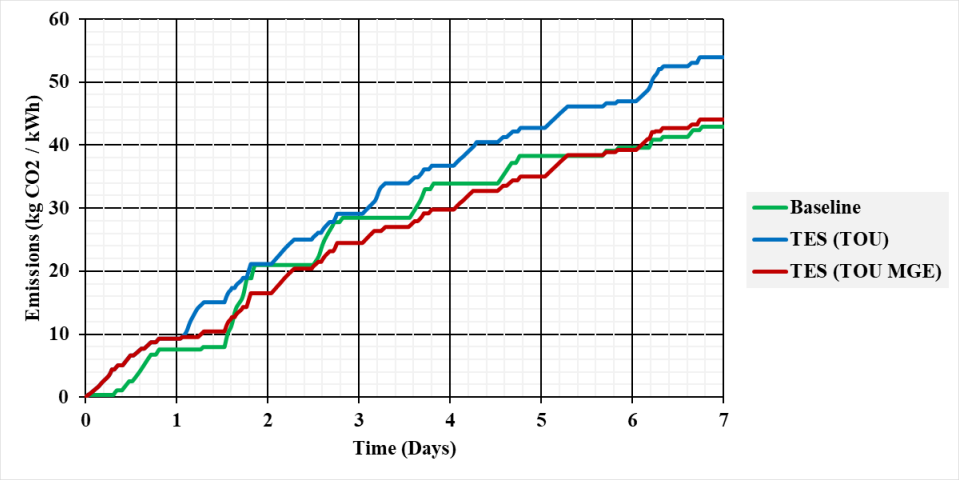


Figure 127: Grid Emissions of Summer Extreme week in Sacramento, CA

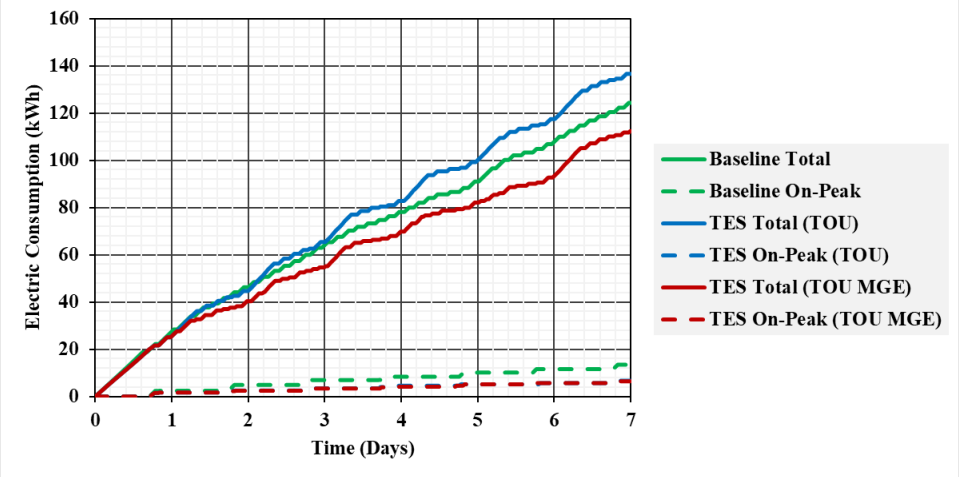


Figure 128: Electric Consumption of Winter Extreme week in Sacramento, CA

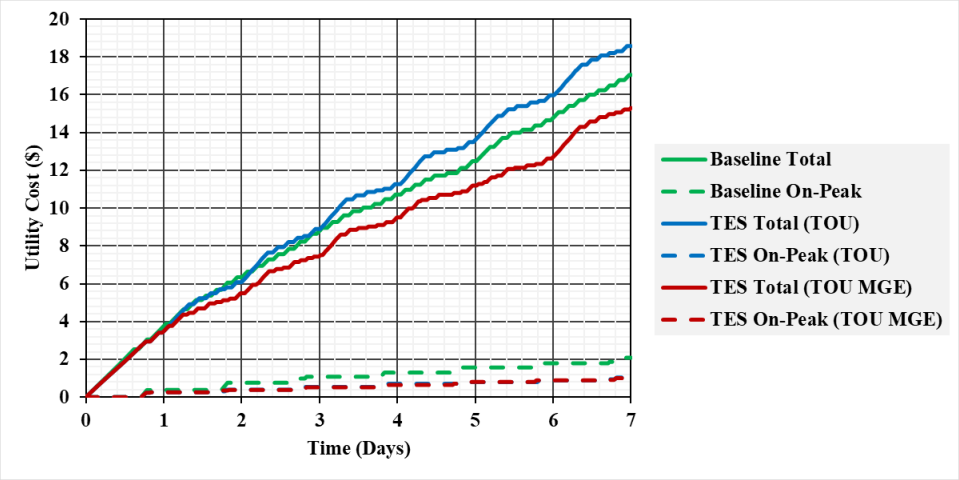


Figure 129: Utility Cost of Winter Extreme week in Sacramento, CA

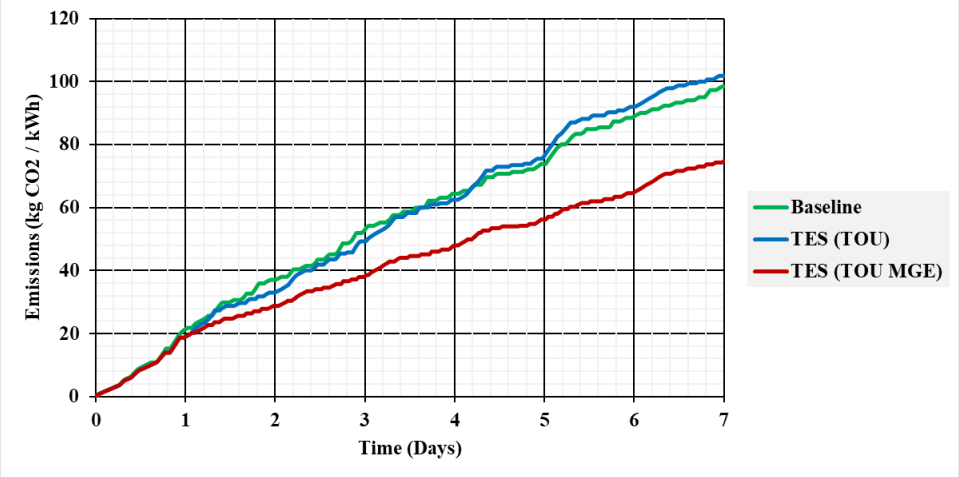


Figure 130: Grid Emissions of Winter Extreme week in Sacramento, CA

VITA

Ph.D. has taught me patience, perseverance, and purposefulness!!

It led me to question myself, my existence, and my passions. I am so many things today that I wouldn't be without my doctoral program.

I didn't know this when I took a flight from Islamabad, Pakistan to join Bredesen Center (7430 miles to be exact) on July 26th, 2018. "Brutal yet beautiful" sums up my journey. I still remember the despair because of loneliness, the anxiety because of imposter syndrome, and the numbness from often burning myself out. But I also remember the excitement and enthusiasm of new experiences and achievements.

While adjusting to a new life, I found many amazing learning opportunities.

From the very first day, I was interested in exploring practical solutions to use my work beyond the scientific world. I took many courses to increase my knowledge about policy, science outreach, and entrepreneurship. Participated in programs and even won awards. From getting best student paper nominations to being awarded a 2023 UTK volunteer of distinction, I want to credit all of my achievements to my most amazing advisor for his guidance, and kindness.

As of May 2023, I am interviewing a clean energy consultancy company as an Energy Analyst. I hope to continue creating a broader impact through my work, as a researcher, as a writer, and as a future mentor.

The things I am truly passionate about, Ph.D. has taught me this too!!